AD NUMBER

AD850556

NEW LIMITATION CHANGE

TO

Approved for public release, distribution unlimited

FROM

Distribution authorized to U.S. Gov't. agencies and their contractors; Administrative/Operational Use; NOV 1968. Other requests shall be referred to Support Technology Division [APF], Air Force Aero Propulasion Laboratory, Wright-Patterson Air Force Base, OH 45433.

AUTHORITY

AFAPL, per DTIC Form 55

AFAPL-TR-68-63

CHECKOUT TECHNIQUES FOR
FLUIDIC SYSTEMS

EDWIN U. SOWERS III

F. RAY SEKOWSKI

Bowles Engineering Corporation

TECHNICAL REPORT AFAPL-TR-68-63

APR 1 7 1969

A

NOVEMBER 1968

AIR FORCE AERO PROPULSION LABORATORY
AIR FORCE SYSTEMS COMMAND
WRIGHT-PATTERSON AIR FORCE BASE, OHIO 45433

CHECKOUT TECHNIQUES FOR FLUIDIC SYSTEMS

EDWIN U. SOWERS III

F. RAY SEKOWSKI

THIS DOCUMENT CONTAINED
BLANK PAGES THAT HAVE
BEEN DELETED

NOTICE

When Government drawings, specifications, or other data are used for any purpose other than in connection with a definitely related Government procurement operation, the United States Government thereby incurs no responsibility nor any obligation whatsoever; and the fact that the Government may have formulated, furnished, or in any way supplied the said drawings, specifications, or other data, is not to be regarded by implication or otherwise as in any manner licensing the holder or any other person or corporation, or conveying any rights or permission to manufacture, use, or sell any patented invention that may in any way be related thereto.

This document is subject to special export controls and each transmittal to foreign governments or foreign nationals may be made only with prior approval of Support Technology Division (APF), Air Force Aero Propulsion Laboratory, Wright-Patterson Air Force Base, Ohio 45433.
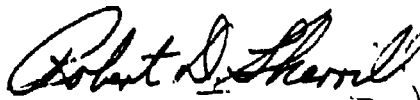
FOREWORD

This report, "Checkout Techniques for Fluidic Systems", presents the results of work performed by Bowles Engineering Corporation under Air Force Contract AF 33(615)-5296. It was accomplished under the direction of Mr. William H. Kemper (APFG), of the Air Force Aero Propulsion Laboratory, Wright-Patterson Air Force Base, Ohio 45433.

Appreciable contributions to the reported program effort were made by Dr. W. A. Walston and P. Bauer, their studies being summarized by B.E.C. Technical Memoranda included in this report, and by P. Cain in the performance of numerous laboratory tests.

This report was submitted by the authors on 7 May 1968.

This technical report has been reviewed and is approved.

ROBERT D. SHERRILL, Chief
Ground Support Branch
Support Technology Division

ii

ABSTRACT

Bowles Engineering Corporation has demonstrated the feasibility of checkout techniques for Fluidic circuitry. Sensors, instrumentation techniques, and checkout procedures have been defined which has been shown, by laboratory tests, to be successful in establishing levels of functional performance, and in isolating causes of circuitry malfunctions. The program was sponsored by the Air Force Aero Propulsion Laboratory.

It has been established that the most accurate means of establishing level of functional performance, to determine if the performance of a system is satisfactory or is outside of allowable limits, is through the use of primary sensors, such as certain pressure transducers and piezoelectric crystals. Primary sensors detect functional signals directly.

Acoustic sensing techniques, a secondary sensing procedure, has been applied, with a high level of success, to the isolation of anomalies causing malfunction. An accelerometer has been mounted to a circuit plate to sense the secondary acoustic energy generated by a group of operating elements on the circuit plate. This sensed acoustic signal has been converted into an amplitude vs. frequency acoustic signature, through the use of sonic and ultrasonic spectrum analyzers. It has been demonstrated that different anomalies cause distinguishingly different changes in the acoustic signature, thus permitting detection and definition of the anomalies causing malfunctions. The results realized in the isolating of malfunction causes through the use of secondary acoustic techniques is considered to be highly significant.

The present report presents the results of the checkout techniques program, during which the applicability of a group of candidate sensors were evaluated for use in the checkout of both analog and digital circuitry.

TABLE OF CONTENTS

v

TABLE OF CONTENTS---Continued

TABLE OF CONTENTS---Concluded

LIST OF ILLUSTRATIONS

LIST OF ILLUSTRATIONS---- Continued

x

LIST OF ILLUSTRATIONS----Continued

xi

LIST OF ILLUSTRATIONS----Continued

LIST OF ILLUSTRATIONS---- Continued

LIST OF ILLUSTRATIONS----Continued

LIST OF ILLUSTRATIONS----Concluded

LIST OF TABLES

SECTION I

INTRODUCTION

1. BACKGROUND

The growth of the field of Fluidics since the late 1950's has been phenomenal. A large and continuously increasing number of applications of Fluidic controls have been implemented. The high level of interest in Fluidic systems is a consequence of the inherent reliability and ruggedness of Fluidic circuitry and a potential for low cost. With the performance characteristics of no-moving-part Fluidic elements being a function of channel geometry as formed into an appropriate material, the maintenance of desired performance reduces primarily to the maintenance of the integrity of a static material structure. With the selection of materials and fabrication techniques appropriate to the application, highly reliable performance may be realized, with greatly minimized maintenance requirements and under extremes of shock, temperature, and radiation.

The established need for reliability and ruggedness in many areas of automatic control has led to a concentration of effort in the Fluidics field to develop and apply Fluidic control systems. The area of Fluidic system checkout has, heretofore, received minimal attention. Under the sponsorship of the Air Force Aero Propulsion Laboratory, therefore, Bowles Engineering Corporation has completed a program to establish applicable techniques for instrumenting Fluidic circuitry with which to define the state of circuit performance and to diagnose causes of malfunction. The results of this program are presented by this report, and are highly encouraging. Techniques have been established, and demonstrated, by which functional performance of Fluidic systems may be checked out, and through which the causes of system malfunction may be defined.

2. PROBLEM STATEMENT

Sensors and sensing techniques are required which provide, through an organized checkout procedure, the means of evaluating the functional performance of Fluidic circuitry. In addition, the sensors and sensing techniques must establish the causes of malfunction to permit prescription of the appropriate corrective actions. To define the problem more precisely, it is necessary to establish the level of checkout which is of primary concern, and to consider a typical checkout sequence.

Of primary interest are techniques and procedures applicable to a flight line system checkout. The first concern is to check out a supposedly functioning Fluidic system. Here the objective is to determine whether the functional performance is within prior established limits. If not, a second objective is to diagnose the cause of malfunctions so as to prescribe either appropriate healing where this may be accomplished in-place, or alternately, removal and replacement of a non-healable circuit grouping. The development of laboratory techniques for bench

1

testing of faulty circuitry is not of prime concern, although techniques applicable to flight line checkout techniques may be highly suitable for bench checkout procedures.

It is necessary to make this distinction to establish requirements which candidate sensors and sensing technique must satisfy. As an example, flight line sensors and sensing techniques may not degrade system reliability, as by the addition of tubing and fittings (with added potential leakage sources) for the remote attachment of sensors; the sensors must themselves be fail-safe in terms of system performance. The size and coupling means of applicable sensors must be compatible with circuitry packaging concepts. These constraints, which are applicable to a flight line checkout, do not necessarily apply to laboratory instrumentation.

A typical checkout procedure is outlined below:

CHECKOUT PROCEDURE SEQUENCE

1. Check to establish that the system input/output characteristics fall within established acceptable performance limits.

2. Check for absence of indications of impending failure.

3. If results of steps 1 and 2 are positive, checkout is complete. If results of either step 1 or 2 is negative, proceed with checkout.

4. Isolate circuit grouping containing malfunction cause.

5. Define cause of malfunction and healing procedure.

6. Perform appropriate healing. If defined anomaly is in-place healable, carry out prescribed procedure. If not an anomaly healable in-place, replace unsatisfactory circuit grouping (as an integral module).

7. Re-initiate sequence with step 1.

An examination of the checkout procedure serves to establish a number of broad functional objectives of circuitry checkout instrumentation.

o   The instrumentation must have sufficient resolution to distinguish between satisfactory and unsatisfactory performance.

o   The means used to detect the cause of unsatisfactory performance should exhibit sufficient resolution to detect and define an anomalous condition of an amplitude which causes the limit of

2

the input/output performance specifications to be approached.
These amplitudes are frequently quite small.

o   The information generated by the checkout instrumentation and
related equipment should require the minimum possible inter-
pretation, to minimize checkout errors. Some degree of automation
of the checkout procedure is probably desirable, depending upon the
specific system, to minimize human error.

3.   GENERAL APPROACH

The program carried out by BEC was implemented by a three phase effort,
outlined as follows:

o   PHASE I - SENSOR SELECTION AND EVALUATION

A survey of sensors and sensing techniques was performed and
candidate sensors selected. Functional failure of typical analog
and digital elements was defined. An extensive evaluation of the
candidate sensors was carried out to establish applicability to the
detection of performance degradation and/or detection of malfunction
causes, as applied to analog and digital elements and simple circuitry.
The compatibility of the sensors with typical packaging concepts and
effects of environment on the sensors were investigated. Recommen-
dations concerning the applicability of the candidate sensors were
prepared.

o   PHASE II - EVALUATION OF INTEGRATED CIRCUITRY INSTRUMENTATION
AND HEALING TECHNIQUES

Based on the conclusions of Phase I, sensing techniques considered
most applicable were applied in the instrumentation of typically
packaged analog and digital integrated circuitry and evaluated.
Techniques for in-place healing of circuitry were investigated.

o   PHASE III - DEMONSTRATION OF FEASIBILITY OF A CHECKOUT
PROCEDURE FOR AN ANALOG CONTROL SYSTEM

A two-module analog controller was instrumented and a semi-automatic
checkout procedure implemented to demonstrate the technical feasi-
bility of Fluidic System Checkout Techniques.

The results of the effort as outlined above are submitted by this report, together
with a summary, conclusions, and recommendations for future work.

3

SECTION II

SUMMARY

Much effort has been successfully directed to the development of Fluidic systems for a broad range of controls applications, the inherent reliability and minimized maintenance of Fluidics being much desired. Bowles Engineering Corporation has completed a program directed toward an area which has heretofore received little attention, that being the establishing of checkout techniques for Fluidic systems. This area will become increasingly more important as more Fluidic systems reach operational status.

Through the BEC program, which is described by this report, the feasibility of instrumentation arrangements and procedures for use in checkout of Fluidic systems have been demonstrated, the objectives of checkout procedures being essentially to establish the level of performance and to isolate causes of malfunction. The program was sponsored by the Air Force Aero Propulsion Laboratory under Contract No. AF 33(615)-5296, with the effort directed by Mr. W. H. Kemper, APFG.

A group of candidate sensors were selected for investigation and evaluation. Two types of sensors were considered; primary sensors, which sense functional signals such as pressure and flow, and secondary sensors, which detect secondary indicators of the state of a circuit such as the thermal profile of a circuit plate or the high frequency noise generated by a functioning element. The applicability of these sensors, and techniques for their use, for both analog and digital Fluidics circuitry, were investigated through tests with elements and circuitry. The most suitable sensors and techniques were selected and made use of in demonstrating the feasibility of a checkout procedure for a Fluidic feedwater controller for a Naval propulsion steam generator.

The results of the program indicate that primary sensors provide the most accurate means of evaluating the level of performance, sensing directly the functional signals. A miniature pressure transducer, piezoelectric crystals, and flow anemometers, were shown to be desirable primary sensors.

Secondary sensing techniques, namely the sensing of acoustic energy and analysis of the amplitude vs. frequency signature of the sensed acoustic energy, were shown to be highly successful in isolating anomalies causing primary performance malfunctions. It was shown that one accelerometer mounted to a circuit plate could isolate anomalies occurring at various locations on a circuit plate containing a group of functioning elements. The capability to isolate malfunction causes through secondary acoustic techniques, stems from the demonstrated fact that different anomalous conditions, such as

5

variations in supply, or bias pressure, or damage to a circuit structure, each cause a distinguishingly different change in the acoustic signature. These differing changes then serve to identify specific anomalies. The accomplishments realized in the area of fault isolation, a difficult instrumentation task, are highly significant and are considered to represent an advance in the state-of-the-art.

Further work is necessary to move Fluidic system checkout techniques from feasibility to operability. The development of sensors and related peripheral equipment specifically for use in Fluidic system checkout should lead to a lower cost of instrumentation. Approaches to minimizing the amount of sensing equipment which is mounted permanently to Fluidic circuitry require investigation, the objective being the reduction of cost and complexity of instrumentation which "goes along" with the circuitry. Along this line, means of transmitting information concerning the condition of Fluidic circuitry (as the acoustic energy generated by elements) from the circuitry to externally located sensing equipment requires study.

SECTION III

SELECTION OF CANDIDATE SENSORS

A discussion of sensor objectives and requirements is presented by this section. A literature survey of technical references and manufacturer's catalogs was carried out to select a group of candidate sensors which appeared compatible with the defined sensor objectives. The candidate sensors are each described, defining the supplier, model number, specifications, and reasons why each was considered applicable.

The objectives and requirements of primary and secondary sensors differ significantly, hence will be treated separately.

1.   SENSOR OBJECTIVES AND REQUIREMENTS

Two types of sensors are considered necessary for the checkout of Fluidic circuitry. The first type is those sensors which are capable of monitoring functional or primary performance. This group of sensors monitors directly the system functional signals, most commonly pressure or flow signals. The second group of sensors detect secondary phenomena which are related to the functional state of Fluidic circuitry.

It is considered probable that primary sensors are necessary for the reliable establishment of satisfactory performance, by directly monitoring functional system signals. The secondary sensors offer a potentially effective means of establishing the mode of failure producing a malfunction, and the amplitude of the anomaly. Such failure modes as development of a leak, contamination of an element's input or output channel, or a loss of supply pressure, all induce some change in the structure of an element's flow field. This in turn effects changes in such secondary indices of performance as local static temperature, temperature gradients and profiles, and the acoustic energy generated by a functioning Fluidic element. These secondary indices may be sensed and used to generate information concerning the operating state of a circuit and, hopefully, causes of malfunction.

a.   Primary Sensors

The function of primary sensors is to monitor and permit display of the functional primary system signals. The signals are normally in the form of pressures (most commonly) or flows, and changes in these quantities.

Where sensing the primary signals of analog circuits, the prime concern is with accurate sensing of signal levels, which reflects a need for good linearity, low hysteresis, and stability. High frequency response is not required. In sensing the primary performance of digital elements, a sufficiently high frequency response

7

is of more concern than a high degree of linearity. Digital element signals are defined more in terms of square wave or pulse rise times, shapes of leading and trailing edges and time relationships between pulses. Consequently, a frequency response compatible with rise times of a fraction of a millisecond is a prime requirement, and linearity is a more secondary concern.

In addition to the fundamental requirements of satisfactorily sensing primary signals, the primary sensors should be of such a physical configuration that they can be coupled to Fluidic circuitry without interfering with primary performance. This is of prime importance with digital circuitry where a mounting arrangement which effects a discontinuity in transmission passages may cause significant functional signal degradation. The capability of flush mounting with a channel wall, or mounting of a small sensing device in a channel, is desired.

The sensor and the means of mounting should not reduce the reliability of the functional system. Consequently, the coupling of external tubing to a circuit for the remote mounting of a sensor is not desirable, since this introduces potential sources of leakage. In order not to reduce system reliability the sensor must in itself be fail-safe. If the sensors fails it should not impair system performance. A sensor which in failing would permit dissociated fragments to be transported down a channel into an amplifier nozzle is highly undesirable.

The size and physical configuration of sensors must be compatible with typical concepts of packaging Fluidic system circuitry.

b. Secondary Sensors

Secondary sensors offer the capability of generating highly valuable information concerning the state of Fluidic circuits. This group of sensors offer a potential means of detecting the causes of malfunction with a minimum number of sensors and/or at a lower cost than by accomplishing the same objective through primary sensors.

A given performance degradation can usually be caused by more than one mode of failure. The problem is to define which mode of failure has occurred, to establish the appropriate corrective measures. As an example, one type of performance degradation of an analog circuit is an unacceptable shift in the output signal from the desired level for a given input signal. This degradation can be the result of a large number of failure modes, including a change in supply pressure, a shift in the setting of a bias adjust valve, a leak, or a contaminated receiver, at some amplifier within the circuit. One approach would be to couple pressure transducers to the supply pressures, inputs, and outputs of all the circuit elements. Then, by process of elimination and a complex comparison of appropriate signals, the problem could be isolated. This is, of course, an impractical approach in terms of both cost and complexity.

8

A number of secondary sensing techniques offer, ideally, a highly attractive alternate. As an example, a sensor capable of generating a thermal map for a complete circuit offers a possible means of locating, through use of one sensor, the cause of a circuit malfunction by the location and nature of changes in the thermal profile. The acoustic energy generated by operating elements also presents great possibilities. Prior tests conducted by BEC to examine the acoustic energy amplitude vs. frequency signature generated by an operating amplifier yielded encouraging results. The tests have shown that by inducing different modes of failure, detectable and differing changes occur in the acoustic signature. The potential thus exists that a single sensor of acoustic signals, with appropriate related equipment, may detect and define the cause of failure within a group of elements.

Two prime functional requirements must then be satisfied for secondary sensing techniques to be applicable. The sensitivity of the technique must be sufficient to detect the small magnitudes of anomalies causing malfunction (malfunction being defined as just exceeding the specified limitations of primary performance). The technique must also be capable of distinguishing between the various modes of failure.

The same requirements of not affecting system performance, of not reducing system reliability, and of compatibility with packaging concepts, described for primary sensors apply to secondary sensors.

2. CANDIDATE SENSORS

The sensors selected as having potential applicability to the checkout of Fluidics circuitry are defined in this section. The selection of the sensors included consideration of the general sensor objectives and requirements as given in Section III-1, as well as the sensing requirements as dictated by the definition of failures of Section IV.

a. Pressure Transducers

Strain gage and other types of pressure transducers have been used for static and low frequency dynamic testing of Fluidic elements since the beginning of the Fluidic technology. Most of these transducers by virtue of their large physical size, add volume to the circuit to be tested. For high frequency analog circuitry and digital circuitry, this effects an undesired degradation of system signals.

During the catalog search, a miniature pressure transducer was found which could be mounted in such a way as to become an integral part of the wall of a pneumatic channel, so that no additional volume is added to the circuit. This transducer manufactured by Scientific Advances, Inc. (Model SA-SD-M7) was used in the initial phases of the program. Later in the course of the program,

9

another transducer model was developed which possessed the same general performance characteristics with improvements in handling and mounting characteristics. This improved transducer, (Model SA-SD-M-6H) was used in the later portions of the program.

In addition to their small size (0.25 in.dia.) and capability of being incorporated as part of the channel wall, the transducers have other advantages which make them applicable to Fluidic checkout procedures.

 o The pressure sensitive areas is small (.028 sq.in.) providing nearly point pressure measurement.

 o The transducer consists of four strain gages bonded to a small diaphragm so that failure of the strain gages will not interfere with the functional performance of the Fluidic element being tested.

 o The linearity and hysteresis is ±0.5% of full scale. For a 2 psi transducer, this means the reading is accurate within 0.01 psi, and for a 15 psi transducer it is accurate within 0.075 psi.

 o The small diaphragm permits the transducers to have a high frequency response; its resonance frequency being 15,500 cps.

 o The pressure transducers are available for a large number of pressure ranges, providing good coverage of checkout pressure sensing requirements.

Summary of Technical Data:

  Supplier: Scientific Advances, Inc.
  Model: SA-SD-M-6H
  Size: .25 in.dia. × .25 in. thickness
  Pressure Sensitive Area: 0.028 in^2
  Input Voltage: 3V d.c. or a.c. rms
  Full Scale Output: 30 mv
  Bridge Resistance: 120 to 200 ohms
  Overpressure: 50% over rated range
  Linearity and Hysteresis: ±0.5% FS
  Calculated Natural Frequency: 15,500 cps
  Pressure Ranges(psid): ±2, ±5, ±10, ±15, ±30, ±100

b.   Flow Anemometry

The use of hot-wire and hot-film anemometers is a highly developed part of current Fluidic technology. Such anemometers operate on the principle that convective heat transfer from a hot body placed in a cooler fluid medium will vary directly with the velocity at which the fluid sweeps past the body. If the body is an electrically excited conductor having a resistivity which varies with temperature, its total resistance will vary as a function of fluid velocity. Hot-wire and hot-film anemometers, therefore, consist essentially of calibrated conductors, probe-mounted for insertion in fluid streams, together with suitable instrumentation for detecting and displaying its electrical output signals which are a function of fluid flow velocity.

Presently available anemometers of this type can be designed with exceptional sensitivity to low-flow velocities. Unfortunately, however, their sensitivity is inherently non-linear, necessitating careful calibration to attain accuracy over wide velocity ranges. Accordingly, these devices are most commonly used for qualitative measurements including, signal-to-noise ratios in Fluidic devices.

In spite of this limitation, however, anemometry is potentially suitable as a sensor approach for Fluidic control system checkout purposes. This is particularly true where either qualitative sensing or relatively crude quantitative measurements are required. Such capability is generally adequate for digital circuit evaluation and offers a limited potential for analog circuit measurements. Moreover, probes can be built in a size suitable for direct incorporation in the inlet and output passages of virtually any type of fluid amplifier.

The hot wire selected as being most suitable for checking out Fluidic elements is the model 55A52, manufactured by Disa Electronics. The principal reasons for selecting these probes are:

o   The probe consists of a wire (.0002 in. dia.) mounted between two needles of 0.8 mm length with a 0.45 mm spacing between them. Being of such miniature size, these probes are capable of being mounted directly into the flow channels of pneumatic elements with a minimum disturbance to the functional flow characteristics.

o   The maximum air flow velocity which the probes are capable of detecting is 150 m/sec which is normally sufficient for use with digital elements.

o   The frequency response of a hot wire anemometer system is a function of the rate at which the electronic circuitry can supply power to the wire or film being used. A hot wire probe connected to a bridge circuit and servo amplifier which keeps the probe

11

resistance constant, and hence the probe temperature virtually constant, is defined as a constant temperature anemometer system. The output of the system is actually a measurement of the power delivered to the flowing medium by the probe. A Disa type 55D05 constant temperature anemometer system was selected to be used with these probes. This system can be used to an upper frequency limit of 50 KC which is more than sufficient for the testing to be performed.

o   Because the hot wire anemometer system is capable of detecting large flow velocities with high frequency content, it possesses the capability of detecting performance characteristics of digital elements and the ability to detect meaningful deviations in performance degradation.

o   The most common failure of the hot wire is wire burn-out which when it occurs, will not affect the functional performance of the element being tested.

The hot film probe chosen to be evaluated as a sensor of primary flow performance is the Disa Electronics type 55A90/91 miniature flush-mounted probe. It was selected for the following reasons.

o   This type of probe can be flush mounted in a flow channel wall and so become a part of the wall, thereby adding no disturbances to the flow.

o   Its miniature size (dia. of approx. 0.2 in.) is compatible with Fluidic element flow channels.

o   Unprotected platinum probes may be obtained for use in gaseous media capable of detecting flow velocities up to 500 m/sec. (Quartz-coated platinum films are also available which are capable of detecting liquid flow velocities up to 10 m/sec.)

o   Using the Disa type 55D05 anemometer system with the hot film probe provides a system response capability of 50 KC.

o   The sensitivity and frequency response of these probes make them useful as detectors of both the primary functional characteristic and meaningful performance degradation of digital elements.

o   Failure of these probes generally consists of film burn-out or contamination of the film. Neither of these failure modes would effect the functional performance of the element under test.

12

Summary of Technical Data:

Constant Temperature Anemometer

Supplier: Disa Electronics
Type: 55D05
Type of Operation: 10:1 and 1:1 bridge ratio
Probes: Hot-wire or Hot-film
Probe Resistance Range: 1 to 50 ohms
Frequency Range: 0 to 50 K Hz, depending on probe
and condition of measurement
Output Voltage: approx. 1 to 7 volts
Output Impedance: approx. 500 ohms
Power Supply: Built-in, batteries

Hot Wire Probe

Supplier: Disa Electronics
Type: 55A53
Wire Material: Platinum-plated tungsten
Wire Diameter and Length: 0.005 mm x 0.45 mm
Length Supporting Legs: 0.8 mm
Probe Body Diameter: 0.9 mm
Resistance at 20° C: 1.4 ± 0.3 ohms
Maximum Air Flow Velocity at 1 atm: 150 m/sec

Hot Film Probe

Supplier: Disa Electronics
Type: 55A90/91
Film Material: Platinum
Film Length: approx. 1 mm
Film Width: approx 0.20 mm
End Diameter of Probe: 4.75 mm
Maximum Velocity gases: 500 m/sec

c.   Piezoelectric Crystals

Piezoelectric crystals are, as the name implies, pressure sensitive electric
crystals. Whenever a pressure is applied to a piezoelectric crystal, an
electrical charge is produced. PZT Bimorph ceramic crystals, manufactured
by Piezoelectric Division of Clevite Corporation were selected for evaluation.
These elements consist of two layers of piezoelectric material with a layer of
thin metal sandwiched between them. The layers of crystal material are secured

13

together face to face so that when a force is applied to the bimorph material, the strain in the crystals causes a corresponding voltage differential to be developed between two electrode terminals.

Although we have already selected strain gage pressure transducers to be evaluated as pressure sensors, it is believed that piezoelectric crystals possess certain characteristics which would be beneficial during certain tests.

o They generate an electric charge when a pressure is applied to the crystals. This characteristic appears especially applicable in monitoring the pressure pulses produced in digital circuits.

o They can be designed to meet the small physical size and shape desired. They can be mounted in the sidewall of the pneumatic channels, and thus becoming a part of the sidewall, do not effect the operational characteristics of the element being tested.

o Because of their physical construction, they would not influence the Fluidic performance if crystal breakdown should cause the device to stop functioning as a sensor.

o Their frequence response characteristics are a function of their physical size (length, width, and thickness). Again their size can be designed to meet the necessary frequency response characteristics of digital elements.

o Their low cost makes them particularly attractive where multi-channel monitoring is required.

Summary of Technical Data:

Little data is given on piezoelectric crystals except for their performance characteristics while mounted in typical non-Fluidic configurations. Their sensitivity and frequency response is greatly dependent on the mounting configurations used. Therefore, these sensors will be evaluated with respect to mounting con-figurations which are applicable to Fluidic elements.

d. Infra-Red Sensing

Infra-red radiometry has been developed in recent years so that a high level of sensitivity has been achieved. IR techniques are used extensively in mapping the thermal contours of land, water, and cloud formations. More recent developments have found IR sensing a practical method of locating defective components in electronic circuits and defective bonding in printed-circuit

14

boards. It is therefore, a possibility that their application to check out Fluidic circuits may produce meaningful data.

Fluidic elements contain a variety of nozzles through which gases are accelerated due to pressure drops across them. The static temperature of the gas at the nozzle throat is less than the temperature (essentially stagnation) in the relatively wide channels upstream of the nozzle. This temperature difference in the gas will extend in some manner to the material forming these elements. By monitoring the surface temperature of the elements, temperature gradients should be detected which are related to the nominal pressure changes occurring within the Fluidic elements. Abnormal pressure changes should produce corresponding thermal gradients which differ from those produced when the elements performance was satisfactory. As an example, if a supply pressure nozzle were completely blocked by contamination, no flow or expansion of gases would occur and thus no temperature gradient across the nozzle would exist. Therefore, the surrounding medium would approach room temperature which is a deviation from the normal operation. It is conceivable that a relationship between changes in the surface temperature gradient and performance degradation could be accomplished in this manner.

A portable radiation thermometer manufactured by the Barnes Engineering Company (model PRT-4) was selected for evaluation as a performance sensor for Fluidic elements because of these characteristics.

o   The PRT-4 radiation thermometer is capable of detecting temperatures ranging from 10°F to 110°F, which adequately covers the expected range of thermal gradients on the surface of Fluidic elements and circuits.

o   Its response of 50 m/sec is more than sufficient to detect changes in the thermal state of Fluidic circuit plates.

o   A checkout procedure which would involve using this device would require no connections to the Fluidic elements flow channels, and therefore, would not add any anomalies which would cause functional performance degradation.

o   The resolution of the Model PRT-4 I.R. thermometer is approximately 0.02° C. If considering the isentropic flow of air through a nozzle with a nominal pressure drop of 1 psi, a 0.02° change in air static temperature in the nozzle throat would reflect a change of approximately 0.001 psi in the nozzle pressure drop. With the I.R. thermometer monitoring resultant changes in the circuit structure temperature, the sensitivity in detecting pressure changes will be less, but hopefully still useful.

15

o   The minimum field of view of the I.R. thermometer is .4 inches
diameter. This is sufficiently small to permit its use in plotting
thermal maps of functioning elements, with a matrix size small
enough to be meaningful.

The relatively large size of this I.R. thermometer and the fact that it must be
used in excess of one foot from the circuit precludes its use for checking out
Fluidic circuits where space is at a premium.

Its primary use in this program is to evaluate the effectiveness of thermal
mapping techniques in indicating performance degradation. If the thermal
mapping technique proves useful, suitable I.R. probes could possibly be
developed.

Summary of Technical Data:

Supplier: Barnes Engineering Company
Model: PRT-4
Temperature Range: 10°F to 100°F
Resolution: 0.02°C
Field of View: 2° at half energy point
Target Distance: 1 foot to infinity, with target filling field of view
Response Time(63%): 50 m/sec
Dimensions of Optical Head: 5-1/2 in.dia. x 5 in.long

e.   Thermistor

The thermistor provides an alternate method of detecting temperature changes in
a Fluidic circuit. A thermal map, or temperatures at selected locations, may be
obtained by monitoring the outputs of small thermistors embedded in the circuit
structure.

The thermistor exhibits a number of fundamental advantages as compared to an
I.R. thermometer. A thermistor of small size (.043" diameter bead) may be
embedded in the circuit structure in close proximity to channel walls. In this
position, the gain factor between operating fluid temperature change and the
surrounding medium temperature change is maximized. Secondly, a small
thermistor may be located in the immediate vicinity of circuitry locations where
the greatest temperature changes occur as, at a nozzle throat. As a consequence
of these two factors, it is probable that greater sensitivity to pressure changes
may be realized with appropriately located thermistors than with an I.R. sensing
device. One disadvantage of the thermistor, however, is that each point
temperature to be monitored required a thermistor, a pair of lead wires, and coupling
to, most commonly, some type of a bridge circuit.

16

Although a large variety of temperature sensors are available today, their performance specifications are relatively similar. Thermistors manufactured by Fenwal Electronics, Inc., model GB32J2 were selected to be evaluated based on the following:

o   They are inexpensive which is desirable, particularly if several sensors were required to be permanently mounted in a circuit plate as part of a checkout technique.

o   Because of their miniature size, these thermistors permit point temperature measurement and are capable of being embedded into the majority of Fluidic circuits marketed.

o   Being embedded in the structure material of Fluidic circuits, these thermistors could not cause any functional performance degradation if they should fail.

o   The average sensitivity of the selected thermistor based on its resistance change between $0^{\circ}C$ ($32^{\circ}F$) and $50^{\circ}C$ ($122^{\circ}F$) is approximately $100\,\Omega/^{\circ}C$ ($55.5\,\Omega/^{\circ}F$). This sensitivity should be sufficient to detect temperature variations associated with the functional performance characteristics and performance degradation of Fluidic circuits.

Summary of Technical Data:

   Supplier: Fenwal Electronics, Inc.
   Model: GB32J2
   Sensitivity: $100\,\Omega/^{\circ}C$ (average between $0^{\circ}C$ and $50^{\circ}C$)
   Time Constant: 2 seconds
   Resistance: $2,000\,\Omega$ ±20% at $25^{\circ}C$
   Dimensions: 0.043 in. dia. bead

f.   Accelerometer

Associated with the operation of Fluidic circuits is an audible acoustic noise in the form of a hissing sound. To the trained observer, this acoustic noise gives a gross indication of the circuit's performance. A typical example is that which often occurs in the testing of digital counting circuits where one can often detect the absence, or miss, of a count just by listening to the circuit's acoustic noise. A change in the acoustic intensity is heard marking the presence of each count. This suggested the possibility of detecting these acoustic signals by more sophisticated means and analyzing their content to produce meaningful and repeatable characteristics which could be related to the circuit's performance status.

17

A potential method of detecting these acoustical pressure disturbances is by mechanical vibration sensing. Acoustic pressure disturbances developed within fluid circuit passages will transmit characteristic frequencies to the surrounding medium which, for mechanical vibration sensing, is the material of which the Fluidic circuit was fabricated.

The device selected for detecting mechanical vibration is a Bruel and Kjaer (B & K) model 4333 accelerometer, chosen for the following reasons:

o   The sensitivity of 16 mV/g is considered to be adequate.

o   The frequency response is flat within ± 1db, to 15 KHz with the resonance frequency being 60 KHz. It is foreseen here that signature changes due to performance degradation can only be interpreted if they are related to the signature of satisfactory performance. Therefore, the frequency range to 60 KC could be used to establish the reference performance signature and deviations from this would be related to performance degradation. A flat response characteristic of the accelerometer is not necessary because only changes from the normal amplitude of the frequency signature will be related to performance degradation of a Fluidic circuit.

o   The small size of this accelerometer will permit mounting onto Fluidic elements or circuits.

Summary of Technical Data:

        Supplier: B & K Instruments, Inc.
        Model: 4333
        Size: 1.4 cm hex. x 1.6 cm
        Mounting Means: 10-32 NF Stud, probe, magnetic base
        Voltage Sensitivity: 16 mV/g
        Acceleration Range: 0.01 to 2,000g
        Frequency Range: 2 to 14,000 Hz, ± 1 db
        Natural Frequency: 60 KHz
        Acoustic Sensitivity: Less than $0.2 \mu V/\mu bar$

g.   Microphone

In the preceding section, the mechanical vibration of the circuit structure resulting from acoustic disturbances in the passageways was to be detected by an accelerometer. These acoustic disturbances may also be detected by a microphone, as the sound is radiated to the ambient air through the vents in Fluidic circuits.

18

Much of the acoustic signature of Fluidic elements is generated in the inter-
action region where the power jet is acted upon by the control jets. The
power jet also impinges on the receiver section in this region. In many
amplifier configurations, the interaction region vents through large holes
into the surroundings, where a small microphone may be conveniently located.

The "Massa" sound detection system chosen for evaluation consists of two
microphones (models M-213 and M-215) with a preamplifier (model M-114B)
and a 60 db amplifier (model M-185). This system was selected on the basis
of the following.

o   The size of the microphone permits a variety of mounting techniques
     which would be applicable to Fluidic circuit packaging techniques.

o   The high sensitivity of the microphones, model M-215 - 12.5 μV/μbar
     and model M-213 - 8 μV/μbar, permits good resolution in detecting
     amplitude changes which can be related to circuit performance
     degradation.

o   A large frequency spectrum of 20 cps to 70 K cps for the M-215 and
     20 cps to 90 K cps for the M-213 is available for locating changes
     occurring from performance degradations.

o   Rise times of 3-1/2 μsec and 2-1/2 μsec for the M-215 and M-213
     respectively, allows measurement of extremely fast transients.

o   Having a microphone mounted external to the Fluidic circuit will not
     interfere with the circuit's functional performance and if failure of
     the microphone should occur, no anomalies would be induced into the
     functioning Fluidic circuit.

Summary of Technical Data:

        Supplier: Massa Div. of Cohu Electronics, Inc.
        Model: M-213 and M-215 microphones, M-114B preamplifier,
                 M-185 amplifier and power supply
        M-213 Microphone
                Sensitivity: 8μ V/μbar
                Frequency Response: 20 cps to 90 K cps
                Rise Time: 2-1/2 μsec
                Dimensions: 0.236 in. dia. x 0.5 in.
        M-215 Microphone
                Sensitivity: 12.5 μV/μbar
                Frequency Response: 20 cps to 70 K cps
                Rise Time: 3-1/2 μsec
                Dimensions: 0.344 in. dia. x 0.75 in.

19

M-114B Preamplifier

    <u>Gain:</u> ap:)x. 1

    <u>Noise:</u> a)x. $10\,\mu V$

M-185 Amplifier (Power Supply

    <u>Gain:</u> 60 d.

    <u>Calibrated A. enuator:</u> 70 db range

SECTION IV

DEFINITION OF ELEMENT FAILURE

In order to define element failure, it is necessary to define the parameters of primary performance and then establish allowable limits for deviations of these performance parameters. It is these deviations which the primary sensors must be capable of detecting. It is also the magnitudes of anomalies leading to these deviations that secondary sensors must detect.

Allowable deviations in primary performance for analog and digital elements are defined in the following along with modes of failure which cause malfunction.

1. FAILURE OF ANALOG ELEMENT

There are two types of deviations of performance from the desired nominal. One is the fabrication tolerance band and the second is deviation in performance for a specific circuit which has been adjusted to provide the desired functional performance. It is not the first, but the second type of deviation, which is degradation of performance, that is of immediate concern.

Figure 1 shows a photograph of a typical analog amplifier element. A continuous supply pressure is directed into the power nozzle reservoir which is located on the center line of the element to the left of the photograph. A power jet issues from the nozzle exit into the interaction region downstream of the exit. This power stream impinges on a three channeled receiver section. The center channel is vented. The two outer channels are signal output channels. The two nozzles on either side of the power nozzle are control jets. A change in a control, or input, signal causes a deflection of the power jet, and consequently an increase in the output pressure in the output channel on the opposite side of the amplifier, with a decrease at the near sided output. The change in output pressure is greater than the change in input pressure and hence the element exhibits pressure gain. The output may be taken either from a single output channel or as the ΔP across the two outputs in a push-pull manner, depending on the application of the amplifier.

Figure 2 shows the nominal performance characteristic of a typical analog element when loaded into an amplifier of the same size. Performance may be defined in terms of:

- o Pressure gain
- o Pressure recovery at saturation
- o Operating range
- o Null output (output signal when control signals are equal)
- o Signal to noise.

21
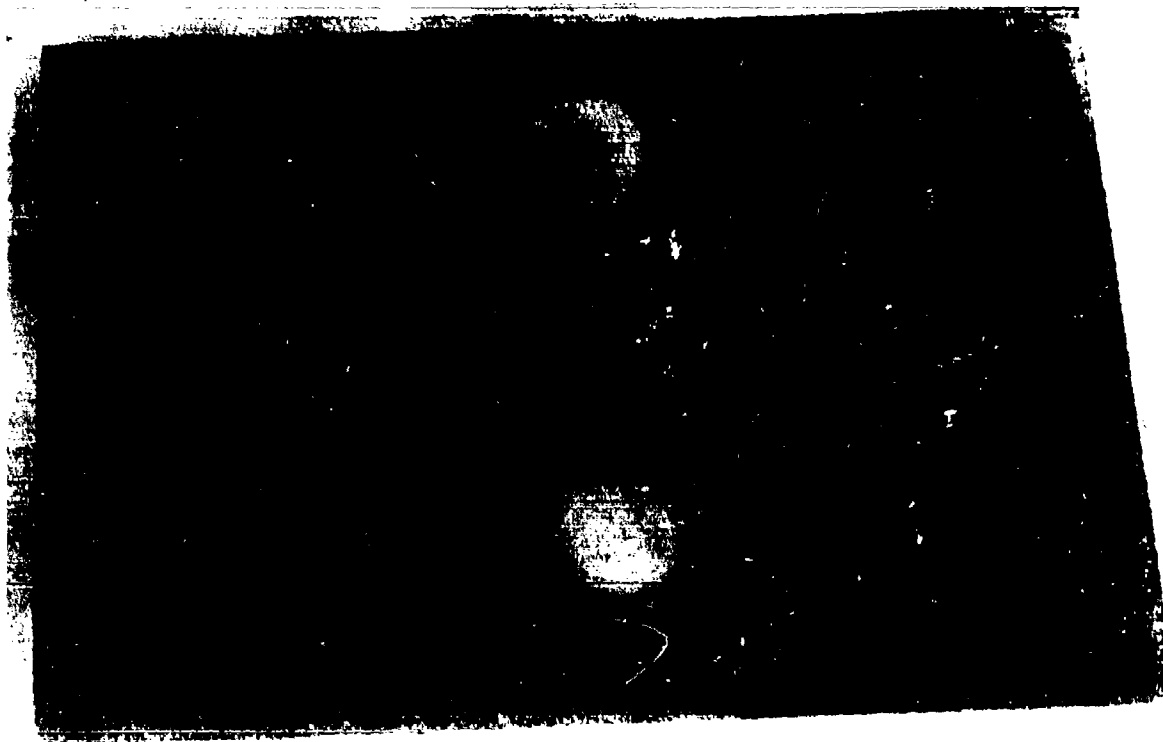
Figure 1. Typical Analog Amplifier Element

P_{O1}
PSIG

P_O (MAX)
45% P_S

LINEAR
RANGE
20% P_S

PRESSURE
GAIN 2.5

5% $P_S \leq P_{C1} \leq 30\% P_S$

P_{C2} - PSIG

SINGLE SIDE OPERATION

LINEAR
RANGE
±35% P_S

PRESSURE
GAIN 3.5

ΔP_{IN} - PSIG

DOUBLE SIDE OPERATION

P_{C1}
P_{O1}
P_S
P_{C2}
P_{O2}
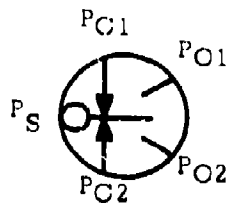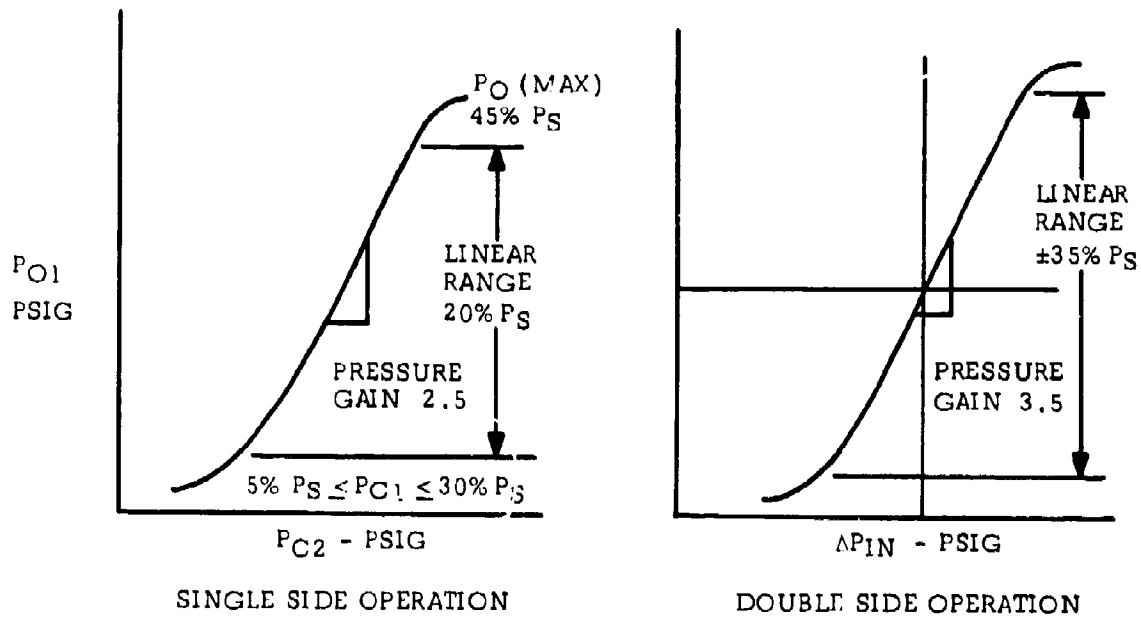
SYMBOL FOR BEAM DEFLECTION
ANALOG AMPLIFIER
(SAE)

P_S	=	SUPPLY PRESSURE
P_{C1}	=	CONTROL PRESSURE
P_{C2}	=	CONTROL PRESSURE
P_{O1}	=	OUTLET PRESSURE
P_{O2}	=	OUTLET PRESSURE
ΔP_{IN}	=	$P_{C2} - P_{C1}$
ΔP_{OUT}	=	$P_{O1} - P_{O2}$

Figure 2. Typical Analog Amplifier
Characteristics

23

BEC Technical Memorandum, TM-116, (Appendix I) presents typical allowable fabrication performance limits and allowable degradation of performance limits in terms of the above parameters. The allowable performance degradations given by TM-116 was used as a standard in the evaluation of sensors applied to analog elements.

Table I lists for an analog element the modes of failure, or anomalies, which may cause a degradation in each of the above defined performance parameters. As can be seen, degradation can be caused by a relatively large number of failure modes and, conversely, many of the failure modes can cause a degradation in a number of performance parameters.

TABLE I. PERFORMANCE DEGRADATION AND CAUSITIVE MODES OF FAILURE

PERFORMANCE DEGRADATION	CAUSITIVE FAILURE MODES
1. Change in Pressure Gain	Deformation of Control Nozzle Deformation of Power Nozzle Deformation of Receiver Change in Load Leakage
2. Change in Pressure Recovery	Change in Supply Pressure Deformation of Power Nozzle Deformation of Receiver Change in Load Leakage
3. Change in Operating Range	Change in Supply Pressure Deformation of Power Nozzle Deformation of Receiver Change in Load Leakage
4. Change in Output Null	Change in Supply Pressure Change in Bias Signal Deformation of Control Nozzle Deformation of Power Nozzle Deformation of Receiver Change in Load Leakage
5. Change in Signal to Noise Ratio	Deformation of Receiver Deformation of Power Nozzle Deformation of Control Nozzle Excessive Control Signals

24

The modes of failure given by Table I. include two types of anomalies; pressure anomalies and physical anomalies. Changes in supply pressure and bias pressures fall within the former category. They are not directly related to the physical structure of an element. Physical anomalies are those which relate directly to the physical structure. They are either caused by a failure of the structure (as a crack, loss of a seal, or chipping or wearing away of parent material) or by the entry and lodging of foreign material within an element (as contamination). Deformation of nozzles or receivers may be caused by either structural failure or the lodging of foreign material.

2. FAILURE OF DIGITAL ELEMENTS

The desired performance characteristics and allowable degradation of performance of digital elements is much more difficult to define than for an analog element. A detailed and thorough discussion of the subject is presented by BEC Technical Memorandum, TM-106, given in Appendix I.

As indicated by the memorandum, the performance of digital elements may, to a partial extent, be defined in terms of steady-state switching pressure and hysteresis along with input and output pressures vs. flow characteristics, which are readily determinable. However, the satisfactory functioning of digital elements is strongly a function of dynamic or transient parameters, such as waveform, switching times, pulse duration, and time relationships between signals, which are more difficult to define and to detect.

The memorandum defines steady-state and transient performance parameters, describes allowable performance deviations, and defines anomalies causitive of circuitry malfunctions. The information presented was used as a basis for evaluation of digital element sensors.

25

SECTION V

EVALUATION OF SENSORS

This section presents the results and conclusions of an evaluation of the candidate sensors. The capability of primary signal sensors to detect performance degradation, as defined by Section IV, was evaluated. The secondary sensors were evaluated with respect to their capability to 1) detect the levels of anomalies leading to the allowable limit of performance degradation, and 2) to define the cause of performance degradation. The degree of performance degradation as related to the magnitude of causitive anomalies was investigated. Also considered was compatibility of the sensors with typical circuit packaging concepts and the effects of environmental conditions on the candidate sensors.

1. PRELIMINARY ACOUSTIC STUDIES

A phenomenon inherent to the operation of Fluidic elements is the radiation of acoustic energy. This acoustic energy offers a highly desirable means of detecting a Fluidic circuit's performance degradation and the potential to determine the cause of the malfunction. To a person with much experience with Fluidic circuitry, the audible noise a circuit generates during operation provides information concerning it's functional state. This observation inspired BEC, prior to the present program, to do some initial research into the potentials of acoustic radiation as a performance indicator. It was shown that the introduction of a number of anomalies did produce detectable changes in the frequency spectrum detected by a microphone, with a potential of relating characteristics of signature changes to the introduced anomaly. It was concluded that further exploitation of this technique was highly desirable.

Within the present program, preliminary studies were carried out to learn more about the nature and sources of acoustic noises. Experiments were conducted with an accelerometer and microphone to select the sensor possessing the greatest potential. Instrumentation techniques were developed to sense and display these acoustic noises in a usable manner.

a. Acoustic Source Study

In order to achieve a better understanding of the sources of acoustic radiation in a Fluidic element, preliminary tests were conducted on a model 1786 analog amplifier, of a configuration as shown by Figure 1. Detection of the acoustic radiation was accomplished by an accelerometer attached to the circuit and by a microphone at the side vents. Sources of prominent acoustic frequencies were detected and are defined in Figure 3, so as to define the relationship to the element's structure and pressure performance characteristics.

27
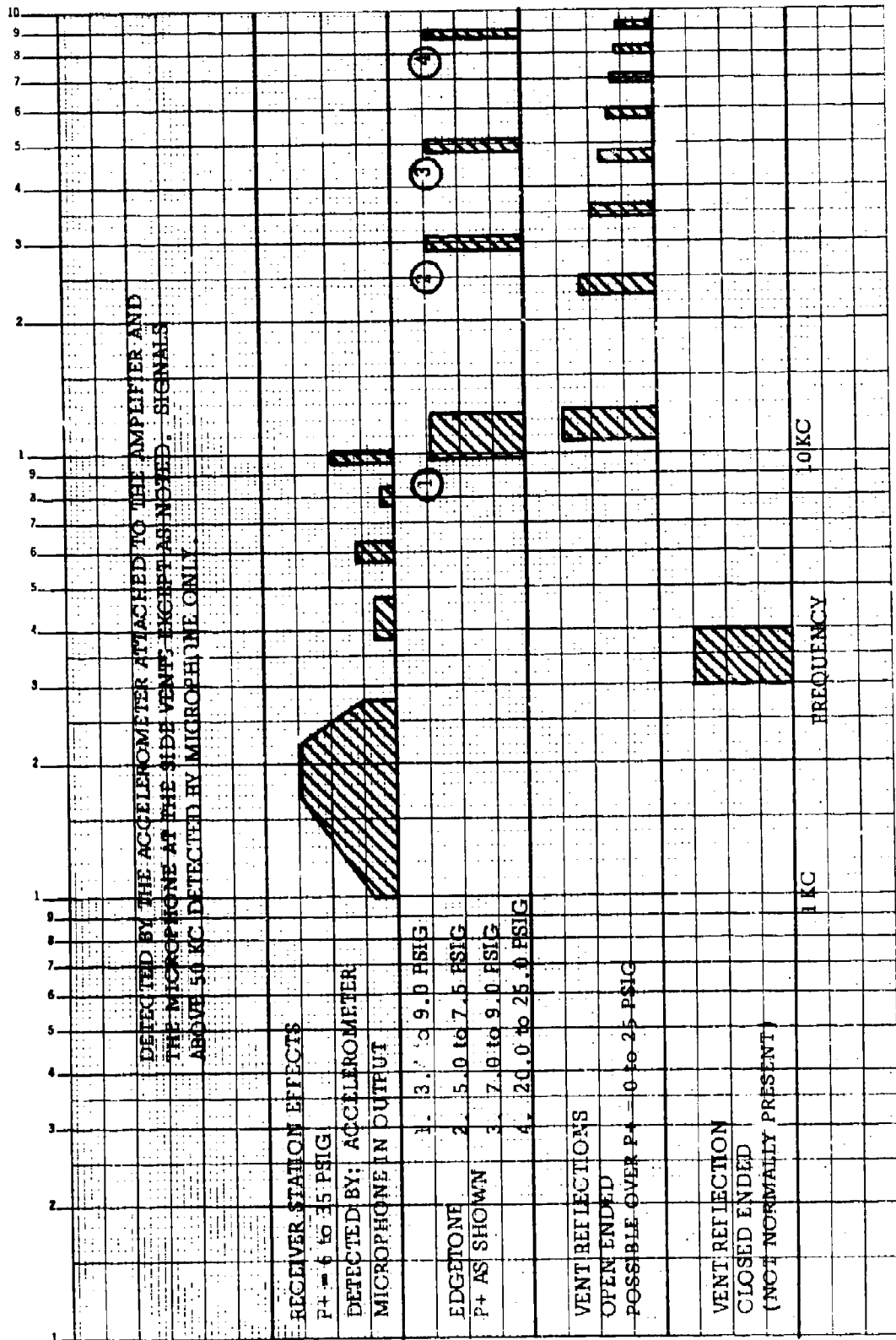
Figure 3. Secondary Acoustic Characteristics of Model 1786 Analog Amplifier

DETECTED BY THE ACCELEROMETER ATTACHED TO THE AMPLIFIER AND
THE MICROPHONE AT THE SIDE VENTS EXCEPT AS NOTED. SIGNALS
ABOVE 50 KC DETECTED BY MICROPHONE ONLY.

RECEIVER STATION EFFECTS
P+ = 6 to 35 PSIG

DETECTED BY: ACCELEROMETER
MICROPHONE IN OUTPUT

1. 3.0 to 9.0 PSIG
2. 5.0 to 7.5 PSIG
3. 7.0 to 9.0 PSIG
4. 20.0 to 25.0 PSIG

EDGETONE
P+ AS SHOWN

VENT REFLECTIONS
OPEN ENDED
POSSIBLE OVER P+ 0 to 25 PSIG

VENT REFLECTION
CLOSED ENDED
(NOT NORMALLY PRESENT)

FREQUENCY

1 KC   10 KC

The primary intent of Figure 3 is to relate the generated frequencies detected to their generating source and give a general idea of the relative amplitudes generated by that source, but there is no relationship displayed between the amplitudes of the frequencies detected due to the various sources.

A group of frequencies between 1 KC and 10 KC were related to the receiver section of the amplifier. These frequencies were caused by acoustic reflections from the downstream end of the output channels and from discontinuities in the lines connecting the outputs to the loads; these reflections acting on the power jet induced periodic oscillations.

A phenomenon occurring when a free jet impinges on an edge is the generating of acoustic signals known as an edgetone. Early work in this area was conducted by Brown[1][2] and subsequently by Powell [3]. Experimental testing on the 1786 analog amplifier has shown the detection of frequencies with the characteristics of edgetones. As is typical of edgetones, a number of eigen frequency stages were observed, as is shown in Figure 3, with the eigen frequency stages and the frequencies within each range being a function of the power jet velocity (or P_S).

Periodic oscillations caused by reflection of acoustic signals from the innermost edge of the side interaction region vent back to the power jet were observed. These frequencies are shown in Figure 3 as "vent reflections – open ended." The periodic nature of these reflections are similar to that of an open ended organ pipe (pressure node termination) of length nominally equal to the dimension from the power nozzle exit to the inside edge of either of the side vents. This dimension represents 1/2 wave length for the fundamental nominal frequency of 12 KC. Eight (8) harmonics of the fundamental were observed. Note that the lower eigen frequency edgetone of nominally 12 KC corresponds closely to the fundamental frequency related to that of the open ended vent reflection. When operating with a supply pressure that induces the lower frequency edgetone, a high intensity 12 KC oscillation occurs, due to reinforcement of the jet edgetone oscillation by the vent reflections.

Figure 4 shows a photograph of frequencies due to open ended vent reflection as they appear on the Panoramic Ultrasonic Analyzer after being detected by the Massa microphone system. The pressure settings of the element and the sweep width scale settings are shown in the figure. The first spike shown to the left is the zero frequency spike associated with the internal noise of the sensing and recording equipment, more commonly referred to as the 60 cps noise spike. The second spike from the left is the fundamental of 12 KC. It is of such amplitude that it exceeded the calibration grids of the recording screen. The other spikes to the right are the harmonics at approximately 24 KC, 36 KC, 48 KC, 60 KC, 72 KC, 84 KC, and 96 KC.

29
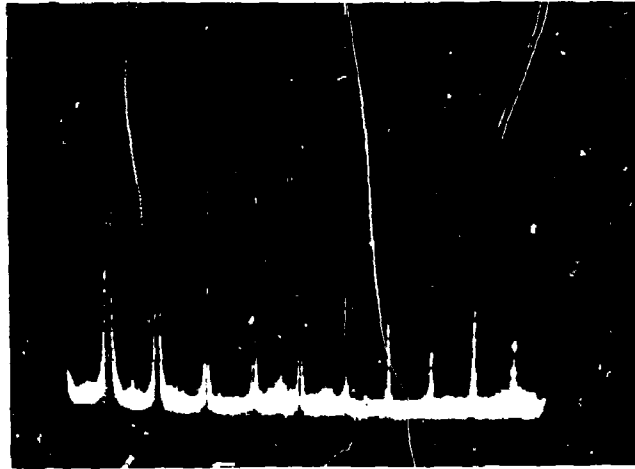
$$P_S \quad = \; 19.6 \; psig$$

$$P_{B1} \quad = \; 0$$

$$P_{C1} \quad = \; 0$$

SENSOR: Microphone
Center Frequency - 50 KC
Bandwidth   - 100 KC
Calibration   -   10 KC/Div.

Figure 4.   Pressure Node Vent Reflection Frequencies

It was observed that a large amplification of the open-ended vent reflections was achieved by locating a solid body external to the vent at pressure antinode locations for the fundamental frequency This indicates the desirability of locating any reflective object, as a metal circuit cover or an instrumentation item, at other than 1/4, 3/4, or 5/4 wave lengths from the region where the interaction region intersects with the inner edge of the vent. An amplitude of oscillation of the power jet may otherwise be affected which is large enough to cause a degradation of the element's primary performance.

A periodic oscillation related to reflection from the outer edge of the vent side chamber was induced by closing the vent exhaust holes. These periodic characteristics were similar to a closed organ pipe (pressure antinode termination) of length equal to distance from the power nozzle to the outside edge

30

of the vent chamber. This produced characteristic frequencies between 3 KC and 4 KC which are shown in Figure 3 as "vent reflections closed ended." These frequencies are not normally detected during normal element functional performance where the vents are opening.

Consideration of the results of this test show for this amplifier, where prominent frequency components of the acoustic signature occur and the source, and in addition indicates some anomalous conditions which should be detectable by this means. The lodging of a particle in a receiver channel or an obstruction in the element output line should be detectable, by introducing a new acoustic reflection surface. Deformation of a receiver tip should cause a change or destruction of an existing edgetone frequency component. A change in supply pressure will cause a change in edgetone frequency within a given eigen-frequency stage or cause a shift to a new eigen-frequency stage, both of which should be detectable.

b. Acoustic Instrumentation Optimization Study

A laboratory study aimed at optimization of acoustic sensing instrumentation was carried out. Two specific objectives were to maximize sensitivity to small changes in state of elements and to achieve satisfactory repeatability. Tests were carried out with an analog and a digital element, and instrumentation settings which led to a desirable display of information were established. The use of both a microphone and an accelerometer as the sensing device was investigated.

The first series of tests conducted were on a model 3126 analog amplifier. The acoustic sensing device selected for these tests was the Massa microphone system. A test jig was fabricated so that the microphone position with respect to the element under test would be kept constant. When locating an acoustic sensor in the near field of a source, it is imperative that the position of all bodies in the area be unchanging. This is a prerequisite to realizing repeatability of the acoustic signal sensed by the microphone.

Figure 5 shows the block diagram of the instrumentation used. The signal detected by the microphone was coupled through the preamplifier to the amplifier. The amplifier attenuator settings were at 0 db. The output of the Massa amplifier was monitored by a Panoramic SB-15a ultrasonic analyzer.

The Panoramic analyzer embodies a narrow band pass filter, the tuned frequency of which is varied continuously with time. The sweep of the filter tuned frequency is coupled to the horizontal axis of a cathode ray tube, with horizontal position calibrated in terms of the filter tuned frequency. The output of the filter is coupled to the vertical axis of the cathode ray tube. In operation, the display tube presents a trace of the amplitude of the frequency components of the inputted acoustic signal.

31
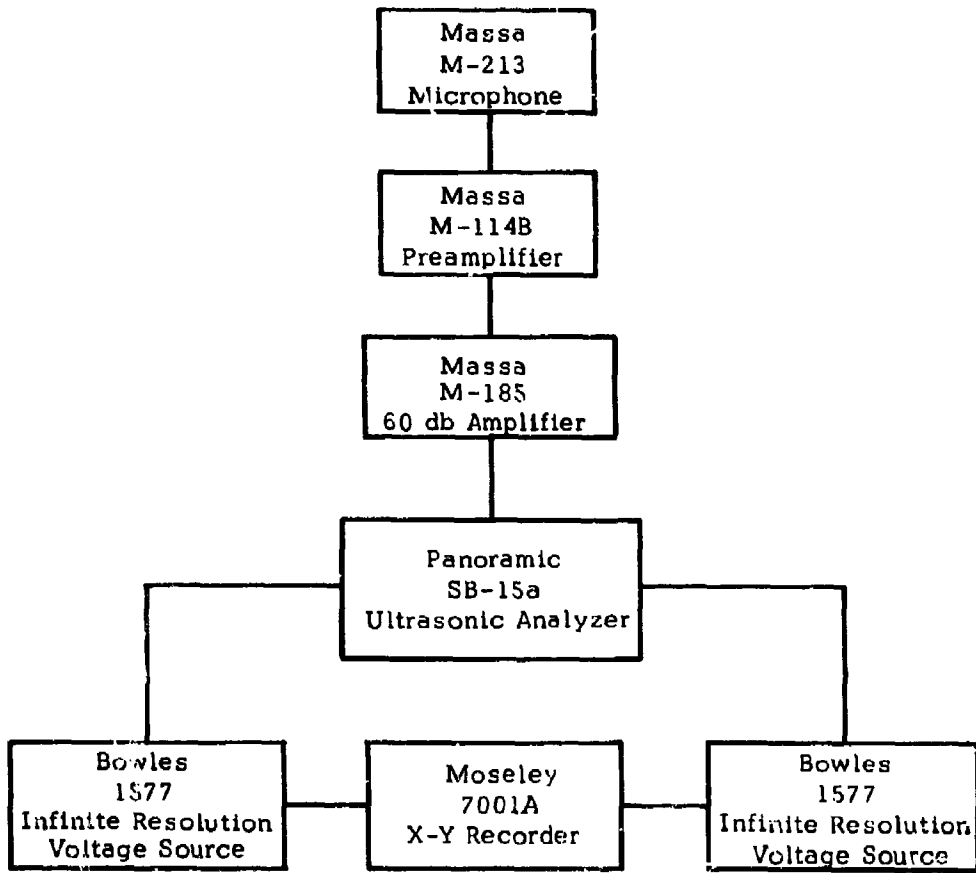
Figure 5.   Instrumentation Block Diagram For Analog
             Amplifier Acoustic Signature Test

32

While some components of the accoustic signature of an element are of a defineable periodic nature, as edgetones and vent reflections, much of the signature is in the nature of noise. The randomness associated with the noise is reflected as differences between two acoustic signature traces generated by the Panoramic analyzer.

The requirements of optimized sensitivity and optimized repeatability must be traded off to achieve a satisfactory compromise. The analyzer offers a number of variables through which this compromise may be effected. The range of frequencies analyzed may be varied. Increasing the frequency range reduces the resolution, thus improving repeatability and decreasing sensitivity. The effects are reversed by decreasing the range considered. Varying degrees of filtering may be applied to the output of the analyzer narrow band pass filter prior to display; thus simultaneously improving repeatability and decreasing sensitivity or in the reverse manner.

For the analog amplifier tests, positive results were realized with the following settings of the Panoramic ultrasonic analyzer controls:

o	Center frequency	–	75 KC
o	Sweep width	–	150 KC
o	I F Bandwidth	–	Auto
o	Amplitude scale	–	Linear
o	Sweep rate	–	Min
o	Video Filter	–	Full ON (clockwise)
o	Input Atten Cont	–	4 db
o	Input Atten Step	–	0 db
o	I F Atten	–	20 db
o	Marker	–	OFF

The horizontal and vertical output of the ultrasonic analyzer were recorded on an X-Y recorder which was coupled through Infinite Resolution DC Voltage Sources. The purpose of these are to null out the high DC component present on the horizontal and vertical output of the ultrasonic analyzer. The front panel settings of the X-Y Recorder were as follows:

o	X Range	–	0.1 V/inch
o	X Variable	–	2-1/2 inch equal 100 KC
o	Y Range	–	0.1 V/inc'
o	Y Variable	–	Cal position

33

Initial testing of the set-up described above resulted in the sweep rate of the ultrasonic analyzer (which is driving the horizontal axis of the X-Y recorder) being too fast for the response of the recorder vertical axis, and therefore, caused a filtering effect (overdamped condition of the vertical axis). A minor modification to the sweep rate circuit of the analyzer reduced the sweep rage from 1 second to 20 second full scale.

Figure 6 shows typical results from these tests. Changes in supply pressure (P_S) were induced. Changes in the relative amplitude of the acoustic signature were recorded over a frequency range of 0 to 150 KC. The figure shows that a large amplitude change occurred in the signature with a 50% change in supply pressure, and that the sensitivity was sufficient to readily distinguish a 10% change.

Although the test results above were encouraging, the need for further work was indicated, to improve the detecting and monitoring techniques in order to improve the resolution to a state where it would detect performance degradation within the allowable deviation limits set in section IV-1.

A second test series was carried out to accomplish two objectives. First, to improve the instrumentation technique used for the prior test, and second, to investigate these techniques as applied to a digital element. The element selected to be tested was a digital flip-flop, model 4709. A description of a 4-input flip-flop and its steady-state characteristics can be found in TM-106 (Appendix I). The sensor selected to be evaluated is the B & K model 4333 accelerometer. The accelerometer was mounted directly to the element over the interaction region.

Figure 7 shows the instrumentation block diagram for this test. A Tektronix AC preamplifier with a fixed signal gain of 10 was used to amplify the output of the accelerometer. The signal was then monitored by a Panoramic model LP-1a sonic analyzer with its auxiliary function unit. Instrumentation settings which yielded desirable results are given in the following. The front panel controls of the frequency analyzer system were set as below:

o   Scale Selector   –   2.5 mv

o   Input Mult   –   X 1

o   Input Pot   –   5

o   Center Frequency   –   10 KC

o   Sweep Range   –   5,000 Lin

o   Vertical Calib. Selector   –   Lin

o   Aux Functions   –   10 sec sweep

34
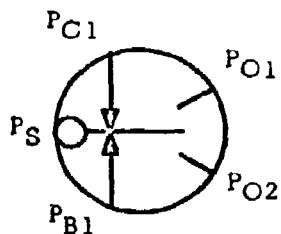
Steady State Conditions:

P_{C1} = 1 psig

P_{B1} = 1 psig

P_S = 10 psig (———)

P_S = 11 psig (....)

P_S = 15 psig (---)

ELEMENT: Analog Amplifier
Model 3126

SENSOR: Massa Microphone
Model M-213
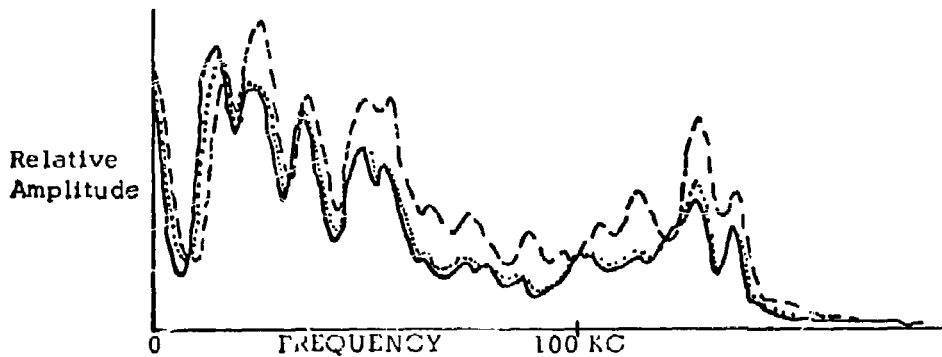
Figure 6.   Acoustic Signature Instrumentation Test #1
Supply Pressure (P_S) Changes
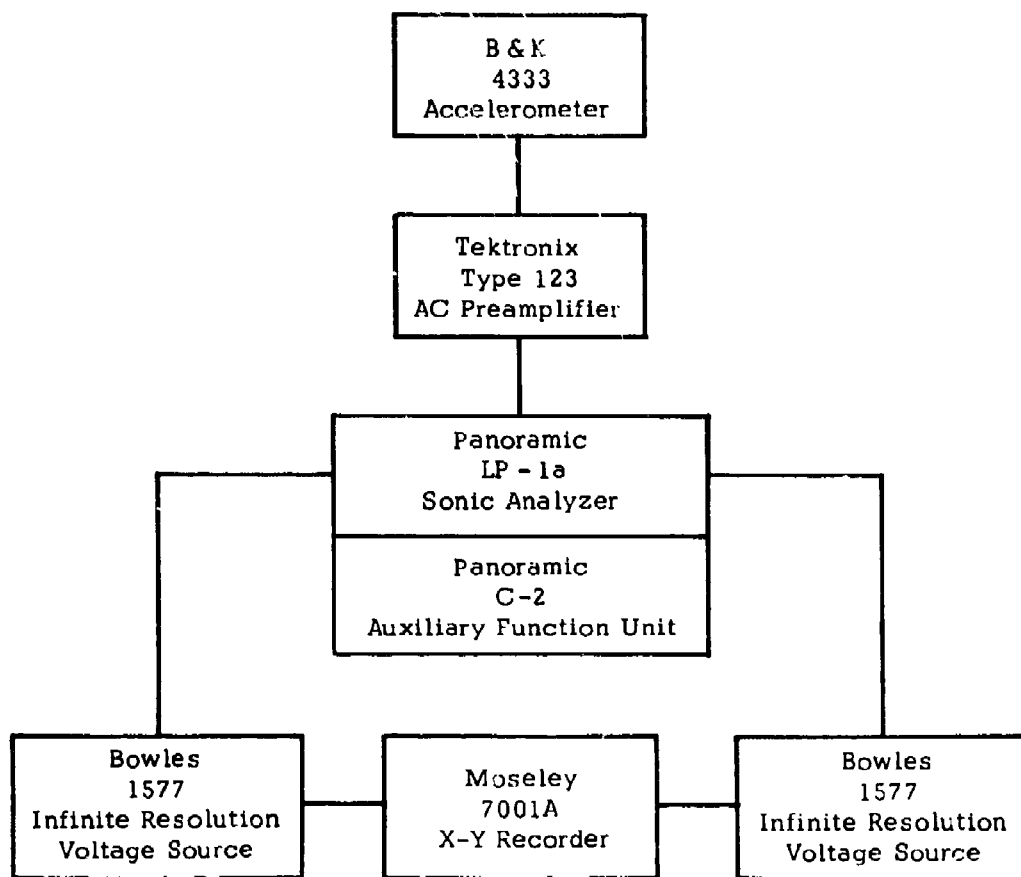
Figure 7. Instrumentation Block Diagram for Digital Flip-Flop
Acoustic Signature Test

o   Spectra Sensitivity   -   Line
    Compensation

o   I F Bandwidth (cps)   -   200

o   Sweep Width Factor   -   1

o   Smoothing Filter   -   4

The horizontal and vertical output from the sonic analyzer were recorded by the
X-Y recorder. The Infinite Resolution DC Voltage Sources preceding the recorder
null out the high DC component of the analyzer outputs. The front panel control
settings of the Moseley X-Y Recorder were as follows:

o   X Range   -   0.2 V/inch

o   X Variable -   5 inches = 2 KC

o   Y Range   -   20 mv/inch

o   Y Variable -   Cal position

The earlier described analog amplifier test results suggested that there are
particular frequency bandwidths more sensitive to element performance changes
than other sections of the signature. Before actually selecting the sonic
analyzer for this test, preliminary tests were conducted using the ultrasonic
analyzer. Various bandwidths over the frequency range of 0 to 150 KC were
investigated to select the one showing the best potential (the greatest change
in signature for an induced anomaly) of detecting performance degradation. The
area presenting the best sensitivity for the digital flip-flop test was in the band-
width between 7 KC and 12 KC. Since the sonic analyzer was capable of
monitoring this frequency range, has the capability of selecting sweep speed
of 1 or 10 seconds full scale, and the capability of selecting five degrees of
smoothing filters, it was used for this test.

Figures 8 and 9 show typical results of the digital flip-flop secondary acoustic
test. Figure 8 shows the changes that occurred in the signature due to a change
in the control signal, P_{C1}, from 0 psig to 0.1 psig. No change of switched
state (changing output from leg P_{O2} to P_{O1}) occurred. The change in signature
is due to an increase of control pressure from 0 to 0.1 psig. The large change
in signature for this small pressure change indicates a high sensitivity to small
changes in the performance state of the element.

Figure 9 shows the change occurring in the acoustic signature due to a change
of switched state. The output was switched from leg P_{O2} to leg P_{O1}. For both
signatures, control pressures were zero. The data shows that the acoustic
signature can determine the switched state of a digital element.

Comparison of Figure 8 and Figure 9 show that the changes occurring in the

37

Figure 8. Acoustic Signature Instrumentation Test #2 Control Pressure (P_{C2}) Changes

Figure 9. Acoustic Signature Instrumentation Test #2
Output State Changes

ELEMENT: Flip Flop
Model 4709

SENSOR: B & K Accelerometer
Model 4333

Steady State Conditions:

Output – P_{O2} (——)
Output – P_{O1} (– – –)

P_S = 1 psig
P_{C1} = 0
P_{C2} = 0

Relative Amplitude

9 KC   10 KC   11 KC

FREQUENCY

39

signature from the nominal condition ($P_S = 1$, $P_{C1} = P_{C2} = 0$, output leg P_{O2}) for the two conditions induced are distinctive from each other in the pattern they produce, i.e., the amplitude changes over the bandwidth investigated are different. It is this condition which makes it possible to determine the type of changes occurring in an element or the type of anomaly induced.

Summary:

These tests established an instrumentation arrangement that yielded satisfactory results in terms of sensitivity and repeatability for a number of specific elements In addition, the considerations discussed provide some insight into possible modifications to instrument different elements. The tests showed that sufficient resolution and repeatability may be realized to detect, by acoustic means, small changes in the operating condition of elements and that the anomaly causing the changes may be defined by typifying characteristics of the acoustic signature changes.

2.   THERMISTOR EVALUATION

The intent of this section is to evaluate thermistors as a detector of secondary indications of performance. This technique is based on the fact that fluid expansion produces temperature gradients and that these changes in temperature will be transferred, to some degree, to the structures of Fluidic control devices. The temperature changes that occur in Fluidic circuitry are related to pressure changes, i.e., the pressure drop across the supply pressure and control pressure nozzles. By mounting thermistors in the structure of the Fluidic circuits it is expected that temperature differences will be monitored to establish satisfactory performance and that deviations in these differences will be related to performance degradation and the anomaly causing it.

Thermistors were calibrated as part of a basic bridge circuit. They were then mounted into the flow channels and the structure of a Fluidic element, close to the channel wall, beneath the exit nozzle of the supply pressure channel. Supply pressure was varied and resultant temperature changes recorded. A theoretical evaluation of this technique to establish its potential was conducted. The results of this effort are presented in the following.

a.   Thermistor Calibration

Two thermistors, model GB32J2, manufactured by Fenwal Electronics, were calibrated against an Atkins temperature system, model 3F01A. These thermistors will be referred to as thermistors T_1 and T_2.

The temperature source for this calibration procedure was an oil bath surrounded by water. Temperature changes were produced by adding ice or boiling water to the water surrounding the oil bath. The oil bath was used for electrical

isolation and to provide a constant reference temperature.

Figure 10 shows the bridge circuit used to calibrate thermistors T_1 and T_2.

$$R_1 = 14.5\ K\Omega$$
$$R_2 = 14.5\ K\Omega$$
$$R_3 = 2.2\ K\Omega$$
$$V = 1.35\ V$$
$$T = 2\ K\Omega \pm 20\%$$
$$@\ 25^\circ\ C$$
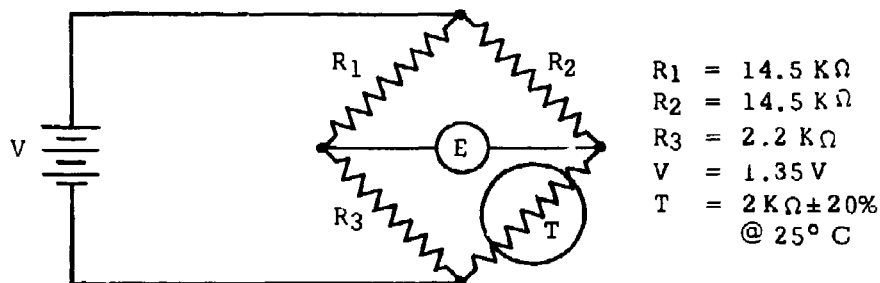
Figure 10. Thermistor Bridge Circuit

The output E was recorded in millivolts. The bridge circuit was designed in such a manner that the power delivered to the thermistor would not raise its temperature more than $1^\circ C$ above its surroundings.

The results of these calibration tests are stabilized and plotted in Figure 11. E_1 is the output of the first bridge containing T_1 and E_2 is the output of the second bridge containing T_2. A spot check was made in air in order to show that little or no current was being conducted through the oil. These points are shown on the graph.

b.   Test Results of Thermistor Evaluation

Thermistors T_1 and T_2, calibrated above, were used to detect temperature changes related to pressure changes. Tests were conducted on a 1786 analog amplifier.

Thermistor T_2 was mounted under the supply pressure (P_S) nozzle in the structural material, close to the channel wall. To accomplish this, a hole of the diameter of the thermistor was drilled from the back of the element to within approximately .003 of the bottom surface of the supply pressure nozzle. The thermistor was then inserted into the hole and potted with epoxy.

T_1 was mounted into the large input tube, where flow was considered to approach stagnation, to monitor the stagnation (or total) temperature. The same bridge circuits used to calibrate the thermistors, shown in Figure 10, were used during this test.

41

T_1, T_2 °F	$E_1 -$ O mV	$E_2 -$ △ mV
33.8	-152	-138
34.0	-149	-143
35.5	-142	-125
39.5	-124	-102
43.4	-100	- 80
47.0	- 91	- 64.5
50.0	- 63	- 49.5
56.8	- 34	- 21.7
59.8	- 22.7	- 10.5
65.6	- 1.4	+ 10.4
71.4	+ 1.6	+ 22.2
96.0	+ 70.0	+ 87.0
118	+109	+115
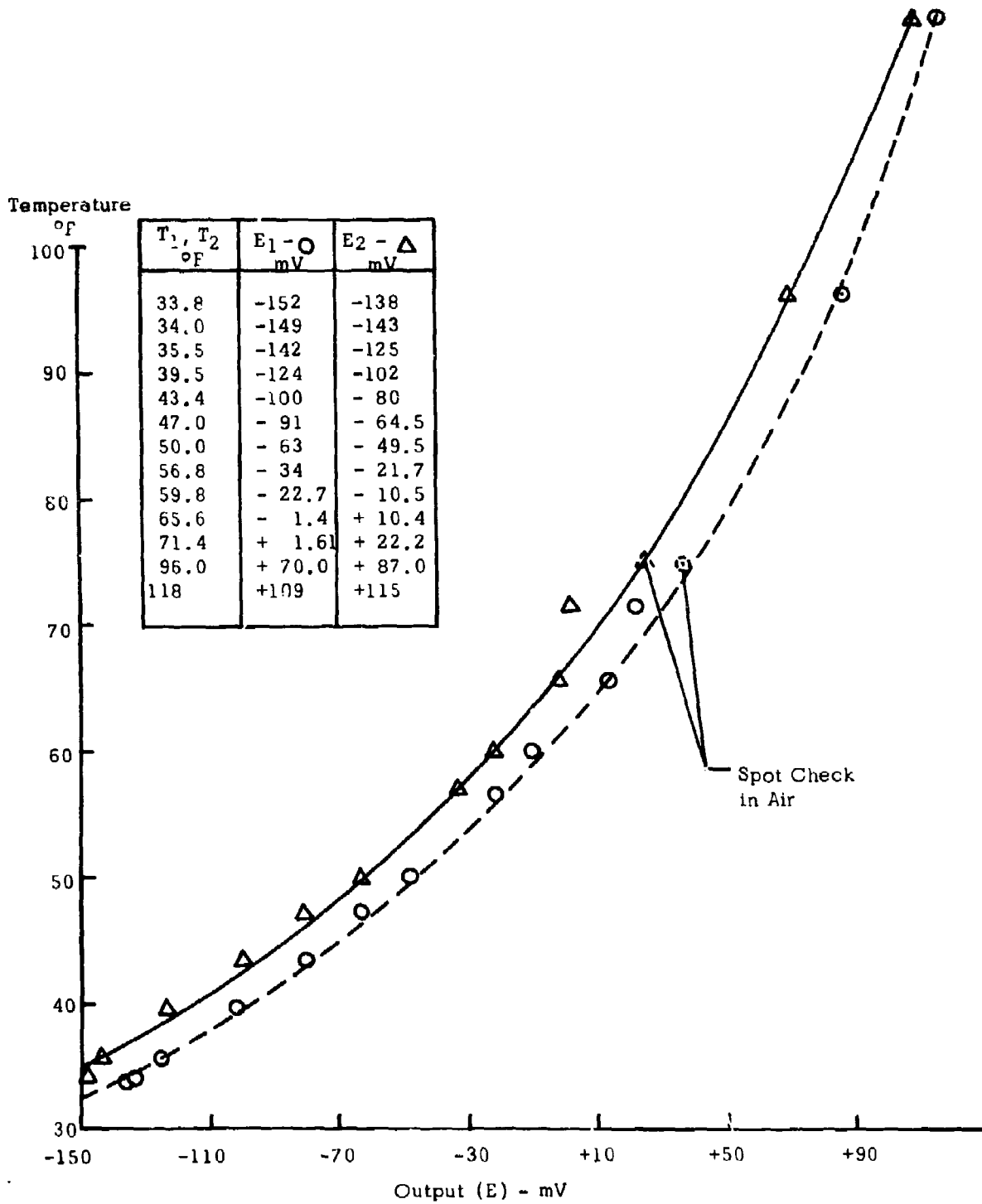
Figure 11. Calibration Curves for Thermistors T_1 and T_2

42

A range of supply pressures were applied. For each new supply pressure value a settling time of 1/2 hour was allowed, then the data for the two thermistors was recorded. A measure of total temperature and temperature at the nozzle exit was thus accomplished for a range of nozzle pressure differentials.

Figure 12 shows a plot of the results of this test, including the tabulated data. The data was taken on a Tektronix oscilloscope, model 502, in millivolts and then transposed to °F with use of the thermistor calibration curves. The incoming air temperature (T_1) remained relatively constant. The plot of T_2 versus P_S shows the decrease in T_2 with increasing P_S.

The results of the described experimental work were inputted into an analytical evaluation of the applicability of thermistors, the results of which are presented in the following discussion.

c.   Theoretical Evaluation.

A theoretical analysis was conducted on using thermistors as detectors of the thermal characteristics of Fluidic circuits. The results of this study are reported in TM-132 given in Appendix II of this report.

The report covers a theoretical evaluation of the expansion of gases through a nozzle under ideal conditions of perfect gas, air with K = 1.4, and isentropic flow. Evaluated under these conditions are the changes in gas temperature at the nozzle throat due to:

o   Stagnation temperature changes

o   Changes in supply pressure

o   Physical dimension changes

o   Changes in ambient temperature.

While small perturbations, as in supply pressure, generate appreciable changes in the static temperature of the gas at the nozzle throat, the static temperature cannot be directly sensed. The temperature sensed by a thermistor located within the element structure, close to the channel wall of a nozzle, is approximately the adiabatic wall temperature. Adiabatic wall temperature, T_{aw}, is given by Geidt [4] as

$$T_{aw} = T_\infty + R (T_{1s} - T_\infty)$$

where:

T_∞ = static temperature in free stream

T_{1s} = total temperature

R = Recovery factor

43

P_S psig	E_1 mV	T_1 °F	E_2 mV	T_2 °F
0	22.7	74.3	40.5	75
5	22.6	74.3	36.0	73.5
10	22.6	74.3	31.5	71.5
15	22.6	74.3	29.2	70.5
20	22.6	74.3	27.0	70.0
25	22.6	74.3	24.5	69.0
30	22.5	74.3	22.1	68.5
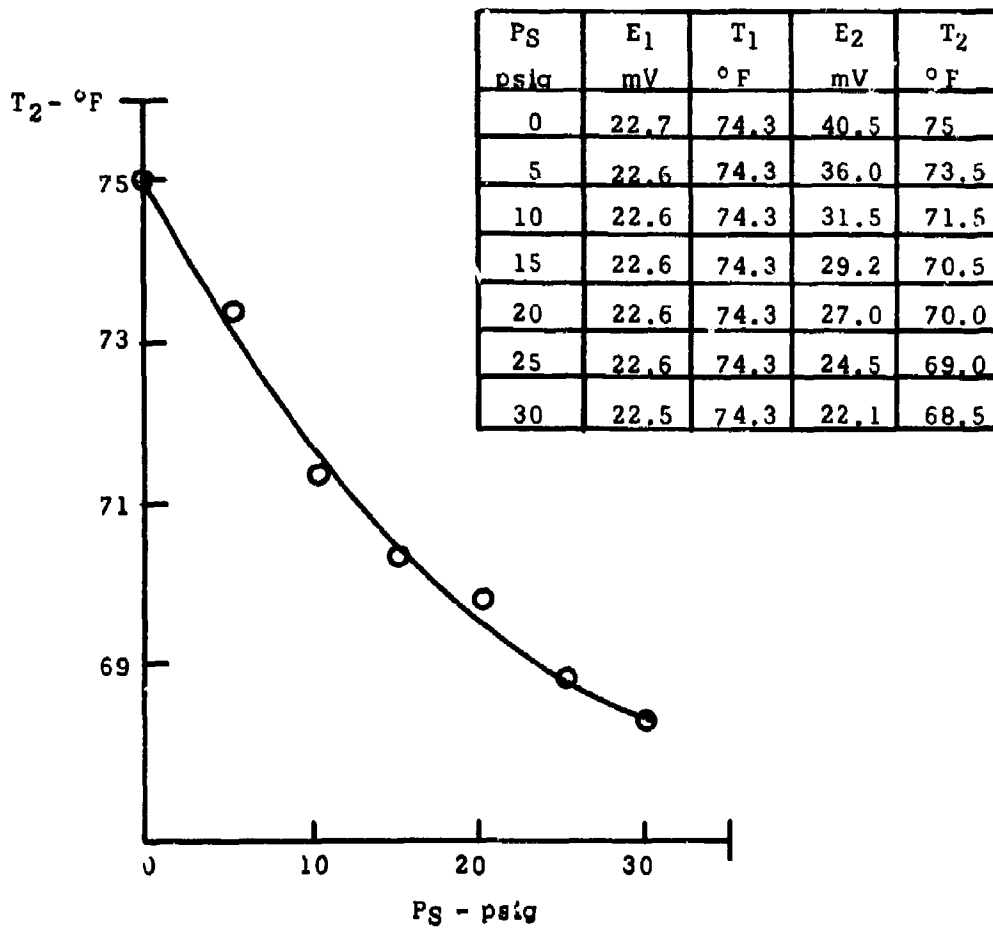
Figure 12. Thermistor Evaluation Test T_2 Temperature Curve for P_S Changes

44

Values for the recovery factor are typically in the region of .95 to less than 1.0. Changes in adiabatic wall temperature are thus small in comparison to changes in static temperature, remaining close to the stagnation temperature. (If the recovery factor were a value of 1, the adiabatic wall temperature would theoretically be the stagnation temperature.) The temperature changes monitored by a thermistor, mounted as described, are thus small.

Evaluation of the test data, described earlier, shows that the temperature monitored did follow that predicted by the adiabatic wall expression with a recovery factor of between .95 and .96.

As pointed out by the TM, the adiabatic wall consideration does not take into account the effect of varying ambient temperatures on the temperature monitored by the thermistor. Where ambient temperature changes are appreciable, difficulty would be experienced in isolating this effect from changes of, for example, supply pressure.

d. Conclusions

It is concluded from the analysis of TM-132 and from the results of laboratory tests that, while thermistors can be satisfactorily mounted in an element, and can detect nominally the adiabatic wall temperature, their use is practical only where ambient temperatures can be closely controlled. Otherwise, meaningful interpretation of monitored temperature changes would be difficult. The possibility does exist of developing techniques for compensation of changes in ambient temperature and would be worthwhile investigating for a case where the thermistor afforded a unique means of performance evaluation.

3. INFRARED THERMOMETER EVALUATION

The Barnes infrared thermometer, model PRT-4, was evaluated as a means of detecting temperature gradients related to the functional performance and functional performance changes of Fluidic elements. The theory relating temperature changes, and thus thermal gradients, to Fluidic functional perfor-marce is explained above in Section 2 - "Thermistor Evaluation" and in TM-132 of Appendix II.

It was considered possible that an I.R. sensor could indirectly detect pressure changes and cause a change in flow and therefore, a change in the fluid flow temperatures. By heat transfer between the fluid operating medium and the body of a Fluidic element, measurable changes in the element body temperature should accompany, following a thermal lag, changes in the fluid flow temperature.

Tests were conducted on an analog Fluidic element, with the I.R. thermometer sensing the temperatures occurring on the outside surface of the element as pressure changes were recorded. An evaluation of the data and the resulting

45

conclusions are given.

a   I.R. Thermometer Tests

The tests were conducted on a 1786 analog amplifier. The temperature distribution over the rear surface of the analog element was monitored by the thermometer. The optical head of the I.R. thermometer, mounted on a tripod, was aimed at the element to sense a field of view of 0.5 in. diameter. Therefore, data was recorded for grid spacings of 0.5 in. x 0.5 in. over the surface of the element. The grid location with respect to the functional channels of the Fluidic element is shown in Figure 13.
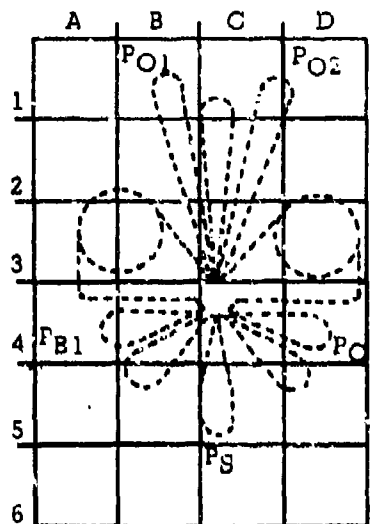
Figure 13.   Grid Locations - I.R. Thermometer Test

The temperature measured by the I.R. thermometer can be read directly from a meter on the front control panel, but this meter, ranging from $10°$ F to $100°$ F did not have sufficient resolution for the small temperature gradients expected during these tests. The I.R. thermometer does provide for a recorder output. The resolution needed was accomplished by expanding the scale of the recorder. A Moseley 7001A X-Y Recorder was used, plotting the output for each temperature measurement for 30 seconds. The average was then recorded as the temperature of the point being measured. Every effort was made to reduce the effects of room air current and room temperature changes during this test by surrounding the I.R. thermometer optical head (sensing device) and the test element with a curtain.

46

The test procedure was as follows. A number of changes were separately
introduced. Specifically, the supply pressure was varied, a control pressure
was changed, and the load applied to the amplifier output was changed.
Following each change, a 30 minute stabilizing period was allowed. Then the
temperatures at each of the grid points were established, taking a 30 second
average for each point. The stagnation temperature of the incoming air (T_O)
was also recorded for each test.

The resultant data is given by Table 11. Test #1 is considered the reference
test, with a supply pressure of 10 psi, and the bias and control pressure each
equal to 10% (1 psig) of the supply. For test #2, the supply pressure was
decreased to 5 psi, with control and bias pressures remaining at 1 psi. For
test #3, the supply pressure was increased to 35 psig, with the control pressures
nominally 1 psig. For test #4, the supply pressure was returned to reference
condition of 10 psi, with a 1 psig bias and 1.5 psig control (a .5 psi differen-
tial input signal). In the last case, test #5, a reduced load area was imposed
on one of the outputs, with the supply pressure, bias and control pressures
being the reference values.

Figures 14, 15, 16, and 17 show typical results in the form of a three
dimensional representation of the thermal maps for tests 1, 2, 4 and 5,
respectively. In considering the three dimensional thermal maps, as well
as the original data, the emphasis should be on qualitative results. The
magnitudes of the sensed temperature differences were of a small enough
amplitude so that the incurred experimental errors were not insignificant. This
fact does not, however, detract appreciably from the observations and conclusions
which may be drawn from the results.

Examination of the thermal map of test #1, Figure 14, shows the temperature of
the rear surface of the element to decrease from the supply pressure reservoir
to exit of the power nozzle and into the interaction region, as is expected. A
temperature drop across the power nozzle of approximately $1^\circ F$ is shown. This
is quite compatible with a differential between total temperature and adiabatic
wall temperature at the nozzle exit of approximately $3^\circ F$ for a pressure differ-
ence of 10 psi (as shown by Table 1, of TM-132 in Appendix II). The tempera-
ture differential on the rear surface of the element will be less than that predicted
by the adiabatic wall equation, due to heat transfer phenomenon in the element
body structure. The map of test #1 also shows the temperature to increase in
passing from the receiver entrance toward the receiver channel outputs. This
reflects, as anticipated, the diffusion of the gas in the receivers, with a
resultant increase in temperature.

The thermal map of test #2, Figure 15, shows that decreasing the supply pressure
from 10 psig to 5 psig reduces the temperature differential across the power
nozzle. Examination of the data of test #3, given by Table II, shows an increase
in the temperature difference across the power nozzle with an increase of supply

47

TABLE II. INFRA-RED THERMOMETER TEST DATA

Test #1 (°F)

	A	B	C	D
1	73.0	72.5	72.0	73.8
2	71.5	71.2	71.1	71.0
3	72.0	69.2	68.9	69.0
4	72.7	71.7	70.5	71.6
5	72.0	72.5	72.3	72.8
6	72.5	74.8	72.3	72.5

P_S = 10 PSI P_{O1} = 1.35 PSI
P_{B1} = 1 PSI P_{O2} = 1.1 PSI
P_{C1} = 1 PSI T_O = 69.3°F
Loads = 6.3×10^{-4} sq.in.

Test #2 (°F)

	A	B	C	D
1	71.7	73.8	71.9	72.5
2	71.1	71.5	71.3	71.3
3	72.1	71.2	70.2	70.5
4	72.2	72.1	71.2	71.6
5	71.3	72.1	72.2	71.8
6	71.5	74.5	72.1	71.9

P_S = 5 PSI P_{O1} = .71
P_{B1} = 1 PSI P_{O2} = .59
P_{C1} = 1 PSI T_O = 68.9° F
Loads = 6.3×10^{-4} sq.in.

Test #3 (°F)

	A	B	C	D
1	70.2	72.6	69.9	70.9
2	69.6	69.0	67.0	68.2
3	70.7	68.0	64.0	64.8
4	71.0	70.5	68.4	68.0
5	70.2	71.0	70.2	70.2
6	70.4	74.5	70.6	70.4

P_S = 35 PSI P_{O1} = 5.5 PSI
P_{B1} = 1 PSI P_{O2} = 3.6 PSI
P_{C1} = .96 PSI T_O = 68.9°F
Loads = 6.3×10^{-4} sq.in.

TABLE II——Continued

TABLE II ---- Continued

Test #5 (°F)

	A	B	C	D
1	71.7	74.4	72.2	72.2
2	71.5	71.3	71.7	70.8
3	72.0	69.8	69.7	69.0
4	72.0	71.2	70.7	71.0
5	71.5	72.0	71.9	72.2
6	72.5	74.4	71.2	71.9

P_S = 10 PSI P_{O1} = 2.5 PSI
P_{B1} = 1 PSI P_{O2} = .85 PSI
P_{C1} = 1 PSI T_O = 68.9°F

Load for P_{O1} = 3.48×10^{-4} sq.in.
Load for P_{O2} = 6.3×10^{-4} sq.in.

Test #4 (°F)

	A	B	C	D
1	72.2	74.3	72.0	71.8
2	71.4	71.5	71.3	70.7
3	72.2	70.2	68.6	69.5
4	72.2	71.5	70.5	71.0
5	71.4	71.8	71.7	71.8
6	73.1	74.2	72.2	71.8

P_S = 10 PSI P_{O1} = 2.8 PSI
P_{B1} = 1 PSI P_{O2} = 0.44 PSI
P_{C1} = 1.5 PSI T_O = 68.4°F

Loads = 6.3×10^{-4} sq.in.

TABLE II---Concluded

$P_S = 10$
$P_C = 1$ $P_C' = 1.35$
$P_B = 1$ $P_G = 1.1$ $T_O = 69.3°F$
LOADS = .0156 X .040

BASE LINE IS 63°
1 INCH = 5°

63°

MODEL - 1786
SENSOR - PT-4 INFRA-RED THERMOMETER

SR5287
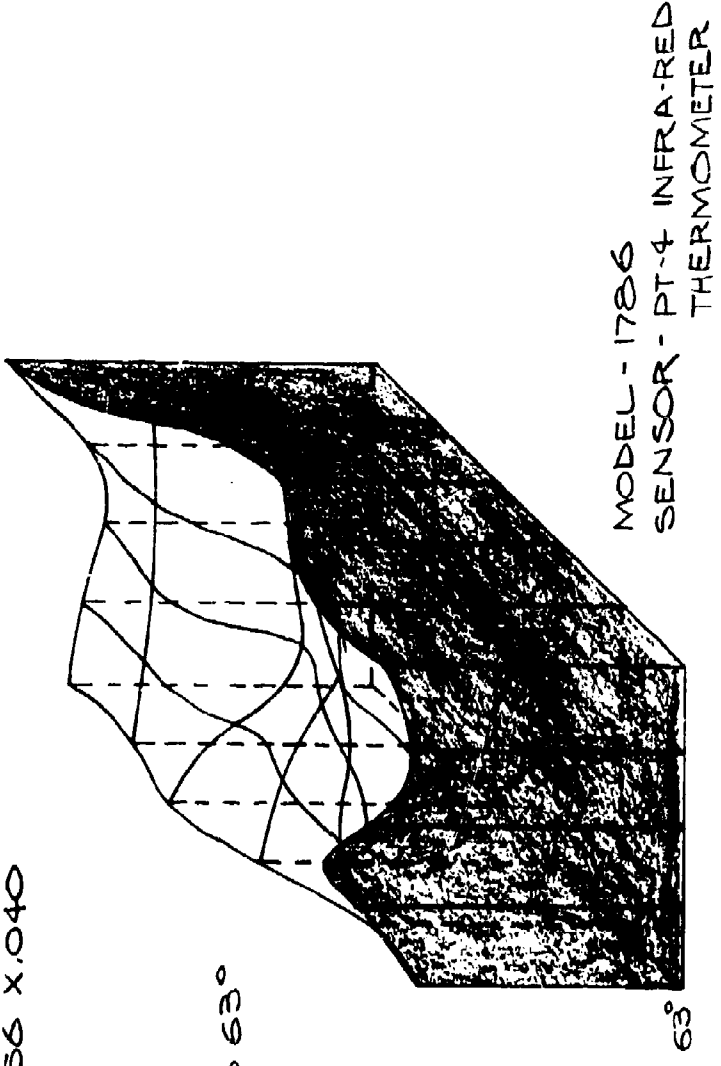
TEST 1 - THERMO-DISTRIBUTION OF ANALOG ELEMENT

Figure 14.

TEST 2 - THERMO-DISTRIBUTION OF ANALOG ELEMENT

MODEL-1786
SENSOR - PT-4 INFRA-RED THERMOMETER

$P_S = 5$
$P_C = 1$ $P_O' = .71$
$P_a = 1$ $P_O = .59$ $T_O = 68.9$
LOADS = .0156 X .040

BASE LINE IS 63°F
1 INCH = 5°

63°F

GR5286

Figure 15.

$P_B = 10$
$P_C = 1.5$ $P_o' = 2.83$
$P_b = 1.0$ $P_o = .44$ $T_o = 68.9°F$
LOADS = .0136 × .040

MODEL - 1786
SENSOR - PT-4 INFRA-RED THERMOMETER

GR5289

BASE LINE IS 62°F
1 INCH = 5°

62°

TEST 4 - THERMO-DISTRIBUTION OF ANALOG ELEMENT

Figure 16.

$P_S = 0$

$P_C = 2.5$ $P_C' = 2.5$

$P_S = P_O = .85$ $T_O = 68.9°F$

LOAD FOR $P_O' = .0087 \times .040$

LOAD FOR $P_O = .0156 \times .040$

$65°$
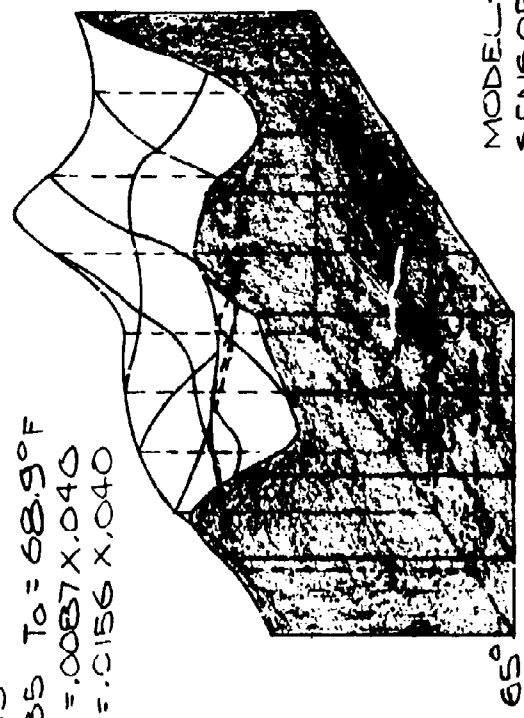
MODEL-1786
SENSOR- PT-4 INFRA-RED
THERMOMETER

BASE LINE IS 65°F
INCH = 5°

TEST 5 - THERMO-DISTRIBUTION OF ANALOG ELEMENT

Figure 17.

GR5290

53

pressure from 10 psig to 35 psig.

Figure 16, the thermal map for test #4, shows the effect of introducing an input signal pressure difference, with supply pressure being the reference value of 10 psig. Comparing Figure 16 with Figure 14, shows that a change in the thermal map was induced by the input signal. A concise reason for the indicated changes is difficult to make, since the thermal phenomenon occurring is quite complex. Within the interaction region, the air issuing from the power and control nozzles, which exhibit one value of stagnation temperature, entrains and mixes with ambient air of a different stagnation temperature. A mathe-- matical description of the thermal phenomenon downstream of the power nozzle exit is hence quite complex.

Figure 17 presents the thermal map for test #5, where the supply, bias, and control pressures were the reference values, and a smaller than normal load area was imposed in air output leg. An observable difference as compared to the test #1 map, occurred.

b.   Conclusions

It is concluded that indications of the performance state of Fluidic elements can be realized by use of I.R. sensing techniques. However, the changes introduced for the above described tests were significantly larger than the small changes of interest, as defined by Section IV. In view of the small temperature changes detected during the tests, and the bounding limits as prescribed by adiabatic wall theory (which predicts small temperature changes), it is concluded that the I.R. sensing technique has insufficient sensitivity to circuit changes to be practical for most checkout applications.

4.   EVALUATION OF SENSORS FOR APPLICATION TO ANALOG CIRCUITRY

An extensive test program was performed to evaluate sensors and sensing techniques which were considered most promising for the satisfactory in- strumentation of analog circuitry. The test program was directed to the evaluation of sensing techniques as applied to a single element and to a simple integrated circuit. The latter case is considerably more complex, where concerned with detecting the degradation of one element within a functioning group of elements.

The basis for evaluation was the capability of the sensing techniques to detect specified allowable deviations in primary performance and the capability to detect and define the level of anomaly leading to this limit of performance degradation.

Another facet of the test program was relating the magnitudes of failure mode anomalies to changes in primary performance.

54

Previous tests and evaluation of sensors indicated two types of sensors with the greatest potential of applicability to analog circuitry. The miniature pressure transducers, model SA-SD, manufactured by Scientific Advances, Inc., were considered the most accurate and the most applicable means of monitoring primary performance. The use of secondary acoustic sensing techniques appeared to exhibit the greatest potential for detection and definition of the causes of malfunction. Previous testing of the Massa M-213 microphone and the B & K model 4333 accelerometer yielded positive results, hence these sensors were selected for this test series.

During the test, the emphasis was directed to secondary acoustic sensing. There were few unknowns concerning the applicability of the miniature pressure sensors. Prior consideration of the sensors indicated that performance was as specified by the manufacturer and that installation could be satisfactorily accomplished. Sensitivity was satisfactory. The related equipment is the same as that for the more common types of strain gage pressure transducers. Hence the effort was directed to secondary acoustic sensing where considerable information was desired.

In the following, the test procedure is described and the test set-up and instrumentation defined. The results of the tests are given, with test data included. Finally, the conclusions generated by the test are submitted.

a.   Test Procedure

Figure 18 shows the analog test circuit. It consists of three stages of model 1786 analog amplifiers. Provisions were made to disconnect the first stage element from the second and third elements so that data could be obtained for three modes of operating conditions. The primary objectives for each of the three test modes was to relate the level of the failure mode anomaly induced to the level of performance degradation, to evaluate the sensitivity and resolution of the secondary acoustic sensor in detecting the level of the anomaly related to the allowable set primary performance deviation limits, and to define the cause of the anomaly by typifying signature changes. The nominal operating pressure values for the three modes of testing conducted are listed in Table III with Figure 19 showing the circuit diagrams.

The first mode consists of having only the first element operating. Primary and secondary indications of performance data were recorded for satisfactory functional performance. Anomalies were then introduced into this element while changes in the primary and secondary indications of performance were recorded. The data was then evaluated to determine the resolution of the secondary sensor in detecting the element's performance degradation, and to relate the failure mode anomaly to the level of performance degradation.

55
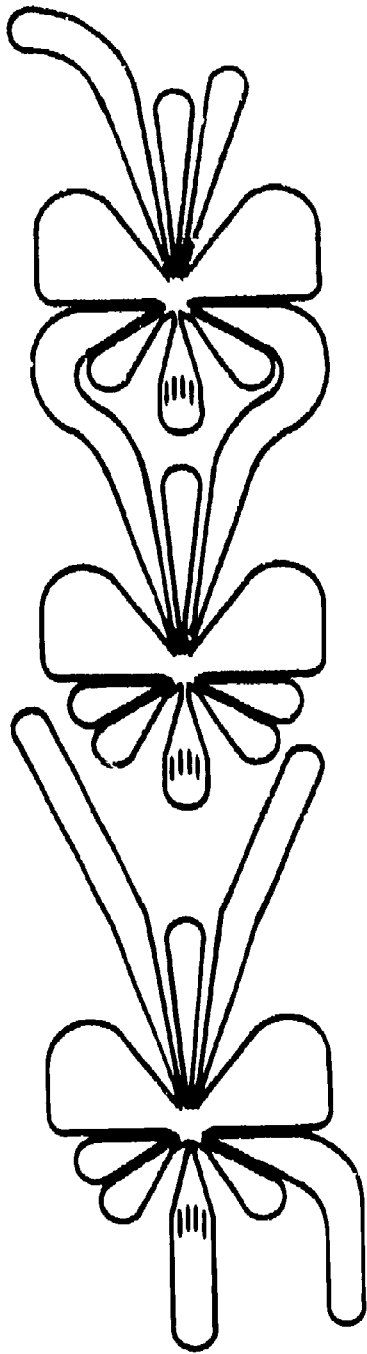
Figure 14. Three Stage Analog Circuit
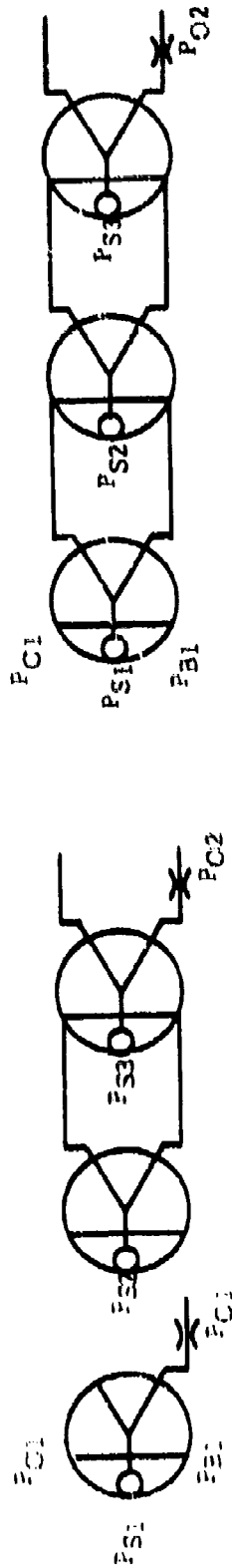
(a)

(b)

Figure 15. Circuit Diagram of Three Stage Analog Amplifier for Test Modes (a) #1 and #2 and (b) #3

56

	P_{S1} (psig)	P_{S2} (psig)	P_{S3} (psig)	P_{B1} (psig)	P_{C1} (psig)	P_{B2} (psig)	P_{C2} (psig)
Mode #1	10	0	0	1.5	1.5	0	0
Mode #2	10	18	35	1.5	1.5	2.7	2.7
Mode #3	10	18	35	1.5	1.5	-	-

The second mode of testing performed was with the second and third stages operating separately from the first stage. The objective was to determine if changes in the secondary acoustic signature could be detected as anomalies were induced into the first element while it was operating in the vicinity (on the same circuit plate) of other elements generating total acoustic signature components of the same order of magnitude or larger.

In the third mode of testing, the first stage element was interconnected to the second stage, so that the three elements presented a three stage amplifier circuit. The reason for this was to determine if changes in the secondary acoustic signature, due to the induced anomalies in the first stage would be amplified, nullified, or remain constant by interconnecting elements to form circuits. In a manner similar to that for the single element, the data was evaluated to determine the resolution of the secondary sensor in determining the performance degradation of the three stage amplifier circuit, and to relate the magnitude of a failure mode anomaly (introduced into the first stage) to the level of performance degradation.

Performance deviation limits for a single stage analog amplifier have been established in Section IV of this report. For the third mode of testing, allowable performance deviation limits were established. The following allowable circuit performance degradation limits for a three stage analog amplifier were considered to be realistic.(Actual requirements vary with specific applications).

Primary Characteristic	Maximum Allowable Change
o Gain	±5%
o Max. Recovery Pressure	-10%
o Operating Range	-10%
o Output Null	± 5% of Operating Range
o Signal/Noise Ratio	Minimum value of 50.

57

Changes greater than these specified are considered a malfunction.

Various pressure and physical anomalies were induced into the first stage element while the three modes of test described above were conducted. The anomalies induced are somewhat typical of those which could occur in a functional Fluidic analog circuit. The anomalies for each test are listed in Table IV below.

TABLE IV. ANOMALY DEVIATION VALUES FOR THREE MODES OF TESTING – THREE STAGE ANALOG AMPLIFIER

Anomaly	Nominal Value	Mode 1 Deviation Values	Mode 2 Deviation Values	Mode 3 Deviation Values
P_{B1} Changes	1.5 psig	1.3 psig 1.4 psig 1.5 psig 1.6 psig	1.3 psig 1.4 psig 1.5 psig 1.6 psig	1.4 psig 1.5 psig 1.6 psig
P_{S1} Changes	10 psig	9 psig 10 psig 11 psig	8 psig 9 psig 10 psig 11 psig	9 psig 10 psig 11 psig
P_{O1} Contamination	6.4×10^{-4} sq.in. *	6.4×10^{-4} sq.in. 5.6×10^{-4} sq.in. 4.4×10^{-4} sq.in. 4.2×10^{-4} sq.in.	6.4×10^{-4} sq.in. 5.6×10^{-4} sq.in. 4.4×10^{-4} sq.in. 4.2×10^{-4} sq.in.	6.4×10^{-4} sq.in. 5.6×10^{-4} sq.in. 4.4×10^{-4} sq.in. 4.2×10^{-4} sq.in.
Center Vent Closure	6.4×10^{-4} sq.in.	6.4×10^{-4} sq.in. 4.8×10^{-4} sq.in. 3.2×10^{-4} sq.in. 0.0 sq.in. (off)	6.4×10^{-4} sq.in. 4.8×10^{-4} sq.in. 3.2×10^{-4} sq.in. 0.0 sq.in. (off)	6.4×10^{-4} sq.in. 4.8×10^{-4} sq.in. 3.2×10^{-4} sq.in. 0.0 sq.in. (off)
Chipped Splitter		Reduction of .005 in. .020 in.	Reduction of .005 in. .020 in.	Reduction of .005 in. .020 in.

* – Lodged Particle

P_{B1} changes consist of varying the ideally constant bias pressure to an element. This anomaly may occur due to events similar to that causing the P_S anomalies, or by contamination of an upstream dropping orifice.

P_S changes consist of varying the supply pressure to the first stage. This anomaly may occur when there is a change in the supply pressure regulator adjustment, because of vibrations, a drop in the supply pressure from the compressor, or contamination of the supply pressure regulator.

P_{O1} refers to contamination of the receiver channel of the output leg of the first element. This contamination was induced by placing various levels of Duco cement in the receiver channel, near the receiver tips, to reduce the receiver area to the values shown in Table IV. This was a simulation of small particle contamination build-up over long periods of time. The last P_{O1} contamination shown in Table IV was a reduction in receiver area caused by lodging a large particle in the receiver tip area. This was done to investigate the effects caused by large particles such as a chip of circuit material, or foreign particles entering through the vent regions and lodging in a receiver.

Center vent closure anomaly were produced by connecting a valve to the center vent channel by a length of polyflow tubing and varying the valve orifice size. This anomaly grossly simulated anomalies occurring in the center vent region such as contamination build-up or particle blockage of the channel. The areas shown are the effective areas of the center receiver and external loading valve in series. The nominal value is that of the center receiver only.

The last anomaly considered is that of chipping a splitter. The splitter is the narrow wedge, with a small radius at its tip, which separates two adjacent receiver channels. These are manufactured within close tolerances. Any significant damage to the tip of a receiver will effect a performance change. Two magnitudes of this anomaly were induced; a breaking off of .005 in. and .020 in. of the splitter tip.

b.   Test Set-Up and Instrumentation

Two considerations entered heavily into the finalizing of a test set-up for this test. First, all physical objectives in the near field had to be as stationary as possible because of the concern with near-field acoustic phenomena. Secondly, means had to be provided for repeatedly sealing and unsealing the three stage amplifier to permit the introducing of various magnitudes of physical anomalies, such as contamination. Figure 20 shows the test stand built to include these considerations. As shown in the picture, all tubing connections to the circuit were kept parallel and of constant length. Whenever the circuit under test had to be removed from the test stand in order to induce physical anomalies, the same physical environmental conditions can be maintained. This also provides for all circuit interconnections to be made external from the immediate environment, such as the circuit changes necessary between the Mode 2 and Mode 3 test. The single elements shown on top of the test stand is acting as a standard load for the last stage output.

59
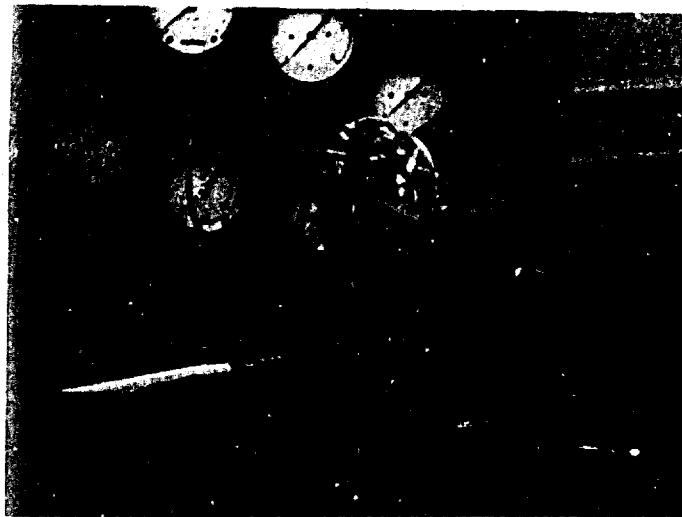
Figure 20. Three Stage Amplifier Test Stand

Also, consideration was given to the supporting structure of the three stage amplifier. A half inch thick steel plate was fastened to a table top as the base for the test stand. Three hold-down clamps were fastened to the steel plate for clamping the circuit down to this plate. A quick release action was also incorporated in the hold-down clamp design so that the circuit could be removed without considerable effort and time being involved. With this arrangement, a unit could be temporarily sealed by placing a gasket between the circuit being tested and the steel plate, thus permitting access to the Fluidic channels and interaction areas in order to induce anomalies.

Figure 21 shows a diagram of the instrumentation set-up used for monitoring the primary function performance data. It consists of strain gage pressure transducers (0 - 5 psi range and 0 - 15 psi range , for monitoring the input and output primary characteristics , respectively), d-c transducer bridges which provide the transducer excitation voltage and output null adjustment, and the X-Y recorder which plotted the transducer's outputs (the input-output characteristics of the circuit being monitored).

The calibration procedure for this recording system is as follows. Inherent to each transducer is a d-c null shift. With zero pressure applied to the pressure transducers, the null balance of the transducer bridge boxes was adjusted so that the X-Y recorder was at its zero input position (the position that results when the input is shorted) and the null shift was eliminated. The X-Y recorder was then calibrated as known pressures were applied to the transducers by

60

INPUT

P_{C1}

OUTPUT

P_{O1} or P_{O2}

```
┌─────────────────┐          ┌─────────────────┐
│     Statham     │          │       CEC       │
│     PL96TC      │          │      4312       │
│Pressure Transducer│        │Pressure Transducer│
└─────────────────┘          └─────────────────┘

┌─────────────────┐          ┌─────────────────┐
│       BEC       │          │       BEC       │
│      1576       │          │      1576       │
│Transducer Bridge│          │Transducer Bridge│
└─────────────────┘          └─────────────────┘

        X  Input  ┌─────────────────┐  Y  Input
                  │     Moseley     │
                  │     7001 A      │
                  │  X-Y Recorder   │
                  └─────────────────┘
```
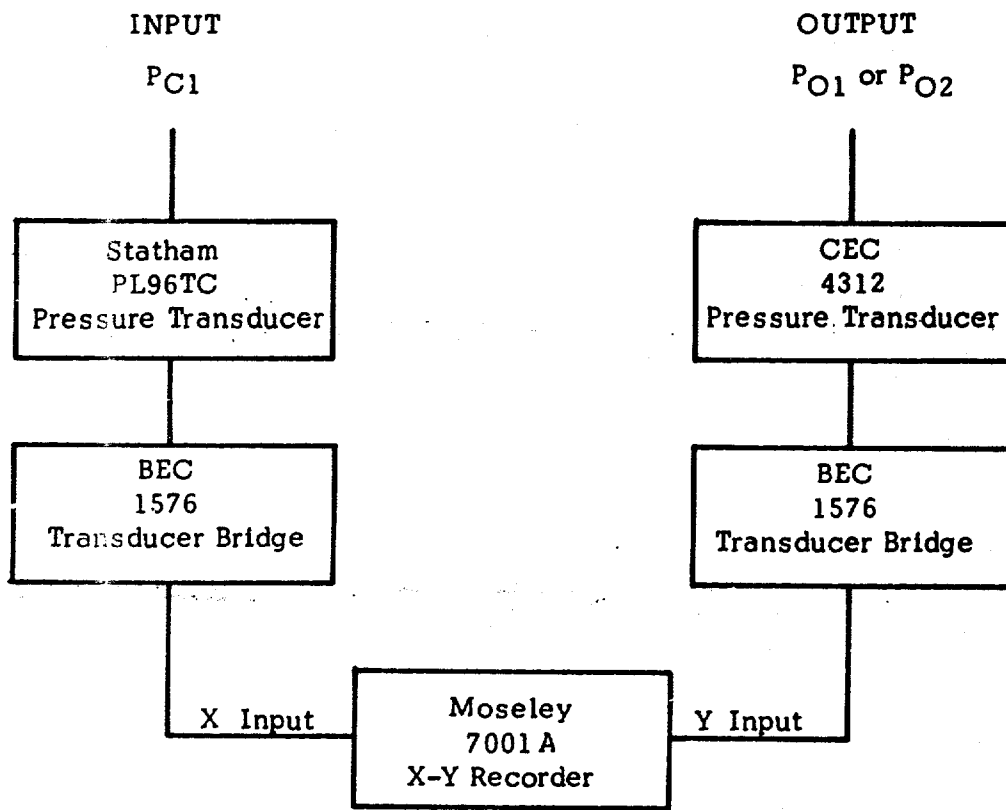
Figure 21. Instrumentation Block Diagram for Primary Performance
Test - Three Stage Analog Amplifier

adjusting the recorder gain to acquire the necessary sensitivity. As an example, for the first mode of test to be performed, that on a single element, the X and Y gain of the recorder was calibrated so that a sensitivity of 1-inch deflection per psi was acquired. A mercury manometer was used to monitor the pressure to the transducers.

A comparison was made between the microphone and accelerometer as an acoustic sensor for this test program. It was concluded that, for the above described test set-up, the accelerometer was the most satisfactory.

With arrangement designed to permit removal and reinstallation of the circuit plate, sufficient repeatability in the relative position of the microphone with respect to the circuit and test set-up tubing could not be realized. As a result, repeatability of the acoustic signature was poor.

The accelerometer could be directly and permanently attached to the circuit plate, thus maintaining constant its position and acoustic coupling with respect to the circuit plate. When removing the circuit plate to introduce anomalies, the accelerometer remained attached to the circuit plate. It was observed, however, that considerable care was necessary in clamping down the circuit plate in always the same way. Differences in structural stresses within the circuit body, caused by inconsistent clamping, appeared to degrade repeatability.

Figure 22 shows the block diagram of the instrumentation set-up for monitoring, analyzing, and recording of the secondary acoustic data detected by the accelerometer. The instrument of primary importance here is the sonic analyzer. Its function is to determine the frequency components and the relative amplitudes of these frequency components that are present in the acoustical characteristics sensed by the accelerometer. As stated earlier, it is the changes in these frequency components and their relative amplitudes which will be related to circuit performance degradation and that provides the foundation for this method of testing. A preamplifier was used between the accelerometer and the sonic analyzer to increase the gain by a factor of 10.

Although the sonic analyzer displays the detected frequency spectrum on its screen, it was necessary to maintain a permanent record of the frequency spectrum signature in order to detect changes in the signature caused by performance degradation. This was accomplished by coupling the horizontal and vertical output provided by the sonic analyzer to an X-Y recorder. This produced a permanent record of the signature displayed on the sonic analyzer's screen. Due to the fact that the spectrum analyzer contained a high DC level component, approximately 9 to 15 volts, DC resolution voltage sources were used to null out this DC shift.

Calibration of the horizontal scale of the X-Y recorder to that of the spectrum analyzer was accomplished by applying known frequencies to the analyzer and

62
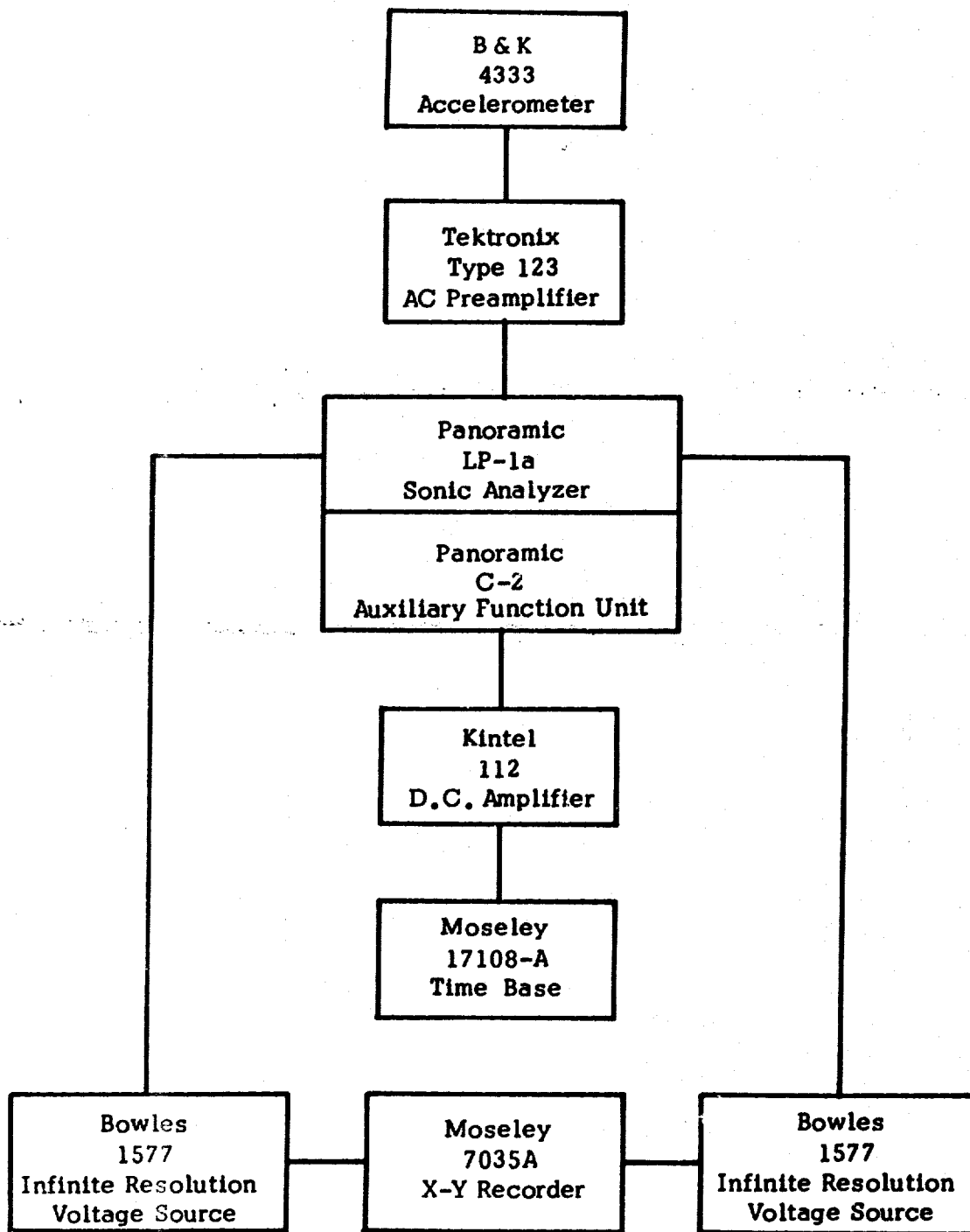
Figure 22. Instrumentation Block Diagram for Acoustic
Signature Test – Three Stage Analog Amplifier

adjusting the bandwidth of the analyzer and the sensitivity of X axis of the recorder to the resolution desired. Calibration of the vertical axis was not extremely critical since primary importance was placed upon the relative amplitude change detected, and not the actual magnitudes of the signals. Therefore, the sonic analyzer was adjusted to display signal amplitudes within the limitations of its screen and the X-Y recorder was adjusted to present the maximum sensitivity of the changes detected, and yet stay within the limitations of its recording area. All instrumentation settings for this test are given in Table V.

TABLE V. Instrumentation Control Panel Settings for Acoustic Signature Test - Three Stage Analog Amplifier

Sonic Analyzer Settings

Input Multiplier	–	X 1
Input Pot	–	1.1
Vertical Calibration Selector	–	Linear
Scale Selector	–	5
Center Frequency	–	12.5 KC
Sweep Range Selector	–	5 KC Bandwidth *
Auxiliary Function Switch	–	Tw-ln **
Spectra Sensitivity Compensation	–	Line
I F Bandwidth	–	200
Sweep Width Factor	–	1
Smoothing Filter	–	5 (max)

X-Y Recorder Settings

X gain adj – Variable position between 10 to 100 mv/inch
     Set for 1 KC ~ 1 inch

X gain adj – Variable position between 0.1 and 1 v/inch

Kintel Amplifier Settings

Gain	–	100

External Time Base Settings

Rate	–	10 seconds per inch

* 1 KC bandwidth for test involving expanded scale
** Condition necessary to use external Horizontal Time Base

During preliminary test using the instrumentation set-up described above, data showed that the signature displayed on the X-Y recorder was not the same as that observed on the sonic analyzer. It was determined that the horizontal sweep rate of the sonic analyzer and thus, the horizontal sweep rate of the X-Y recorder were too fast for the vertical frequency response of the X-Y recorder and caused the signature to be over-damped. This problem was resolved by connecting an external time base unit to the horizontal sweep circuit of the sonic analyzer permitting the selection of any sweep rate desired. An amplifier was placed between the time base unit and the sonic analyzer in order to provide the proper voltage gain necessary to drive the sonic analyzer. Through use of the external time base, a recorder horizontal sweep rate of approximately 10 sec/in was achieved.

c.   Test Results

The data for each of the introduced modes of failure, along with a discussion of the results for each failure mode, are presented by this section.

The format of data presentation is the same for each of the failure modes. The format is defined by the following, the sequence given being that adhered to for each failure mode.

Primary Performance Curves - Single Element:

This figure presents the primary input/output curves of the single element for each level of anomaly.

Performance Deviations - Single Element:

The dimensionless performance parameters are presented for each level of anomaly, as determined from the primary performance curves. The allowable deviation limits for each parameter are given, through which the maximum acceptable magnitude of the anomaly may be established. The relationship between the magnitude of the anomaly and the resultant change in primary performance is shown.

Acoustic Signature - Single Element:

The acoustic signature of the single element for each magnitude of anomaly is given, with coding relating each signature to the anomaly magnitude.

Acoustic Signature - Single Element plus Decoupled Group:

This presents the acoustic signature of test mode 2, where the second and third stage amplifiers are activated, but decoupled from the first stage. In this case, the intent was to establish the capability to detect an anomaly in one element where unrelated, higher intensity, acoustic energy from other

65

elements was present. It was desired to determine whether or not the character-
istic signature changes detected for the element where the anomaly occurred
would be "washed out" by other higher intensity noise sources. This differs
appreciably from the 3rd test mode where considering the three stage amplifier.
In this case, an anomaly in the first stage will normally cause some change in
state of the second and third stages and thus alter their components to the total
signature. Coding relates the signature curves to the magnitude of anomalies
introduced into the first stage.

Primary Performance Curves - 3 Stage Amplifier:

The input/output primary performance curves for the interconnected three stage
amplifier are given for each level of anomaly introduced into the first stage
element. All data related to the 3 stage amplifier falls within the consideration
of the 3rd test mode.

Performance Deviation - 3 Stage Amplifier:

The dimensionless performance parameters for the 3 stage amplifier are given
for each level of anomaly introduced into the first stage. The allowable
deviations in performance for the 3 stage amplifier are shown. The level of the
anomaly in the first stage which leads to malfunction of the circuit may thus be
established.

Acoustic Signature - 3 Stage Amplifier:

This presents the acoustic signature of the complete 3 stage amplifier circuit.
Appropriate coding relates the signature curves to the anomaly amplitudes in-
troduced into the first stage.

The terminology used in presenting and discussing the results of this test are
given by Table VI.

TABLE VI. DEFINITION OF TERMS - THREE STAGE ANALOG AMPLIFIER TEST

P_S	-	Supply Pressure
P_{SO}	-	Supply Pressure at Nominal Conditions
P_B	-	Bias Pressure
P_{BO}	-	Bias Pressure at Nominal Conditions
P_C	-	Control Pressure
P_{CO}	-	Control Pressure at Output Null
P_N	-	Output Pressure when $P_C = P_{SO}$
P_{NO}	-	Output Pressure at Nominal Conditions
G	-	Gain - $\Delta P_{OUT} / \Delta P_{IN}$
G_O	-	Gain at Nominal Conditions
$====$	-	Allowable Deviations Limits from G_O, P_{NO}, P_{RO}, or P_{UO} and P_{LO}
P_R	-	Maximum Pressure Recovery at Saturation
P_{RO}	-	Maximum Pressure Recovery at Nominal Conditions
P_U	-	Upper Limit of Operating Range when Linearity is Within 3%
P_{UO}	-	Upper Limit of Operating Range at Nominal Conditions
P_L	-	Lower Limit of Operating Range when Linearity is Within 3%
P_{LO}	-	Lower Limit of Operating Range at Nominal Conditions
A_R	-	Receiver Nozzle Area
A_{RO}	-	Receiver Nozzle Area Nominal
A_C	-	Center Vent Nozzle Area
A_{CO}	-	Center Vent Nozzle Area Nominal

67

Failure Mode #1 - Bias Shift

Changes in the bias pressure of the first element were induced
as the three modes of test were conducted. The magnitude of the
change from the nominal bias pressure of the first element for
each mode of testing are given in Table IV.

Shown in Figure 23 are the changes in the input-output charac-
teristic curve that resulted from these induced bias pressure
anomalies. Extracted from these curves are the primary perfor-
mance characteristics which are plotted in Figure 24, along with
the allowable deviations in primary performance as specified in
Section IV. The only performance characteristic which exceeded
the allowable performance deviation limits was the output null.
According to the limitation set on the output null, the maximum
P_{B1} change permitted is approximately 1% or .015 psi.

Figure 25 shows the changes in the acoustic signature, resulting
from the induced P_{B1} anomalies for the single element test, over a
5 KC bandwidth. Figure 26 shows an expanded scale, 1 KC band-
width, of the center frequency (12.5 KC) of Figure 25. The intent
here is to show that if an indication of performance degradation
is presented by the 5 KC bandwidth signature, better resolution in
determining the level of the anomaly is possible by looking at a 1
KC bandwidth of the area in question. Considering the level
differences of the signatures detected, changes in bias pressure of
1% can be detected.

Figure 27 shows the changes occurring for the second mode of test
performed. Changes occurring in these signatures were activated
by the same bias pressure changes as those for the single element
test. Therefore, the same changes in primary performance apply
here. Comparing the changes in the signature shown in Figure 27
for an element operating within a group of other elements, but not
interconnected, shows that changes in the bias pressure level could
be detected with a resolution approaching that for the single element
test. The primary difference detected here is shown by the zero
reference line. The total acoustic signature detected contained a
much larger DC average component so that the zero reference had
to be shifted two inches (equivalent to 2.85 mV) in order for the
total signature to appear within the limits of the recording paper.
Activation of the two decoupled higher power level elements did
not "wash out" the first stage amplifier signature. The signature
shape in the 12 KC to 15 KC region was not greatly changed nor were
the changes in signature, due to the bias anomalies, appreciably altered.

68

Figure 28 shows the changes resulting in the primary performance input-output curves for the third mode of testing (3 stage amplifier) as P_{B1} changes were induced to the first stage. This input-output characteristic curve is a plot of input signal to the first element versus the output of the last element. Extracted from the primary performance curve are the primary performance characteristic changes as shown in Figure 29. The primary performance characteristics, due to this anomaly, show little change except for that of the output null. A bias change of ±6% from the nominal of 1.5 psig effected the limiting values of output null shift.

Figure 30 shows the changes that resulted in the acoustic signature for this third mode of testing as the bias anomalies were induced. The acoustic signature change displays good resolution in detecting the level of performance degradation related to the allowable performance degradation limits.

Figure 23. Failure Mode #1 - Bias Shift
Primary Performance Curves - Single Element

70

PRESSURE GAIN

$P_{SO} = 10$ psig $P_{RO} = 1.5$ psig

$G_O = 2.3$

$====$ = ±2% of G_O

OUTPUT NULL

$P_{SO} = 10$ psig $P_{BO} = 1.5$ psig

$P_{RO} = 1.05$ psig

$====$ = ±1% $(P_{UO} - P_{LO})$ at P_{NO}

MAX. PRESSURE RECOVERY

$P_{SO} = 10$ psig $P_{BO} = 1.5$ psig

$P_{RO} = 3.85$ psig

$----$ = −5% of P_{RO}

OPERATING RANGE

$P_{SO} = 10$ psig $P_{BO} = 1.5$ psig

$P_{UO} = 3.75$ psig

$P_{LO} = 1.05$ psig

$====$ = 90% of $(P_{UO} - P_{LO})$
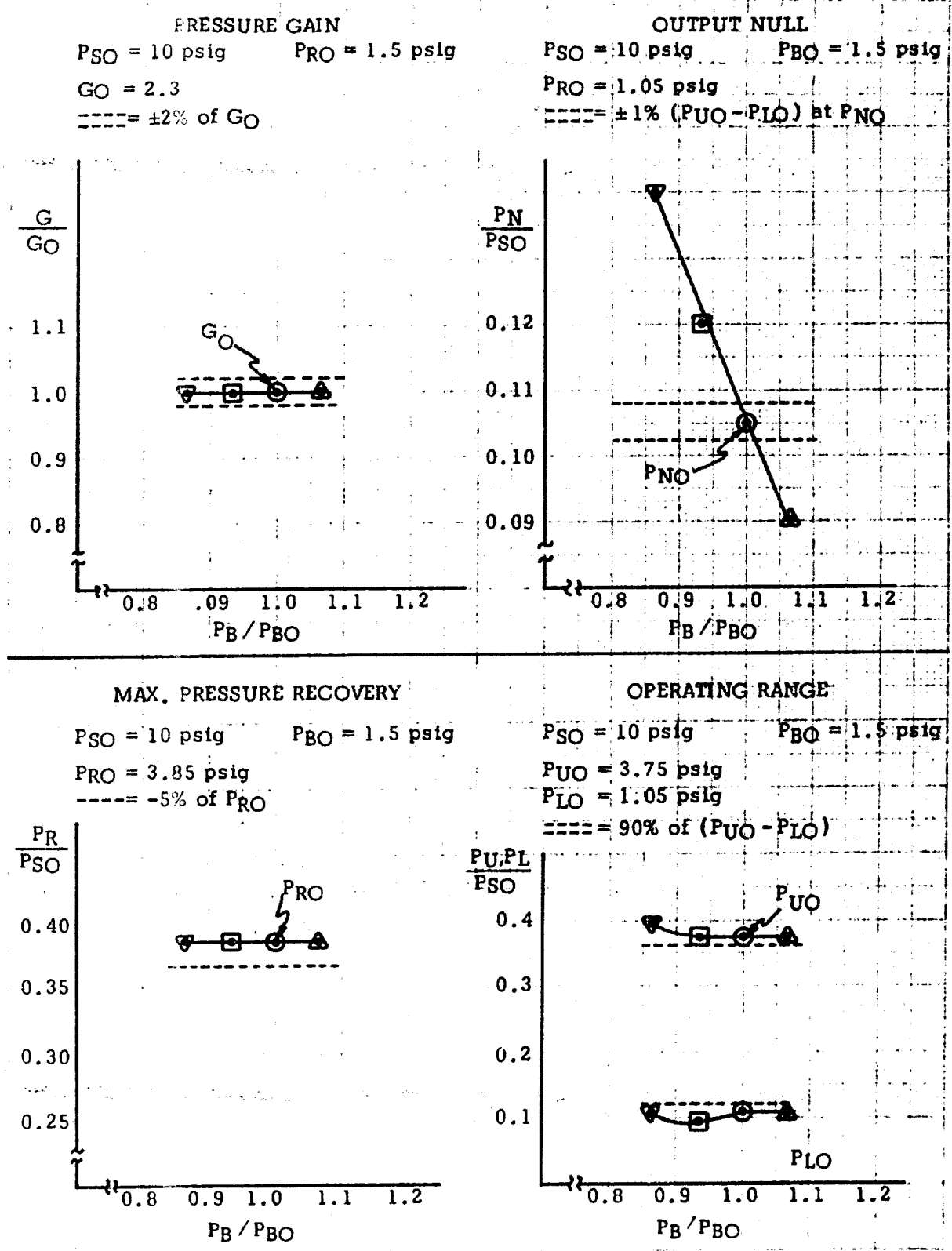
Figure 24.   Failure Mode #1 − Bias Shift
Performance Deviations − Single Element

71

Relative Amplitude

Zero Reference

FREQUENCY RANGE

11BC   11HC

Figure 21. Failure Mode #1 - Bias Shift
Acoustic Signature - Single Element

72

Relative
Amplitude

12 KC   FREQUENCY RANGE   13 KC
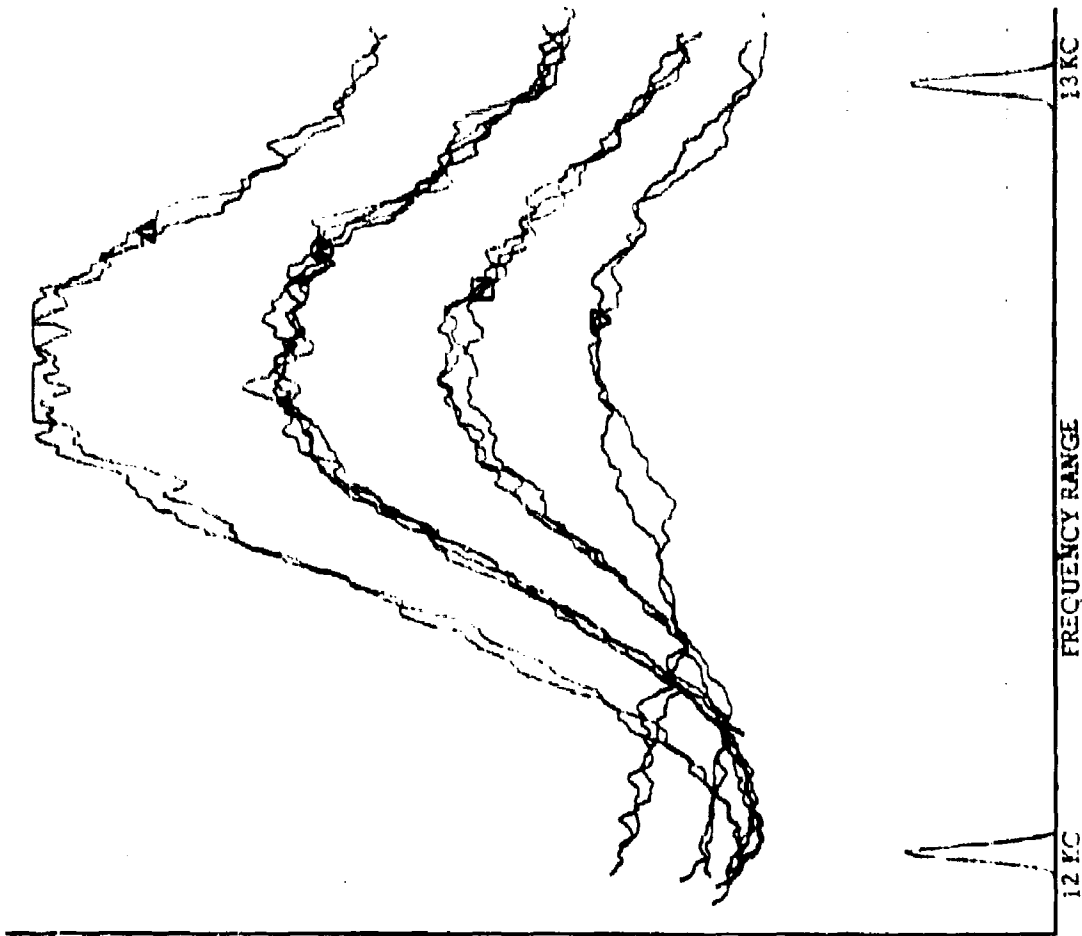
Figure 26. Failure Mode #1 – Bias Anomalies
Acoustic Signature – Single Element (Expanded Scale)
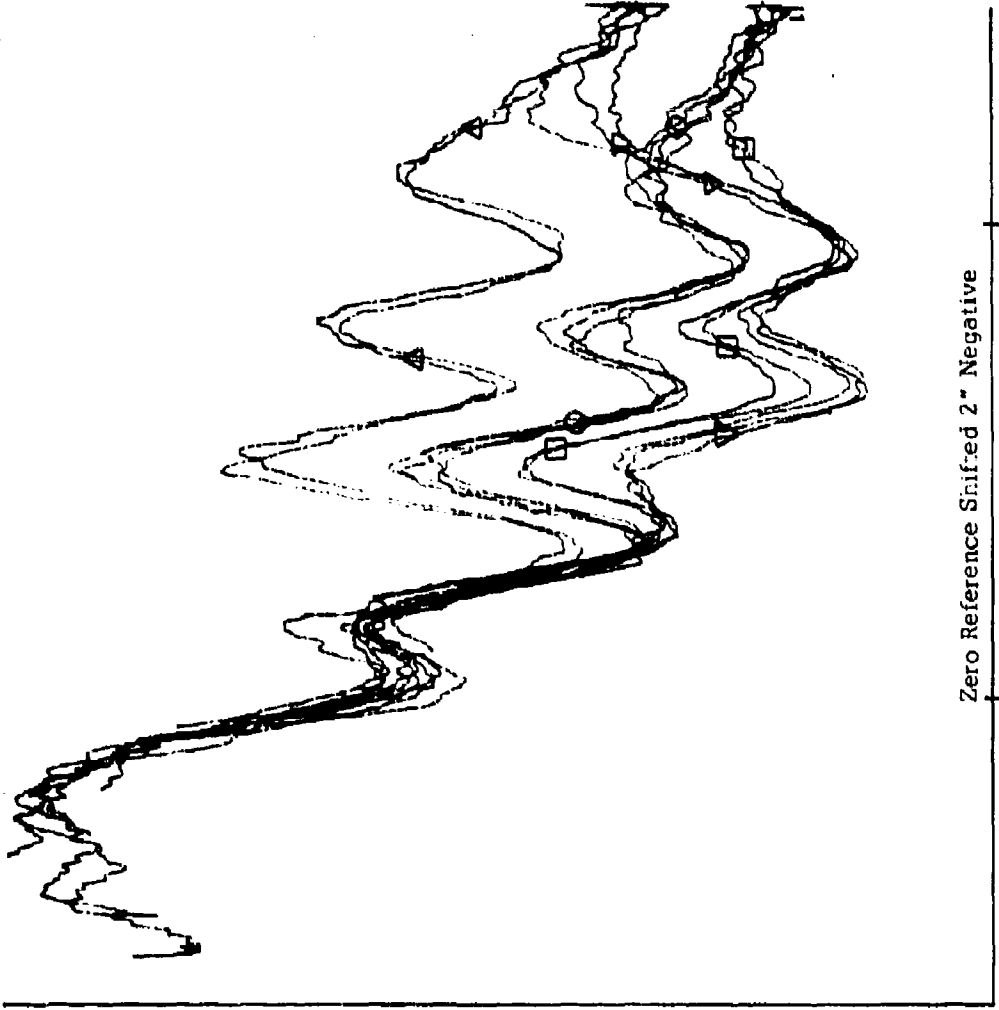
Figure 27. Failure Mode #1 - Bias Shift
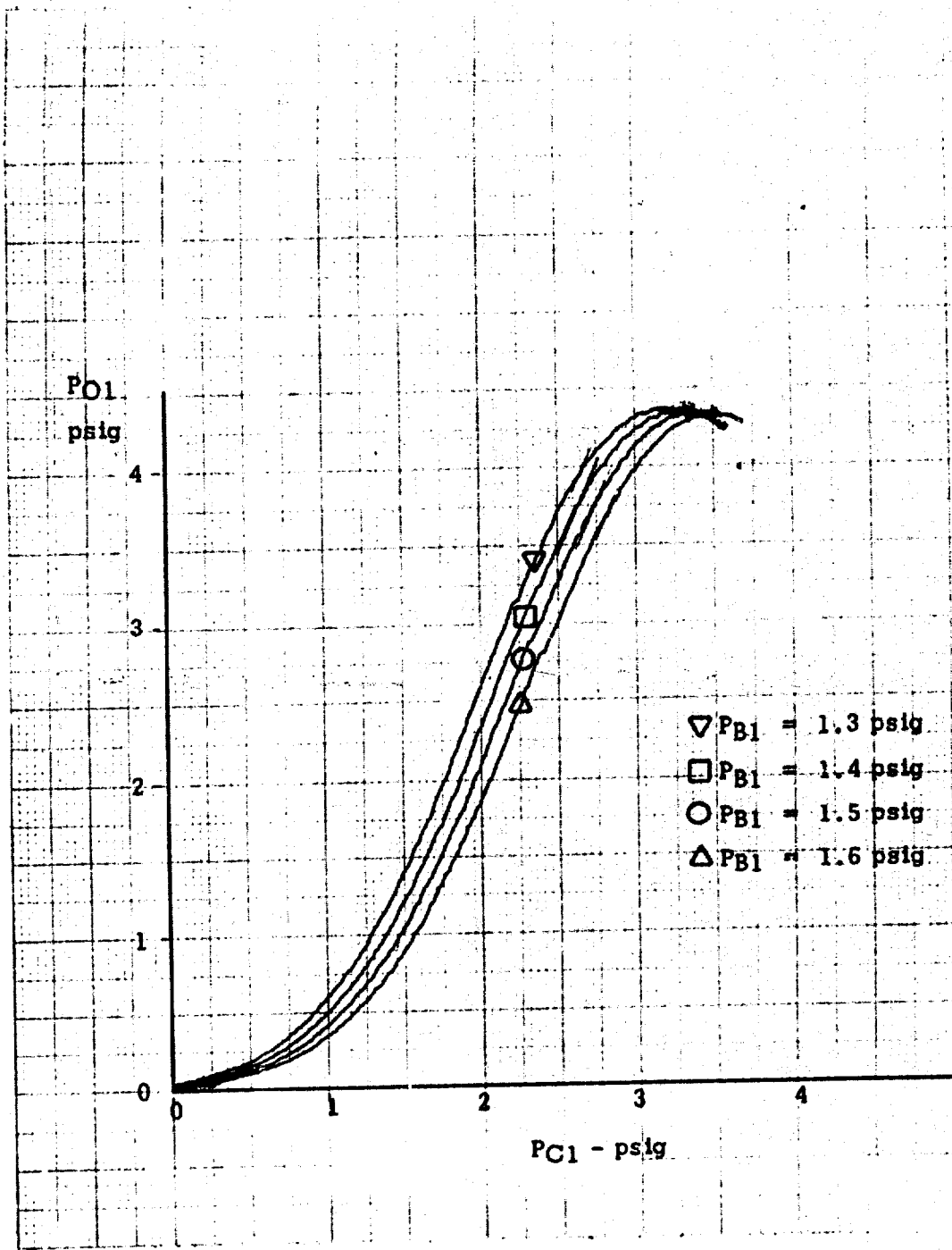Acoustic Signature - Single Element plus Decoupled Group
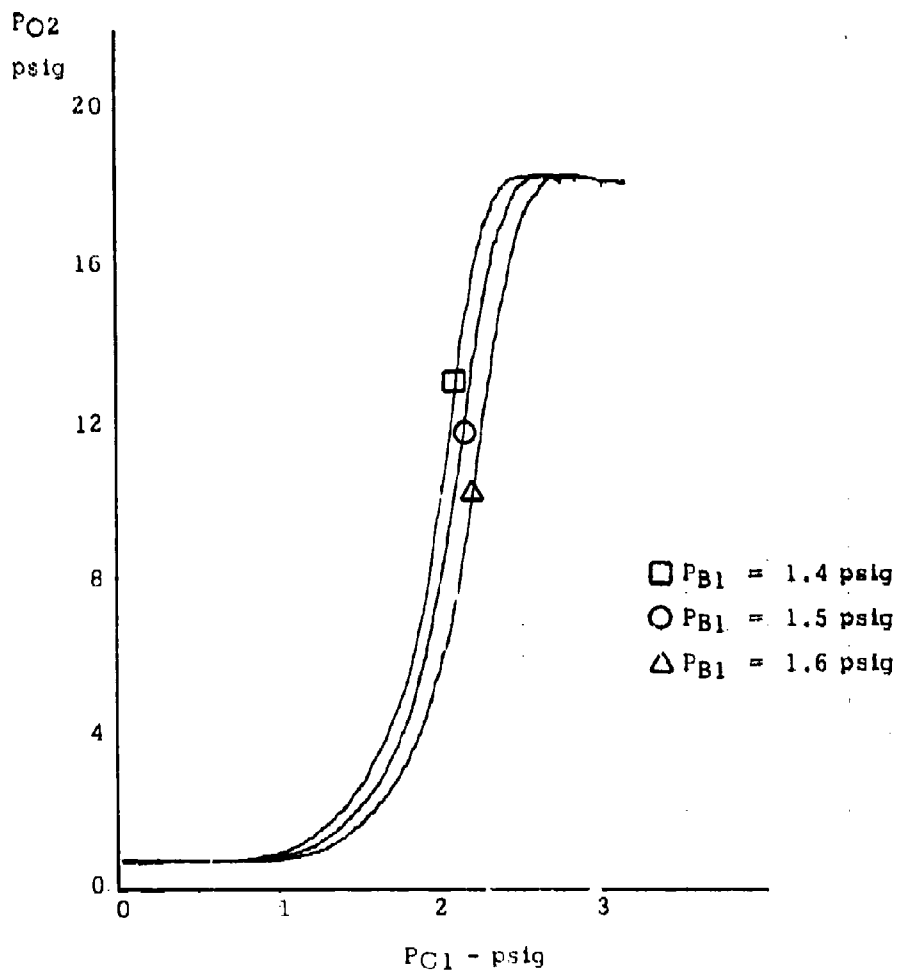
Figure 2e. Failure Mode #1 - Bias Shift
Primary Performance Curves - 3 Stage Amplifier

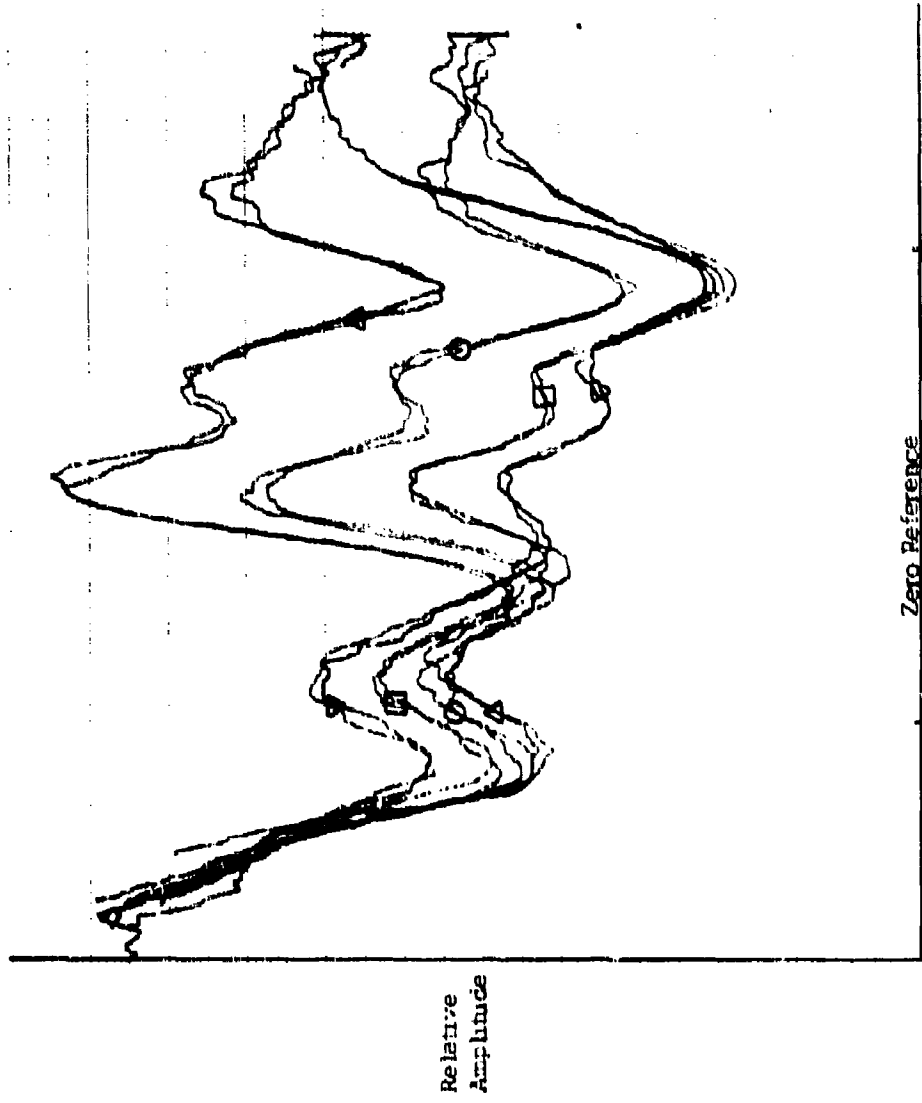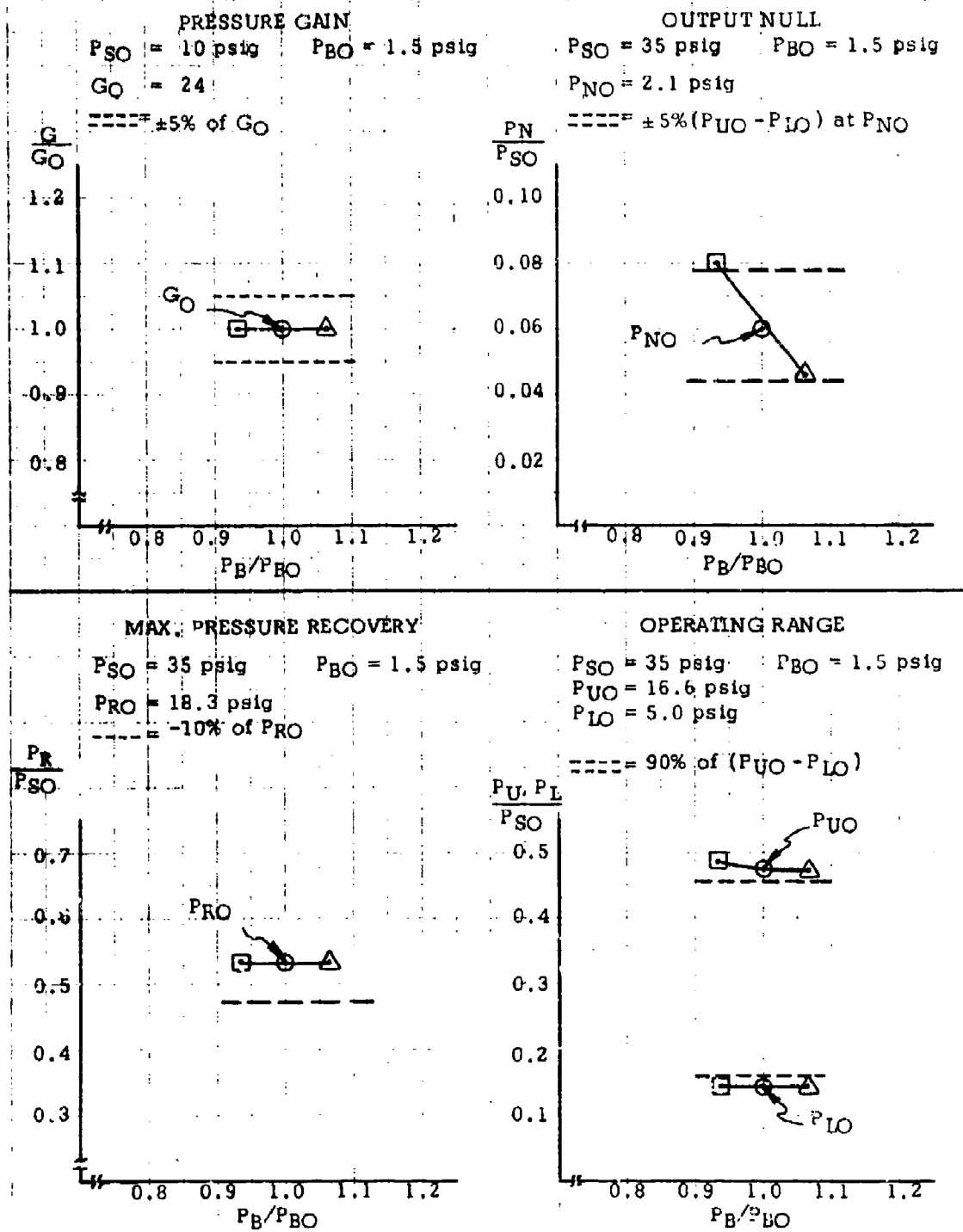Figure 29. Failure Mode #1 – Bias Shift
Performance Deviations – 3 Stage Amplifier

Relative
Amplitude

Zero Reference Shifted 1" Negative

11KC   FREQUENCY RANGE   14KC
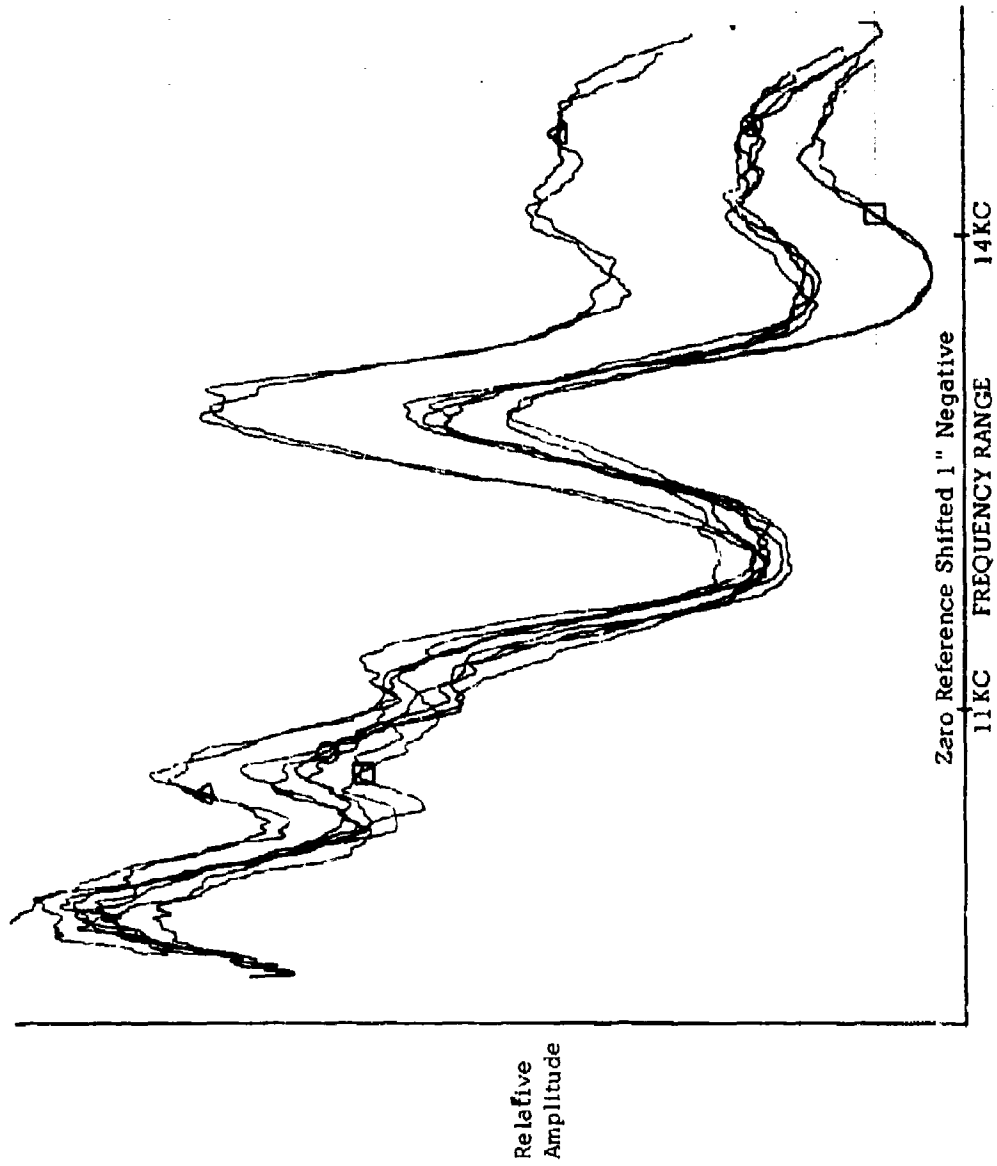
Figure 30. Failure Mode #1 – Bias Shift
Acoustic Signature – 3 Stage Amplifier

Failure Mode #2 - Supply Pressure Changes

Various changes in supply pressure were induced into the first element as the three modes of test were conducted. The magnitude of changes from the nominal supply pressure (P_S) of the first stage element for each mode of testing conducted are given in Table IV.

Figure 31 shows the primary input-output characteristic changes for the single element that resulted from the changes induced in the supply pressure. Extracted from these curves are the primary performance characteristics, which are plotted in Figure 32, along with the allowable deviation in primary performance as specified by Section IV. Although the maximum recovery pressure, operating range, and output null exceeded the allowable performance deviation limits for the supply pressure changes induced here, the characteristics determining the maximum change in supply pressure permitted (before the circuit is considered malfunctioning because it exceeds its allowable limits first) is that of output null. According to Figure 32, the limitation set on the output null will only permit a P_{S1} change of 3% (0.3 psi).

Figure 33 shows the changes in the acoustic signature for the single element as a result of the P_{S1} anomalies. Four traces were recorded for each supply pressure setting to determine the stability and repeatability of the detecting signature. Based on the differences between signature changes in the area of 12.5 KC and the repeability of the signatures for the fixed pressure levels, changes in supply pressure of 3% represent the minimum that can be detected. The desirability of improving trace repeatability to obtain better resolution was indicated by this test. This was subsequently accomplished later in the program.

By comparing Figure 25 of the acoustic signature changes for bias anomalies to Figure 33 for that of the acoustic changes for supply pressure anomalies, it is apparent that the changes from the base line signature for these two anomalies are quite different. Bias anomalies caused the greatest changes in the signature between the bandwidth of 12 to 15 KC, while supply pressure anomalies effected the most significant changes in the signature between the bandwidth of 10.5 to 12.5 KC. This shows that typifying signature changes can be related to the cause of the anomaly.

78

Figures 34 and 35 show the changes occurring in the secondary acoustic signature for a bandwidth of 5 KC and 1 KC, respectively, for the second mode of test performed. Changes occurring in these signatures were activated by the same supply pressure changes as that during the first mode of testing. Therefore, the same changes occurring in the primary performance characteristics apply here. Evaluation of Figures 34 and 35 show that, for a supply pressure failure in one element, performance degradation occurring in that element under conditions where other elements in the area were activated and generating acoustic energy, could be detected by changes in the secondary acoustis signature. As in the test performed for bias anomalies, the acoustic signature generated by elements activated for this test did cause an additional DC level increase, shown in the figures by a zero axis shift of 2 inches (2.85 mV) in order for the signature to fit within the limitations of the recording paper.

Figure 36 shows the changes resulting from the P_{S1} variation to the first stage element for the third mode of test performed; all three stages connected together to form an amplifier circuit. This input-output characteristic curve is a plot of the input signal to the first element vs. the output from the last stage element. As shown in the input-output performance curves of Figure 36 and the primary performance characteristics data given in Figure 37, the anomalous deviations in P_{S1} produce little or no change in the primary characteristics except where a drastic change of 40% ($P_{S1} = 6$ psig) from the nominal value of 10 psi was made. Considering the allowable performance degradation limitations for the 3 stage amplifier, as indicated in Figure 37, a change of 2 psi or greater (20%) is necessary in the supply pressure to the first stage in order for the circuit to be considered malfunctioning.

Figure 38 shows the acoustic signature changes for a 5 KC bandwidth signature as supply pressure to the first stage was changed ±10% (±1 psi) from its nominal value of 10 psi for this third mode of testing. Since these signatures show the potential of detecting variations of 1 psi with relatively good resolution and it takes a change of approximately 2 psi before the circuit is considered malfunctioning, this test shows the potential of the secondary detection technique in detecting impending failures, as well as detecting a state of malfunction.

The signature for the three stage amplifier changes in a similar manner to that for the single stage, the signature level decreasing with increasing supply pressure. The changes in the acoustic signature differs appreciably from that where a bias anomaly was

79

introduced into the first stage of the three stage amplifier (Figure 30). In the latter case, large changes occur in the 13 to 15 KC region which do not occur where the supply pressure was varied, indicating typifying differences in signature changes for different anomalies.

Figure 31. Failure Mode #2 – Supply Pressure Changes
Primary Performance Curves – Single Element

81

Figure 32. Failure Mode #2 - Supply Pressure Changes
Performance Deviations - Single Element

82

Relative
Amplitude

11KC   FREQUENCY RANGE   14KC
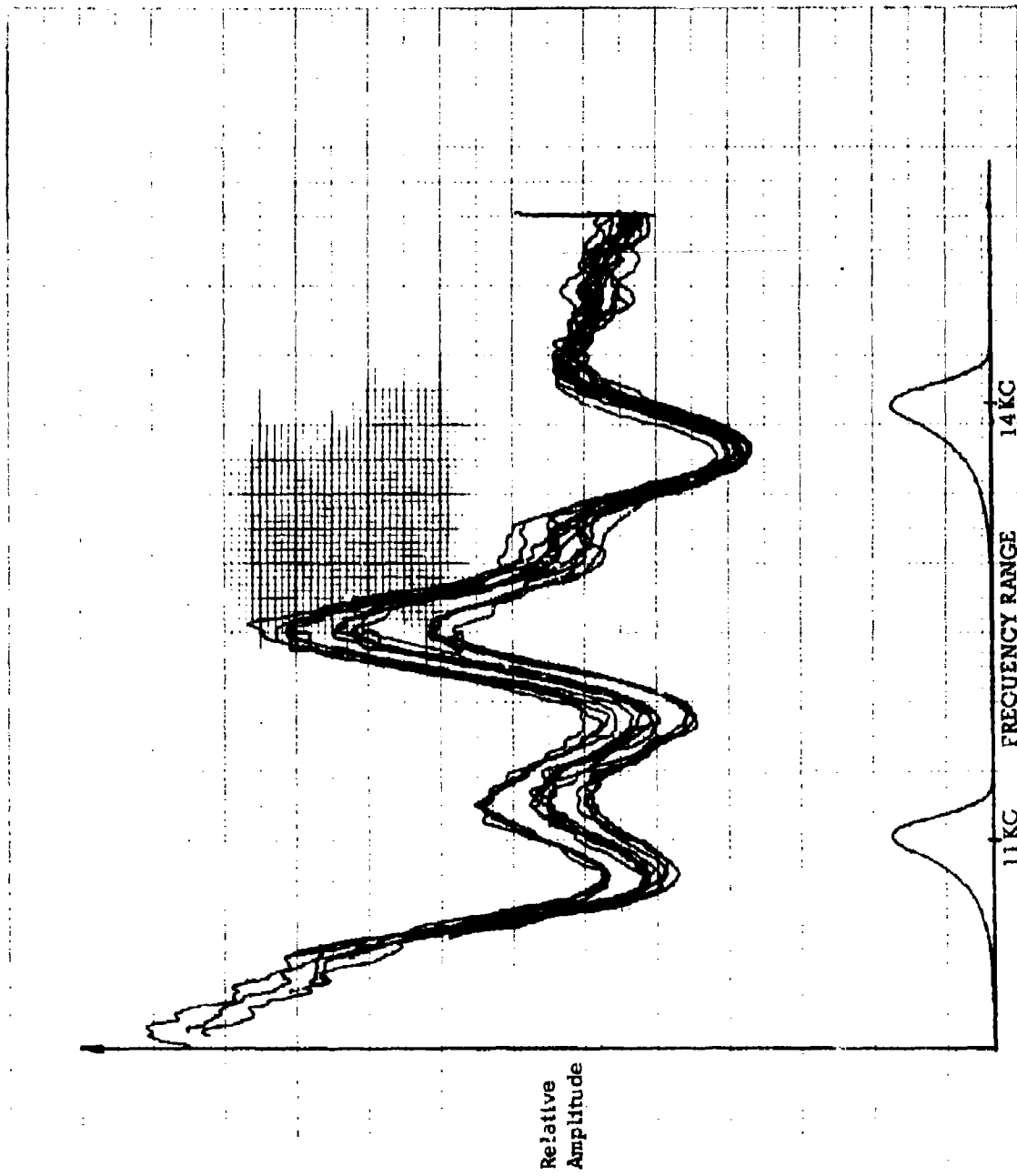
Figure 33. Failure Mode #2 - Supply Pressure Changes
Acoustic Signature - Single Element

☒ P_{S1} = 8 psig

Zero Axis Shifted 2" Negative

11KC   FREQUENCY RANGE   14KC

Figure 34. Failure Mode #2 – Supply Pressure Changes
Acoustic Signature – Single Element plus Decoupled Group

Relative
Amplitude
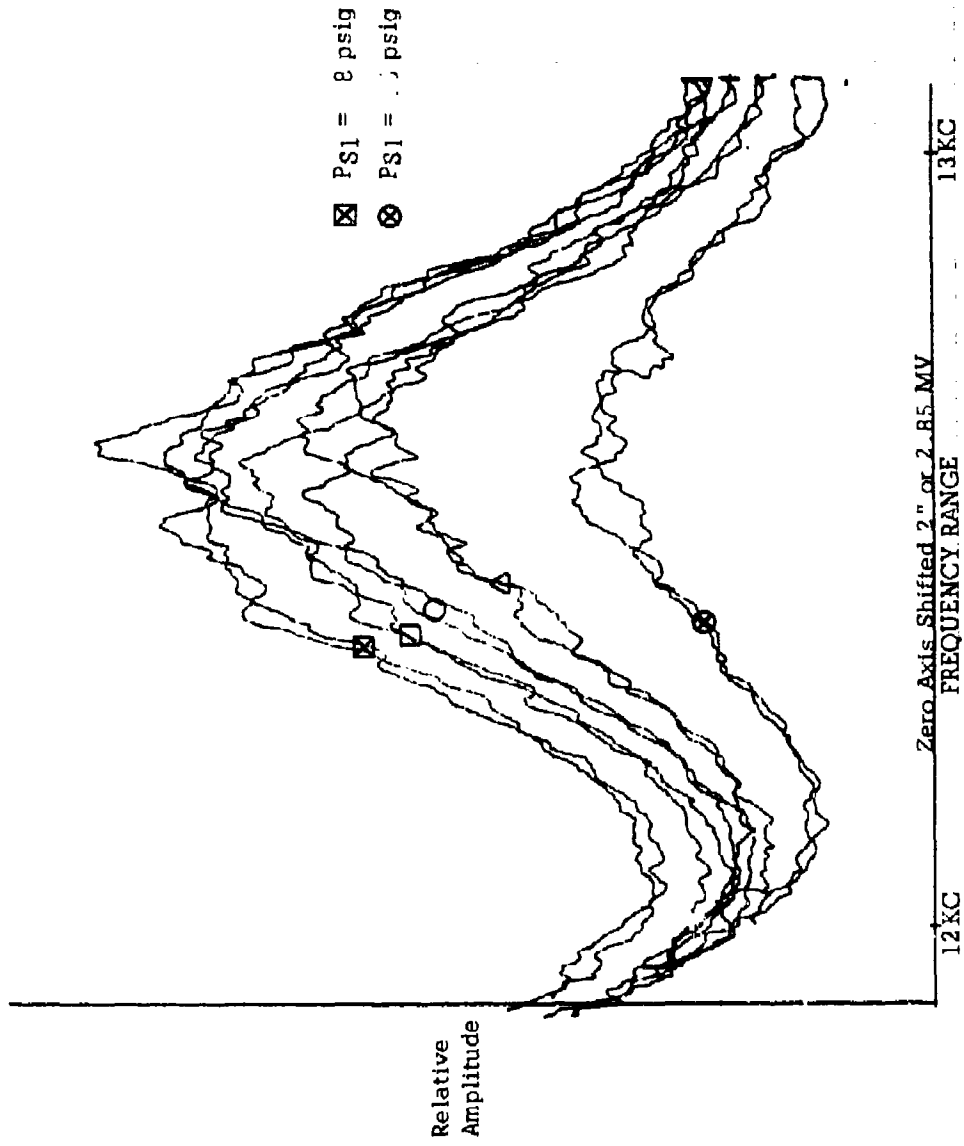
Figure 35. Failure Mode #2 – Supply Pressure Changes
Acoustic Signature – Single Element plus Decoupled Group (Expanded Scale)
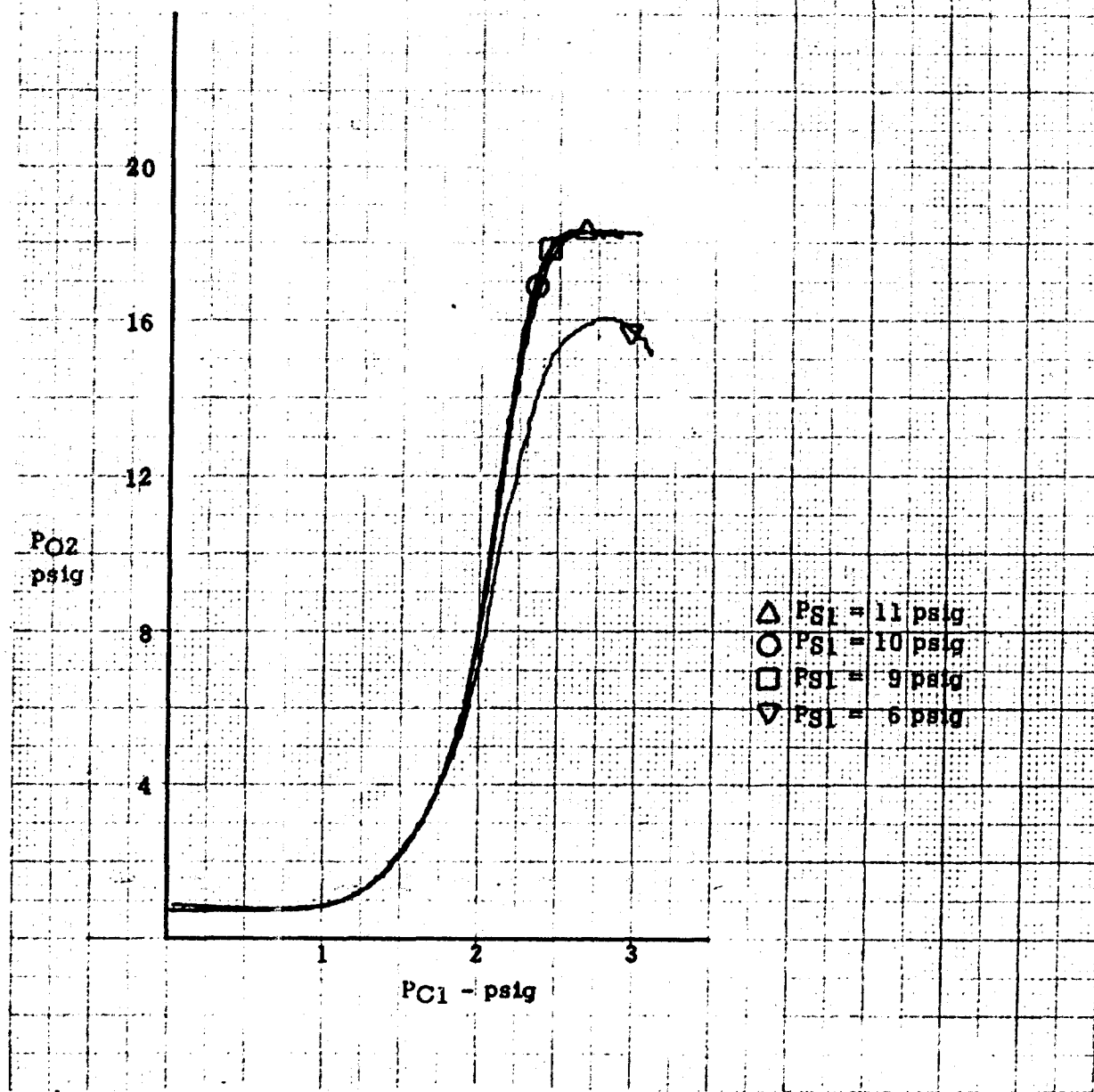
Figure 36. Failure Mode #2 - Supply Pressure Changes
Primary Performance Curves - 3 Stage Amplifier

PRESSURE GAIN

$P_{SO} = 12$ psi

$G_O = 26$

$----$ = ±5% of G_O

$\frac{G}{G_O}$

OUTPUT NULL

$P_{SO} = 35$ psig

$P_{NO} = 2.1$ psig

$----$ = ± 5% ($P_{UO} - P_{LO}$) at P_{NO}

$\frac{P_N}{P_{SO}}$

MAX. PRESSURE RECOVERY

$P_{SO} = 35$ psig

$P_{RO} = 18.3$ psig

$----$ = -10% of P_{RO}

$\frac{P_R}{P_{SO}}$

OPERATING RANGE

$P_{SO} = 35$ psig

$P_{UO} = 16.0$ psig

$P_{LO} = 6.4$ psig

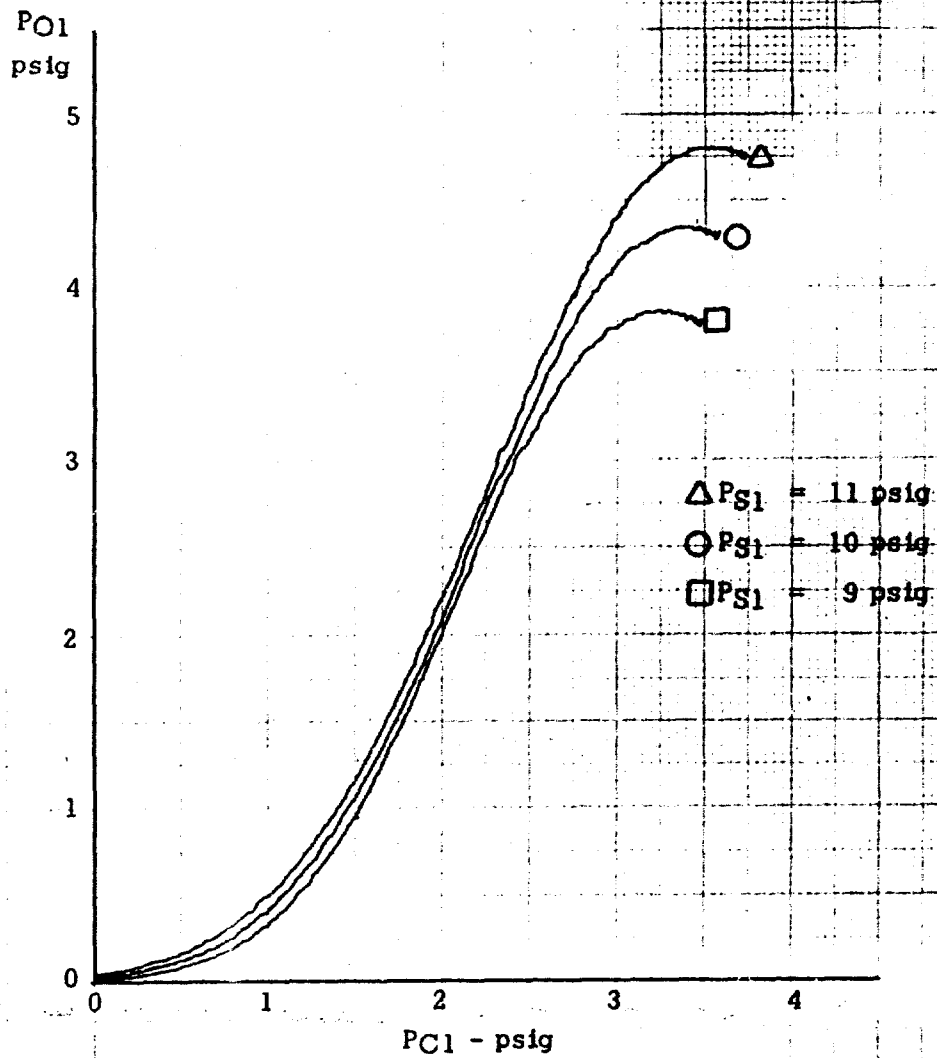$----$ = 90% of ($P_{UO} - P_{LO}$)
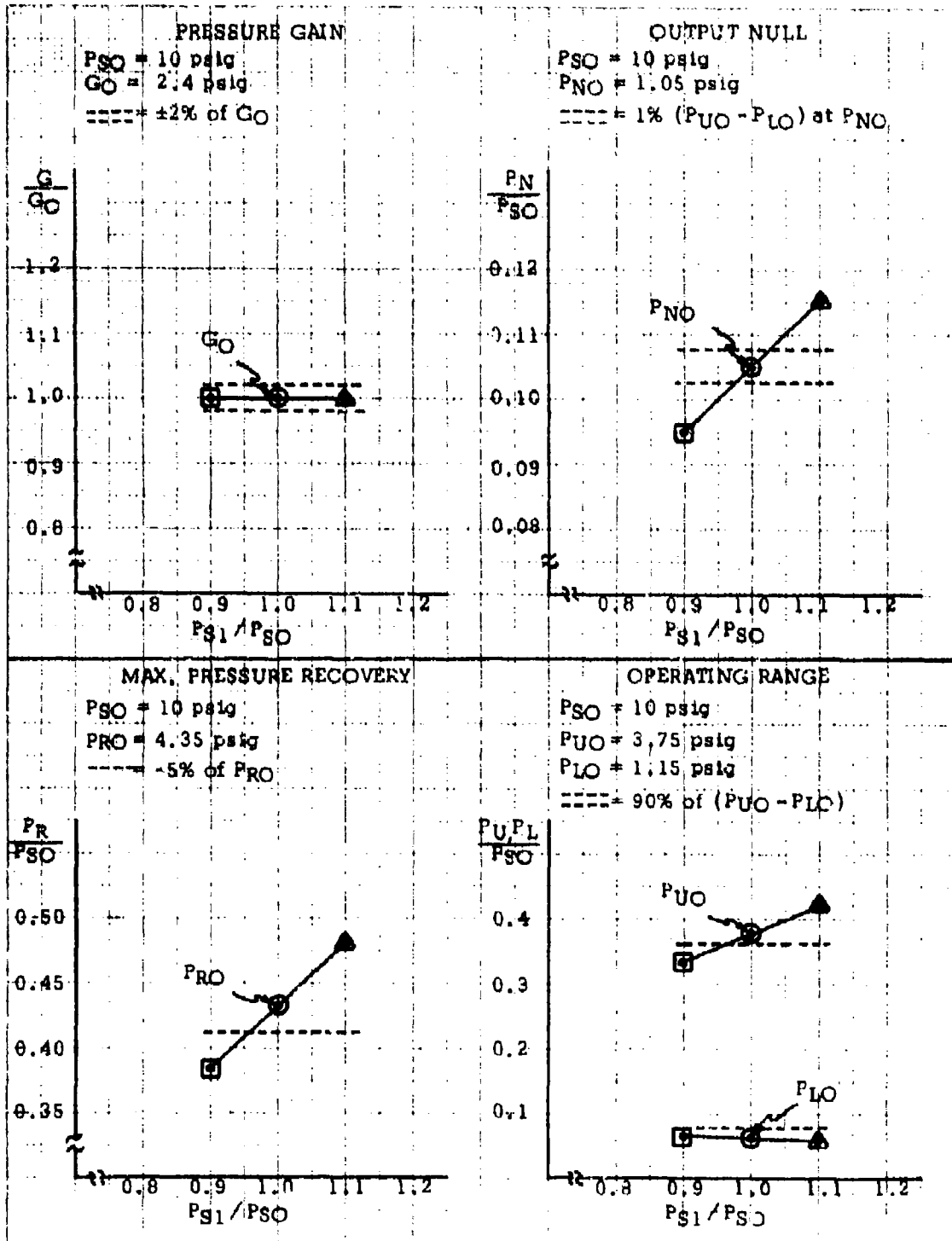
$\frac{P_U P_L}{P_{SO}}$
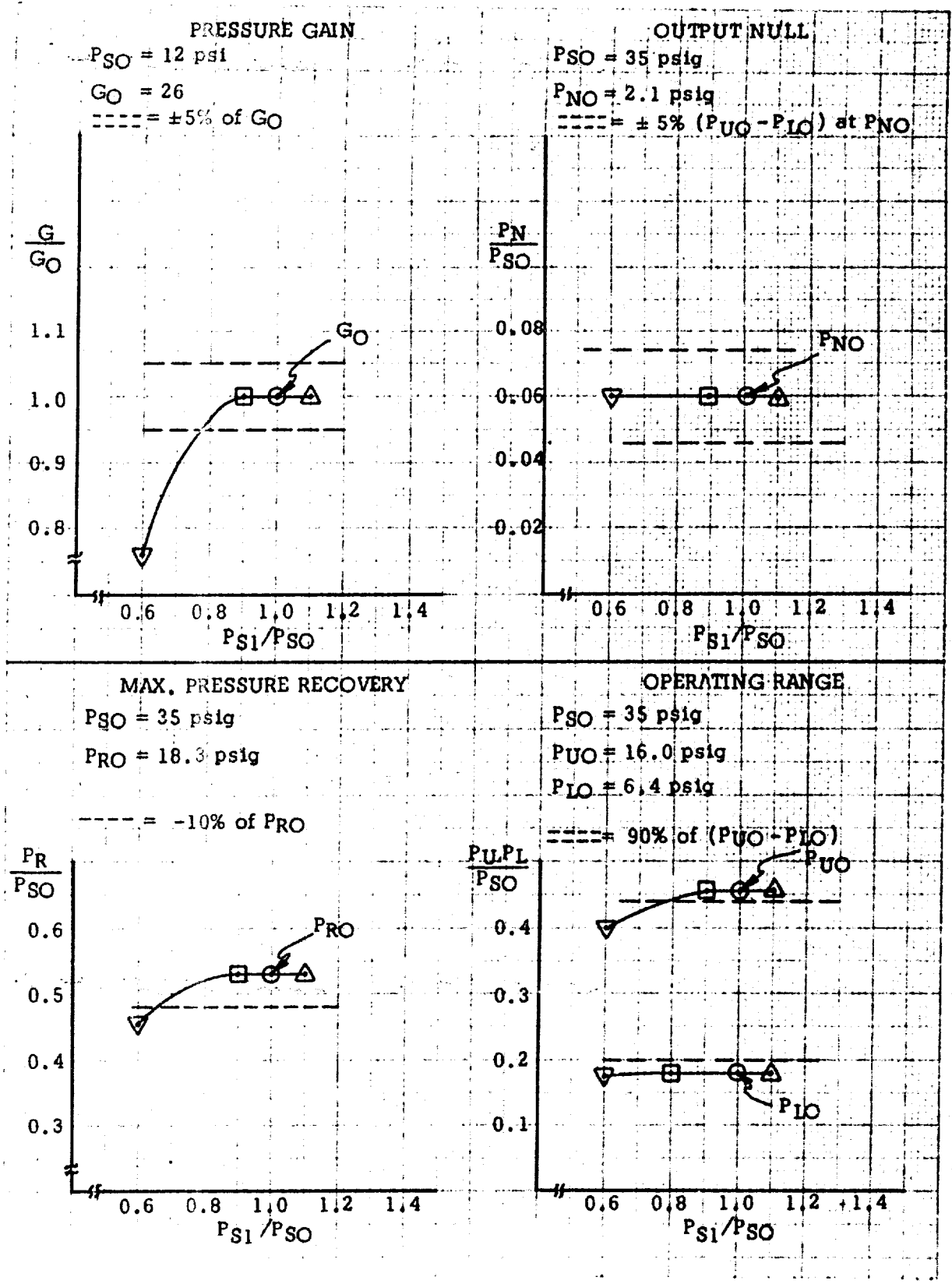
Figure 37. Failure Mode #2 – Supply Pressure Changes
Performance Deviations – 3 Stage Element

87
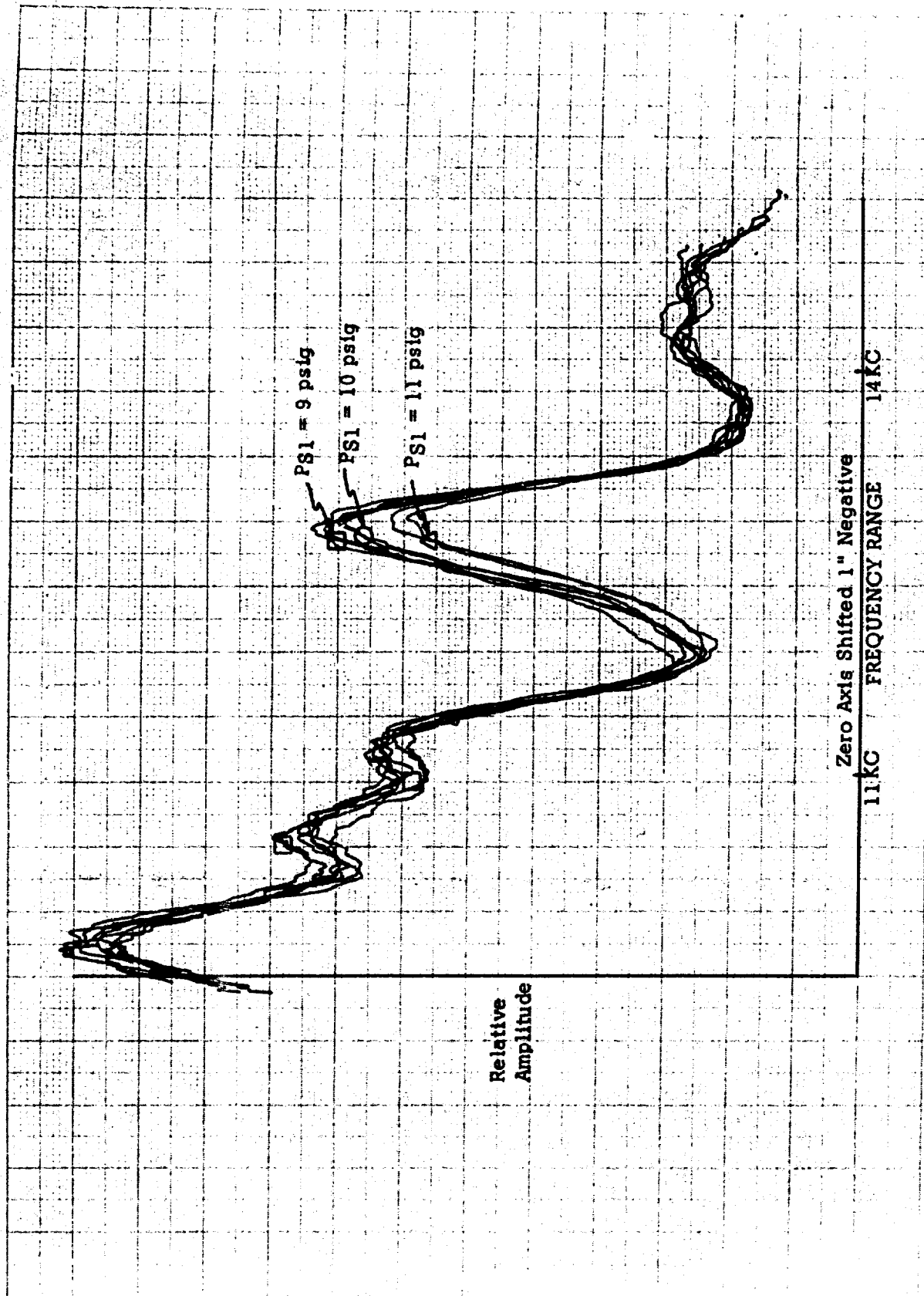
Figure 38. Failure Mode #2 - Supply Pressure Changes
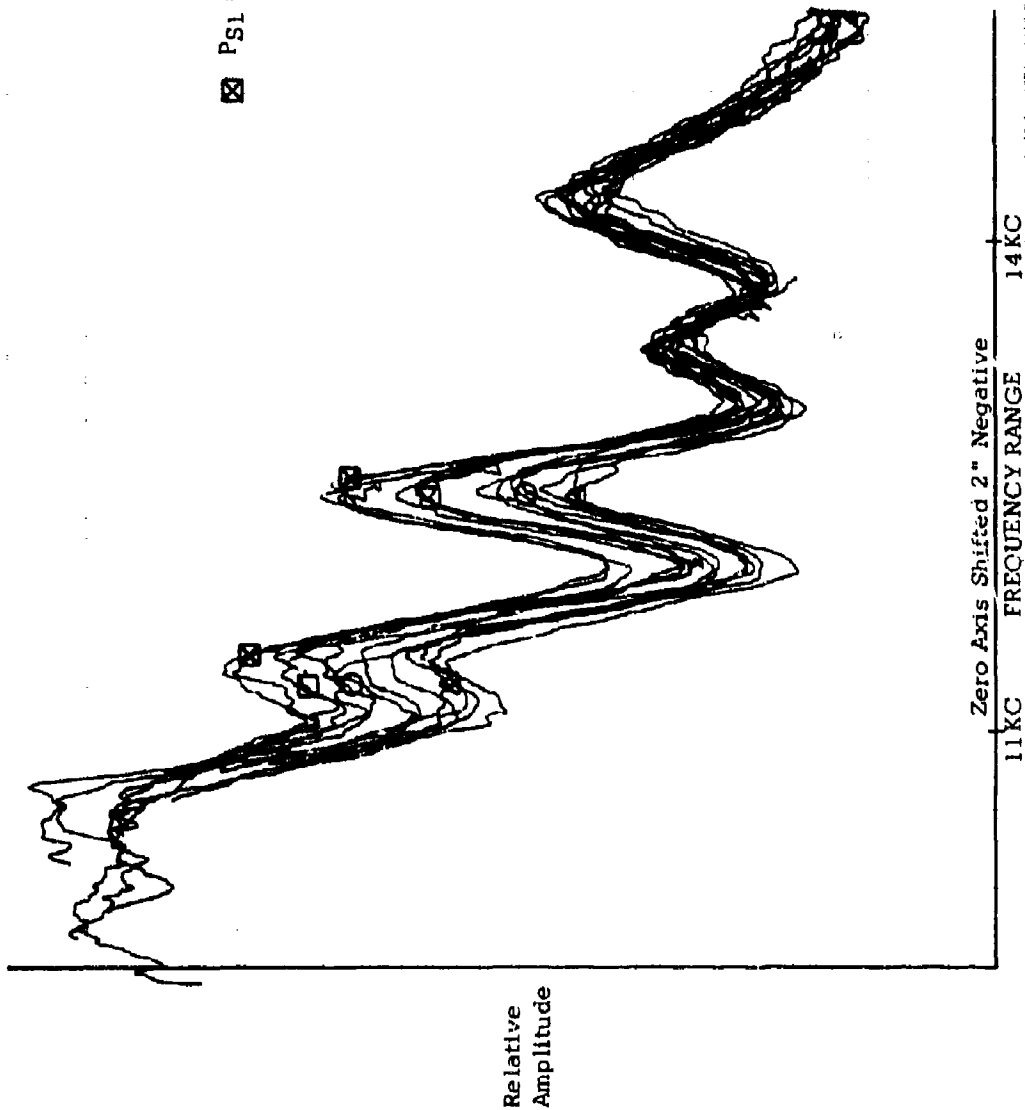Acoustic Signature - 3 Stage Amplifier

Failure Mode #3 - Receiver Contamination

Where the pressure anomalies of failure modes 1 and 2 were conducted on a permanently sealed unit, physical anomalies such as receiver contamination were conducted on a circuit possessing a temporary sealing technique, using hold-down clamps and a gasket seal. This is the primary reason for the changes in the base line primary performance and in the base line acoustic signatures that will be observed during these tests. The contamination induced during these tests is described in part 4.a. of this section, with Table IV defining the area reduction for each of the test modes performed.

Figure 39 shows, for the single element, the changes in primary performance input-output characteristic curves due to the various levels of the anomaly induced. Generated from these curves are the changes in primary performance characteristics, which are shown in Figure 40, along with the allowable performance deviations. All levels of the anomaly induced exceeded the allowable performance deviation limits, indicating the sensitivity of the element to a significant build-up of contamination in the receivers.

Figure 41 shows the changes occurring due to these receiver contamination anomalies, in the secondary acoustic signature. An increase in the signature level with increasing contamination occurs in the 10 KC region, with sensitivity marginally sufficient to detect allowable deviation limits. It should be noted that the signature change due to the particle contamination is easily distinguished from that for the wall build-up contamination. The signature changes due to both wall build-up contamination and a lodged particle differ significantly from the changes due to bias or supply pressure anomalies..

Figure 42 gives the changes in the secondary acoustic signature for the second test mode. The changes in the signature are quite similar to those for the test performed on the single element. This indicates that contamination in one element within a group is detectable.

Figure 43 shows the changes in the input-output characteristics for the third test mode, due to receiver contamination of the first element. Figure 44 shows the resultant changes in the primary performance characteristic of the three stage amplifier. As for the element test, each level of anomaly led to malfunction.

Figure 45 shows the changes caused by these induced anomalies in the secondary acoustic signature for the three stage amplifier. As with the earlier discussed contamination signatures, contamination due to a lodged particle may be easily distinguished. The three stage amplifier signature changes due to receiver contamination also differ distinguishably from those for bias and supply pressure anomalies.

89
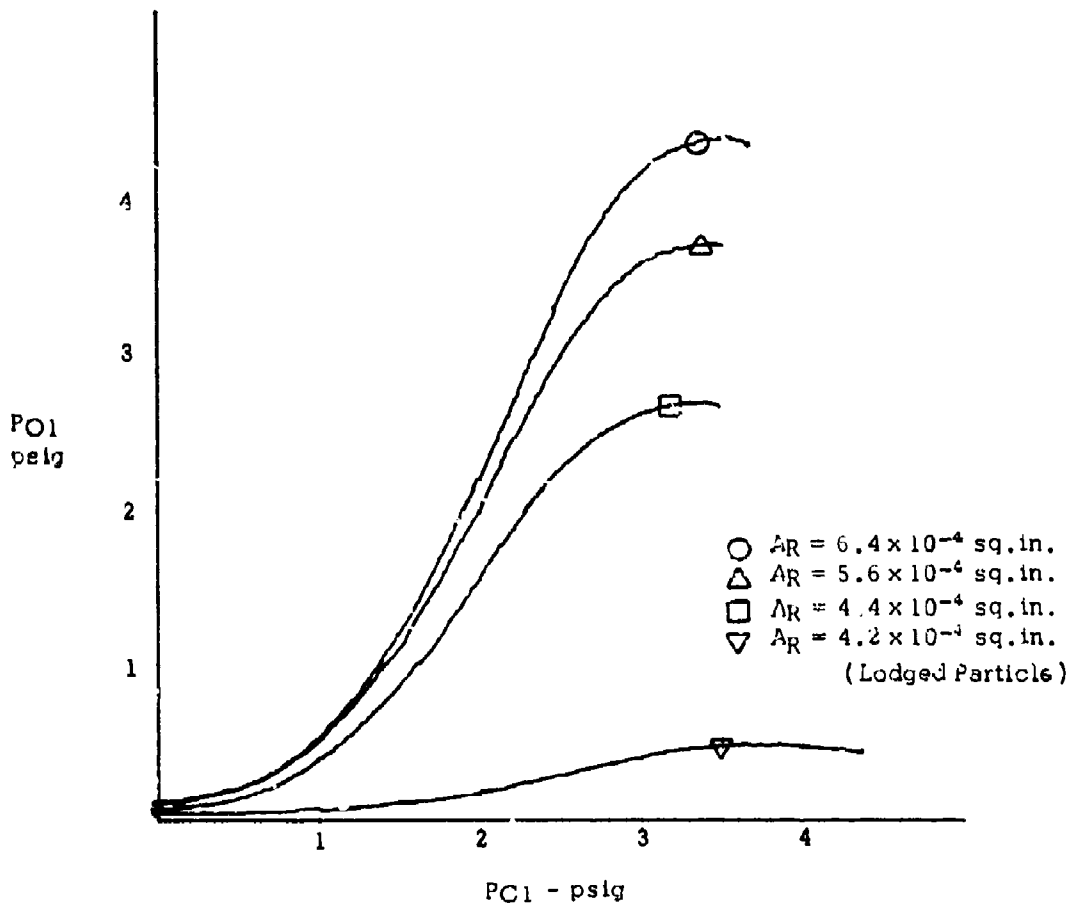
Figure 39. Failure Mode #3 – Receiver Contamination
Primary Performance Curves – Single Element

Figure 40. Failure Mode #3 – Receiver Contamination
Performance Deviation – Single Element

91

Relative
Amplitude

FREQUENCY RANGE
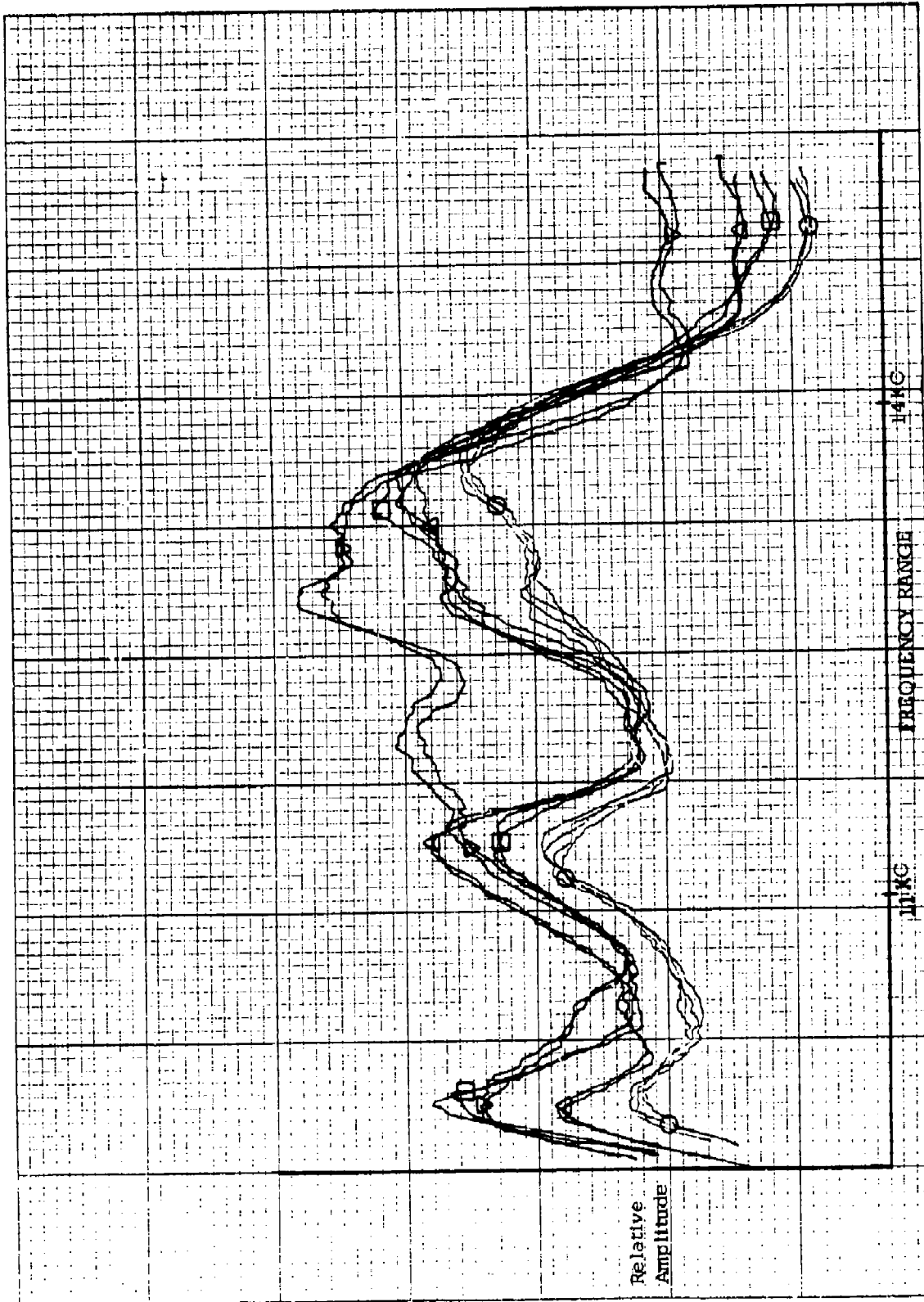
Figure 41. Failure Mode #3 – Receiver Contamination
Acoustic Signature – Single Element

92

Figure 42. Failure Mode #3 - Receiver Contamination
Acoustic Signature - Single Element Plus Decoupled Group
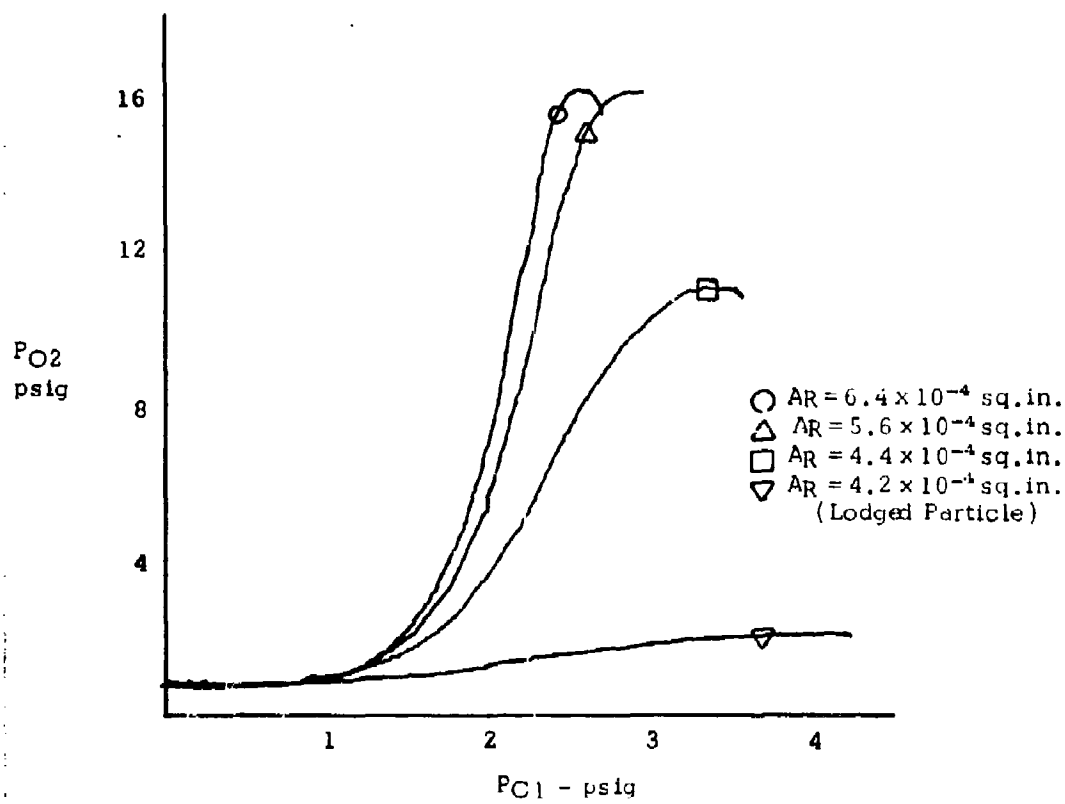
Figure 43. Failure Mode #3 – Receiver Contamination
Primary Performance Curves – 5 Stage Amplifier

PRESSURE GAIN
$P_{SO} = 10$ psig $A_{RO} = 6.4 \times 10^{-4}$ in²
$G_O = 21.2$
==== $= \pm 5\%$ of G_O

OUTPUT NULL
$P_{SO} = 35$ psig $A_{RO} = 6.4 \times 10^{-4}$ in²
$P_{NO} = 2.2$ psig
==== $= \pm 5\%$ $(P_{UO} - P_{LO})$ at P_{NO}

MAX. PRESSURE RECOVERY
$P_{SO} = 35$ psig $A_{RO} = 6.4 \times 10^{-4}$ in²
$P_{RO} = 16.1$ psig
---- $= -10\%$ of P_{RO}

OPERATING RANGE
$P_{SO} = 35$ psig $A_{RO} = 6.4 \times 10^{-4}$ in²
$P_{UO} = 15.2$ psig
$P_{LO} = 5.2$ psig
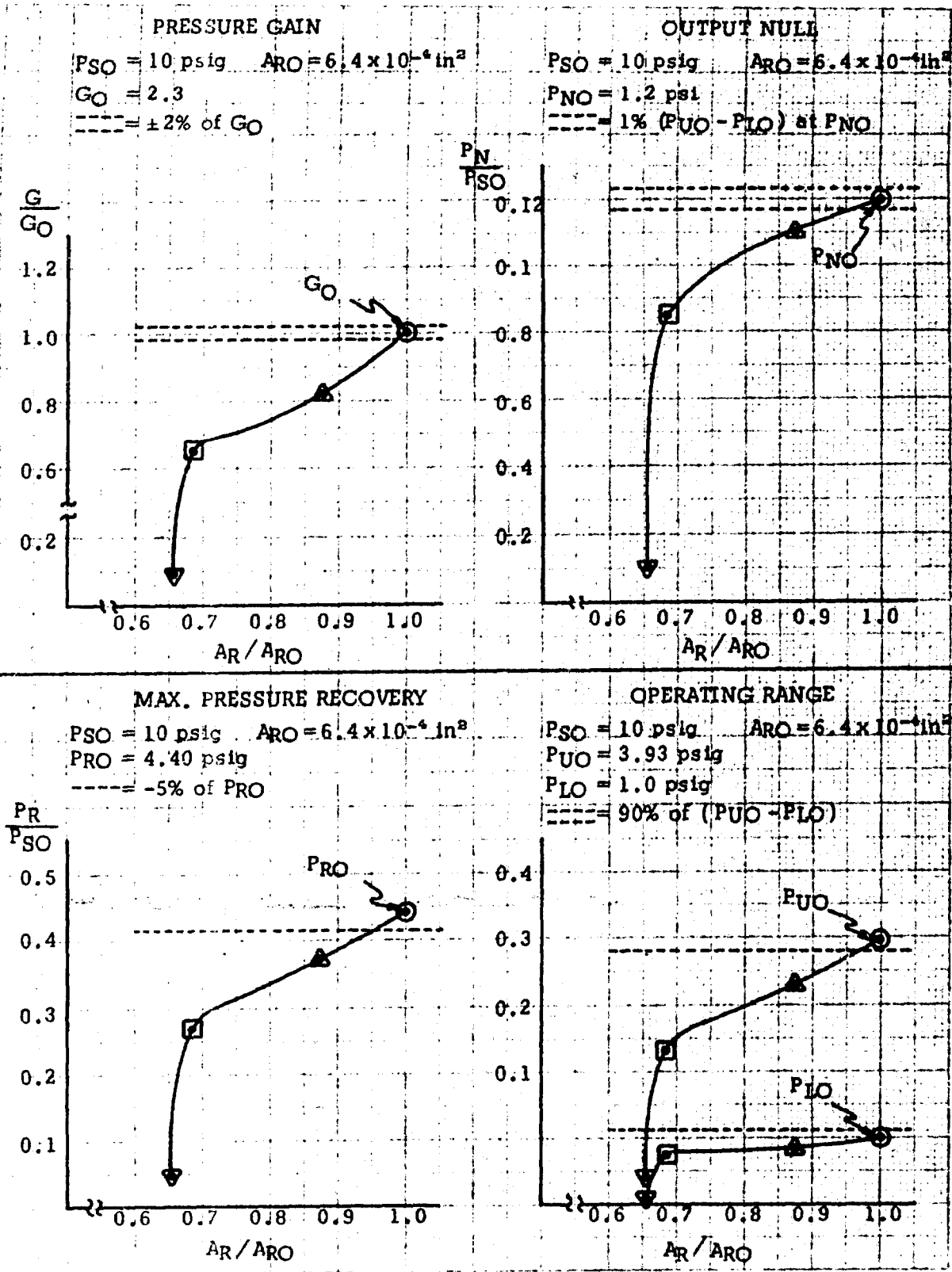==== $= 90\%$ of $(P_{UO} - P_{LO})$
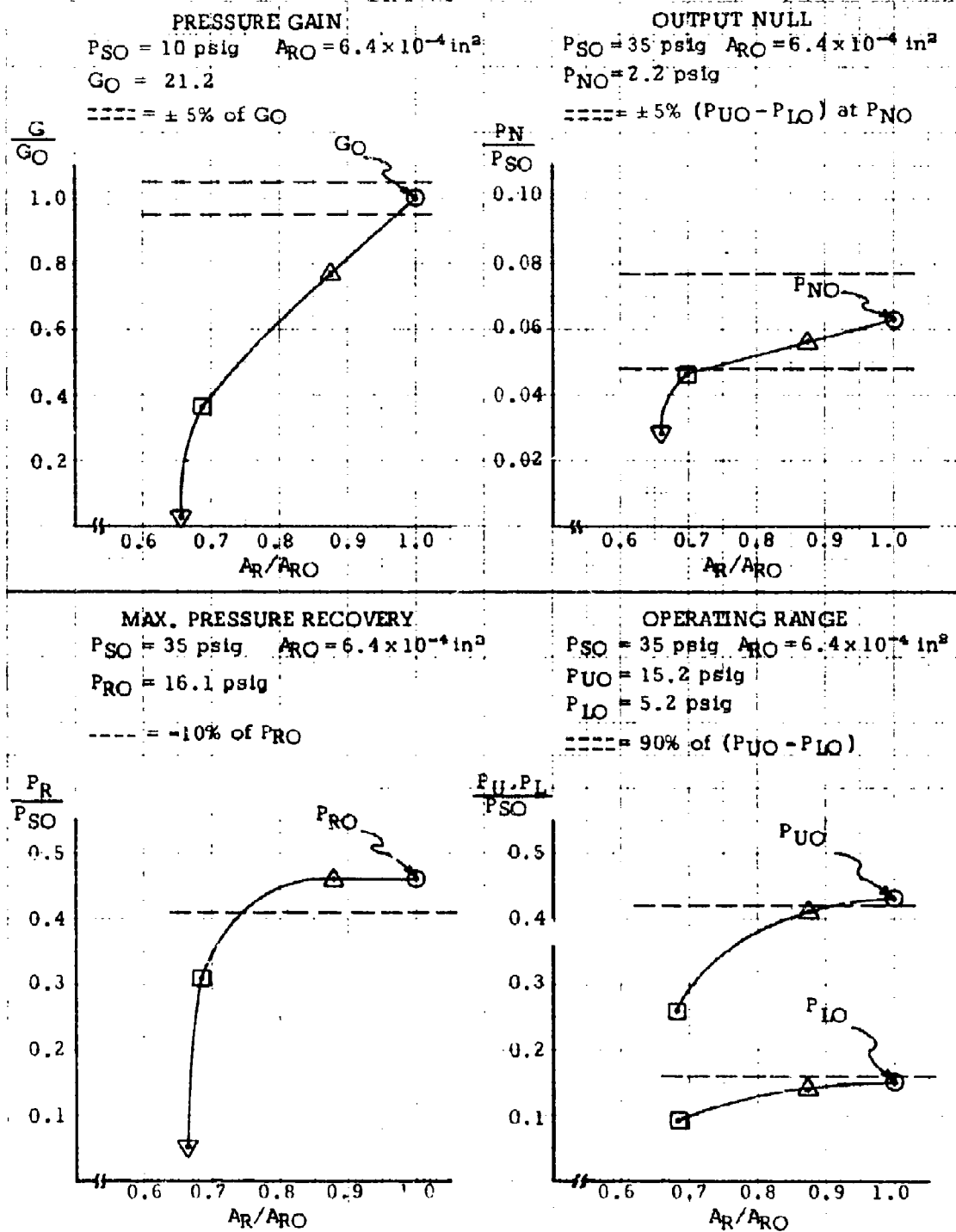
Figure 44. Failure Mode #3 – Receiver Contamination
Performance Deviations – 3 Stage Amplifier

95
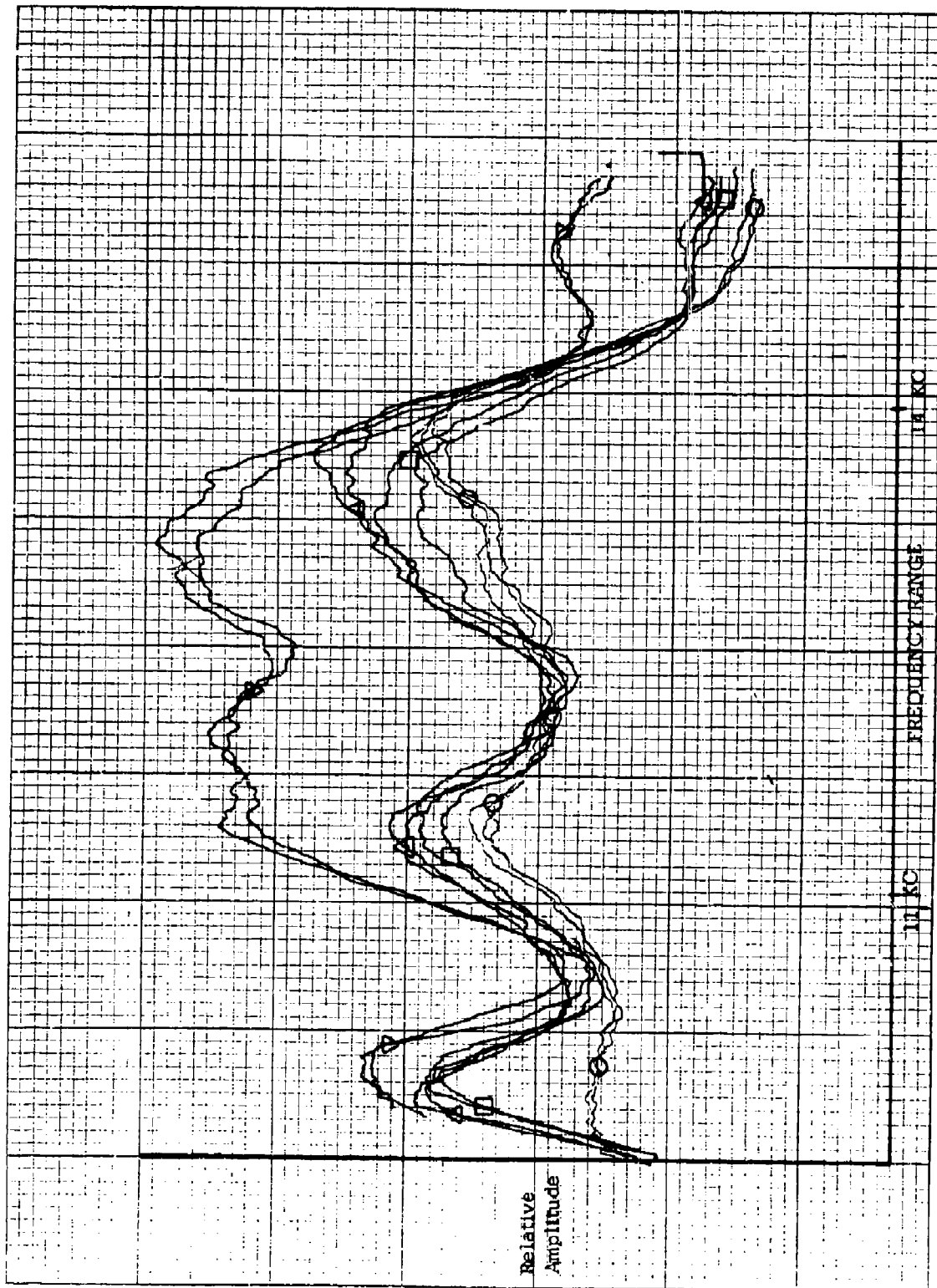
Figure 45. Failure Mode #3 — Receiver Contamination
Acoustic Signature — 3 Stage Amplifier

Failure Mode #4 – Center Vent Closure Anomalies

Center vent closure anomalies were accomplished by connecting
a valve to the center vent with a length of polyflow tubing and
varying the orifice size of the valve. Table IV gives the tabu-
lated orifice size induced for each mode of operation.

Figure 46 gives the input-output characteristics and changes in
these curves for the various center vent closure anomalies for
the first mode of testing. It is shown in this figure the importance
of this center vent because of the changes occurring in these
curves when its area is reduced, and in particular, the erratic
input-output curve that occurs when this center vent is blocked
off. Figure 47 shows the primary performance characteristics
determined from Figure 46. For each level of vent closure,
failure was induced. The allowable limits of null shift prohibit
a vent closure reduction of more than 3%.

Figure 48 shows the changes that occurred in the secondary acoustic
signature due to these center vent closure anomalies. The figure
shows that as the magnitude of the anomaly increased (area de-
creasing), within the bandwidth between 12 to 14 KC, the secon-
dary signature decreases in a logical manner. It is also observed
here that positive going changes occur in the signature, as the
anomaly is increased, at the extreme ends of the signature in the
area of 10 KC and 15 KC. These unique proportional changes that
occur are quite different from those of the anomalies induced
previously, which shows the potential of defining the cause of the
anomaly by typifying signature changes. Better resolution of this
anomaly could be achieved by expanding the scale or increasing the
gain of the detecting circuit.

Figure 49 shows the changes that occurred in the secondary acoustic
signature as the same anomalies were induced into the first stage
element for the second mode of testing. These changes in the sig-
nature occurred in the same manner as that for the first mode of testing.
The results indicate that a typifying signature for this anomaly can
be detected in the presence of other active elements.

Shown in Figure 50 is the primary input-output characteristic curves
for the third mode of testing with Figure 51 showing the primary per-
formance data determined from the input-output curves. The first
level of closure causes malfunction by unacceptably reducing the
operating range. The second and third levels of closure causes a
highly erratic output signal.

97

Figure 52 shows the changes occurring in the secondary acoustic signature for the three stage amplifier as the anomalies were induced into the first element. These changes are similar to those occurring in Figure 48 for the single element test and those occurring in Figure 49 for the single element within a group of elements. This test shows the potential of defining the anomaly due to the characteristic of a decreasing signature in the 13 KC area with an increasing signature at the ends of the bandwidth at 10 KC and 15 KC. The decreased in amplitude at 13 KC from the nominal to the first level of closure appears sufficient to detect the allowable level of this anomaly.
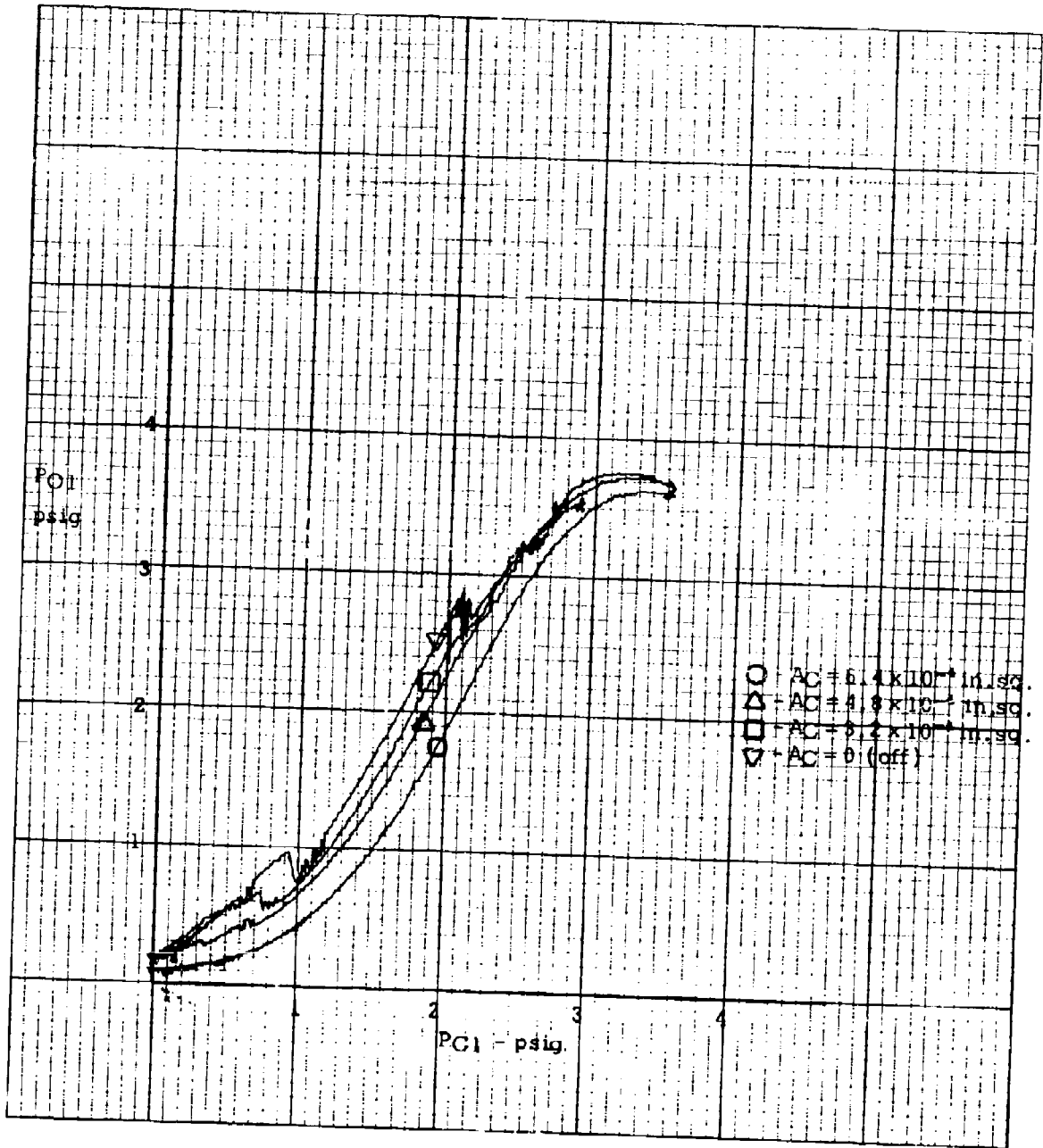
Figure 46. Failure Mode #4 - Center Vent Closure
Primary Performance Curve - Single Element

99

PRESSURE GAIN

$P_{SO} = 10$ psig $A_{CO} = 6.4 \times 10^{-4}$ in^2
$G_O = 2.0$

$\mathtt{----} = \pm 2\%$ of G_O
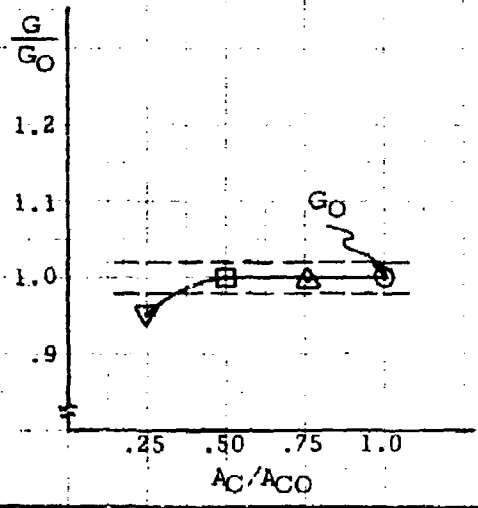
OUTPUT NULL

$P_{SO} = 10$ psig $A_{CO} = 6.4 \times 10^{-4}$ in^2
$P_{NO} = 0.96$ psig

$\mathtt{----} = \pm 1\%$ $(P_{UO} - P_{LO})$ at P_{NO}

$\dfrac{G}{G_O}$

1.2

1.1

1.0

.9

G_O

.25   .50   .75   1.0
A_C/A_{CO}

$\dfrac{P_N}{P_{SO}}$

0.20

0.15

0.1

0.05

P_{NO}

.25   .50   .75   1.0
A_C/A_{CO}
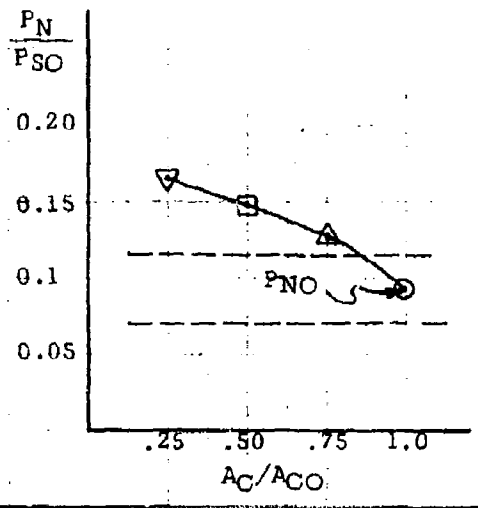
MAX. PRESSURE RECOVERY

$P_{SO} = 10$ psig $A_{CO} = 6.4 \times 10^{-4}$ in^2
$P_{RO} = 3.75$

$\mathtt{----} = -5\%$ of P_{RO}
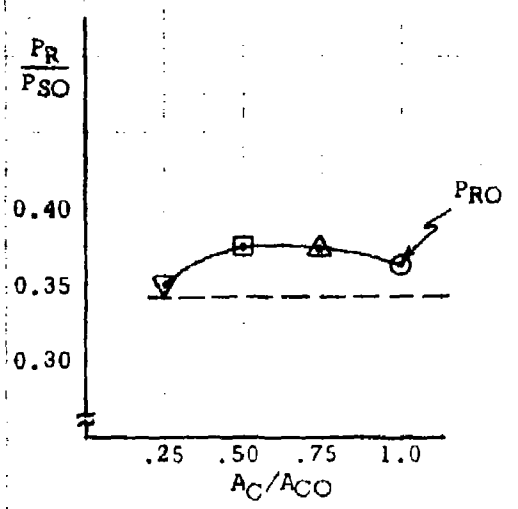
OPERATING RANGE

$P_{SO} = 10$ psig $A_{CO} = 6.4 \times 10^{-4}$ in^2
$P_{UO} = 3.05$ psig

$\mathtt{----} = 90\%$ of $(P_{UO} - P_{LO})$

$\dfrac{P_R}{P_{SO}}$

0.40

0.35

0.30

P_{RO}

.25   .50   .75   1.0
A_C/A_{CO}

$\dfrac{P_U, P_L}{P_{SO}}$

0.30

0.20

0.10

P_{UO}

P_{LO}

.25   .50   .75   1.0
A_C/A_{CO}
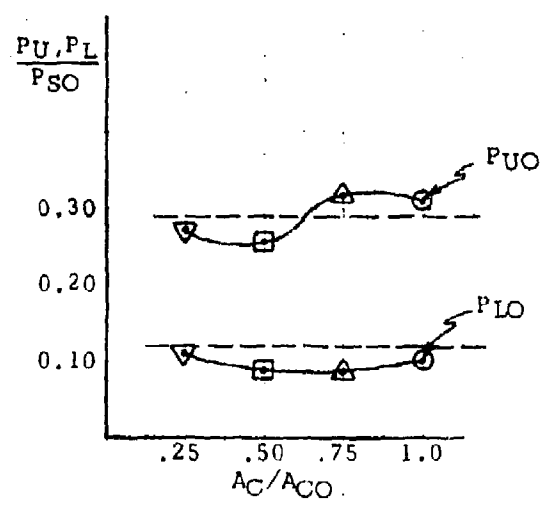
Figure 47. Failure Mode #4 – Center Vent Closure
Performance Deviations – Single Element

100
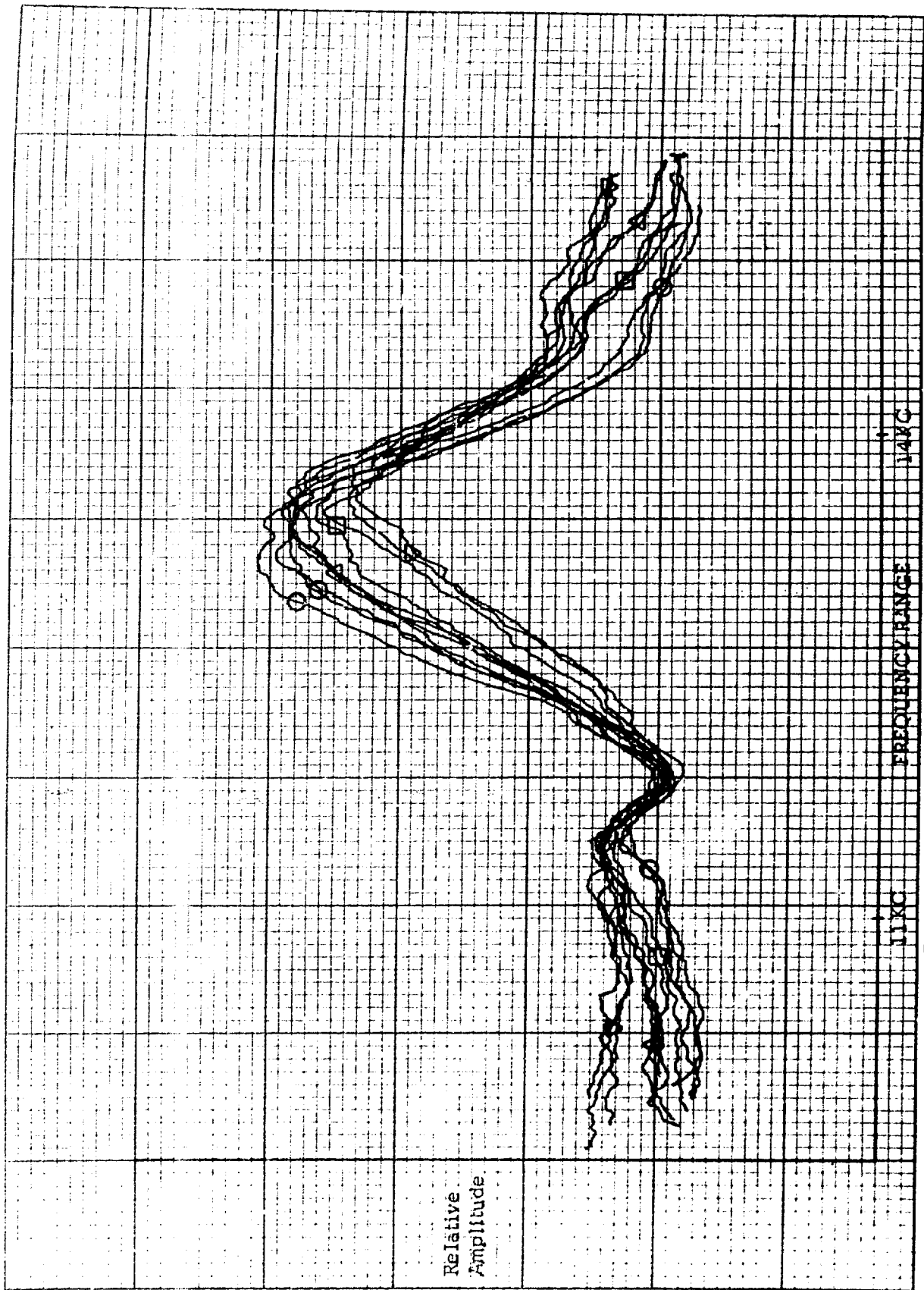
Figure 48. Failure Mode #4 – Center Vent Closure
Acoustic Signature – Single Element

Relative
Amplitude

1KC   FREQUENCY RANGE   19KC
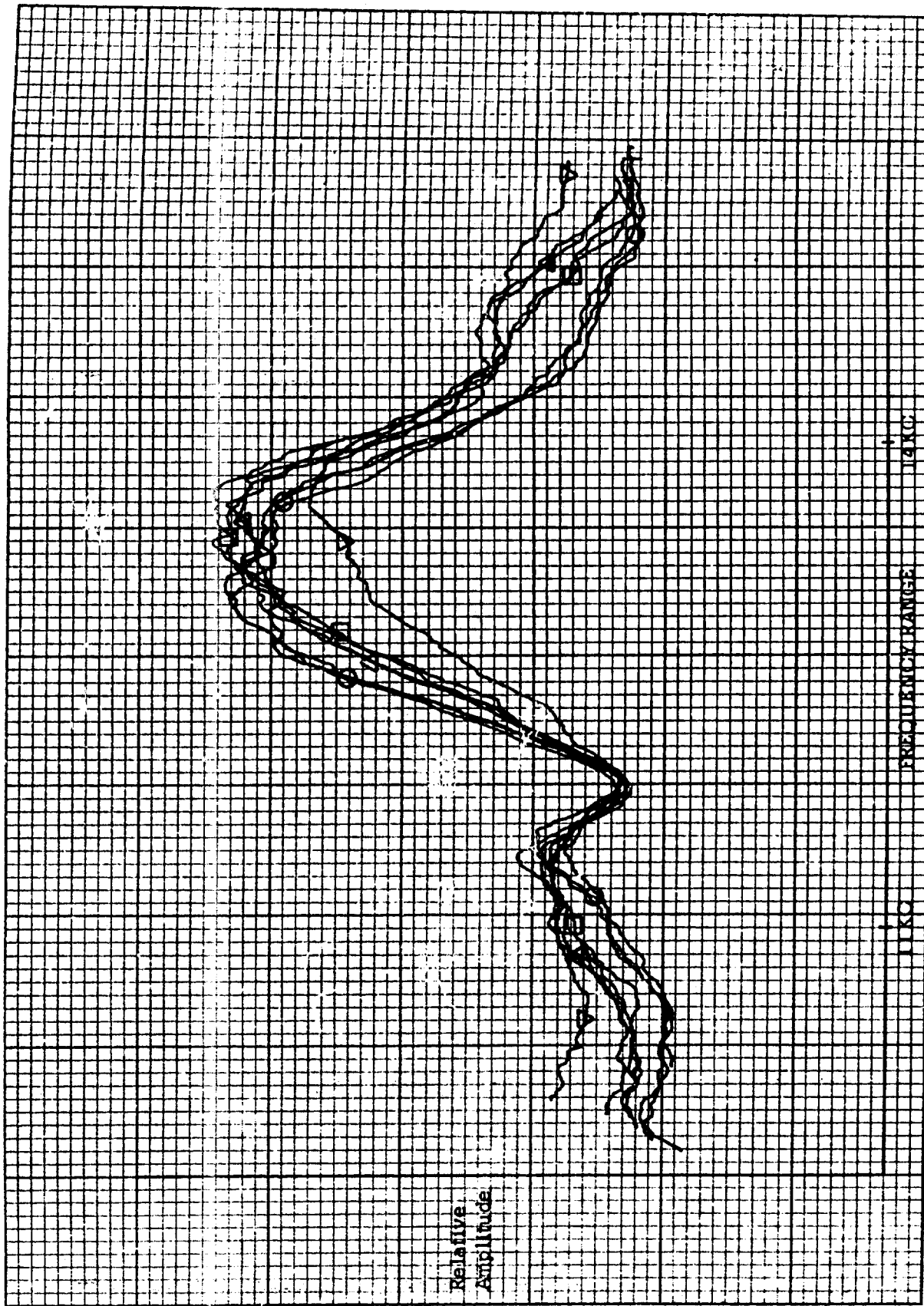
Figure 49. Failure Mode #4 – Center Vent Closure
Acoustic Signature – Single Element Plus Decoupled Group
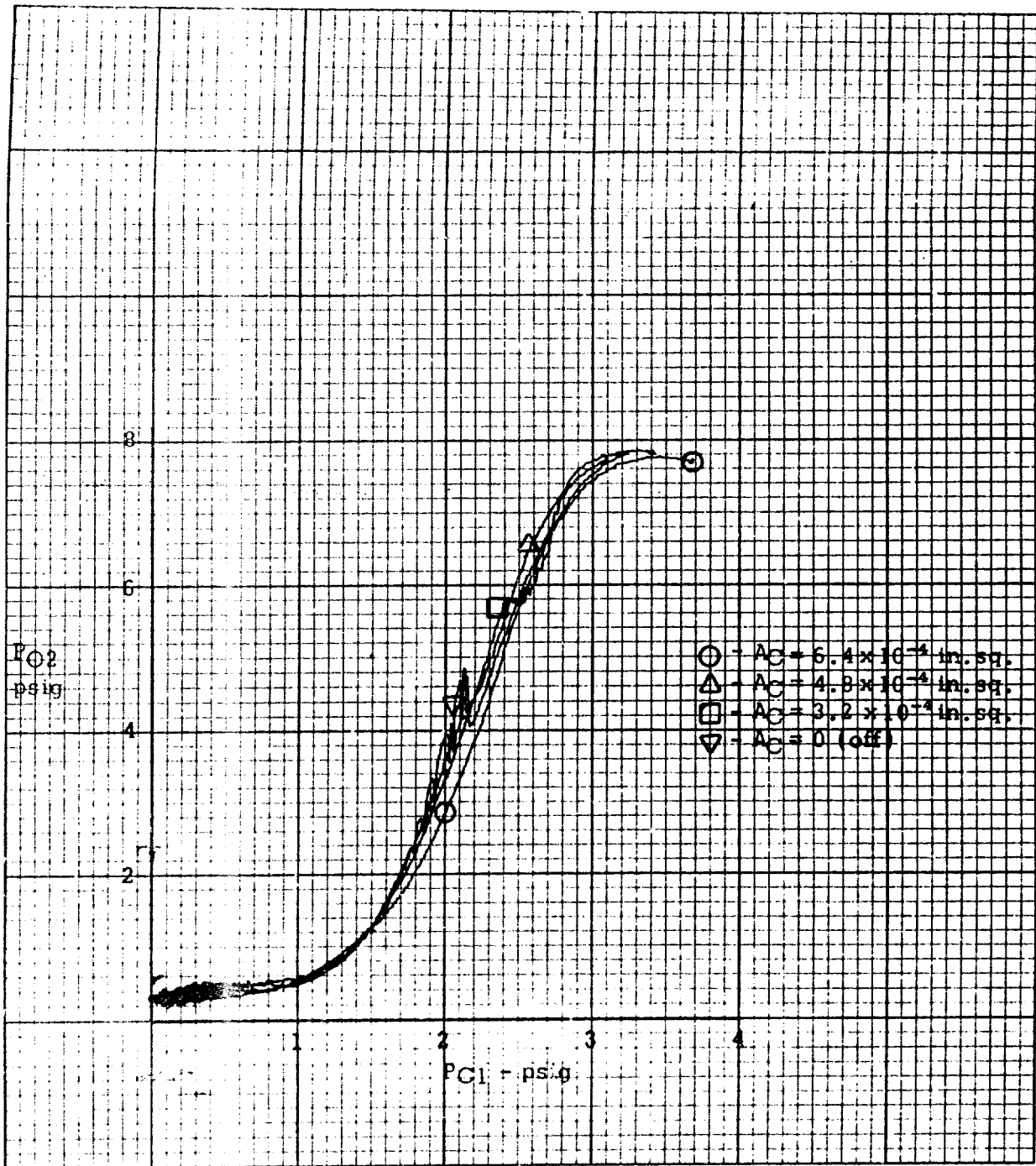
Figure 50. Failure Mode #4 – Center Vent Closure
Primary Performance Curves – 3 Stage Amplifier

103

PRESSURE GAIN

$P_{SO} = 10$ psig $A_{CO} = 6.4 \times 10^{-4}$ in^2
$G_O = 5.7$
‒ ‒ ‒ = ±5% of G_O
▨ = Erratic Signal

$\dfrac{G}{G_O}$

OUTPUT NULL

$P_{SO} = 35$ psig $A_{CO} = 6.4 \times 10^{-4}$ in^2
$P_{NO} = 1.25$ psi
==== = ±5% $(P_{UO} - P_{LO})$ at P_{NO}

$\dfrac{P_N}{P_{SO}}$

1.1
1.0
0.9
0.8

G_O

0.06
0.05
0.04
0.03

P_{NO}

.25   .50   .75   1.0
A_C/A_{CO}

.25   .50   .75   1.0
A_C/A_{CO}

MAX. PRESSURE RECOVERY

$P_{SO} = 35$ psig $A_{CO} = 6.4 \times 10^{-4}$ in^2
$P_{RO} = 7.7$ psig
‒ ‒ ‒ ‒ = -10% of P_{RO}

$\dfrac{P_R}{P_{SO}}$

OPERATING RANGE

$P_{SO} = 35$ psig $A_{CO} = 6.4 \times 10^{-4}$ in^2
$P_{UO} = 6.6$ psig
$P_{LO} = 2.2$ psig
==== = 90% of $(P_{UO} - P_{LO})$

$\dfrac{P_U P_L}{P_{SO}}$

0.4
0.3
0.2
0.1

P_{RO}

0.4
0.3
0.2
0.1

P_{UO}
P_{LO}

.25   .50   .75   1.0
A_C/A_{CO}

.25   .50   .75   1.0
A_C/A_{CO}
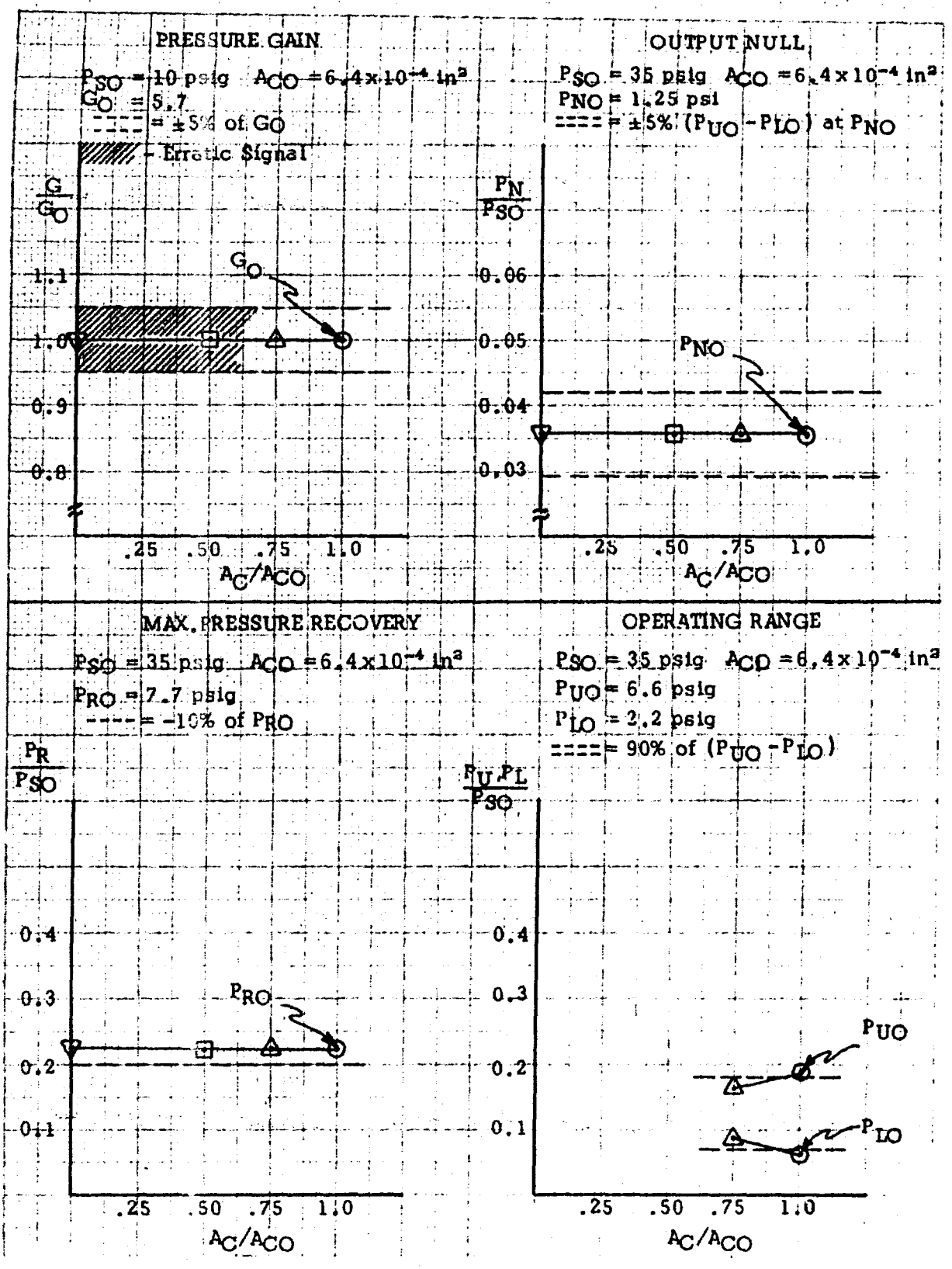
Figure 51.   Failure Mode #4 – Center Vent Closure
Performance Deviations – 3 Stage Amplifier

104
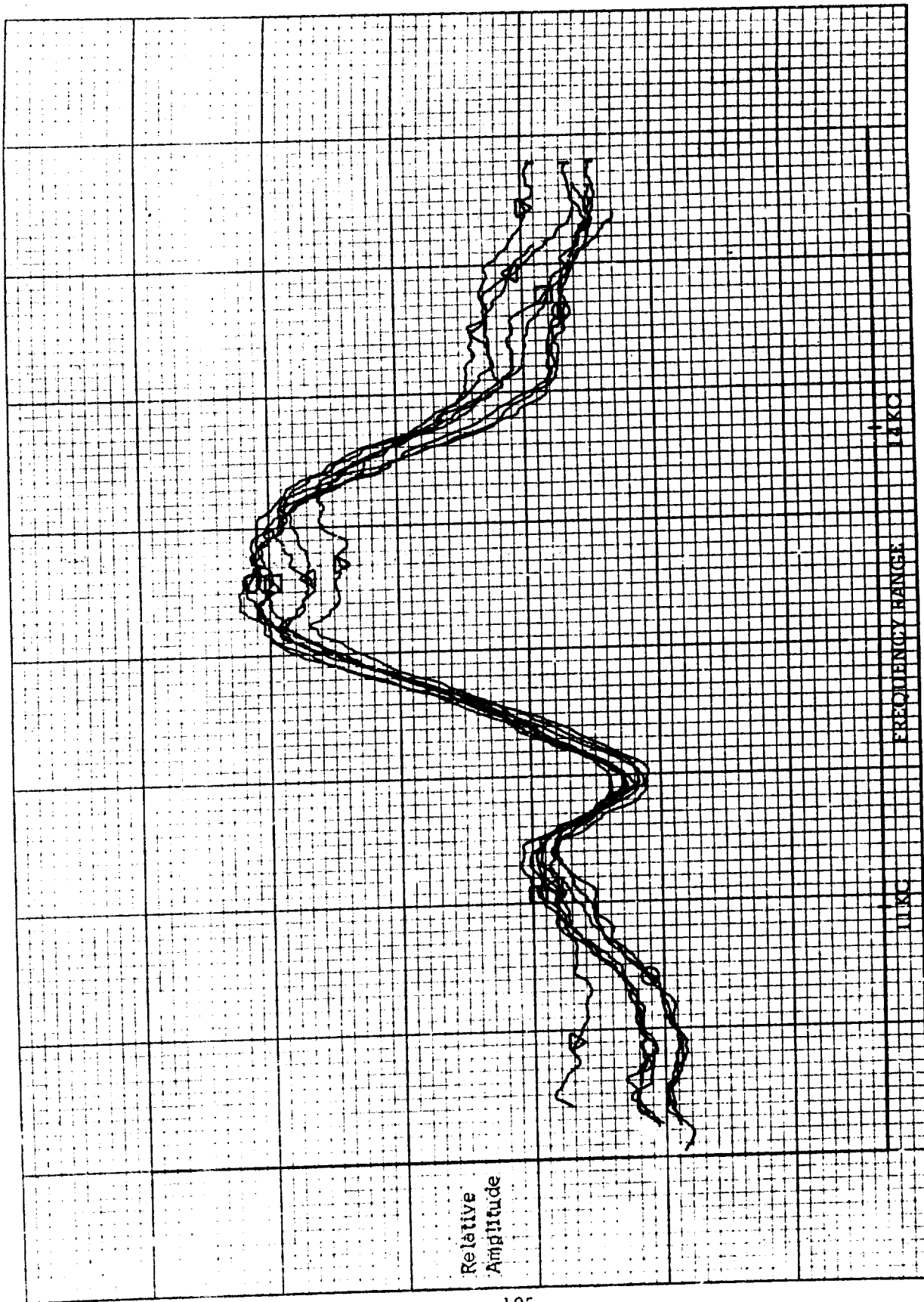
Figure 52. Failure Mode #4 – Center Vent Closure
Acoustic Signature – 3 Stage Amplifier

105

Failure Mode #5 - Splitter Chipping Anomalies

Figure 53 shows the changes that occurred in the primary performance input-output curves for chipping of the splitter tip between the center vent and the P_{O1} output leg. A reduction of 0.005 in. produced a relatively small (but unacceptable) change in the primary characteristic input-output curves while a reduction of 0.020 in. produced quite a substantial change. Figure 54 shows the changes in the primary performance characteristic. The 0.020 inch reduction exceeded the allowable performance deviation limits in all the performance characteristics, while 0.005 chipping caused the limits of gain only to be exceeded, the limit on chipping being approximately .004 inches.

Figure 55 shows the changes in the secondary acoustic signature for the single element, caused by the chipping of the splitter. These changes show that the changes in performance degradation is detectable with sufficient resolution to detect the allowable degradation limit. This anomaly effects changes in the signature which differ from changes due to prior anomalies.

Figure 56 shows the changes that occurred in the secondary signature for the second mode of testing. Resolution is satisfactory. While similarities do exist between the signature changes for this case and for the single element, the similarity is not as good as with prior anomaly tests. It is probable that this was due to damage to the circuit plate. It is anticipated that the chipping of a splitter in one element may be both detected and defined where in the presence of other active elements.
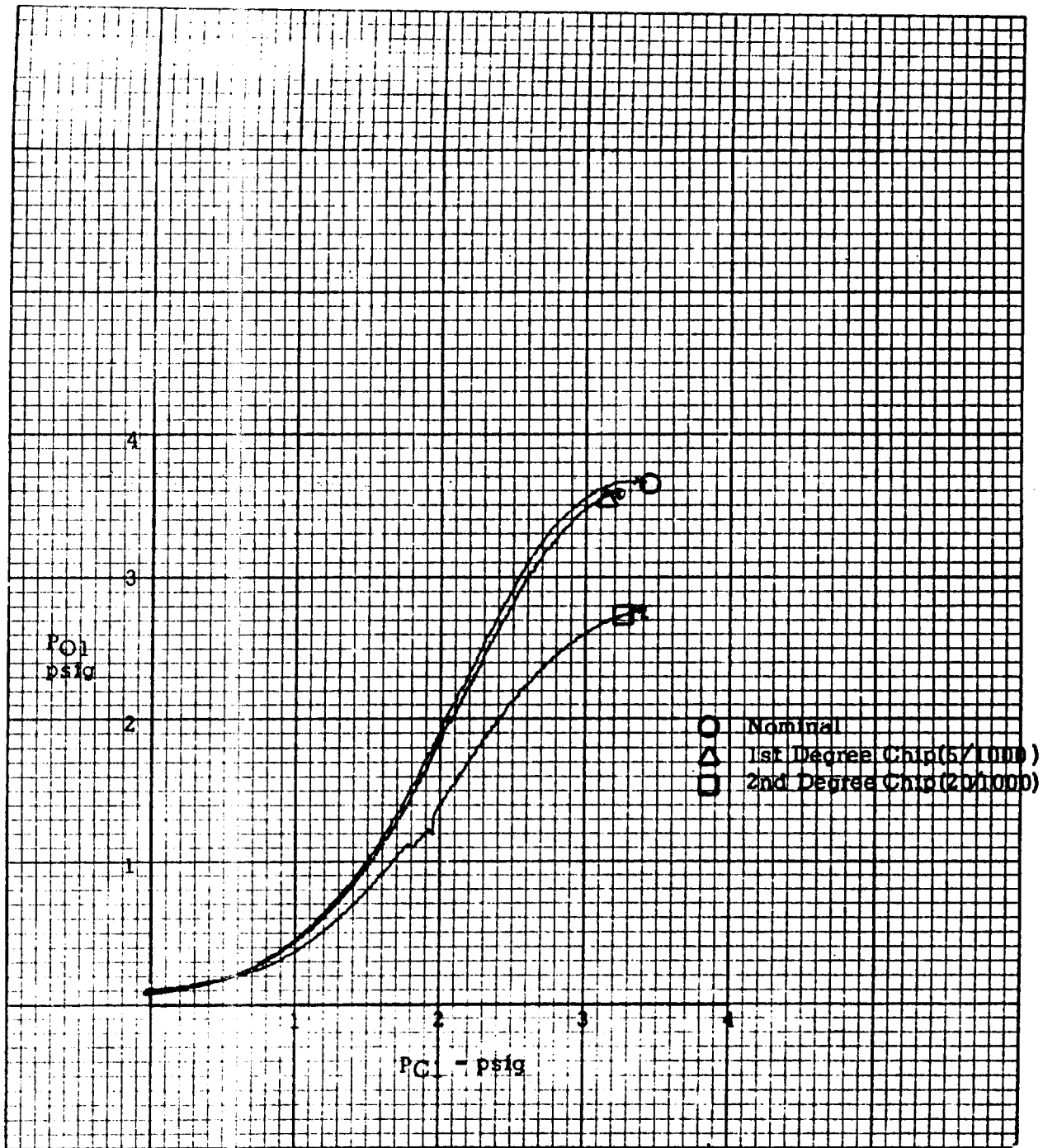
Figure 53. Failure Mode #5 - Chipped Splitter
Primary Performance Curves - Single Element

107
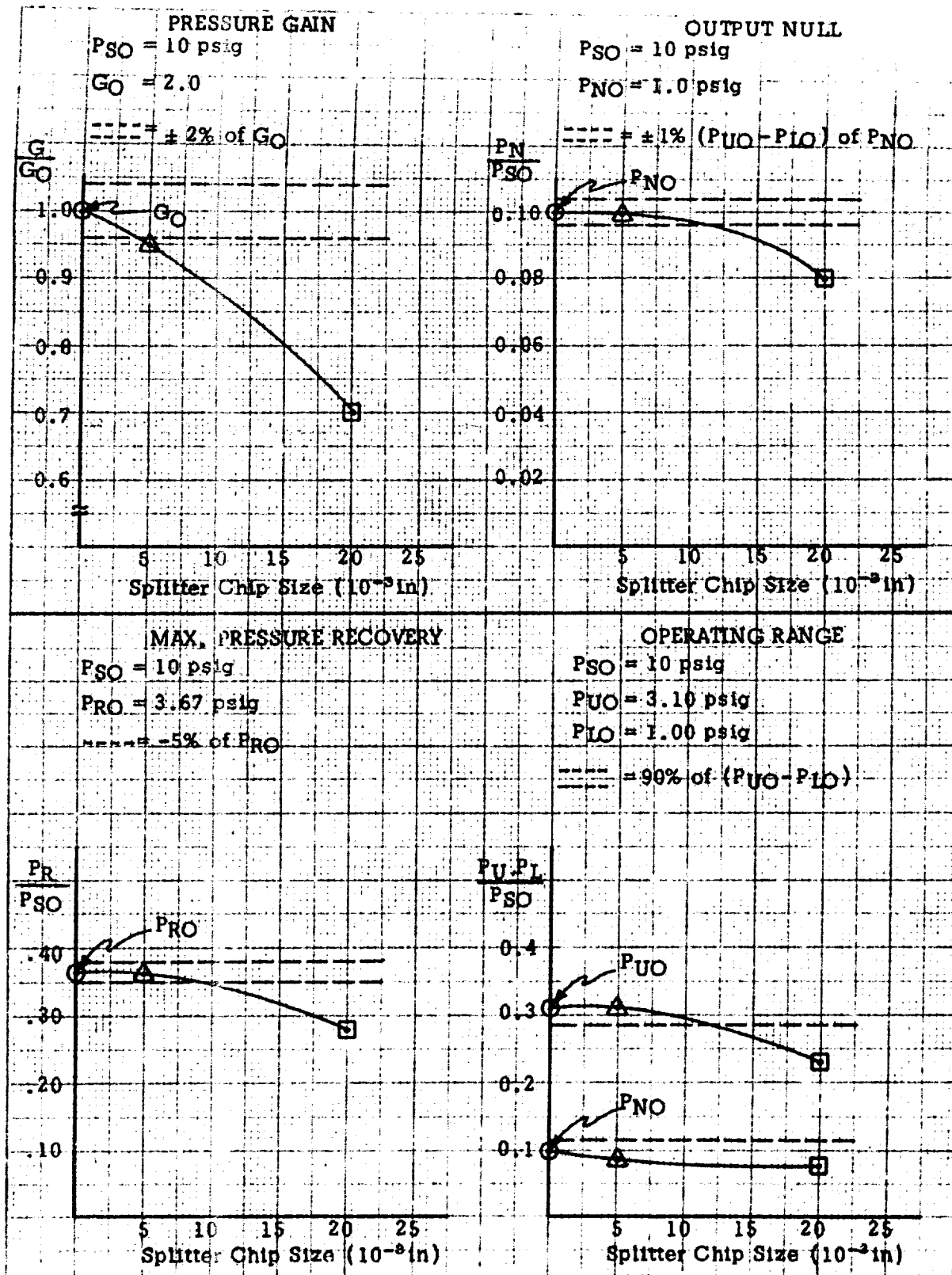
Figure 54. Failure Mode #5 - Chipped Splitter
Performance Deviations - Single Element
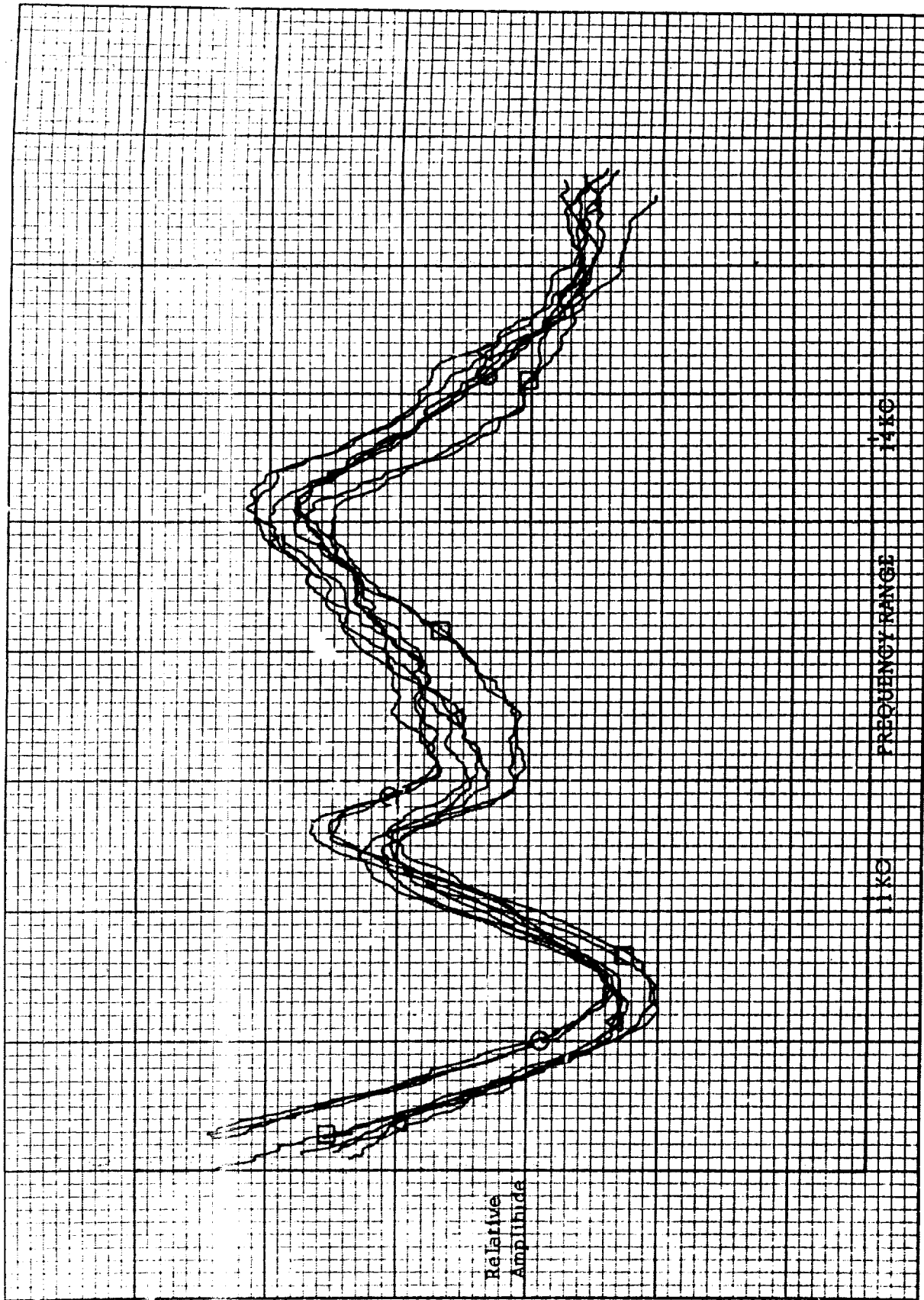
Figure 55. Failure Mode #5 – Chipped Splitter
Acoustic Signature – Single Element plus Decoupled Group
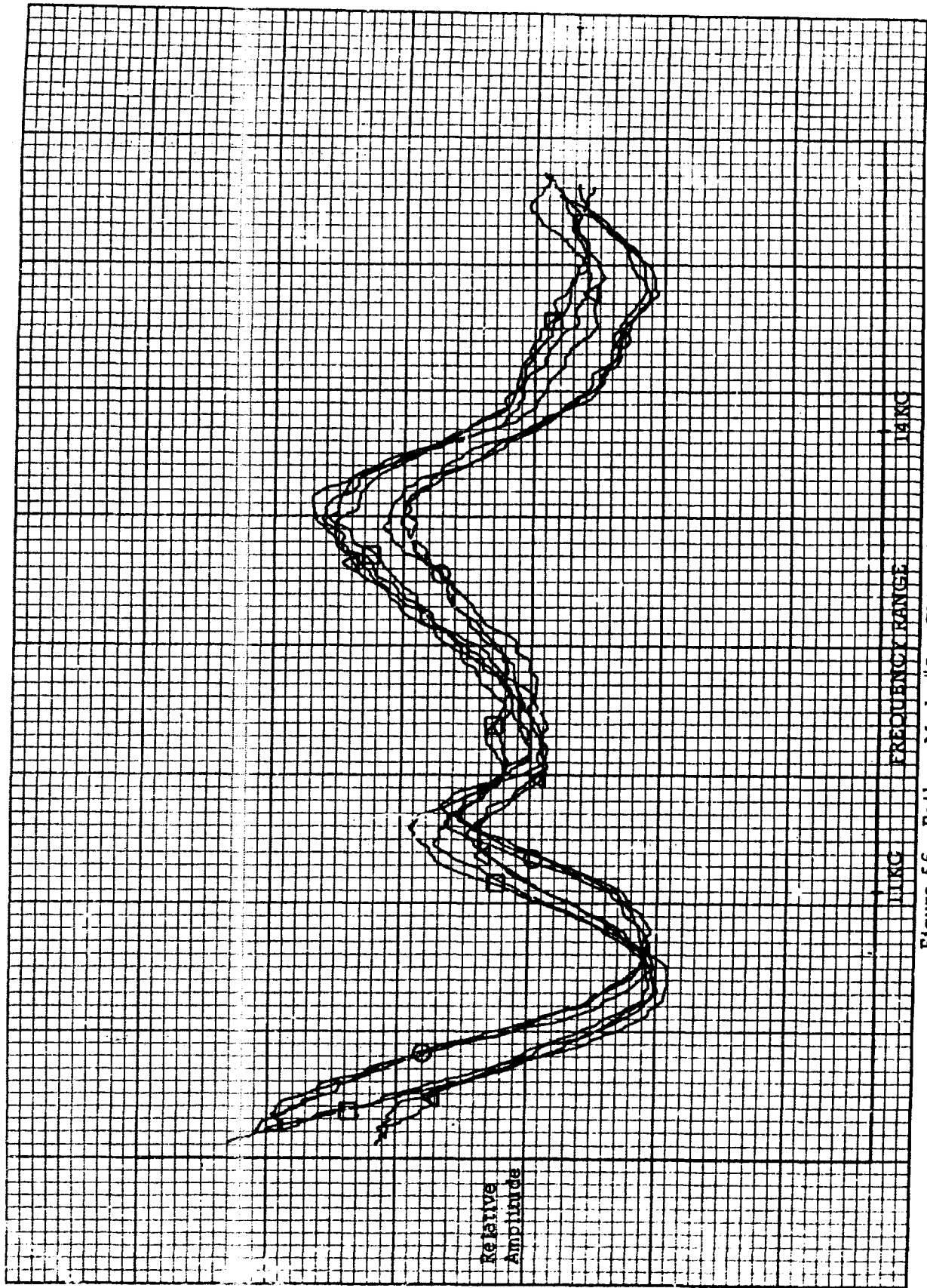
Figure 56. Failure Mode #5 - Chipped Splitter
Acoustic Signature - Single Element

Relative
Amplitude

FREQUENCY RANGE

11KC

14KC

d. Conclusions

In summary, the results of this test series were highly encouraging. In a large percentage of cases sufficient resolution was realized to permit detection of the level of anomaly leading to malfunction of an element and of a 3 stage amplifier circuit.

Comparison of the signatures for the various anomalies shows that typifying differences in signature changes do exist, permitting definition of failure causes. Consideration of the second test mode results indicate that the typifying signature changes associated with an anomaly of an element were not washed out by the acoustic noise of other non-connected but adjacent elements. The changes in the signature of the three stage amplifier circuit were shown to permit the detection of allowable magnitudes of induced anomalies, with differences in the signature changes permitting definition of the various anomalies.

It was concluded from these tests that secondary acoustic sensing techniques exhibit a high potential as a successful means of detecting and defining the anomalous conditions causing the malfunction of analog circuitry.

5. EVALUATION OF SENSORS APPLIED TO DIGITAL ELEMENTS

This section and section 6. present the results of laboratory tests to evaluate sensors for use in monitoring the performance of digital circuitry. This section deals with tests conducted with an element while section 6. deals with tests of a simple digital circuit.

The total group of candidate sensors selected for consideration during this program, along with a description of each of the sensors, is presented in Section III of this report. Considering the characteristics of the individual sensors relative to the performance characteristics and the types of failure of digital elements to be detected, as discussed by Section IV, the following group of sensors were selected as potentially applicable to check out of digital elements and circuits.

- o   Miniature pressure transducer

- o   Hot wire anemometer

- o   Piezoelectric crystal

- o   Accelerometer

- o   Microphone.

111

Included within the total group of sensors were thermistors and an infrared thermometer. It was concluded from an evaluation of these two sensors, as reported by parts 2. and 3. of this section, that neither sensor offers a high degree of applicability to Fluidic systems checkout. These sensors are consequently excluded from the above group.

In the following, the test procedure is discussed, the test setup and instrumentation are described, and the results of laboratory tests are presented.

a.   Test Procedure

Figure 57 shows the digital test element. It is a model 1715A OR/NOR Gate. The input and output channels were elongated to permit the installation of multiple instrumentation for sensor performance comparison. Also shown in Figure 57 are the location of the primary performance sensors and the location of induced physical anomalies.

The Fluidic OR/NOR Gate functions in the following manner. A continuous supply pressure, P_S, effects a power jet which is directed into one of the two output channels, depending upon the input signal rate. A signal into any of the P_C inputs generates an output at P_{O1}. This, then, is the OR output. For no inputs only, the element switches to output P_{O2}, this being the NOR output. The wall attachment effect on the OR side is negated by a spoiling vent, hence the jet will be directed to the OR side only when one or more of the input signals are active.

The test element was sealed with a single-sided sticky tape, clamped down by a Plexiglas cover plate (approximately 1/2 inch thick) which was fastened by screws to the circuit. This arrangement permitted the sealing and unsealing of the element in order to induce physical anomalies. The screws clamping the Plexiglas cover to the circuit were torqued to the same value each time the element was reassembled, thus producing a reasonably repeatable seal and repeatable operating characteristics.

Two modes of test were conducted on this OR/NOR Gate. First, satisfactory performance tests produced the necessary data to evaluate the primary performance sensors and to determine and record the base line acoustic signature to be used as a reference. Second, anomaly tests were conducted to provide primary and secondary performance data as various pressure and physical anomalies were induced.

Dynamic input signals were generated by a Fluidic oscillator and directed into the digital element. These inputs were of nominally a square wave. The input and output signals were monitored by a number of primary sensors which were paired to permit comparative evaluation in sensing the same signal. The output

112
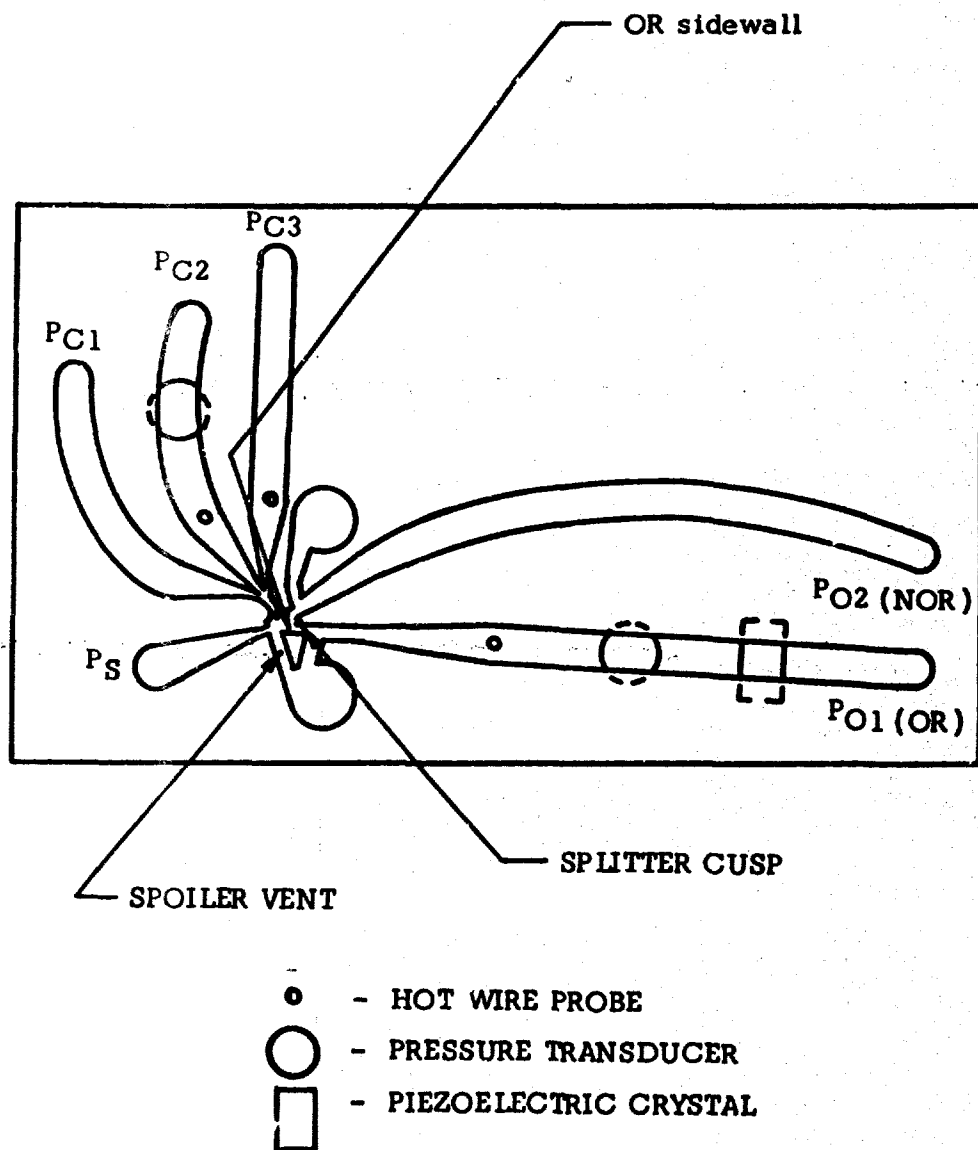
Figure 57. Three Input OR/NOR Test Element

113

of the sensors were simultaneously recorded as a function of time by a multi-channel light galvanometer oscillograph recorder.

A microphone was mounted adjacent to the circuit plate to investigate the potential of acoustic monitoring of primary dynamic performance. An accelerometer was fastened to the element to investigate the capabilities of this secondary sensor to detect and define introduced pressure and physical anomalies, under both steady-state and dynamic conditions.

b.   Test Setup and Instrumentation

The primary sensors selected for evaluation during this test were mounted in position as shown in Figure 57. The hot wire anemometer probes were mounted through a 0.036" diameter hole drilled from the bottom of the circuit so that the probe tip was located in the middle of the flow channel. The miniature pressure transducers were mounted through a 0.25" diameter hole drilled from the bottom of the circuit so that the surface of the pressure transducer was flush with the bottom of the channel. These two sensors were fixed into their positions, and sealed to prevent leaks, with Duco cement.

The piezoelectric crystal was mounted on the top side of the channel. A 1/2" hole was drilled through the Plexiglas cover plate and tapped. The crystal was then mounted on top of the sticky tape gasket which sealed the element. It was locked into position over the channel with a 1/2" Plexiglas screw, with its center drilled out, gripping the crystal only at its outer edges, thus permitting it to flex with pressure to its center surface.

The microphone was mounted under the OR/NOR Gate element approximately 1/2 inch from its bottom surface. The microphone was used in the test to give a gross indication of primary performance by detecting the changes in the average acoustic energy with changes of switched state. The accelerometer, used to monitor the secondary acoustic signature, was mounted directly on the bottom of the element surface over the interaction region. Mounting was accomplished by use of the threaded mounting stud, provided by the manufacturer, which was bonded to the element with Duco cement.

The instrumentation block diagram for monitoring and recording of the secondary acoustic signature detected by the accelerometer is shown in Figure 58. The signals detected by the accelerometer were amplified by the preamplifier which had a fixed gain of 10, and monitored by the sonic or ultrasonic analyzer. The horizontal and vertical output of the ultrasonic or sonic analyzer were connected to an X-Y recorder. DC infinite resolution voltage sources were used to null out the DC shift from the analyzer. Preliminary testing had shown that the signatures recorded with the ultrasonic analyzer lacked sufficient repeatability.

114
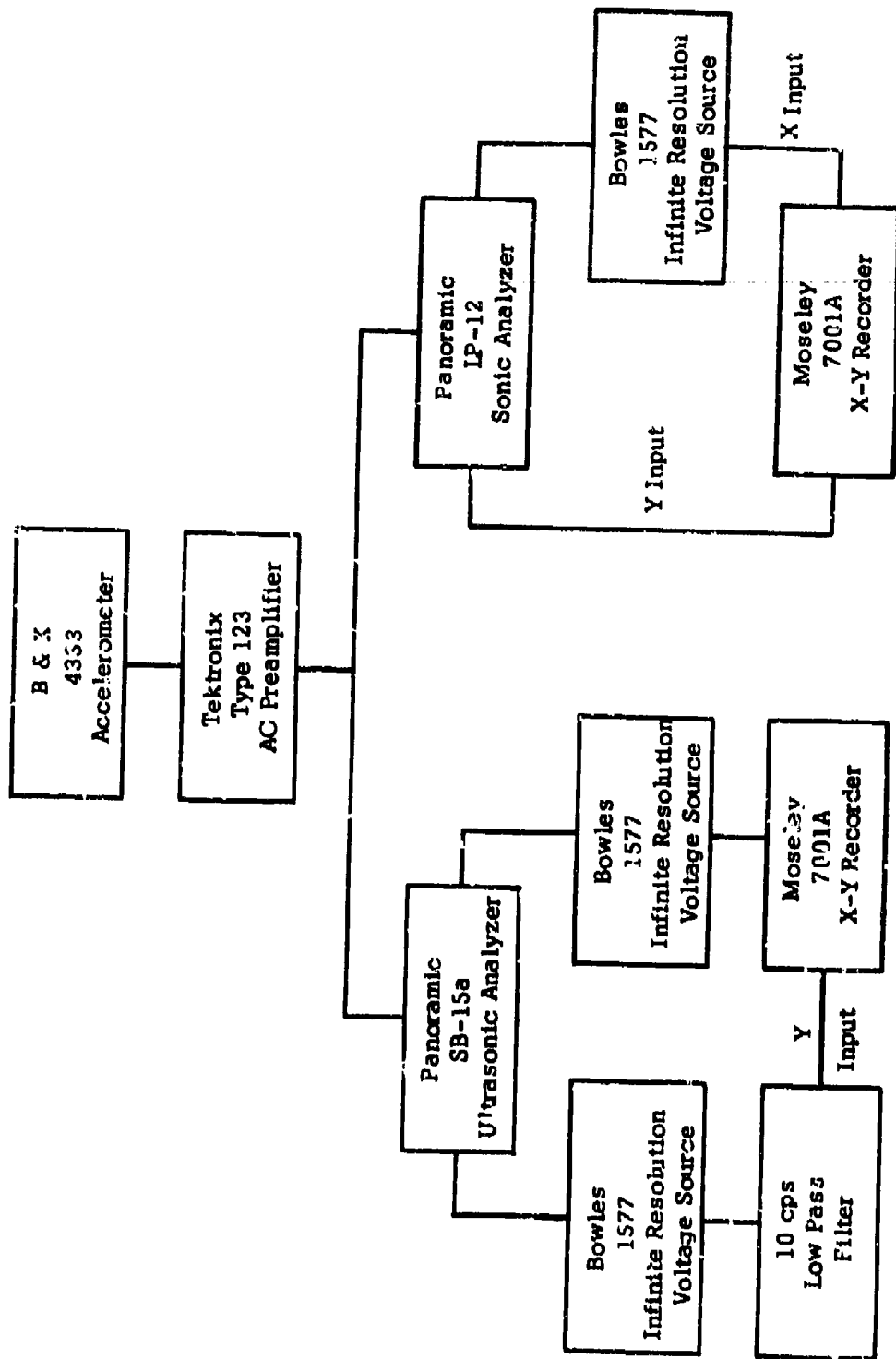
Figure 58. Instrumentation Block Diagram for Acoustic Signature Tests - OR/NOR Gate Element

In order to improve repeatability, a 10 cps low pass filter (60 db/decade above 10 cps) was coupled into the circuit between the analyzer's vertical output and the X-Y recorder. This filter, added to the smoothing filter of the analyzer, produced a more repeatable trace. The front panel control settings for the instruments are given in Table VII.

The instrumentation block diagram for the primary sensors is shown in Figure 59. Although there were two pressure transducers and three hot wires used, the block diagram only shows one of each, because the instrumentation was repeated for the others. A description of the sensors and instrumentation used is as follows:

o   Two miniature pressure transducers, model SA-SD-M-64, manufactured by Scientific Advances, Inc., were used. The first transducer, 0 to 2 psi range, monitored the input PC2. The second, 0 to 15 psi range, monitored the OR output. Modified BEC model 1576 transducer bridges were used for transducer excitation and as the balancing bridge, with modifications made to improve the balancing circuit. A schematic diagram of the bridge circuit is shown in Figure 60.

$$V = 3 \text{ volts}$$
$$R_1 = 25 \text{ K}\Omega$$
$$R_2 = 1.5 \text{ K}\Omega$$
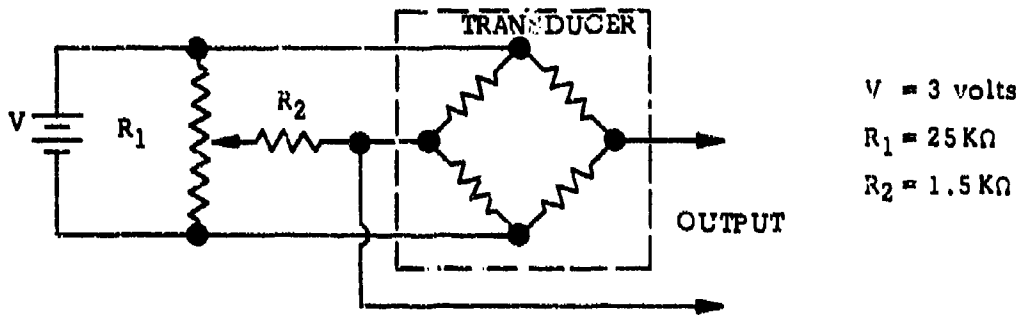
Figure 60. Transducer Bridge Circuit

The output of the transducer bridge circuits were amplified by Consolidated Electrodynamics Corporation type 155 amplifiers, with a gain of 20 and 500 for the PC2 transducer and the OR output transducer, respectively. The output of the amplifiers were monitored by a C.C type 5-124 recording oscillograph. The recording circuits of the oscillograph consisted of a type

116

TABLE VII. INSTRUMENTATION CONTROL PANEL SETTINGS FOR ACOUSTIC SIGNATURE TEST - OR/NOR GATE ELEMENT

Sonic Analyzer

Input Multiplier	X100
Input Pot	10
Vertical Calibration Selector	Lin
Scale Selector	10
Center Frequency	100 cps
Sweep Range Selector	200 Lin
Auxiliary Function Switch	10 sec
Spectra Sensitivity Compensation	Random
I.F. Bandwidth	2
Sweep Width Factor	1
Smoothing Filter	1

Ultrasonic Analyzer

Center Frequency	5 KC
Sweep Width	10 KC
I.F. Bandwidth	Auto
Amplitude Scale	Linear
Sweep Rate	20 sec/full scale
Video Filter	Full ON (clockwise)
Input Atten Step	0
Input Atten Cont	10 db
I.F. Atten	20 db
Marker	OFF

X-Y Recorder for Sonic Analyzer

X gain adj	50 mV, variable set for 1 inch = 25 cps
Y gain adj	50 mV, fixed

X-Y Recorder for Ultrasonic Analyzer

X gain adj	50 mV, variable set for 1 KC 1 inch
Y gain adj	10 mV, fixed

117
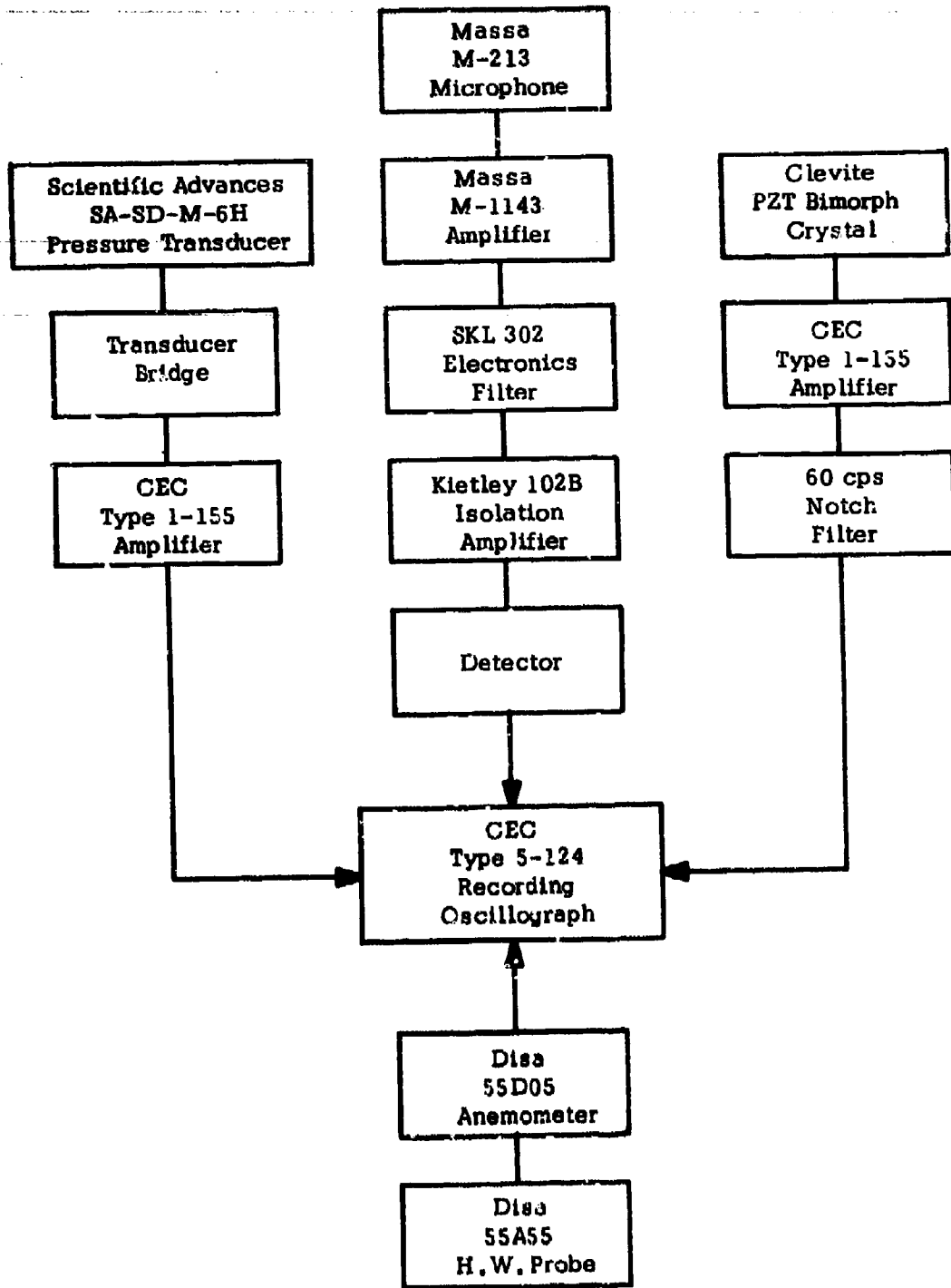
Figure 59. Instrumentation Block Diagram for Primary Performance
Sensor Test - OR/NOR Gate Element

7-363 damping network and a 7-363 type galvanometer for each transducer. The flat (±5%) frequency range of this galvanometer circuit is 0 to 1,000 cps.

o Three Disa Model 55A53 hot wire probes monitored the flow of P_{C2}, P_{C3}, and the OR output channels. These probes were connected to a Disa Model 55D05 constant temperature anemometer which supplied the power to the probes and monitored the flow characteristics. The probe heating resistance ratio was set by selecting 2.4 on the resistance selector switch on the front panel. The output of the C.T. anemometer was recorded on the CEC light galvanometer oscillograph. Type 7-345 galvanometers and damping networks were used which permitted a flat (±5%) frequency range of 0 to 500 cps.

o The instrumentation for recording of the primary performance characteristic with the Massa microphone system was developed by experiment. The final circuit was as shown in the block diagram of Figure 59. The output of the microphone was coupled through the Massa M-114B low noise preamplifier, with an approximate gain of one, to the Massa M-185 amplifier set for 0db attenuation. The output of the Massa system was passed through an SKL Dual Section filter, set to permit a bandpass of 20 KC. The output of the filter was amplified by the Kintel decade isolation amplifier with its gain adjust set at 1,000. The signal was then passed through a detector as shown in Figure 61. The detector consists of a half wave rectifier and filter. It permits detecting the level changes of the 20 KC signal's average intensity. The output of this circuit was monitored by the oscillograph recorder using a 7-304 galvanometer with a flat (±5%) frequency range of 0 - 500 cps.

$C_1 = 8 uf$

$R_1 = 1.9 K\Omega$

$R_2 = 10 K\Omega$
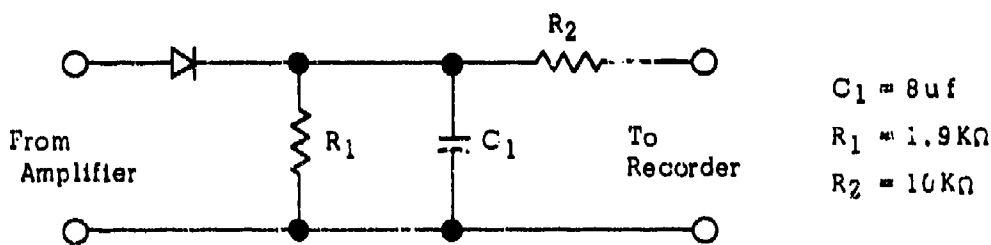
Figure 61. Detector Circuit Diagram

c.   Satisfactory Performance Tests

During this test series with a satisfactorily performing element, data was
taken to permit the comparative evaluation of primary sensors for digital
elements. In addition, base line acoustic signature data was obtained for
use as a reference during subsequent anomaly detection tests.

Figure 62 shows the input/output performance of the OR/NOR Gate as
detected by the various primary performance sensors. The miniature
pressure transducers, selected as being the most accurate of the primary
sensors (based on the manufactured specifications and previous tests) were
used to evaluate the element performance and as a reference when evaluating
the performance of the other primary performance sensors included in this test.

According to the data shown, the OR/NOR Gate was functioning satisfactory
for a single input frequency of 3 cps. The input signal to the OR/NOR Gate
is shown to be noisy. This is an anomaly related to the input signal and
not the OR/NOR Gate. The output traces show that the element was switched
by the narrow input noise spikes which indicated that the OR/NOR Gate would
function properly at higher frequencies and much narrower pulse widths at
its input.

The traces of Figure 62 indicate that for a 3 cps switching frequency, the
sensing capability of hot wire anemometers compared favorably with the
miniature pressure transducers. The representation of waveform generated
by the hot wire follows closely that depicted by the pressure transducer.
The traces do, however, indicate some lag in the anemometer system as
compared to the pressure transducer. The lag is not immediately detected
by observation of the nominal waveform at the recording speed for this test,
but it can be seen in the attenuation of the narrow noise spikes.

The microphone trace is seen to exhibit significant information. The capability
of this sensing means to detect changes in switched state at low frequencies
is definitely demonstrated. It is also shown that accurate evaluation of wave-
form by this means is improbable. The possible potential of an acoustic system
of this nature (described in part d.) is considered to be in the gross monitoring
of switching of one or a group of digital elements by means of a single sensing
device external to the element flow channels.

The trace generated by the crystal, which was mounted over the OR output
channel, demonstrates the capability to detect the signal described by the
pressure transducer in the OR output. The results were considered highly
encouraging, though the need for improvement was obvious.

120
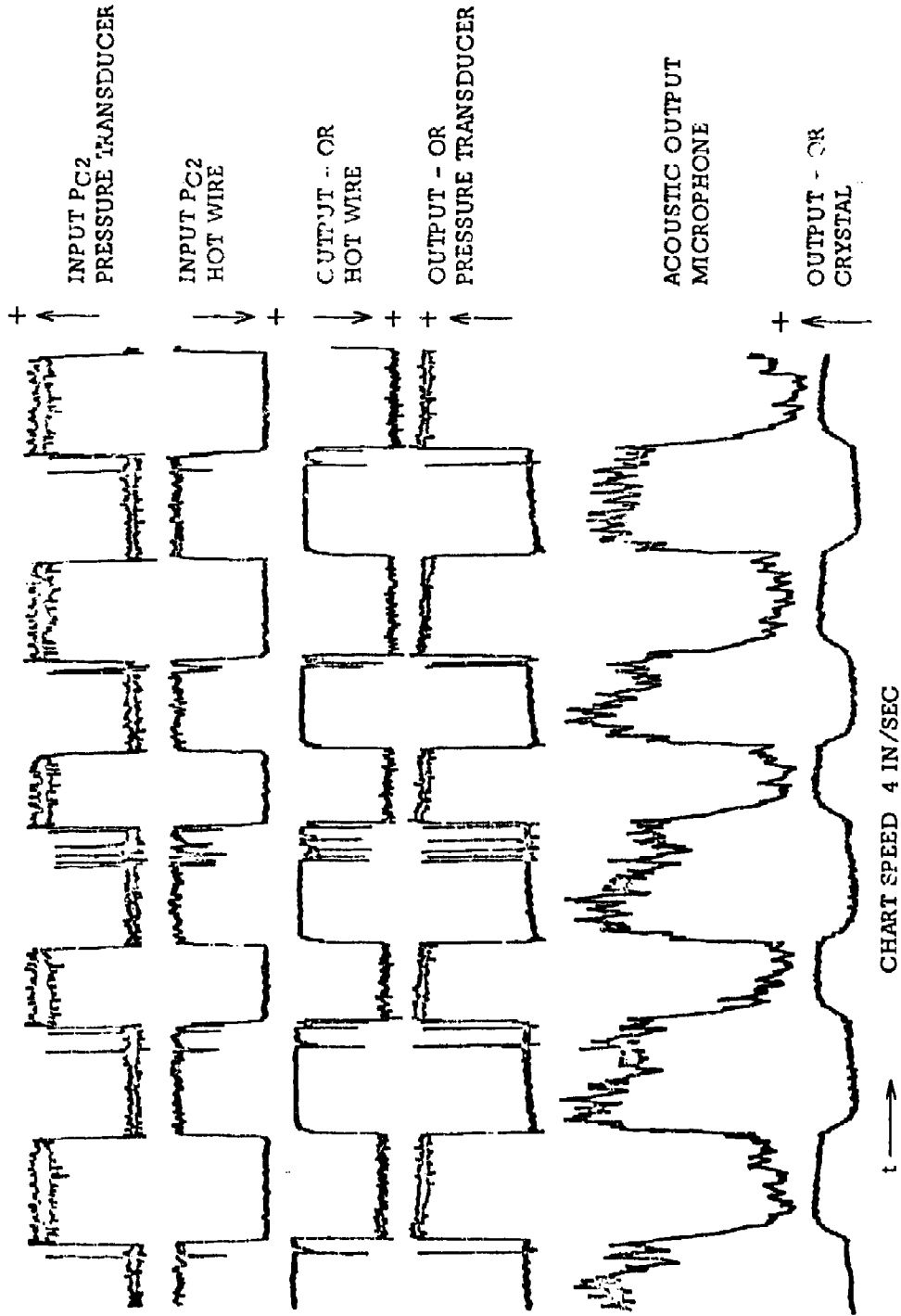
Figure 62. OR/NOR Gate Satisfactory Performance Test
Primary Performance Sensors – Single Input

CHART SPEED 4 IN/SEC

INPUT P$_{C2}$ PRESSURE TRANSDUCER

INPUT P$_{C2}$ HOT WIRE

OUTPUT – OR HOT WIRE

OUTPUT – OR PRESSURE TRANSDUCER

ACOUSTIC OUTPUT MICROPHONE

OUTPUT – OR CRYSTAL

121

Figure 63 shows a section of recording data displaying the primary performance characteristics as detected by the various sensors for two control signals at different frequencies. The input into PC2 is approximately 30 cps while the input into PC3 is approximately 100 cps. The irregularity of the input flow amplitude, Γ_{C3}, is a result of feedback into this channel, when its signal is zero and the input to PC2 is of some amplitude other than zero. This interaction of the two signals is not a desirable characteristic, but it does not constitute a malfunction of the element. The result shows that the OR/NOR Gate will accept two input signals and perform properly. This data demonstrates the capability of the instrumentation in defining the satisfactory dynamic performance of the element under realistic operating conditions.

Comparison of the hot wire anemometer representation of the PC2 signal with that of the miniature pressure transducer shows a definite lag in the hot wire system. This lag is clearly detectable with the higher chart speed of this test. To provide a more accurate description of waveform, the need to reduce lag in the hot wire system is apparent. (Significant improvement was subsequently realized, and is discussed in section 5.)

The microphone trace is shown to contain the same information, albeit with less accuracy, as that sensed by the pressure transducer in the OR output.

Detection of the OR output with the crystal yielded good results. The trace shows sufficient response to monitor pulse rise times of less than a millisecond. This test indicated that the crystal had a high potential as a sensor of digital element primary signals, although the need to decrease the distortion of a sustained signal pressure is apparent. (A large improvement in this area is presented in section 6.)

While conducting tests to establish a static base line acoustic signature trace, a test was performed to determine to what extent frequency of dynamic operation of this element would effect the acoustic signature. Figure 64 shows the results of this test. The trace performed under static conditions ($P_S = 1$ psig, $P_{C2} = 0$) shows a large amplitude signal in the 5.5 KC region and a low amplitude signal in the 0 to 1 KC region. As periodic control signals were introduced, the 6 KC area decreased and the 0.5 to 1 KC means of detecting operating frequency changes. The static base line, used subsequent as a reference for satisfactory operating condition, was as given by the 0 cps trace of Figure 64.

Further evaluation on the static base line acoustic signature monitored by the ultrasonic analyzer was performed to establish the typical signature changes that could be expected during the anomaly test. This test consists of introducing a 0.25 psi DC signal in PC2 to produce a change of state (output switched from NOR to OR) in the element. Figure 65 shows the resulting change in the acoustic signature. Good resolution was displayed.

122
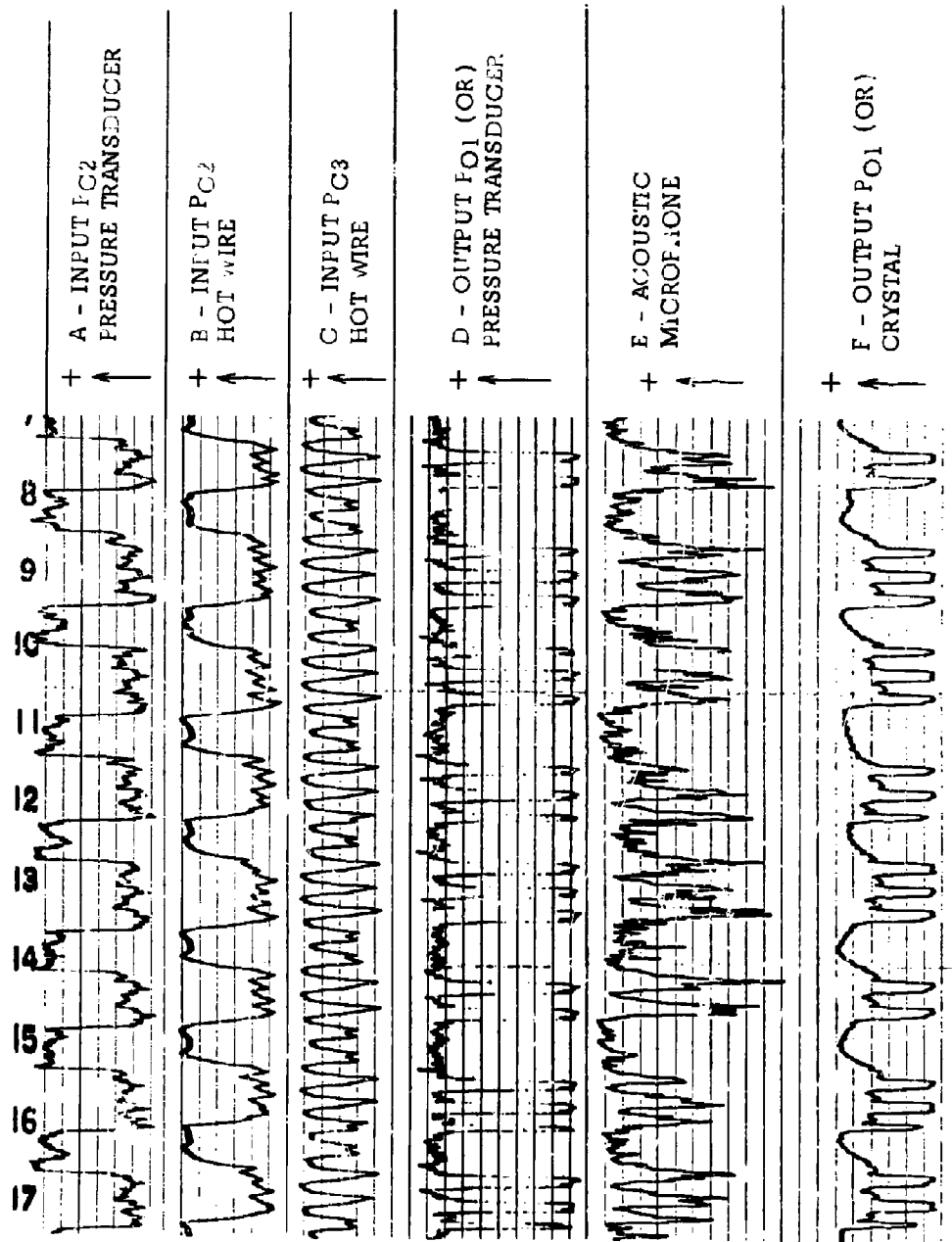
Figure 63. OR/NOR Gate Dual Input Test Primary
Performance Monitoring

CHART SPEED 16 IN/SEC

A - INPUT P_{C2}
PRESSURE TRANSDUCER

B - INPUT P_{C2}
HOT WIRE

C - INPUT P_{C3}
HOT WIRE

D - OUTPUT F_{O1} (OR)
PRESSURE TRANSDUCER

E - ACOUSTIC
MICROPHONE

F - OUTPUT P_{O1} (OR)
CRYSTAL

123

ELEMENT: OR/NOR Gate Model 1715A

SENSOR: Accelerometer. B&K Model 4333

OPERATING CONDITIONS:

P_S = 1 PSIG
P_{C1} = 0 PSIG
P_{C3} = 0 PSIG

○ P_{C2} = 0 PSIG
△ P_{C2} = 0.25 PSIG @ 30 cps
□ P_{C2} = 0.25 PSIG @ 100 cps

Relative
Amplitude

Frequency Range

8 KC

Figure 64. OR/NOR Gate Acoustic Signature Changes Due To
Dynamic Operating Frequencies

124

ELEMENT: CR/NOR Gate Model 171SA

SENSOR: Accelerometer, B&K Model 4333

OPERATING CONDITIONS:

$P_S = 1\ PSIG$
$P_{C1} = 0\ PSIG$
$P_{C3} = 0\ PSIG$

$\bigcirc P_{C2} = 0\ PSIG$
$\triangle P_{C2} = 0.25\ PSIG$

Relative
Amplitude

Frequency Range

8 KC
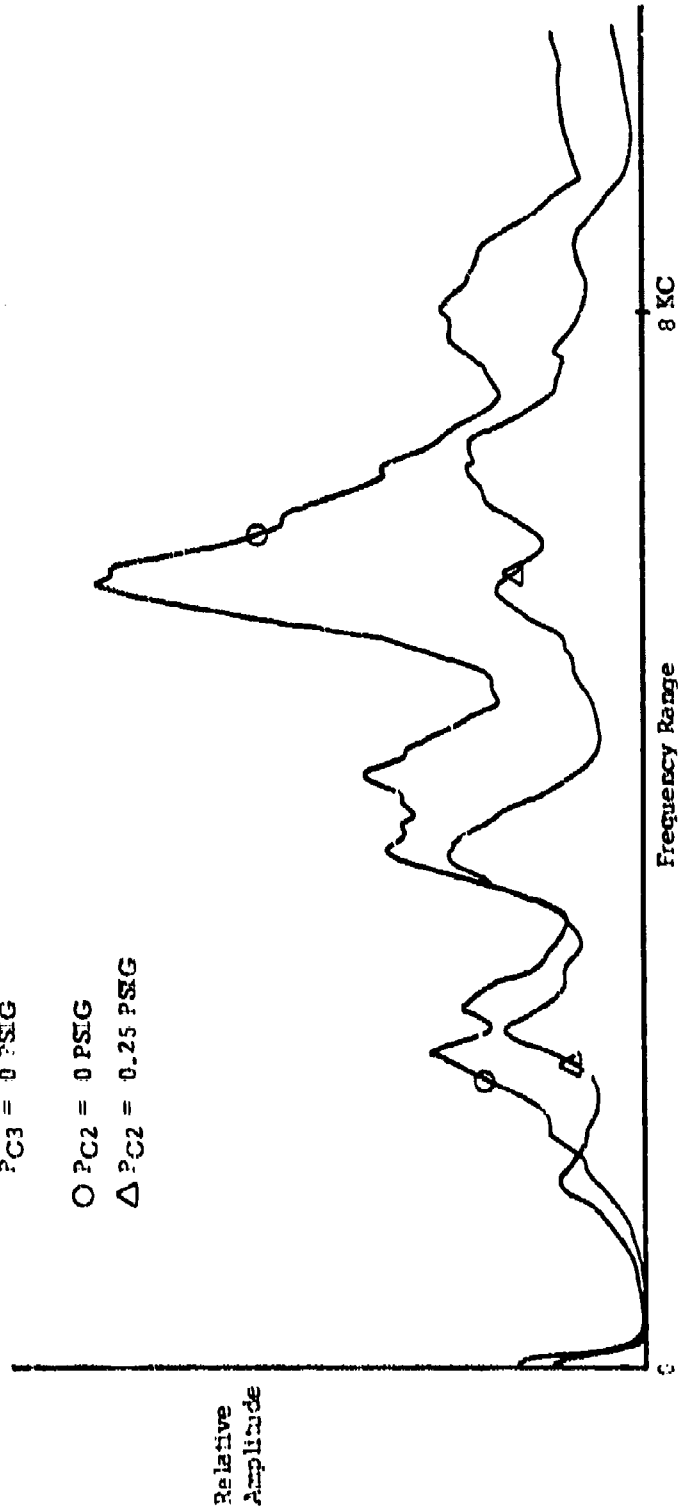
Figure 65. CR/NOR Gate Acoustic Signature Changes
Due To Change of State

125

Tests were also conducted using the accelerometer and sonic analyzer to display the acoustic signature produced in the low frequency region (0 to 200 cps) by detecting the dynamic operating frequency of the test element. Figure 66 shows the results in detecting satisfactory dynamic performance for two control signals at different frequencies of approximately 100 cps and 150 cps being induced into PC3 and PC2, respectively. The results show that detecting the operating frequency of a digital element is possible by secondary means and that the detecting of various simultaneous operating frequencies within an element is also possible. This technique possesses the potential of detecting the various operating frequencies of a group of elements forming an integrated circuit. It will also be shown later that the amplitude of these signatures can be related to pressure anomalies.

d.   Anomaly Detection Tests

The prime objective of this test series was to investigate the capabilities of secondary acoustic sensing to detect and define anomalies introduced into a digital element. The capabilities of primary sensors were established during satisfactory performance tests, hence the consideration of these sensors during the anomaly tests was minimized. The results realized for each of the anomalies introduced are presented in the following.

1.   Supply Pressure Changes

Changes occurring in the static secondary acoustic signature were detected by the accelerometer and recorded as various levels of supply pressure changes were introduced into the OR/NOR Gate. Figure 67 shows these changes. Good resolution in detecting the level of the anomaly is displayed by the figure and as will be realized later when signature changes due to other anomalies are presented, supply pressure changes have their own defining characteristic signature change. A decrease in P_S produces a decreasing amplitude of the signature over the entire bandwidth observed, and an increasing P_S produces an increase in the amplitude of the signature observed. Therefore, both the magnitude and type of anomaly induced is considered to be well presented in these signature changes.

The capability of acoustically detecting supply pressure anomalies under dynamic operating conditions was demonstrated. Figure 68 shows five (5) sections of the 100 cps region of the sonic analyzer as it detected the dynamic performance of the OR/NOR Gate with an inputted 100 cps control signal and with varying supply pressure. The five sections of the 100 cps region, from separate graphs, were placed adjacent to each other in Figure 68 for ease of signature comparison for the various levels of supply pressure. Trace "A" shows the amplitude of the signal due to control pressure only, since $P_S = 0$. Traces "A" through "C" show an increase in the relative
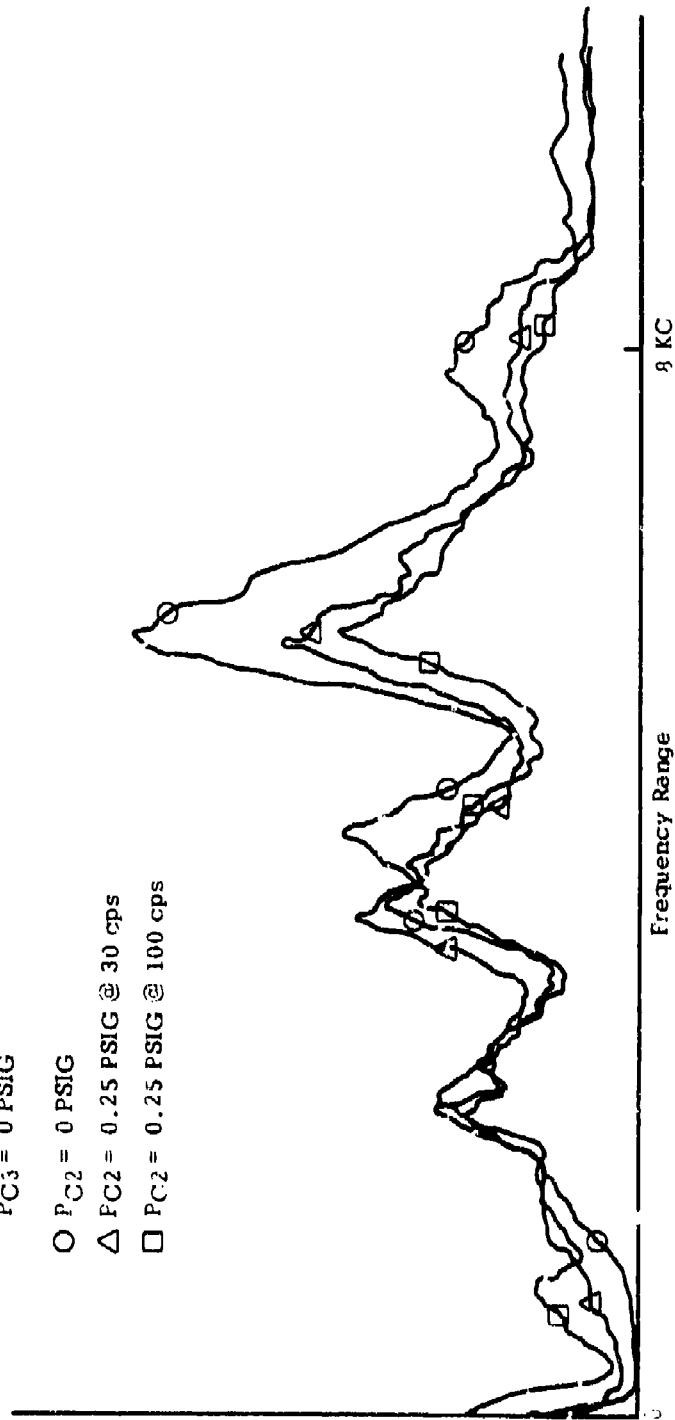
126

ELEMENT: OR/NOR Gate, Model 1715A

SENSOR: Accelerometer, B&K Model 4333

OPERATING CONDITIONS:

P_S = 1 PSIG

P_{C1} = 0 PSIG

P_{C2} = 0.25 PSIG @ 150 cps

P_{C3} = 0.25 PSIG @ 100 cps

Relative Amplitude

100 cps   150 cps   F leg

Frequency Range
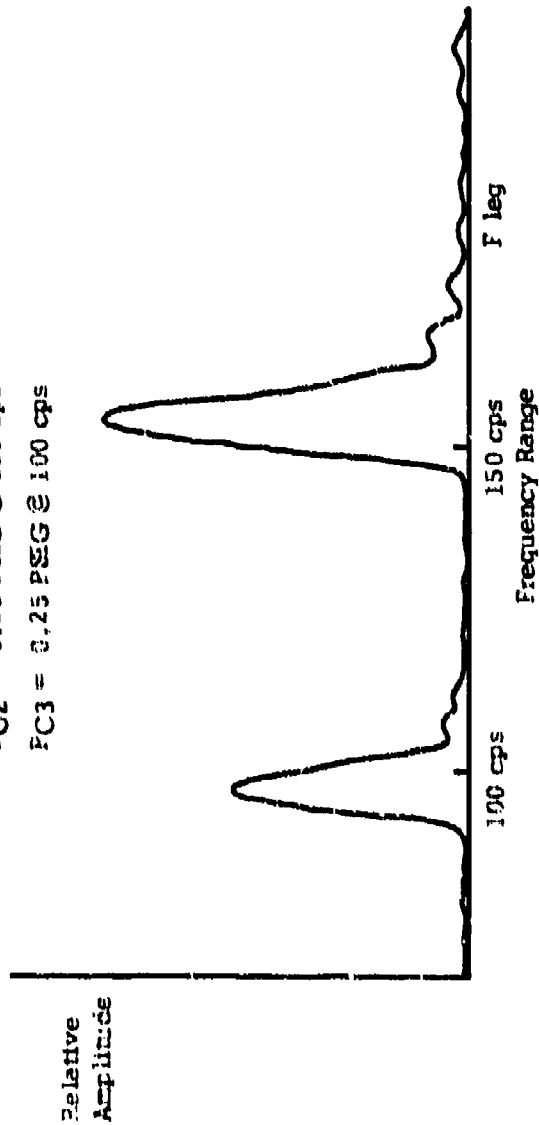
Figure 66. OR/NOR Gate Dynamic Acoustic Signature for Dual Input Control Signals

127

Relative
Amplitude

ELEMENT: OR/NOR Gate, Model 17154

SENSOR: Accelerometer, B&K Model 4333

OPERATING CONDITIONS:

O F_S = 1.5 PSIG

$\triangle$ P_S = 1.0 PSIG

$\square$ P_S = 0.5 PSIG

P_{C1} = P_{C2} = P_{C3} = 0 PSIG
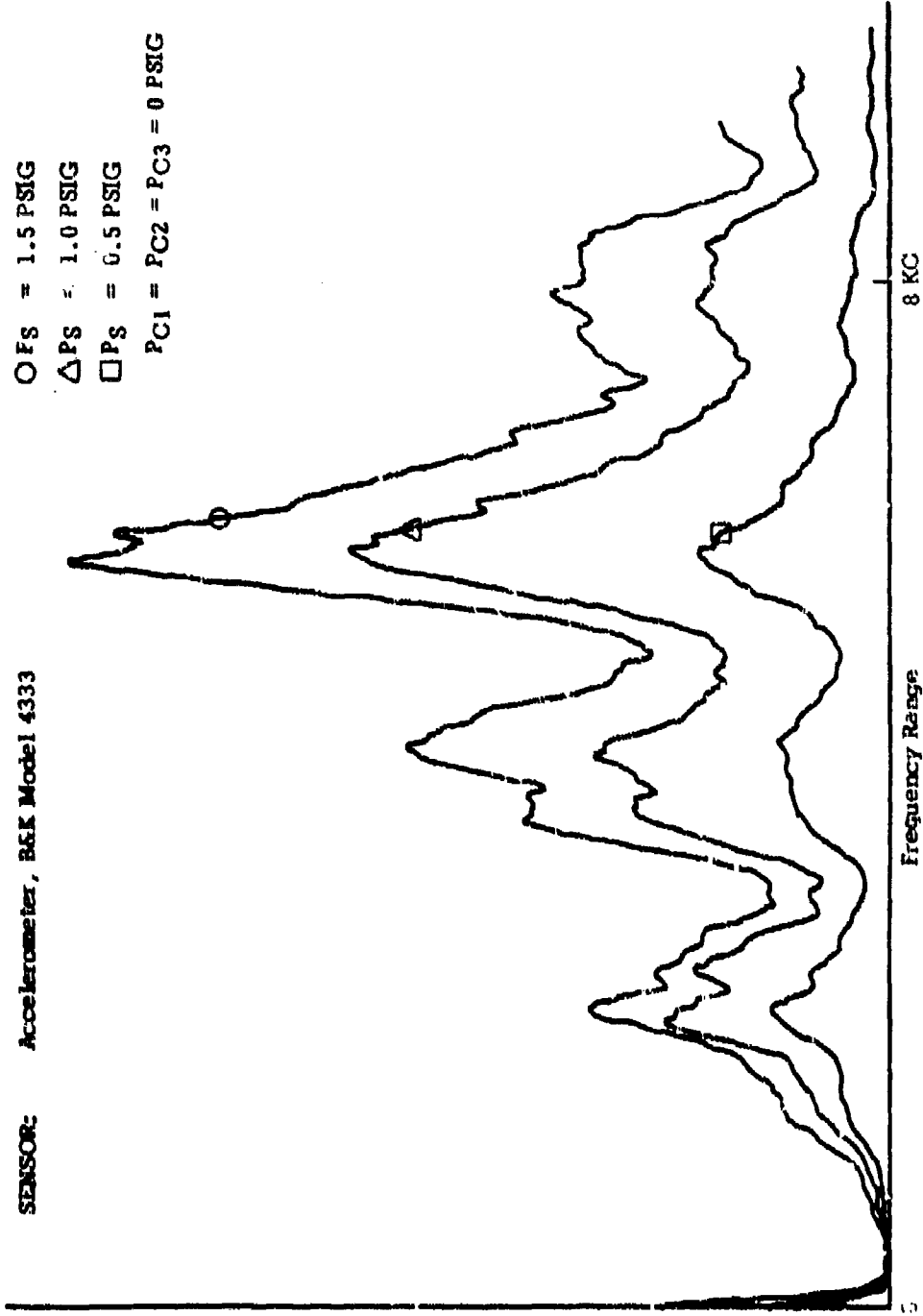
8 KC

Frequency Range

Figure 67. OR/NOR Gate Static Anomaly Detection Test:
Acoustic Signature Monitoring - Supply Pressure
(P_S) Changes.

Figure 68. OR/NOR Gate Dynamic Anomaly Detection Test
Acoustic Signature Monitoring – Supply Pressure
(Ps) Changes

OPERATING CONDITIONS:

PC1 = PC3 = 0

PC2 = 0.25 PSIG Sq. Wave at 100 cps

ELEMENT: OR/NOR Gate, Model 1715A

SENSOR: Accelerometer, B&K Model 4333

Scale: 1" = 25 cps

Relative Amplitude

Frequency

Ps = 0 PSIG (A)

Ps = 0.5 PSIG (B)

Ps = 1.0 PSIG (C)

Ps = 1.5 PSIG (D)

Ps = 2 PSIG (E)

100 cps

amplitudes with an increasing Pg. With the supply pressure activated, the resultant power stream was switched at the input signal frequency. As the supply pressure was increased, the acoustic energy of the oscillating power stream was increased, thus causing the increase in signature amplitude with increasing Pg. Traces "D" and "E" show the changes occurring in the acoustic signal as Pg was increased beyond 1 psig, the nominal value. In the case of Trace "D", the supply pressure was sufficiently large so that the input signal could not consistently effect switching of the power stream, which caused the shown irregularity of the traces. In the case of Trace "E", the supply pressure was increased to such a level that the control signal could not switch the power stream. In the absence of switching, then, the microphone detected essentially the same acoustic changes as in case "A", the effects of the input signal only.

2. Control Pressure Changes

Control pressure changes were effectively detected under dynamic conditions by the accelerometer and sonic analyzer, as shown in Figure 69. Four levels of signal were detected as the amplitude of the 100 cps control input was varied, while the supply pressure was held at a constant 1 psig value. These traces are in the 100 cps region corresponding to the input frequency of the control signal. Shown in the figure is a definite relationship between the level of the control signal amplitude and the relative amplitude of the signal detected by the accelerometer. Switching of the OR/NOR Gate occurred for all traces except for the case where $P_{C2} = 0.1$ psi. As the amplitude of P_{C2} was increased, the trace repeatability shows a greater margin of error (the wide band at the top of each group of traces). This is an indication of over-driving the element with too large a control signal, such as the 0.5 psig input.

In addition to the dynamic detection of control pressure changes, small changes in the static acoustic signature were also observed when changing the level of a static input signal. The capability to differentiate between the two switched states under static conditions has been shown earlier in Figure 65.

3. Splitter Cusp Contamination

Figure 70 shows the changes that occurred in the static secondary acoustic signature for two degrees of splitter cusp contamination. Contamination was simulated by the application of Duco cement. Shown in the figure is a decrease in the amplitude of the signature presented in the 5.5 KC and 8 KC areas related to the level of anomaly induced. Sufficient resolution is shown here to detect these levels of anomaly. The decreasing amplitude in the 6 KC and 8 KC areas is definitive of splitter cusp contamination.

130

ELEMENT: CF/NOR Gate, Model 1715A

SENSOR: Accelerometer, B&K Model 333

OPERATING CONDITIONS:

P_S = 1 PSIG

$P_{C1} = P_{C3}$ = 0 PSIG

P_{C2} = 0.5 PSIG

P_{C2} = 0.25 PSIG

Relative Amplitude

Frequency - cps

P_{C2} = 0.2 PSIG

P_{C2} = 0.1 PSIG

Frequency - cps
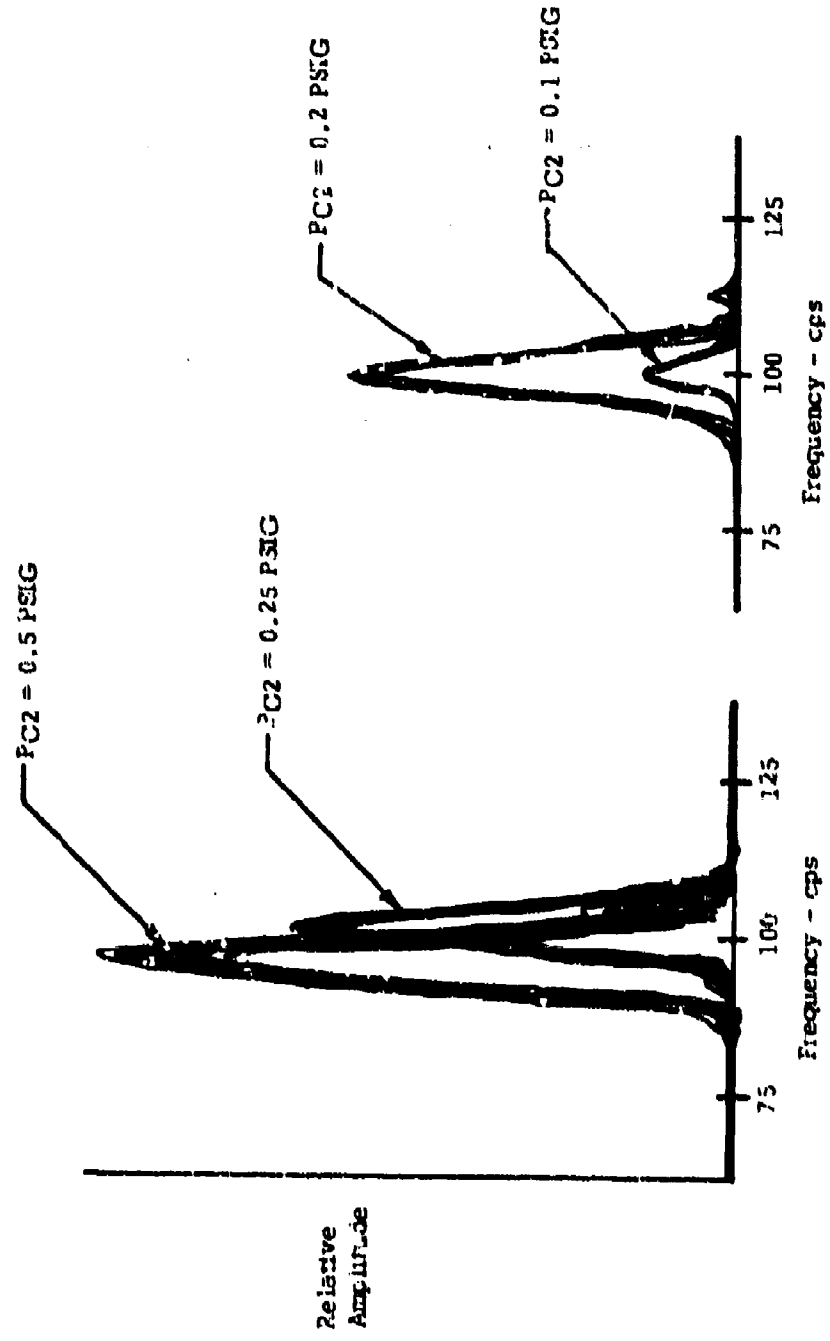
Figure 59. CF/NOR Gate Dynamic Anomaly Detection
Test - Acoustic Signature Monitoring -
Control Pressure (P_{C2}) Changes

131

ELEMENT: OR/NOR Gate, Model 1715A

SENSOR: Accelerometer, B&K Model 4333

OPERATING CONDITIONS:

P_S = 1 PSIG

P_{C1} = P_{C2} = P_{C3} = 9 PSIG

○ – No Contamination

△ – 1st Degree

□ – 2nd Degree

Frequency – cps

8 KC

Relative Amplitude
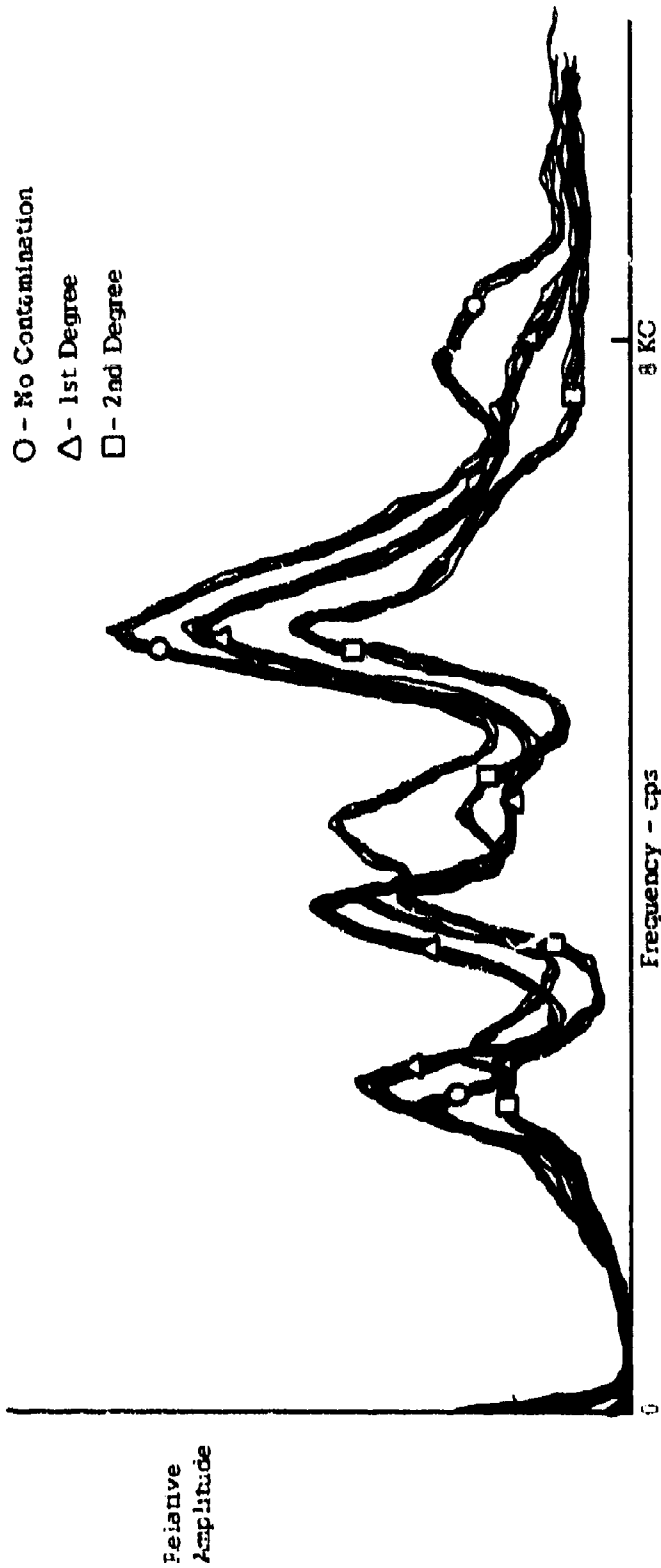
Figure 76. OR/NOR Gate Static Anomaly Detection Test
Acoustic Signature Monitoring – Splitter Cusp
Contamination

4.   Power Nozzle and Spoiler Vent Contamination and
     Splitter Cusp Chipping

Figure 71 shows four (4) static condition traces; the baseline signature, the changes in signature produced by contamination of the supply pressure nozzle, the change in signature produced by contamination of the spoiler vent, and that produced by chipping of the splitter. These three anomalies were plotted on the same graph with the baseline signature to show the appreciable and typifying signature changes for each anomaly.

Figure 72 shows the primary performance of the OR/NOR Gate with the magnitude of contamination of the spoiler vent the same as that of Figure 71. The malfunction caused by this anomaly is shown by the OR output (P_{O1}), as detected by a miniature pressure transducer.

For a number of cases, the power jet remained attached to the OR output side during a zero input signal state. Contamination of the spoiler vent caused an increased wall attachment effect on the OR side which prevented the power jet from dropping back to the NOR output with cessation of the input signal. Examination of the microphone trace shows satisfactory detection of this malfunction by this sensing means also.

Figure 73 shows the primary performance with the splitter cusp chipped the same as that of Figure 71. The noise present in the OR output signal is not acceptable. The malfunction was also detected by the microphone. The microphone trace of Figure 73 shows greatly increased noise as compared to Figure 72.

e.   Conclusions

The conclusions drawn from this test series along with those generated by subsequent tests of a simple digital circuit are summarized in Section 8, Summary of Sensor Applicability.

6.   EVALUATION OF SENSORS APPLIED TO A SIMPLE DIGITAL CIRCUIT

One objective of this test series was to further evaluate primary performance sensors. Tests were conducted to show the results of the piezoelectric crystal performance incorporating improved mounting conditions and to show the results of the hot wire probe performance after improvements were made to the external circuitry. Also, tests were conducted to evaluate the performance of a hot film probe for the first time. The mounting techniques, external circuitry, and test results will be discussed for each sensor.

During previous tests on digital elements, changes in the secondary acoustic signature were to be a successful technique for detecting and defining various

133

OPERATING CONDITIONS:

ELEMENT: OR/NOR Gate
Model 1715A

SENSOR: Accelerometer:
B&K Model 4333

$P^+ = 1$ PSIG

$P_{C1} = P_{C2} = P_{C3} = 0$

—— Base Line
—·—·— Power Nozzle Contamination
········· Spoiler Vent Contamination
—— Chipped Splitter

Relative Amplitude

Frequency

8 KC
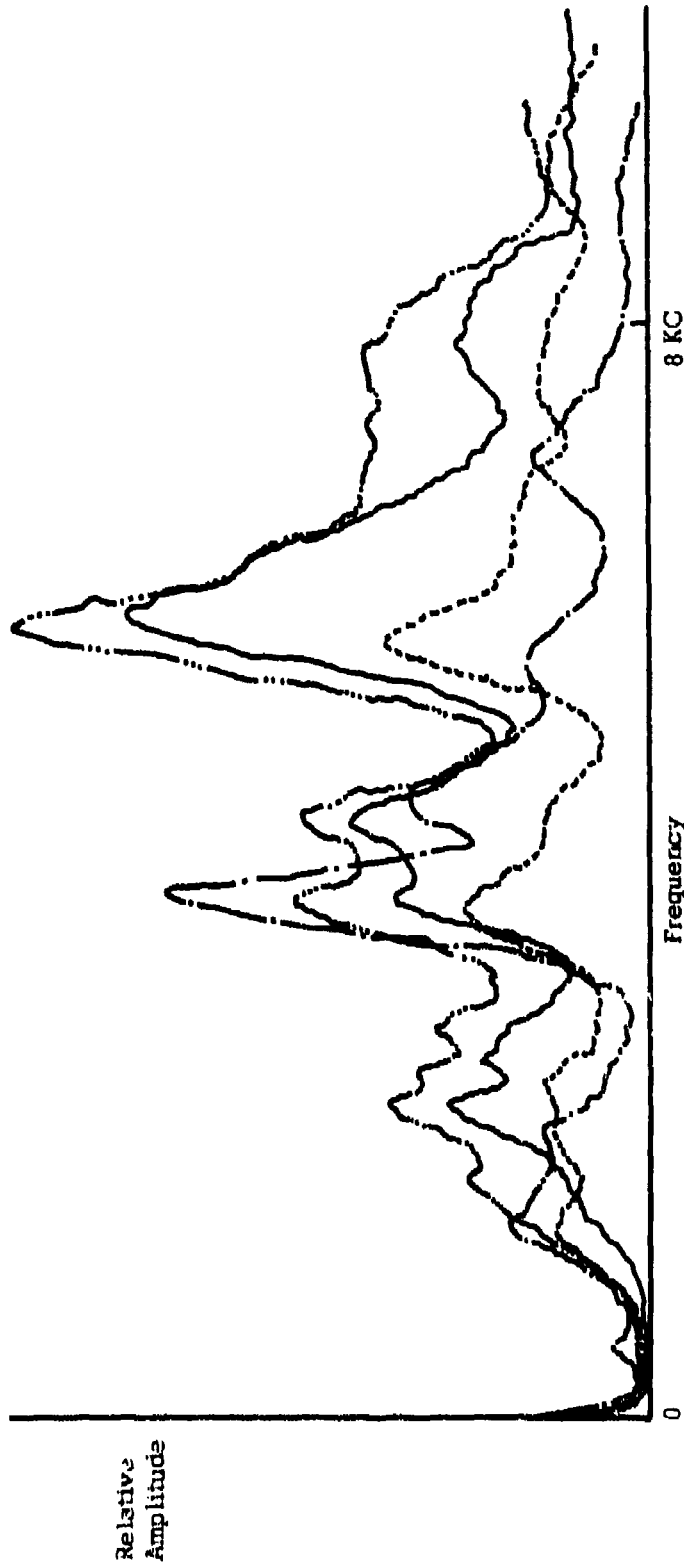
Figure 71. OR/NOR Gate Static Anomaly Detection Test – Acoustic Signature Monitoring – Power Nozzle Contamination, Spoiler Vent Contamination, and Splitter Cusp Chipping

134
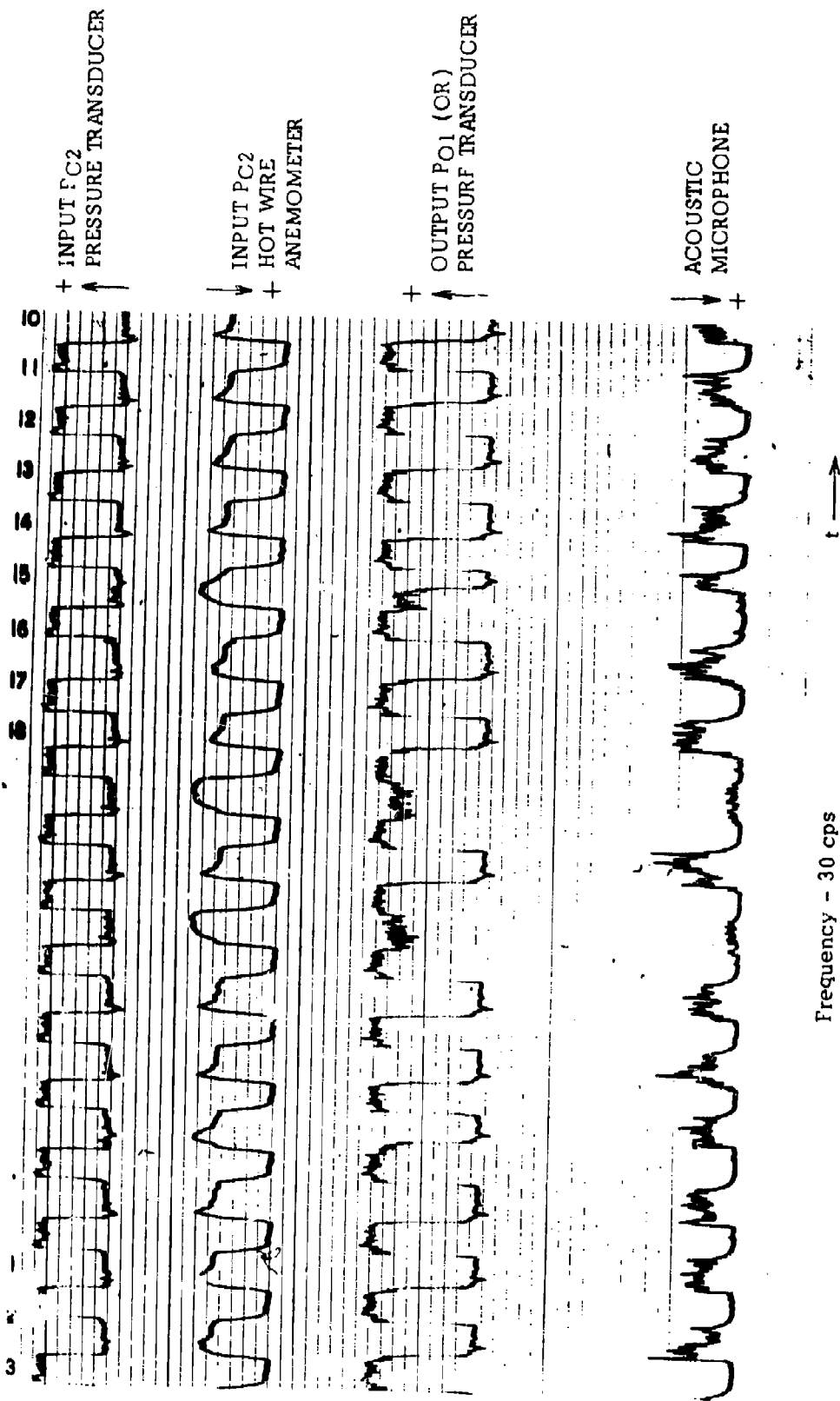
Figure 72. OR/NOR Gate Contamination Test Primary Performance
Monitoring – Spoiler Vent Contamination

Frequency – 30 cps

INPUT P_{C2}
PRESSURE TRANSDUCER

OUTPUT P_{O1} (OR)
PRESSURE TRANSDUCER

ACOUSTIC
MICROPHONE

Frequency – 30 cps
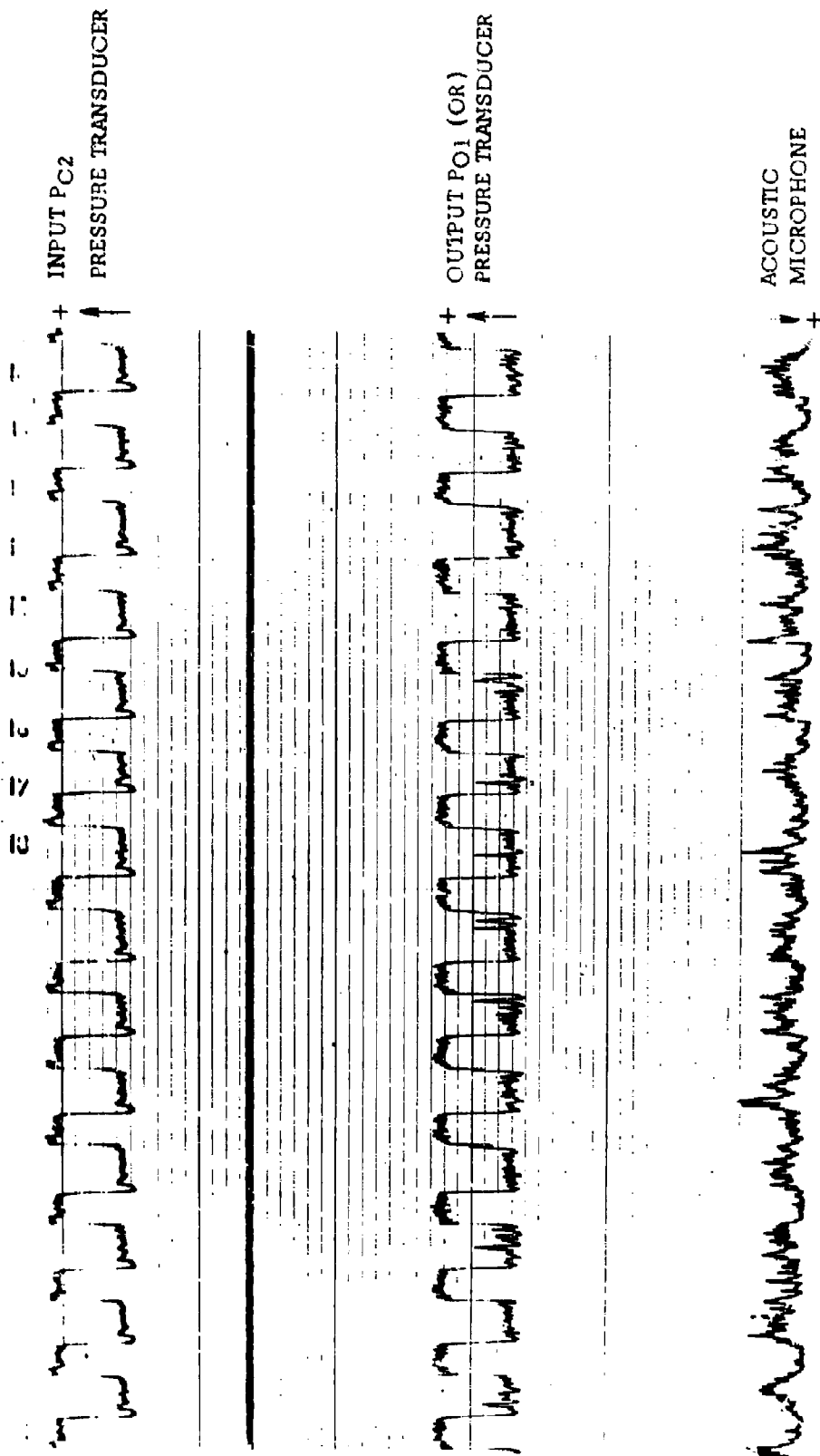
Figure 73. OR/NOR Gate Physical Anomaly, Test.
Primary Performance Monitoring –
Chipping of Splitter Cusp

136

levels and types of introduced anomalies. It was a second objective of this test series to show that this same technique could be employed when more than one element is contained on a circuit plate. The secondary detector was mounted in the near acoustic field of one element while anomalies were induced into another more distant element. The test procedure and results will be discussed.

a.   Test Circuit

The digital circuit selected was a pulse shaper circuit plate which is shown in Figure 74 with its schematic representation. Also shown in the figure are the locations of the primary secondary sensors.

The circuit consists of a Flip-Flop element and an OR/NOR Gate interconnected with feedback. The OR/NOR Gate functions to provide an output at the NOR leg in the absence of all control signals or an output at the OR leg with either one or all of the control signals present. The Flip-Flop element is switched to provide a signal at output leg P_{O1} by a control signal P_{C2}, or switched to provide an output at P_{O2} by a signal P_{C1}. The output signal remains at the most recent switched state even after discontinuation of the respective input signal.

The objective of the pulse shaper network is to produce a signal of narrow pulse width for each cycle of input signal. This is accomplished as shown below.

137
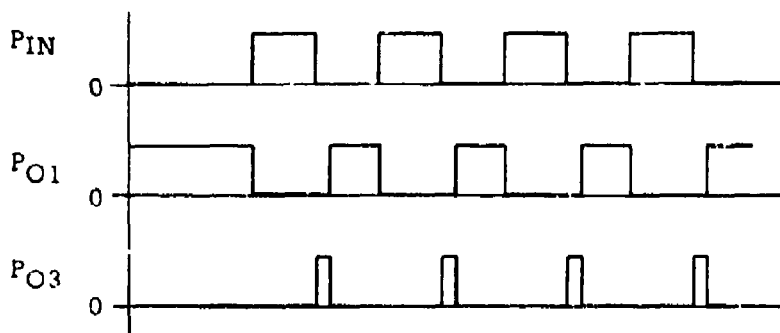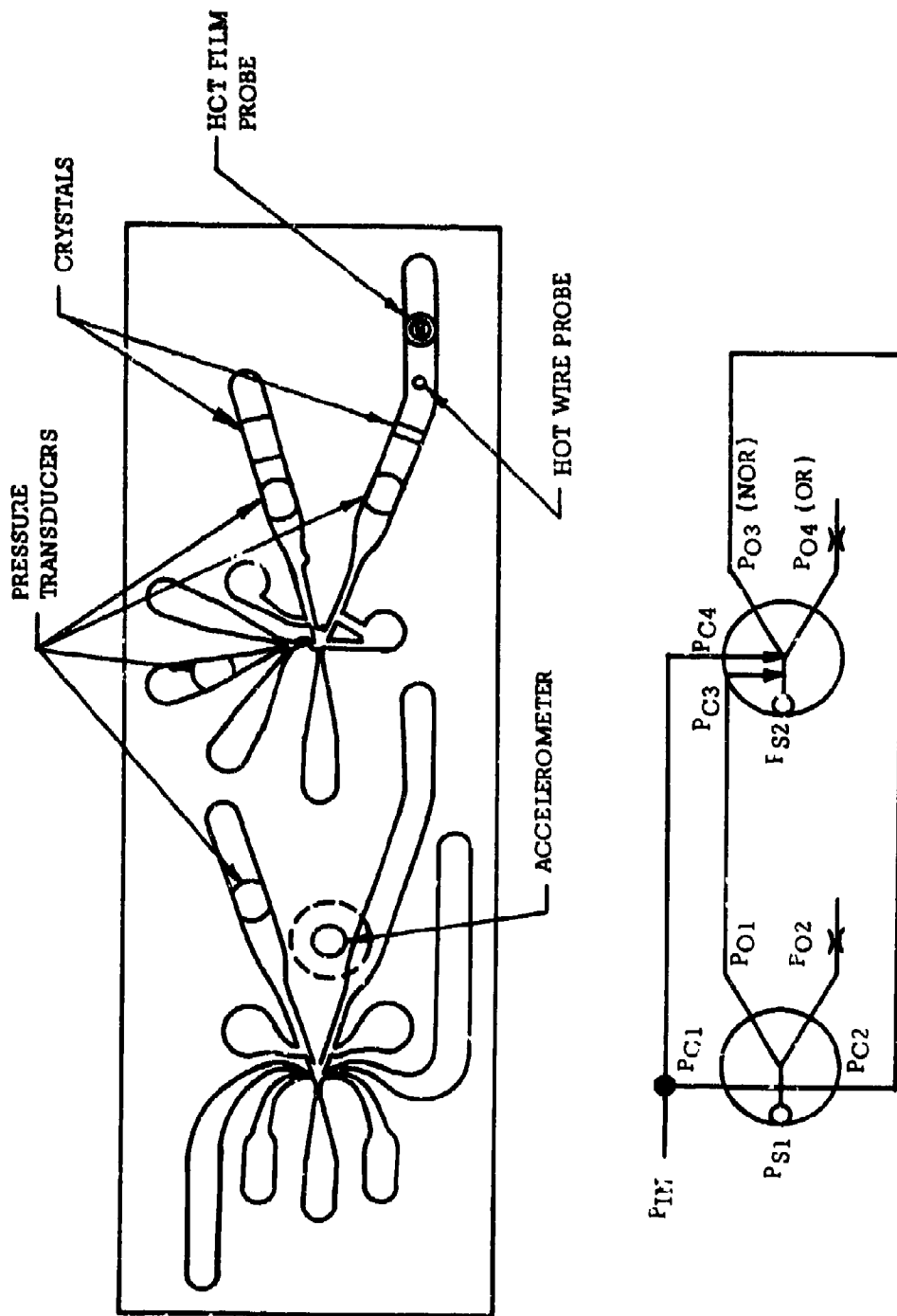
Figure 74. Pulse Shaping Circuit Plate and Schematic

138

With $P_{IN} = 0$, the static state of the network results in the output of the
Flip-Flop being P_{O1} and the output of the OR/NOR being P_{O4}. Thus,
P_{C1}, P_{C2}, and $P_{C4} = 0$. When the first positive pulse of P_{IN} occurs,
the Flip-Flop flow is switched to output leg P_{O2}, or $P_{O1} = 0$. The output
of the OR/NOR Gate remains constant since there is still an input in the
controls. When P_{IN} goes to zero, the Flip-Flop output remains switched to
P_{O2}. P_{C3} and P_{C4} are now both zero, hence the OR/NOR Gate switches
to the NOR leg which is the positive pulse output. The NOR leg is connected
by a feedback path to the Flip-Flop control P_{C2}, causing its output to switch
to P_{O1}, which results in switching the OR/NOR Gate back to the OR output.
The circuit is now in the static (initial) state awaiting the next positive
input signal. The pulse width of the OR or NOR output (either may be used
depending on whether a positive or negative going pulse is required) is
determined by the amount of signal delay selected to be used in the feedback.

b.   Primary Performance Sensors

Four (4) miniature pressure transducers manufactured by Scientific Advances
model SA-SD-M-6H, were mounted to monitor the primary functional perfor-
mance of the test circuit. Since these transducers had already been selected
as the most accurate means of monitoring static and dynamic performance,
they were used as a reference for evaluating the other primary performance
sensors included in this test.

The pressure transducer mounting technique, the bridge circuit, and the
monitoring instrumentation was the same as that described for the OR/NOR
element test in Section 5. The performance of these pressure transducers
is shown in Figure 75. Their ability to detect the functional performance
of this circuit was highly satisfactory and they show that the circuit was
functioning properly.

Two (2) piezoelectric bimorph crystals manufactured by Clevite, a Division
of Brush Instruments, were mounted into the circuit as shown in Figure 74.
The crystals were of two different sizes, 0.25" x 0.25" and 0.55" x 0.06",
in order to determine the effects of size and shape on the sensing performance.
The mounting technique of the crystals was modified, compared to that used
during the OR/NOR element test, in an attempt to improve their performance.
During the element test, the crystal was mounted on the thin film of sealing
tape over the top of the channel, with a screw-down clamping arrangment
fastening the ends of the crystal to the circuit plate. Under these conditions,
it was found that the performance of the crystal was very sensitive to the
pressure applied by the clamping arrangement. As an alternate, the crystals
were mounted through the bottom of the circuit plate, flush with the bottom of
the channel, with a bead of cement around the outside edge of the crystals
to seal off all leaks and fix the crystal in place. The instrumentation circuit

A − OR Output Crystal (0.25" x 0.25")

B − OR Output Pressure Transducer

C − NOR Output Crystal (0.55" x 0 06")

D − NOR Output Pressure Transducer

E − PC3 Pressure Transducer
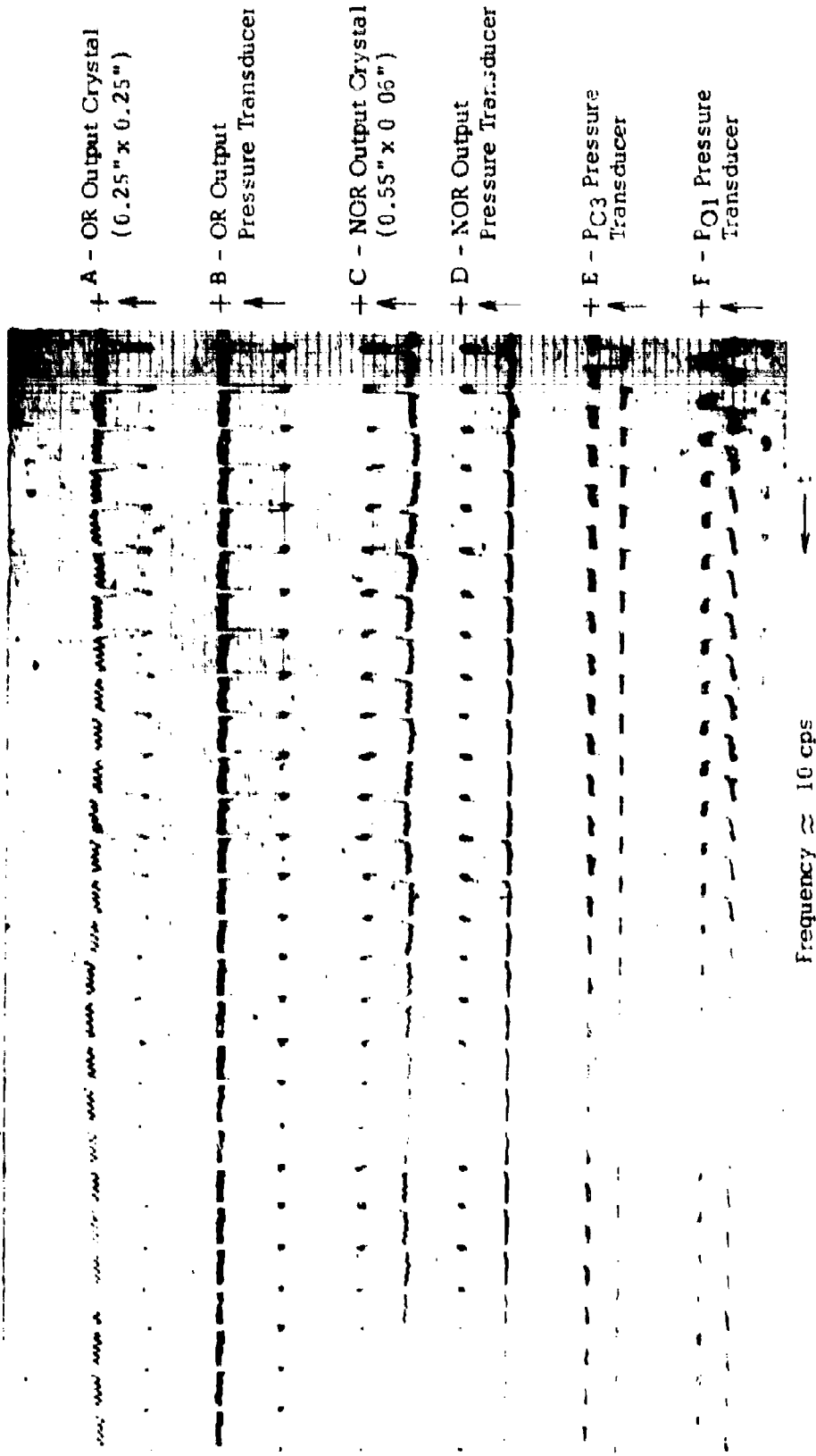
F − PO1 Pressure Transducer

Frequency ≃ 10 cps

Figure 75. Digital Pulse Shaping Circuit Primary Performance Monitoring

for these crystals was the same as that used during the OR/NOR element test
in Section 5., except that a model 7-363 galvanometer and damping unit were
used, permitting a flat (±5%) frequency range of 0 to 1 KC.

Figure 75 shows the performance of these crystals monitoring the OR and NOR
output of the circuit. Also shown in this figure are the signals detected by
the pressure transducers which monitored the same signals, so that evaluation
of the crystals on a comparative basis could be accomplished. The results
show that the crystal's performance was improved, compared to the test results
of the separate OR/NOR Gate element test, as a result of the mounting technique
employed. Although their amplitude characteristics are not necessarily linear,
their performance in detecting pressure changes with respect to the time scale
is highly satisfactory. This characteristic is of primary importance in detecting
dynamic performance of digital circuits. Traces A and C of Figure 75 show that
the size and shapes of the crystals did not produce any detectable dynamic
performance differences except that the larger crystal, with more sensing area
exposed to the pneumatic signal, was of a larger amplitude. The scale for the
larger crystal is approximately half the scale for the smaller one, although the
output had not been calibrated to be directly proportional to pressure. It is also
known that the upper frequency limit will be a function of the crystal's size,
decreasing with increasing size.

A hot wire anemometer probe model 55A52 manufactured by Disa was mounted
in the OR output channel. This sensor, previously tested during the OR/NOR
Gate element tests, produced a meaningful indication of dynamic performance
but exhibited the desirability of decreasing the rise time of the hot wire
anemometry system. During this test, the rise time was improved by eliminating
excess resistance induced by the lead wires to the probe, and by improving
upon the setting of the overheat ratio (defined as the ratio between operating
resistance and the probe resistance) which permits the optimum performance
probe temperature. The more precise setting of the over-heating ratio was
accomplished by setting the "Resistance" switch to the "external" position,
connecting a non-inductive decade resistance box to the "External Resistance"
terminal, and setting this external resistance to within a tenth of an ohm of the
required value. The required external resistance (R_{ext}) was determined by the
equation,

$$R_{ext} = 10 \ (r R_c + R_L)$$

where r is the heating ratio required (which is recommended by the manufacturer),
R_c is the cold resistance of the probe at 20°C, and R_L is any resistance added by
the lead connections. The recording instrumentation for this test was the CEC
recorder as used during the OR/NOR Gate test, except that model 7-364 galva-
nometer and required damping circuits were used permitting a flat (±5%) frequency
response of 0 to 500 cps.

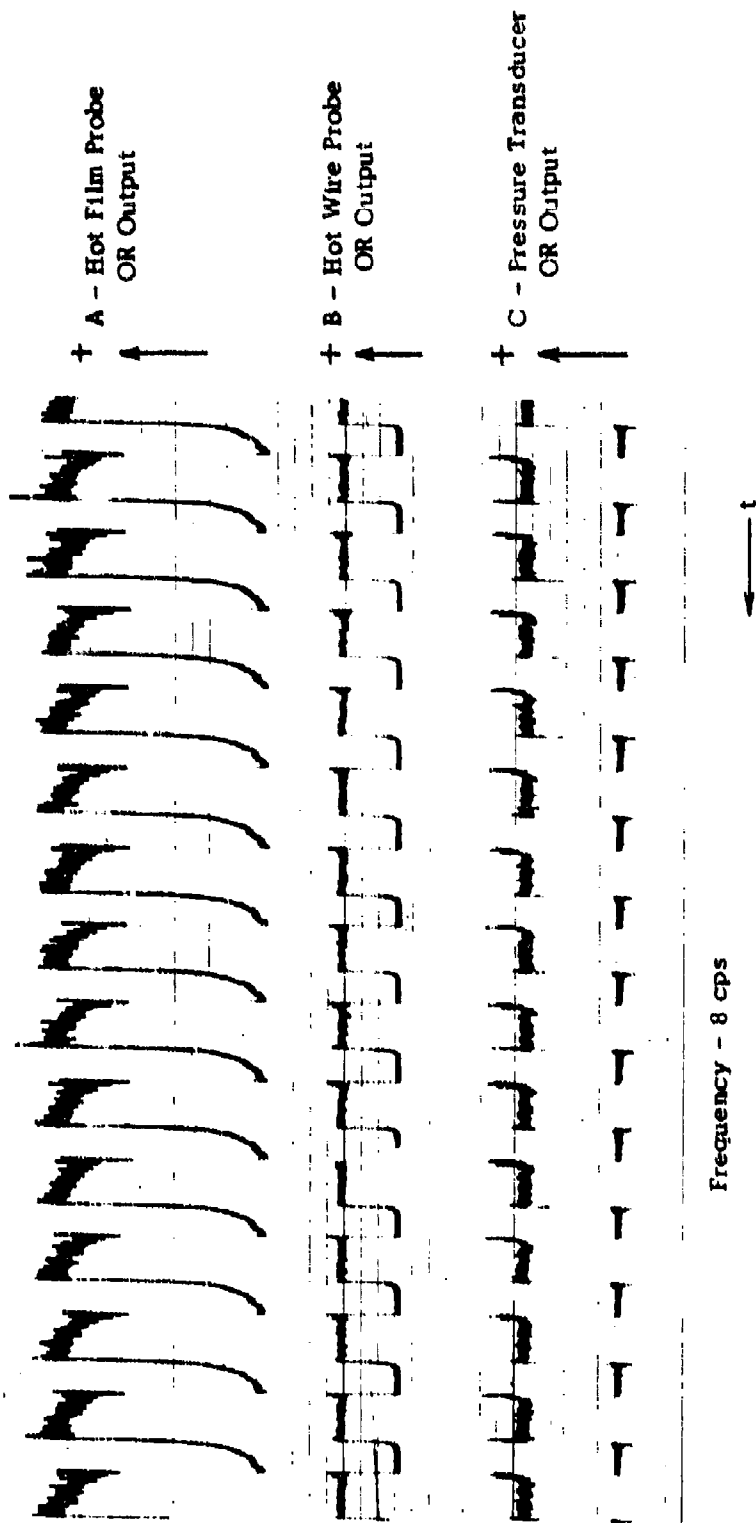The performance of this hot wire probe is shown in Figure 76. The results show

141

Figure 76. Digital Pulse Shaping Circuit
Flow Anemometry Test

A – Hot Film Probe
OR Output

B – Hot Wire Probe
OR Output

C – Pressure Transducer
OR Output

Frequency – 8 cps

142

that its ability to detect dynamic primary performance is highly satisfactory. The adjustments made to the external circuitry led to a considerable improvement in its performance ability compared to the results of earlier tests. Although its amplitude characteristics are inherently non-linear, its ability to detect dynamic flow events, a characteristic of principle interest in digital circuitry, is highly satisfactory.

The flow detecting performance characteristic of a hot film probe was investigated for the first time during this test. As shown in Figure 74, it was mounted in the OR output channel so that it could be comparatively evaluated against the performance of the hot wire probe and the pressure transducer. The probe was a Disa model 55A91. Its design is such that it permit flush-mounting in a flow channel wall without changing the geometry of the circuit or disturbing the flow. This model of hot film probe has a quartz coated film permitting its use in liquids.

The hot film probe was connected to the Disa constant temperature anemometer model 55D05, as was the hot wire probe described above. The "Resistance" switch was set in the "external" psoition and a 280 ohm resistor was connected to the "External Resistance" terminal to provide the proper over-heating ratio, according to the manufacturer's specifications for this model of probe. The anemometer supplied the power to the probe and produced an output proportional to the power delivered. The output of the anemometer was recorded on the CEC model 5-124 recording oscillograph using a model 7-364 galvanometer and damping network permitting a flat ($\pm$ 5%) frequency response of 0 to 500 cps.

Figure 76 shows the performance of the hot film probe along with that of the hot wire probe and the pressure transducers mounted in the same channel. The results show that the hot film probe is capable of detecting qualitative measurements of flow events related to the time scale similar to that detected by the hot wire probe. While poorer dynamic response is shown for the hot film probe, it is believed that the response time can be appreciably improved by optimizing the over-heating ratio.

c.   Secondary Sensing Evaluation

Static tests were conducted to evaluate the secondary acoustic signature technique used in the previous OR/NOR element test as to its capabilities of detecting levels of an anomaly induced in one element with the detector (accelerometer) mounted in the near field of another element. Figure 74 shows the location of the accelerometer as being near the output of the Flip-Flop element. The anomalies were introduced into the OR/NOR Gate element. The instrumentation necessary to monitor and record the signature detected by the accelerometer was similar to that for the static test on the OR/NOR Gate element, as described in Section 5. The mounting of the accelerometer for this test consisted of drilling and tapping a hole at the selected location

143

and mounting the accelerometer on a screw-mounting stud provided by the manufacturer for this purpose.

Figure 77 shows the changes that occurred in the acoustic signature detected for various supply anomalies introduced into the OR/NOR element. The pulse shaper circuit was functioning in its static state (no signal input) for this test. The results of this test show that it is possible to detect anomalies in one digital element by secondary acoustic sensing while the sensor is located in the near field of another digital element. It is believed that centrally locating the accelerometer with respect to the interaction regions of all elements contained within a circuit plate would result in an increase in the sensitivity of the sensing technique.

d. Conclusions

The described test results in conjunction with prior tests of a single digital element, indicate that the evaluated miniature pressure transducer, hot wire and hot film anemometers, and piezoelectric crystal, each offer a satisfactory means of monitoring the primary performance of a simple digital circuit. It was concluded that euqally satisfactory results could be expected with a more complex citcuit.

The capability of acoustic sensing techniques to detect an anomaly in one element in the presence of a second active element was shown. This accomplishment, along with the positive results of acoustic detection tests with a single element, indicated that the secondary acoustic sensing technique should provide an effective means of detecting and defining anomalies in a more complex digital circuit.

The results of this effort are incorporated into Section 8, Summary of Sensor Applicability.

7. PACKAGING AND ENVIRONMENTAL STUDY

A study was carried out to establish means of mounting the candidate sensors to typically packaged Fluidic circuitry. Two packaging concepts were considered. One concept was the modular packaging approach where single circuit plates are attached to one or both sides of a manifold, with a cover placed over each circuit plate, the complete package assembly being a circuit module. Systems may be assembled by the rack mounting and interconnection of the number of modules required to make up the total system. The second packaging concept considered was a stacked circuitry arrangement. In this case, circuit plates and manifolds are stacked into a monolithic assembly which may make up a complete Fluidic system.

144

ELEMENT: PULSE SHAPER

SENSOR: Accelerometer
B&K Model 4333

$P_{S1} = 1$ PSIG

$P_{IN} = 0$

$\triangle - P_{S2} = 0$

$C - P_{S2} = 1$ PSIG

$\square - P_{S2} = 1.5$ PSIG

$\diamondsuit - P_{S2} = 2$ PSIG

Relative
Amplitude

1.75   4.25   6.75
Frequency – KC
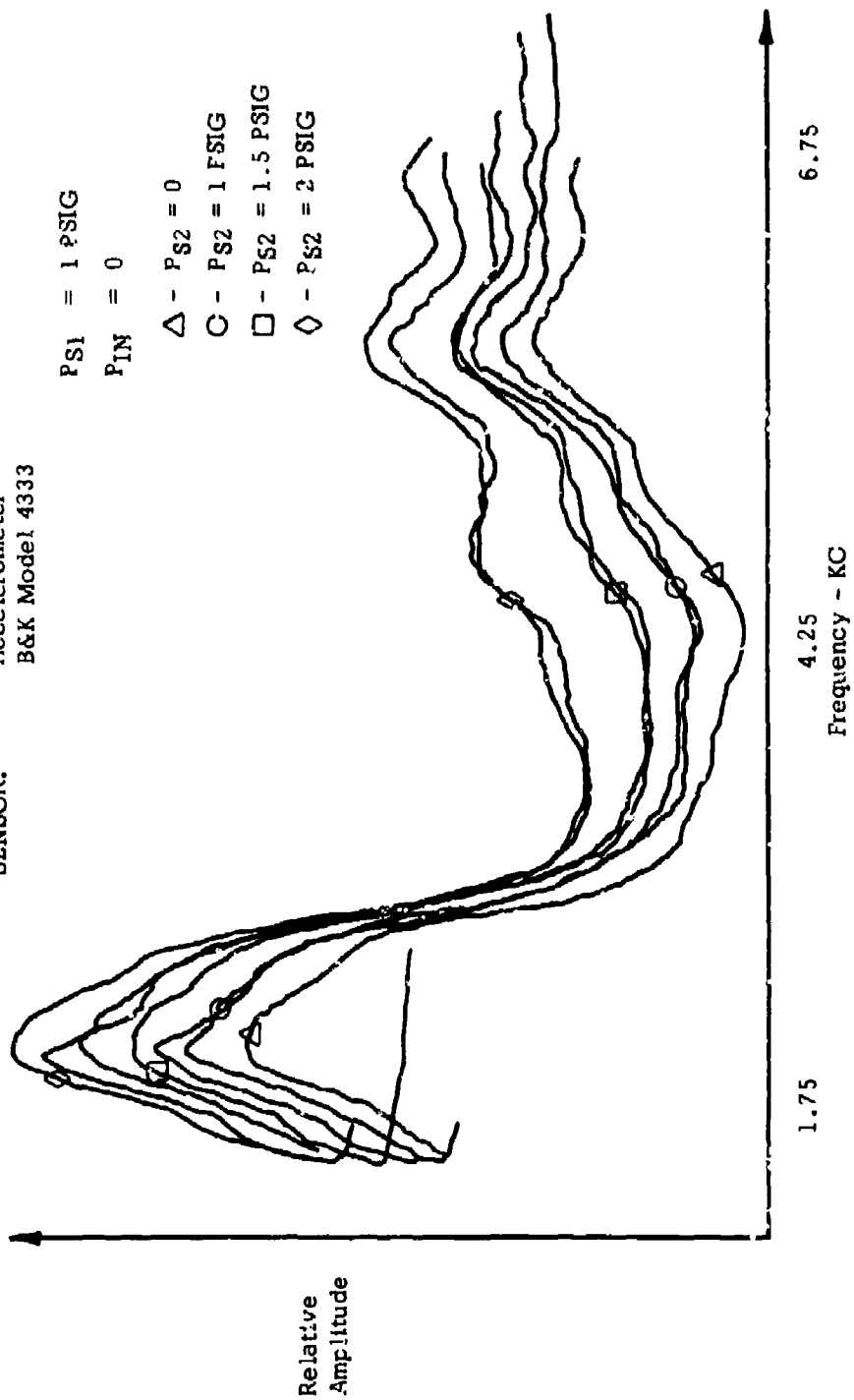
Figure 77. Digital Pulse Shaping Circuit Acoustic
Signature Changes – Supply Pressure
Anomalies

145

The effects of environmental conditions on the candidate sensors was investigated, considering temperature, pressure, humidity, vibration, acoustic energy, and electromagnetic energy.

The results of both investigations are presented by BEC TM-147, "Compatibility of Sensors with Packaging Approaches and Effect of Environment on Sensors" which is located in Appendix III of this report.

In summary, the following candidate sensors are compatible with the modular packaging concept:

- o Microphone
- o Accelerometer
- o Anemometer
- o Miniature Pressure Transducer
- o Thermistor
- o Piezoelectric Crystal.

The sensors listed below are considered to be compatible with the stacked packaging concept:

- o Accelerometer
- o Anemometer
- o Miniature Pressure Transducer
- o Thermistor
- o Piezoelectric Crystal.

The candidate miniature mircophone is not considered suitable to stacked circuitry due to the compactness of the circuitry and lack of common spaces into which groups of elements vent and into which microphones may be mounted. In most cases, mounting of the compatible sensors into a modular package is more easily accomplished than mounting into a stacked circuit arrangement, because of the higher circuit density and less available space in the latter. The infrared thermometer which was used to evaluate the feasibility of I.R. sensing techniques was too large to be practicably mounted as an operational sensor to either type of circuit package.

Most of the sensors are influenced to some degree by one or more of the considered environmental conditions. In some cases, the influence may be negligible. Where this is may not be true, it is considered that appropriate

146

compensation may be made. When selecting sensors for use in a specific
checkout procedure for a Fluidic system, the effects of the encountered
environmental conditions on the sensor characteristics, and consequently
on the accuracy of the checkout procedure, must be evaluated.

8. SUMMARY OF SENSOR APPLICABILITY

Part 2. of Section III defines a group of candidate sensors which were selected
early in the program as being potential sensors of the state of operation of
Fluidic circuitry. Through a program of analysis and testing with analog and
digital elements and simple circuits, the capabilities of these sensors were
evaluated. The results of this program are presented by the present section.

The sensors were evaluated in terms of the capability to detect malfunctions
or to define the causes of malfunctions. The compatibility of the sensors with
two typical types of circuit packaging arrangements was investigated. One
type of package is a modular arrangement where a single circuit plate is
attached to one or both sides of a manifold, with a protective cover then
placed over each circuit plate. The second package type is a stacked circuitry
arrangement, where circuit plates and manifolds are stacked into a multi-
layered monolithic structure. In addition, the effects of environment on the
sensors were investigated. The conclusions drawn concerning each of the
candidate sensors are summarized in the following.

a. Miniature Pressure Transducer

The Scientific Advances, Inc. Model SA-SD-M-6H miniature pressure transducer
is a highly satisfactory sensor of the functional operating signals of both analog
and digital circuitry. This device is a small strain gage pressure transducer
of 0.25 in. diameter and 0.25 in. length, designed so that it may be mounted
flush to a circuitry channel wall. The flush mounting capability permits the
sensing of pressure signals without causing any deformation of the sensed signal.
Pressure range of ± 2, ± 5, ± 10, ± 15, ± 30, and ± 100 psig are available.

The peripheral equipment required for this sensor is a standard d-c transducer
bridge and power supply, which provides the transducer exitation voltage and
the capability of adjusting the output signal null.

The sensor is well suited to accurately establishing the level of performance
of both analog and digital circuitry, to establish whether or not performance
(in terms of pressure signals) is within specified limits. A linearity of $\pm 0.5\%$
of full scale permits the accurate detection of analog circuitry performance.
The natural frequency of 15.5 KHz is sufficient to accurately sense the transient
characteristics pertinent to the satisfactory performance of most digital
circuitry.

147

The pressure transducer may be suitably mounted into both circuit modules and stacked circuitry. Mounting into the circuit plates of circuit modules is readily accomplished. Where mounting into stacked circuitry, it may be necessary to design the circuitry layout to provide the necessary mounting space.

Temperature variations cause a small change in sensitivity of the pressure transducer and in the zero outputs, a 0.01% full scale sensitivity change and 0.05% full scale zero shift per ^{0}F for a temperature compensated model. Where checking out circuitry with small allowable deviations in pressure signal transfer characteristics, it may be desirable in some cases to incorporate a temperature compensation adjustment into the external bridge, to correct for changes in sensitivity without resorting to a pressure calibration.

b.   Flow Anemometers

The Disa Electronics Model 55A52 hot wire probe and type 55A90/91 flush-mounting hot film probe are applicable to the checkout of functional performance of digital circuitry, as defined in terms of mass flow signals. Because of fundamental nonlinear characteristics, and the possibility of calibration changes due to contamination and oxidation, the hot wire and hot film probes are not well suited to the checkout of analog circuitry, where accurate monitoring of signal levels is highly important. Since in the checkout of digital circuitry, the transient characteristics of signals are normally of greater significance than a high degree of accuracy of signal levels, the nonlinearity of the hot wire and hot film probes, and the possibility of small calibration changes, do not present a serious disadvantage.

The model 55A52 hot wire probe is sufficiently miniaturized so that the supporting needles (0.8 mm. long, spaced 0.45 mm. apart) and wire may be inserted into a circuit channel without affecting an appreciable deformation of the sensed signal. The type 55A90/91 hot film probe, with an end diameter of 4.75 mm. may be mounted flush to a circuit channel wall. The hot wire probe has a number of advantages relative to the hot film probe. It is smaller and less costly. The advantages of the hot film probe are no interference with functional signals, less possibility of damage due to contaminants in the operating fluid, and, should cleaning of circuitry be necessary, less possibility of damage during a solvent flushing procedure. The desirability of the hot wire vs. the hot film probe is dependent upon the instrumentation requirements for specific circuitry checkout procedures.

Both probes may be coupled to a Disa type 55D05 constant temperature anemometer system which heats the wire or film to a constant temperature and provides an output signal which may be directed into a wide range of recording or display devices. The frequency range of the anemometer system is zero to 50 KHz, the upper limit being dependent on the probe and conditions of measurement. Evaluation tests made with digital elements and simple circuitry, as

described in parts 5. and 6. of this section, indicate that the frequency response of the anemometer system/probe combination is adequate to define the functional performance of digital circuitry.

Both of the probe types may be readily incorporated into modularized circuitry. For stacked circuitry, the hot wire probe is more suitable, because of its smaller size.

Environmental conditions which lead to variations in the temperature, pressure, or humidity of the sensed operating fluid, may in some cases cause sufficient calibration changes to require the use of calibration curves or multiple anemometer installations (and appropriate electronic circuitry) to null out these effects.

c.   Piezoelectric Crystals

PZT Bimorph ceramic crystals, manufactured by the Piezoelectric Division of Clevite Corporation have been demonstrated by laboratory tests to exhibit good potential as sensors of digital element functional performance. These crystals, when suitably flush-mounted to a channel wall, generate a differential charge potential when deformed by a pressure signal. The crystals are not as well suited to analog circuitry since the output signal (the charge generated by deformation) is not necessarily a linear or easily predictable function of signal pressure. Tests indicate, however, that the linearity is adequate and the response is sufficiently fast to detect the functional performance of digital circuits. The prime advantage of the crystals in comparison to the pressure transducer or hot wire anemometer is a lower cost. Where a checkout procedure for specific digital circuitry requires a relatively large number of functional performance check points, the cost advantage of the crystal sensor may be significant, and may lead to selection of this sensor as the most suitable.

The output of the crystals may be coupled directly to a variety of common display and recording devices when used as a transient sensor, as is the case with digital performance monitoring. A high impedance load is desired to minimize the rate of discharge.

The piezoelectric crystals are highly compatible with both the modular circuit and the stacked circuit packaging concept.

The pressure calibration of the crystals is effected to some degree by temperature variations. It is expected that in most cases, the calibration changes would not greatly effect usefulness as a sensor for digital circuits.

149

d. Infrared Sensing

A Barnes Engineering Company Model PRT-4 radiation thermometer was tested as a means of evaluating the potential of I.R. sensing techniques. It was initially considered that a thermal map of a Fluidic circuit plate, generated by an I.R. sensor, would show variations due to changes of the internal flow field caused by anomalous conditions.

During laboratory tests, changes in the thermal map were induced by a number of anomalous conditions of relatively large magnitude. The sensitivity was not, however, considered sufficient to detect the less gross anomalous conditions that normally cause a malfunction. The possibility of obtaining useful information from thermal maps is further diminished by the effects of variations in operating fluid temperature and external environmental temperature.

It was concluded that I.R. sensing techniques are not well suited to the checkout of Fluidic circuitry.

e. Thermistors

Thermistors are considered to nave a limited usefulness in the checkout of Fluidic circuitry. The thermistors investigated during the program were Fenwal Electronics, Inc., Model GB32J2 units. These are small beads of 0.043 inch diameter which may be mounted within a circuit plate adjacent to a circuit channel wall. The thermistors so located can detect, to some degree, changes in temperature of the operating fluid within the channel, which may indicate a change in operating conditions of a Fluidic circuit.

The response of a mounted thermistor is too slow to be well suited to the sensing of functional performance. It was initially considered, however, that the thermistor might be useful in detecting, through changes in stream temperature, changes in pressure that should remain constant, such as supply and bias pressures. A thermistor located adjacent to a channel wall senses approximately adiabatic wall temperature. This temperature deviates from the stagnation temperature most where the velocity is greatest and the static temperature lowest, which occurs at a restriction such as a power nozzle, and in this location should exhibit the greatest sensitivity to undesired changes in supply pressure. Analytical and test results indicate that while supply pressure changes can be detected by a thermistor, the sensitivity is low when considering typically encountered limits of supply pressure or bias pressure variations. The capability of obtaining meaningful information from thermistors is hindered by the detection of changes in stream stagnation temperature and ambient temperature, both of which may have no effect on supply or bias pressures. Only in cases where large pressure variations are of interest and where stream stagnation temperature and external temperature are nearly constant (or compensation for changes provided) does the thermistor appear to have useful applications. Typically, the external equipment

used with a thermistor is a d.c. power supply and bridge circuit, with the thermistor being one leg of the bridge.

The thermistor, because of its small size, may be easily incorporated into modularized or stacked circuitry.

The environmental condition of greatest concern is temperature. It is probable that much can be done to minimize the effects of changes in stream stagnation temperature and external temperature through the use of multiple thermistors and external compensation circuitry.

f. Accelerometer

Laboratory evaluation tests of a B&K, Inc., Model 4333 accelerometer have shown the accelerometer to be highly effective in the isolation of faults. The accelerometer does not directly detect functional performance. Its value lies in detecting and defining the causes of malfunction of a Fluidic circuit.

It has been demonstrated by laboratory tests that the presence of anomalies, such as supply pressure changes, contamination, and element deformation, may be detected by analysis of the frequency content of the acoustic energy generated by functioning analog and digital circuitry, as sensed by an accelerometer mounted to a circuit plate. Anomalies of the relatively small magnitudes causing performance deviation limits to be reached, have been detected and defined by the changes produced in the amplitude vs. frequency acoustic signature of elements and simple circuits. Each introduced anomaly caused a distinguishingly different change in the acoustic signature. It is highly significant that anomalies occurring in one element of a group of functioning elements have been isolated. This indicates the potential of defining the cause of malfunction of an integrated circuit, such as an analog integrator, through the use of a single sensing element permanently attached to the circuit plate.

The accelerometer tested was of reasonably small size, 1.4 cm. hex. x 1.6 cm., and mountable to circuit plates by means of an adhesive or threaded mounting stud. Smaller accelerometers are available for cases where space limitations do not permit use of an accelerometer of this size. The frequency range of the B&K accelerometer was 2 to 14,000 Hz which appeared to be sufficient.

The accelerometer may be coupled into a Panoramic LP-1a sonic analyzer, or a Panoramic SB-15a ultrasonic analyzer, both of which provide a means of determining the amplitude vs. frequency signature of the sensed acoustic energy. A recorder such as the Moseley 7035a X-Y recorder may be used to record the acoustic signature. Figure 22 shows an instrumentation arrangement used during tests with a three stage amplifier.

151

The accelerometer is compatible with both the modularized and stacked circuit package concepts. In the stacked circuit arrangement, it is necessary to design space into circuit plates for the integral location of an accelerometer, and it may be desirable to use an accelerometer of smaller size.

There is a slight change in the accelerometer sensitivity with temperature changes. Data supplied by the manufacturer allows for sensitivity change compensation if required. Since changes in shape of the acoustic signature are more critical to the isolation of faults than are precise signature amplitudes, it is probable that under most conditions, temperature induced sensitivity changes will not present a problem. Externally introduced vibrations within the signature bandwidth may be either damped out by appropriate package and mounting means or may be factored into the interpretation of the signature.

g. **Microphone**

The Massa M-213 miniature microphone has been shown to be capable of sensing the secondary acoustic energy generated by Fluidic circuitry and thus may be used for fault isolation in a manner similar to that with an accelerometer.

The primary differences between the microphone and acceleromter sensors is the medium through which acoustic energy, much of which is generated in the element interaction region, is transmitted to the sensor. A microphone located in a fixed position close to the vented side of Fluidic elements senses the acoustic energy transmitted by air from the interaction region through the vents to the sensor. In the case of an accelerometer mounted to a circuit, the transmission medium is the structural material from which the circuit is formed.

Tests made with the microphone, though not as extensive as for the accelerometer, indicate that the microphone should be nominally as effective in sensing secondary acoustic energy as the accelerometer. The microphone, in conjunction with a Massa M-114B preamplifier and M-185 amplifier and power supply, when coupled to a spectrum analyzer and recorder should have basically the same capabilities in fault isolation as the accelerometer.

Where the microphone is to be used to isolate faults within an integrated circuit, it is desirable that all of the amplifiers vent into a common space within which the microphone may be located. To achieve repeatability of acoustic signatures, it is necessary that the relative positions of everything within the space be held constant. It was found difficult to sufficiently satisfy this requirement during laboratory tests because of versatilities built into the laboratory set-ups, which would not occur in an operational checkout arrangement.

152

The microphone may be easily incorporated into a modularized circuit, within the space between a circuit plate and the protective cover placed over the circuit plate. Location within a stacked circuit is more difficult, requiring that the circuitry structure be designed to provide a chambe into which to mount the microphone and into which some number of elements may be vented.

Temperature variations may effect the sensitivity of the microphone. As in the case of the accelerometer, since changes in shape of the signature are of greatest importance in defining the anomaly causing a malfunction, small sensitivity changes should not present a problem in many cases. Calibration data as a function of temperature allows for sensitivity compensation if needed. Externally generated noise and vibration within the selected signature bandwidth may be either damped by appropriate packaging and mounting, or may be factored into the interpretation of the signature.

SECTION VI

EVALUATION OF INTEGRATED CIRCUITRY INSTRUMENTATION AND HEALING TECHNIQUES

1.   EVALUATION OF INSTRUMENTATION FOR AN
      ANALOG CIRCUIT MODULE

The investigations described in Section V of this report have shown that for analog elements and a simple analog circuit, the secondary acoustic signature, i.e., the sound and/or vibration emitted by a Fluidic element, provides a means of detecting and defining an anomaly, once its existence has been established by the degradation of primary performance. It has been concluded that primary performance sensors are required to determine overall performance. This section discusses the extension of that technique to a circuit module from the Feedwater Controller, which was chosen as representative of analog controls.

The primary performance of the chosen module was established, with all parameters within specified values, as a base line. Three (3) anomalies were introduced and the primary and secondary characteristics determined. The anomalies were; first, changes in supply pressure (P^+); second, changes in circuit load; and third, introduction of contamination into the circuit.

a.   Description of Circuit to be Tested

The analog circuit chosen for test is part of one module of a Feedwater Controller for a Naval boiler. The module consists of an integrated circuit plate attached to a manifold which supplies pressure to each of the circuit elements. The particular module circuit is shown in Figure 78. A functional block diagram of the complete Feedwater Controller is shown as Figure 79, with the circuit of interest enclosed by dashed lines. The other circuit on the module is substantially identical.

This circuit operates to produce an output signal pressure which is proportional to the difference of the two input signals. In other words, it operates as a typical summing amplifier, so that $\dot{W}_e = \dot{W}_w - \dot{W}_s$. $\dot{W}_e$ is output pressure, $\dot{W}_w$ and $\dot{W}_s$ are the input pressure signals. Typical performance is shown in Figure 80, which presents $\dot{W}_e$ vs. $\dot{W}_s$ for $\dot{W}_w$ a constant, and $\dot{W}_e$ vs. $\dot{W}_w$ for $\dot{W}_s$ a constant.

b.   Test Setup

Pressure transducers were connected through signal conditioners to an X-Y recorder for primary performance. A B&K Model 4333 accelerometer was used
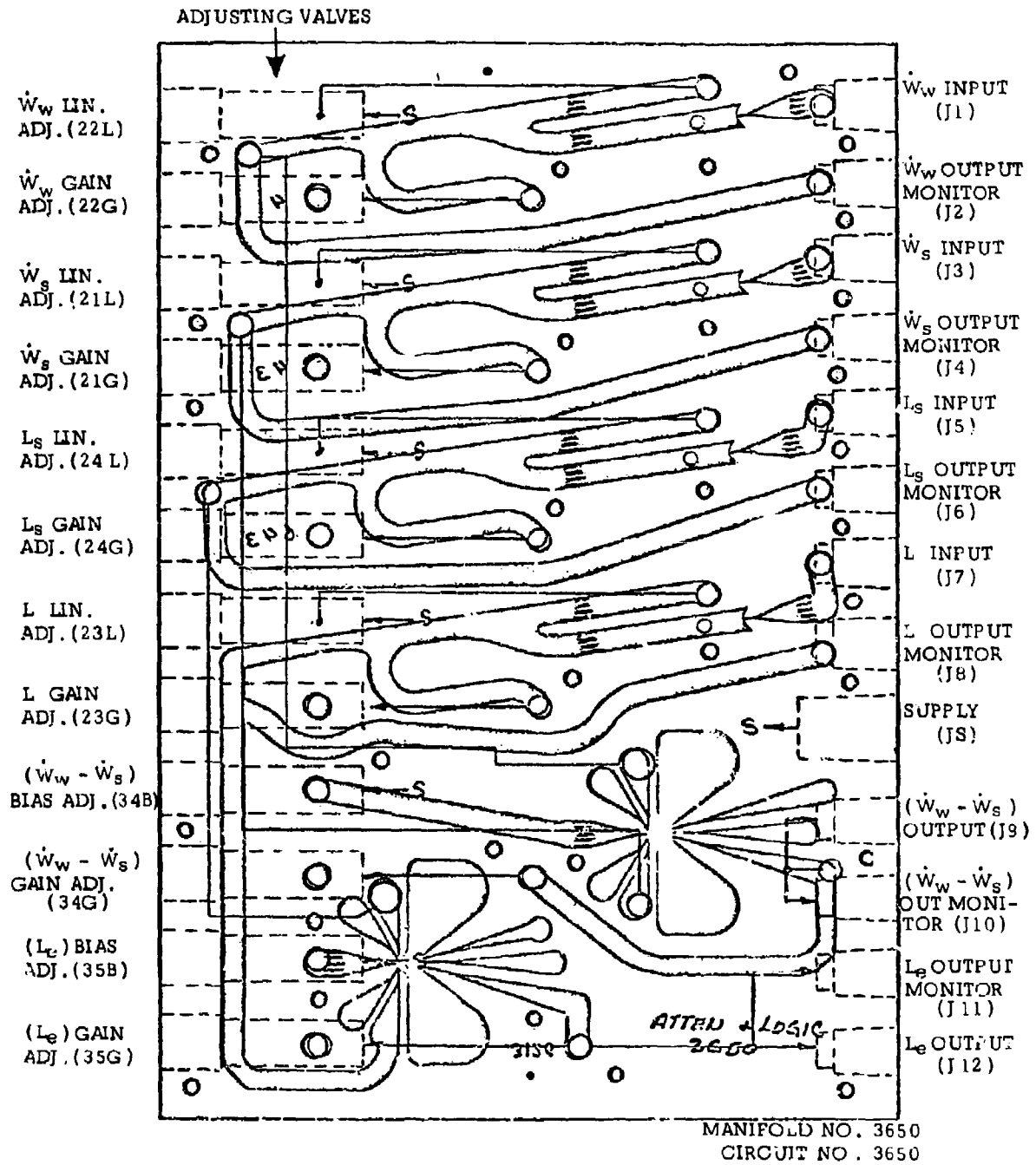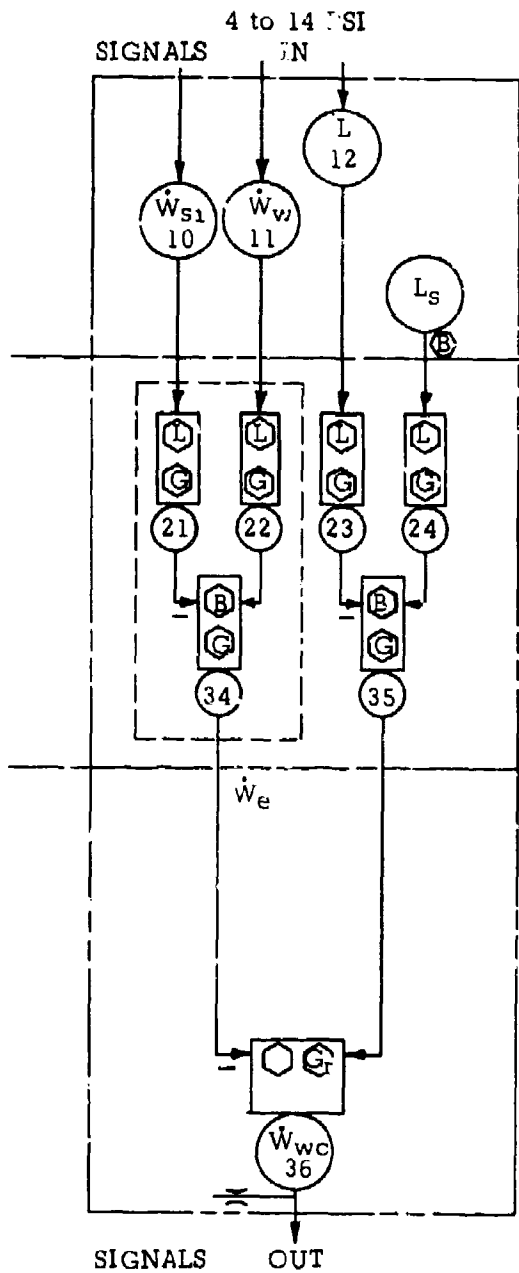
ADJUSTING VALVES

$\dot{W}_w$ LIN.
ADJ.(22L)

$\dot{W}_w$ GAIN
ADJ.(22G)

$\dot{W}_s$ LIN.
ADJ.(21L)

$\dot{W}_s$ GAIN
ADJ.(21G)

L_s LIN.
ADJ.(24L)

L_s GAIN
ADJ.(24G)

L LIN.
ADJ.(23L)

L GAIN
ADJ.(23G)

$(\dot{W}_w - \dot{W}_s)$
BIAS ADJ.(34B)

$(\dot{W}_w - \dot{W}_s)$
GAIN ADJ.
(34G)

(L_e) BIAS
ADJ.(35B)

(L_e) GAIN
ADJ.(35G)

$\dot{W}_w$ INPUT
(J1)

$\dot{W}_w$ OUTPUT
MONITOR
(J2)

$\dot{W}_s$ INPUT
(J3)

$\dot{W}_s$ OUTPUT
MONITOR
(J4)

L_s INPUT
(J5)

L_s OUTPUT
MONITOR
(J6)

L INPUT
(J7)

L OUTPUT
MONITOR
(J8)

SUPPLY
(JS)

$(\dot{W}_w - \dot{W}_s)$
OUTPUT(J9)

$(\dot{W}_w - \dot{W}_s)$
OUT MONI-
TOR (J10)

L_e OUTPUT
MONITOR
(J11)

L_e OUTPUT
(J12)

ATTEN & LOGIC
2600

MANIFOLD NO. 3650
CIRCUIT NO. 3650

Figure 78. Feedwater Control Attenuators and Logic Module

156

SIGNALS

4 to 14 PSI
IN

○─ PRESSURE SIGNALS – MONITORING
CAPABILITY PROVIDED

Ⓑ = BIAS ADJUSTMENT

Ⓖ = GAIN ADJUSTMENT

Ⓛ = LINEARITY ADJUSTMENT

─⟍─ = ORIFICE, .0008 in² EFFECTIVE AREA

Ⓛ
Ⓖ = ATTENUATOR

Ⓑ
Ⓖ = DIFFERENTIAL RELAY

ⒷⒼ = MINIMUM SIGNAL SELECTOR

⬡⬡
⬡⬡ = PROPORTIONAL PLUS RESET
CONTROLLER SUBCIRCUIT

⬡⬡ = RESET CONTROLLER
SUBCIRCUIT

$\dot{W}_e$

SIGNALS   OUT

SIGNAL NOMENCLATURE

$\dot{W}_f$ = FUEL FLOW

$\dot{W}_{ab}$ = AIR FLOW BIAS

$\dot{W}_a$ = AIR FLOW

P_{ss} = STEAM PRESSURE SET POINT

P_s = STEAM PRESSURE

$\dot{W}_s$ = STEAM FLOW

L = WATER LEVEL

L_s = WATER LEVEL SET POINT

$\dot{W}_w$ = WATER FLOW

$\dot{W}_{ac}$ = AIR FLOW COMMAND

$\dot{W}_{fc}$ = FUEL FLOW COMMAND

$\dot{W}_{wc}$ = WATER FLOW COMMAND
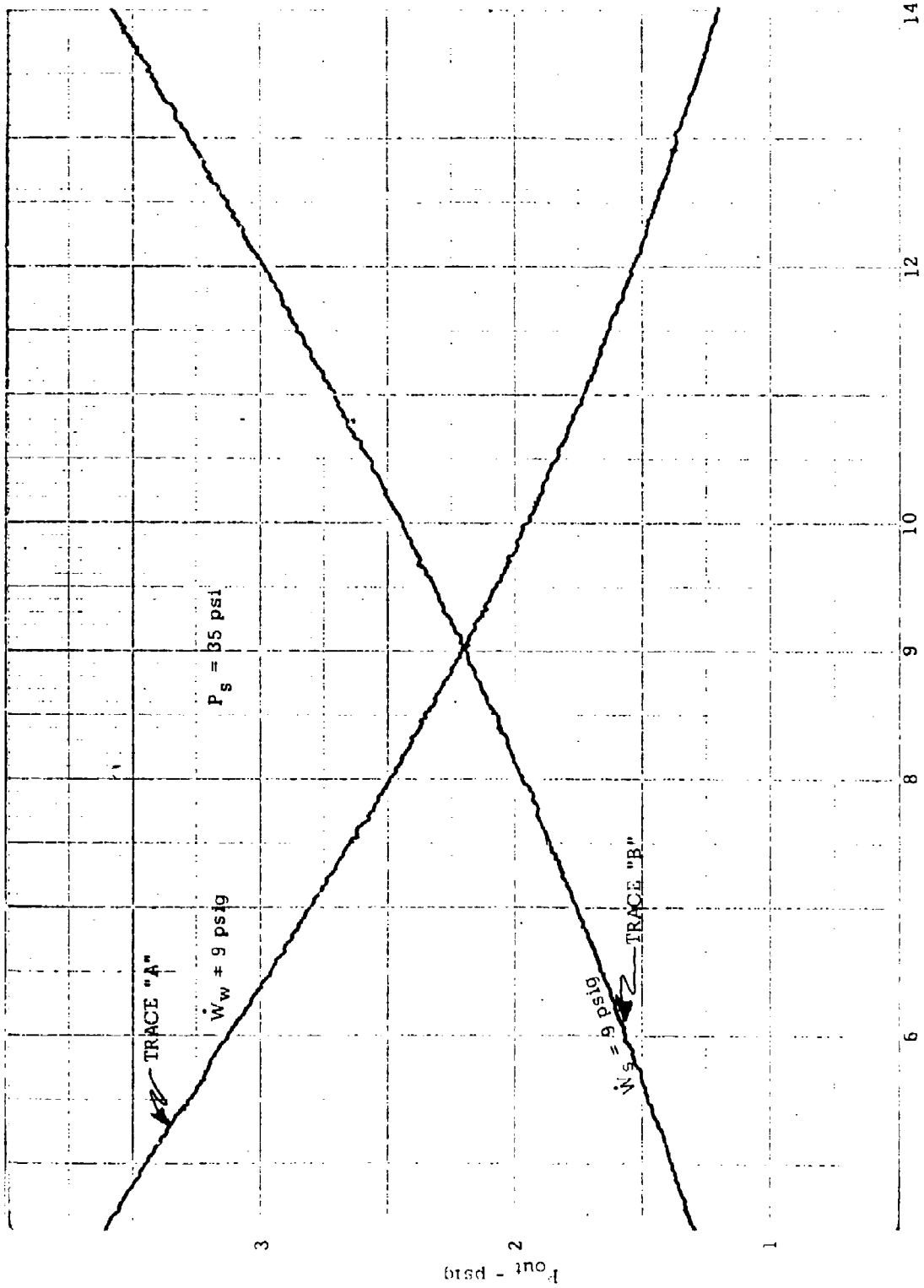
Figure 79. Feedwater Controller

157

Figure 80. Attenuator and Logic Module Test
Primary Performance Monitoring
Satisfactory Performance

to detect changes in the secondary acoustic signature for various anomalies.
Preliminary experiments were performed to determine the optimum position for
the accelerometer. The signal from the accelerometer was analyzed by a
Panoramic ultrasonic analyzer using a band from 15 KHz to 65 KHz. This
signature was then recorded as amplitude vs. frequency on an X-Y recorder.

c. Results Varying Supply Pressure

The supply pressure to the circuit is specified to be 35 psig. A typical
system malfunction is a decrease in supply pressure. Therefore, perfor-
mance with degraded supply pressure is of interest. The primary performance
for supply pressures of 35, 30, 25, and 20 psig is shown in Figure 81. The
nominal null output pressure is shown, about 3.1 psig, and the change in
input required to produce that null can be readily seen. For this circuit,
the allowable null shift is on the order of ±.2 psi.

The secondary acoustic signature for changes in supply pressure is shown
in Figure 82, for the condition where the input pressures are equal. This
acoustic signature is distinctive from that produced by other anomalies
because it changes proportionally along most of the curve. Sensitivity is
sufficient to detect the magnitude of supply pressure variation effecting the
allowable null shift.

d. Results Varying Load

The normal load for this circuit is a 0.020" x 0.040" control port in the next
section of the control. The circuit testing was done with an equivalent load
orifice (0.0008 in²). Typical malfunctions in service could be a complete
blockage (deadended), a small leak, and a complete disconnection (short
circuit). Tests were performed to simulate these conditions, i.e., blocked
or deadended, increased load to 0.0014 in² orifice, and complete dis-
connection.

The primary characteristics are shown on Figure 83 for these loads. The change
from null is readily apparent. The secondary acoustic signatures are shown in
Figure 84. The change in signature occurred primarily in the vicinity of 40 KHz.
An expanded scale display of this region is shown in Figure 85. From this it
can be seen that changes in load produce a change in secondary acoustic
signature quite different from that caused by supply pressure variation, and that
sufficient sensitivity in detecting this anomaly exists.

e. Results From Varying Levels of Contamination

Contamination is a rather subjective parameter, and no exacting method of
measuring, or for that matter, producting contamination exists. Previous
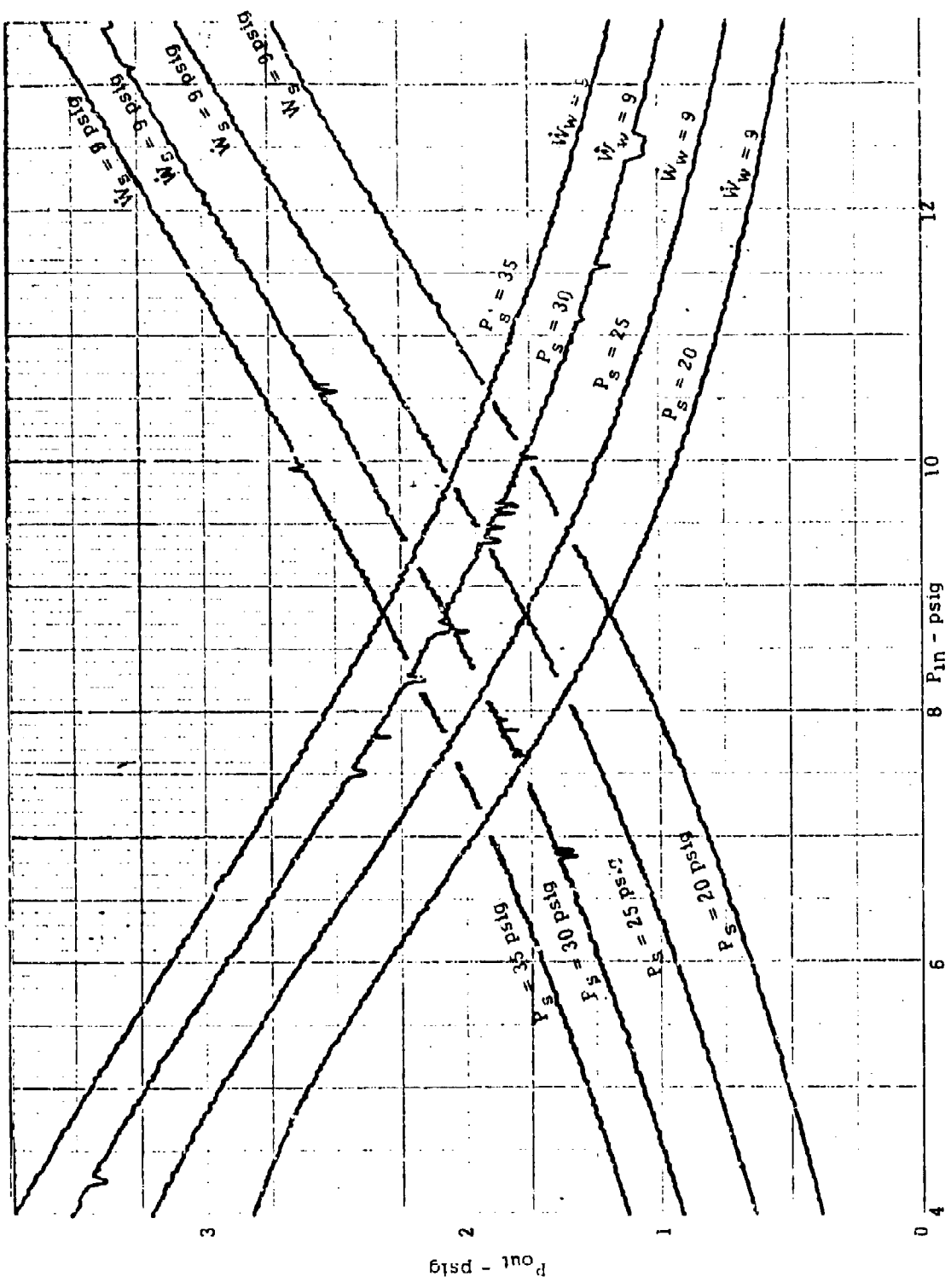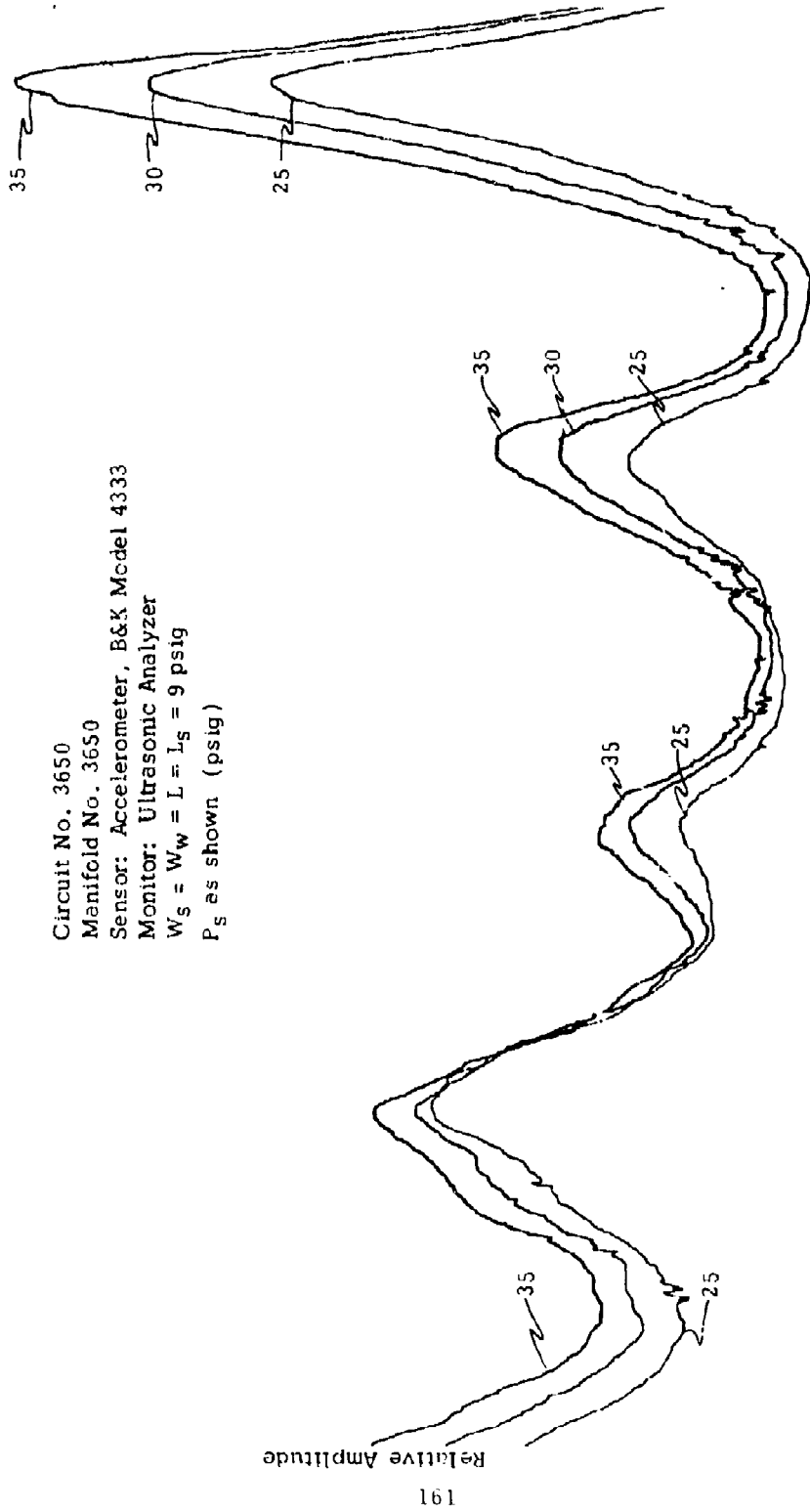experience has shown that a typical contaminating situation exists when

159

Figure 81. Analog Attenuator and Logic Module Test
Primary Detection
Supply Pressure Anomalies

160

Circuit No. 3650
Manifold No. 3650
Sensor: Accelerometer, B&K Model 4333
Monitor: Ultrasonic Analyzer
$W_s = W_w = L = L_s = 9$ psig
P_s as shown (psig)

- Frequency -

Figure 82. Analog Attenuator and Logic Module Test
Supply Pressure Anomalies
Secondary Detection
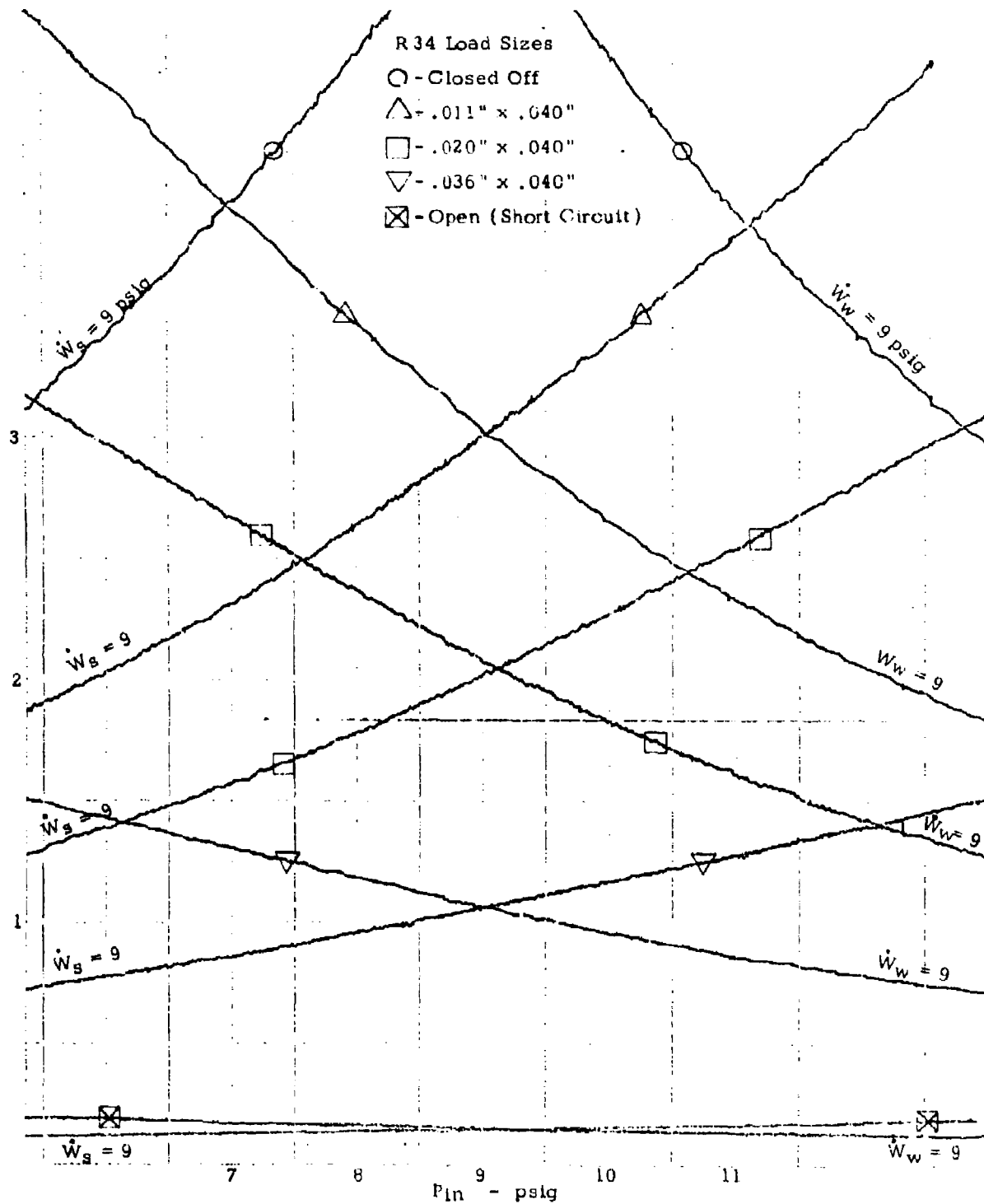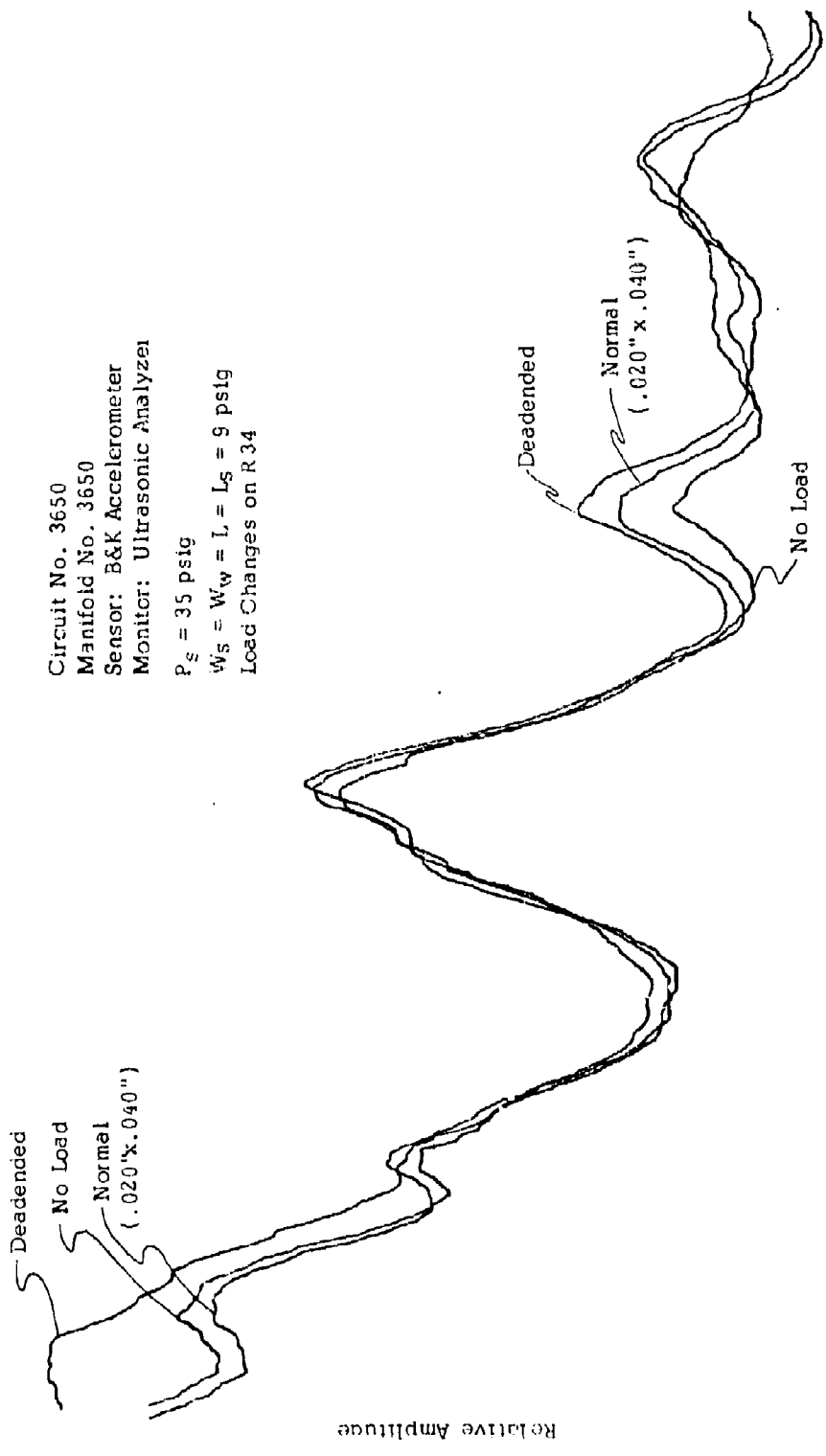
61 KC

23 KC

Relative Amplitude

161

Figure 83. Analog Attenuator and Logic Module Test
Primary Detection - Load Anomalies

Circuit No. 3650
Manifold No. 3650
Sensor: B&K Accelerometer
Monitor: Ultrasonic Analyzer

$P_S = 35$ psig
$W_S = W_W = L = L_S = 9$ psig
Load Changes on R 34

Deadended
No Load
Normal
(.020"x.040")

Deadended
Normal
(.020"x.040")
No Load

Relative Amplitude

– Frequency –

15 KC   52 KC

Figure 84. Analog Attenuator and Logic Module Test
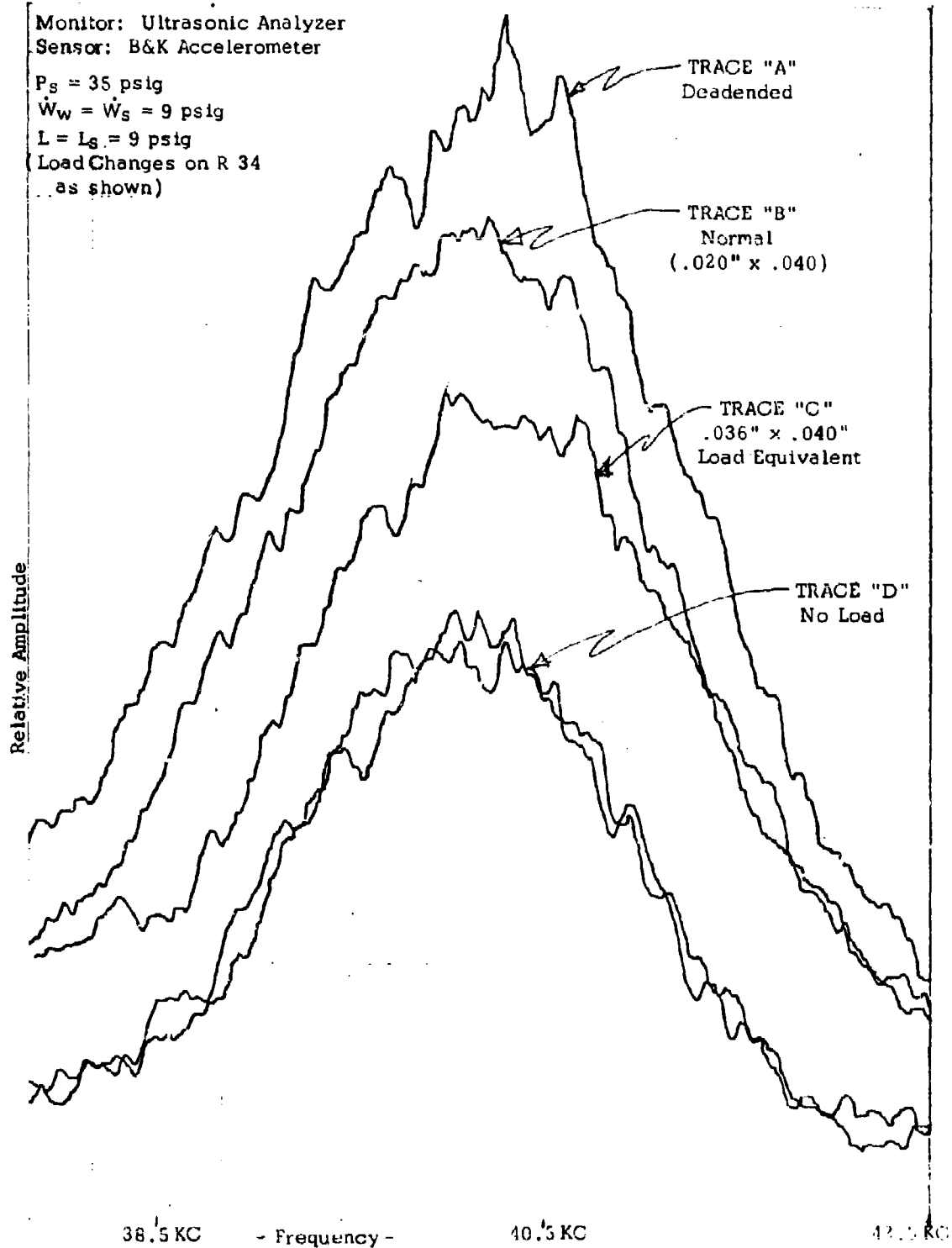Secondary Detection
Load Anomalies – R 34

163

Figure 85. Analog Attenuator and Logic Module Test
Secondary Detection
Load Anomalies

traces of oil are present in the supply air, together with finely divided particulate matter. For this series of experiments, therefore, a drop of oil was introduced in the air supply, and dust was added to the supply air. The dust particles are of a size that will pass through a 0.004 in. x 0.004 in. screen mesh. Three levels of contamination were introduced, but since no measurement has been devised these are referred to as level C1, C2, and C3. Level C2 results from running longer with dusty air than level C1, and level C3 from even longer times.

The primary performance is shown in Figure 86. The change in null is readily apparent, and an increase in output noise may be seen. The data shown is an X-Y recording, so the frequency response of the recorder must be considered in viewing the results. Also, since it was not significant to the test, the input ramp rate used to produce the recording was not noted. It is apparent, however, that the performance was greatly degraded.

The secondary acoustic signature for these levels of contamination are shown in Figure 87. The frequency band between 53 KHz and 64 KHz exhibits some- what random changes with contamination which are attributed to varying build-up of contamination in the nozzles and channels. The changes in the signature in the region from 38 KHz to 53 KHz are somewhat proportional to contamination. This is similar to the results from varying load, and while not due to load restrictions, indicates that changes which degrade output capability will also show a decreasing amplitude in the secondary acoustic signature in the frequency range around 40 KHz.

Figure 88 shows a detectable change in the secondary acoustic signature when the oil was introduced, but prior to the introduction of dust. This is extremely significant because it provides a potential for detecting impending malfunction, before the contamination has built up to the point of primary performance degradation.

2.   EVALUATION OF INSTRUMENTATION FOR A STACKED PAIR OF DIGITAL CIRCUIT PLATES

The previous sections of this report have shown that both pressure transducers and bimorph crystals will monitor primary performance of digital elements, and that accelerometers will detect the secondary acoustic signature. The secondary acoustic signature can determine the type of an anomaly, with the primary sensors detecting performance malfunction. This section discusses the application of that work to a pair of digital circuit plates from the BEC Missile Control. These circuit plates contain two parallel, independent amplifying and pulse-shaping networks.

The primary performance of these networks was established, with all parameters within prescribed operating conditions, as a base line. Three (3) anomalies

C-1 = First degree Contamination
C-2 = Second degree Contamination
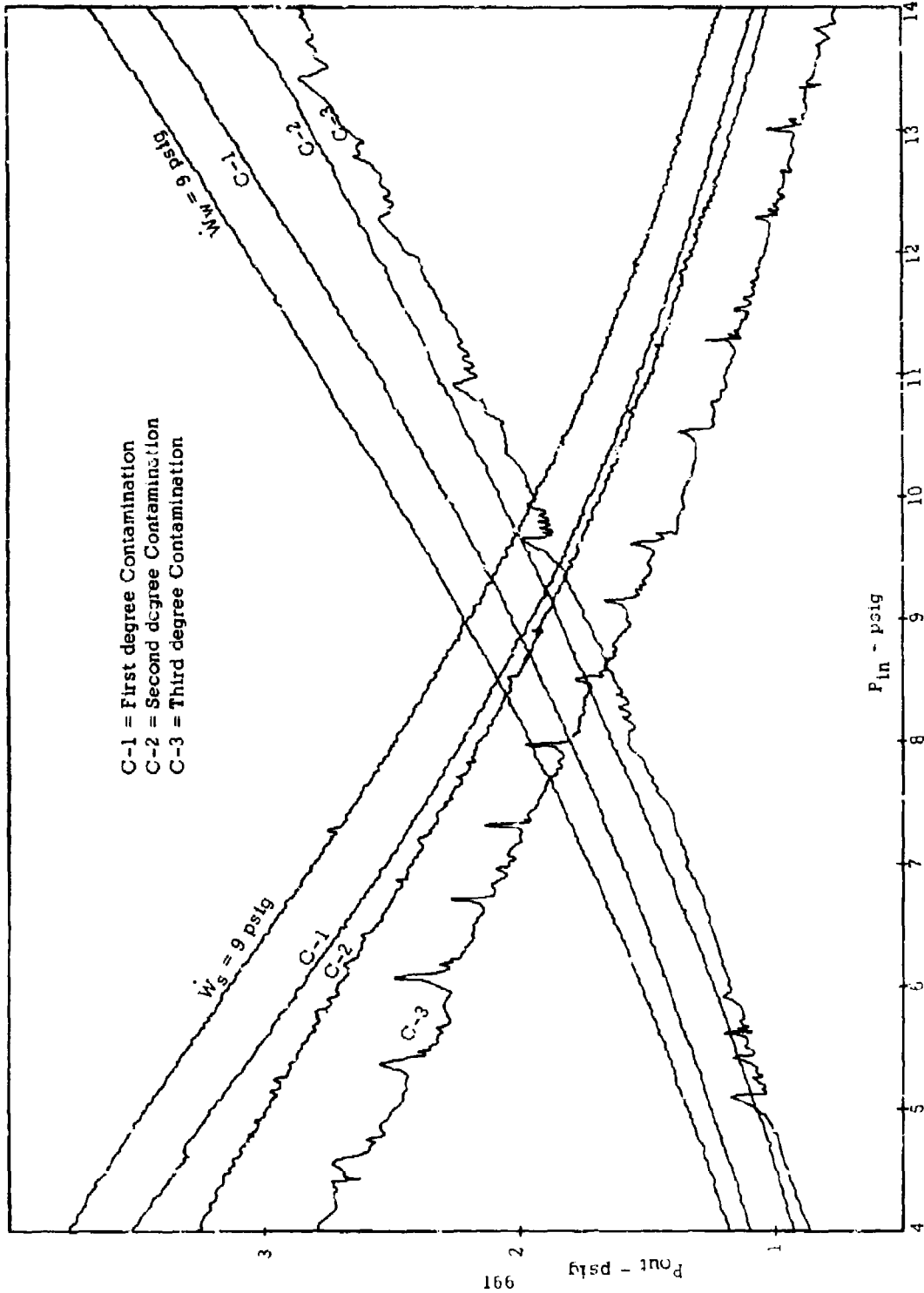C-3 = Third degree Contamination

Figure 86. Analog Attenuator and Logic Module Test
Primary Performance Monitoring
Contamination Anomalies
Relay 34

Circuit No. 3650
Manifold No. 3650
Sensor: B&K Model 4333 Accelerometer

P_S = 35 psig
$W_W = W_S = L = L_S$ = 9 psig

C-1 = First degree of Contamination
C-2 = Second degree of Contamination
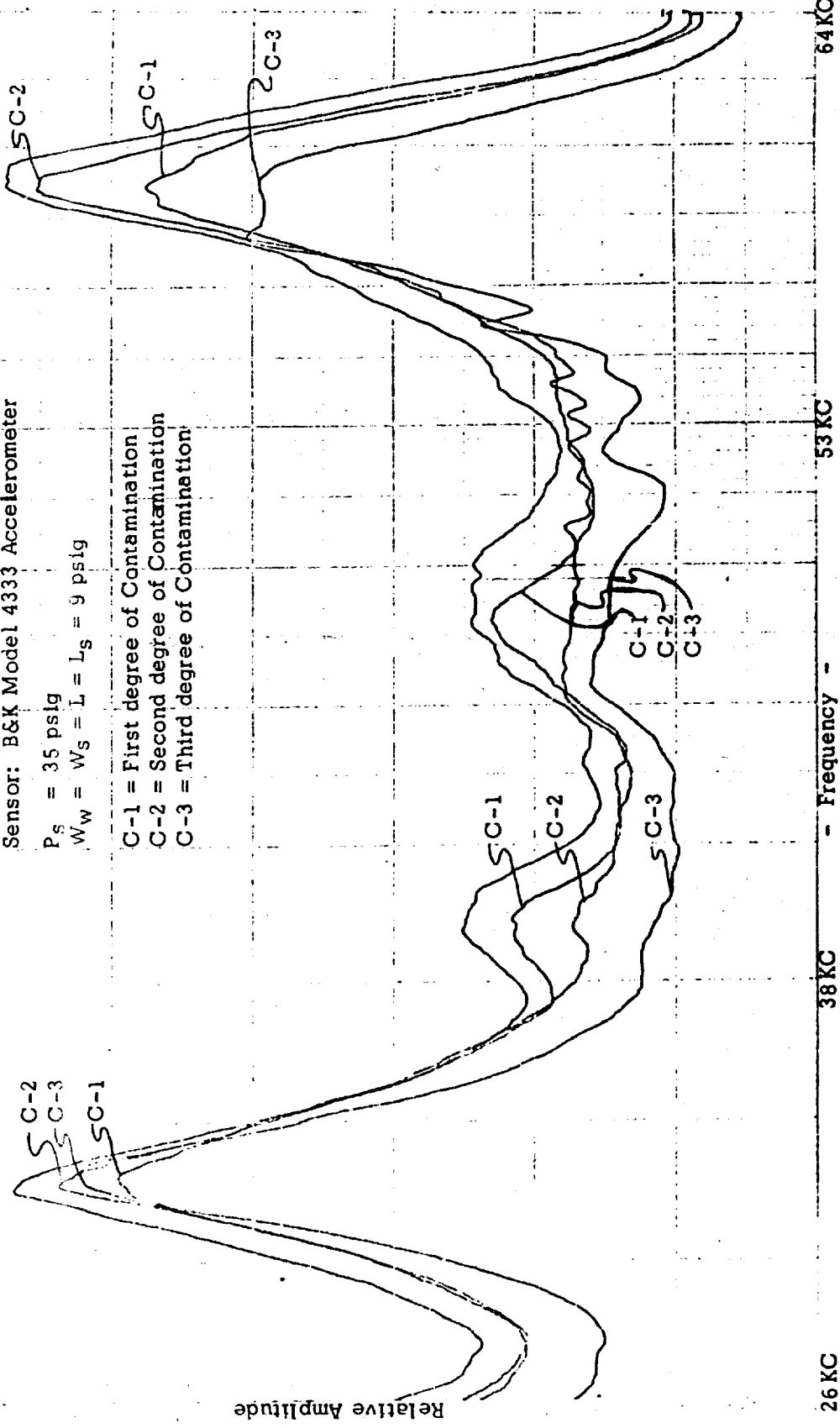C-3 = Third degree of Contamination

Relative Amplitude

26 KC   38 KC   – Frequency –   53 KC   64 KC

Figure 87. Analog Attenuator and Logic Module Test
Secondary Detection
Contamination Anomalies

167

Circuit No. 3650
Manifold No. 3650
Sensor: B&K Model 4332 Accelerometer
Monitor: Ultrasonic Analyzer

P_s = 35 psig

$W_w = W_s = L = L_s = 9$ psig

Oil in P+ Nozzles of R 34 and R 35

Base Line

2 Oil

Relative Amplitude

36 KC
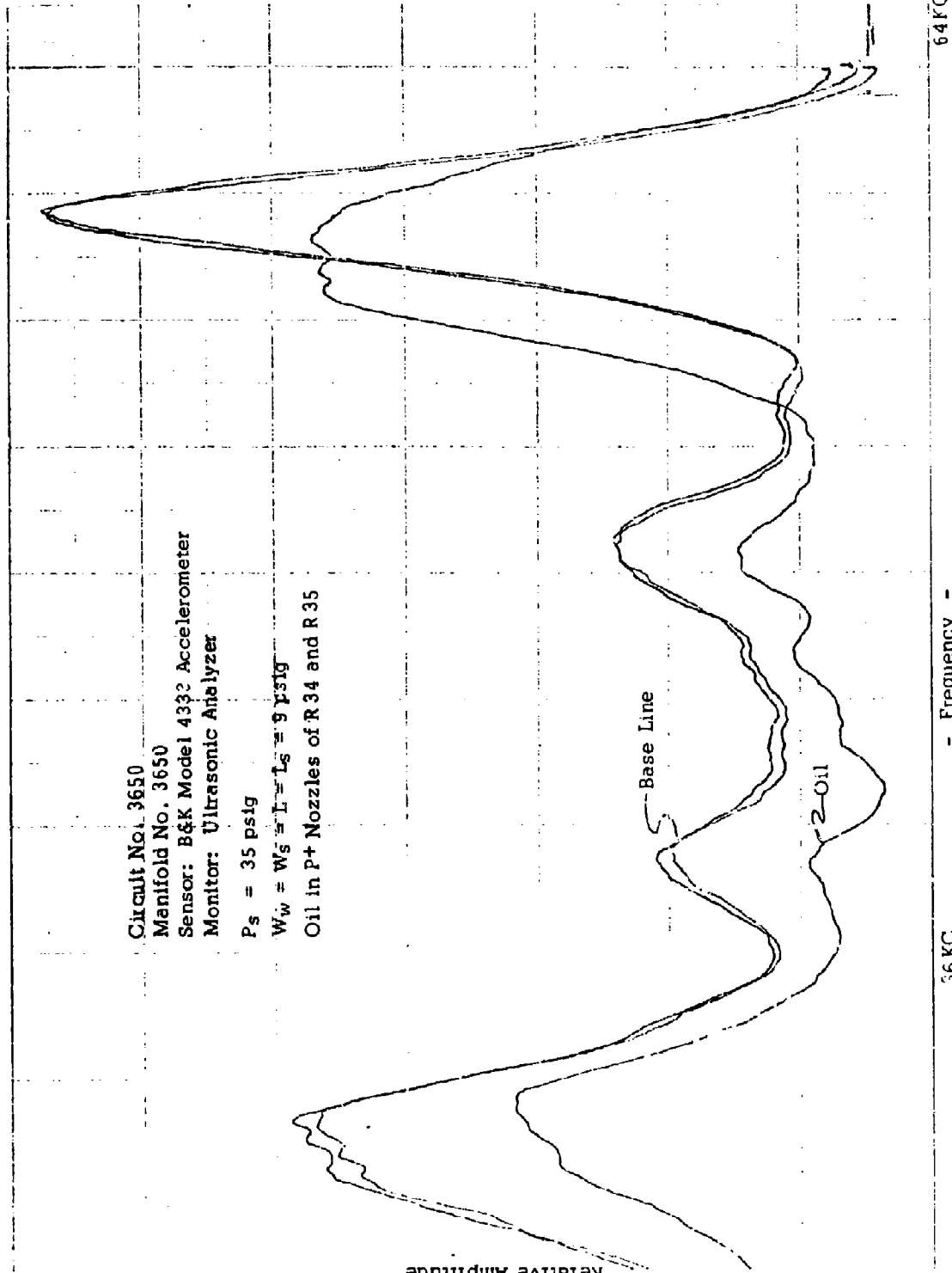
64 KC

- Frequency -

Figure 88. Analog Attenuator and Logic Module Test
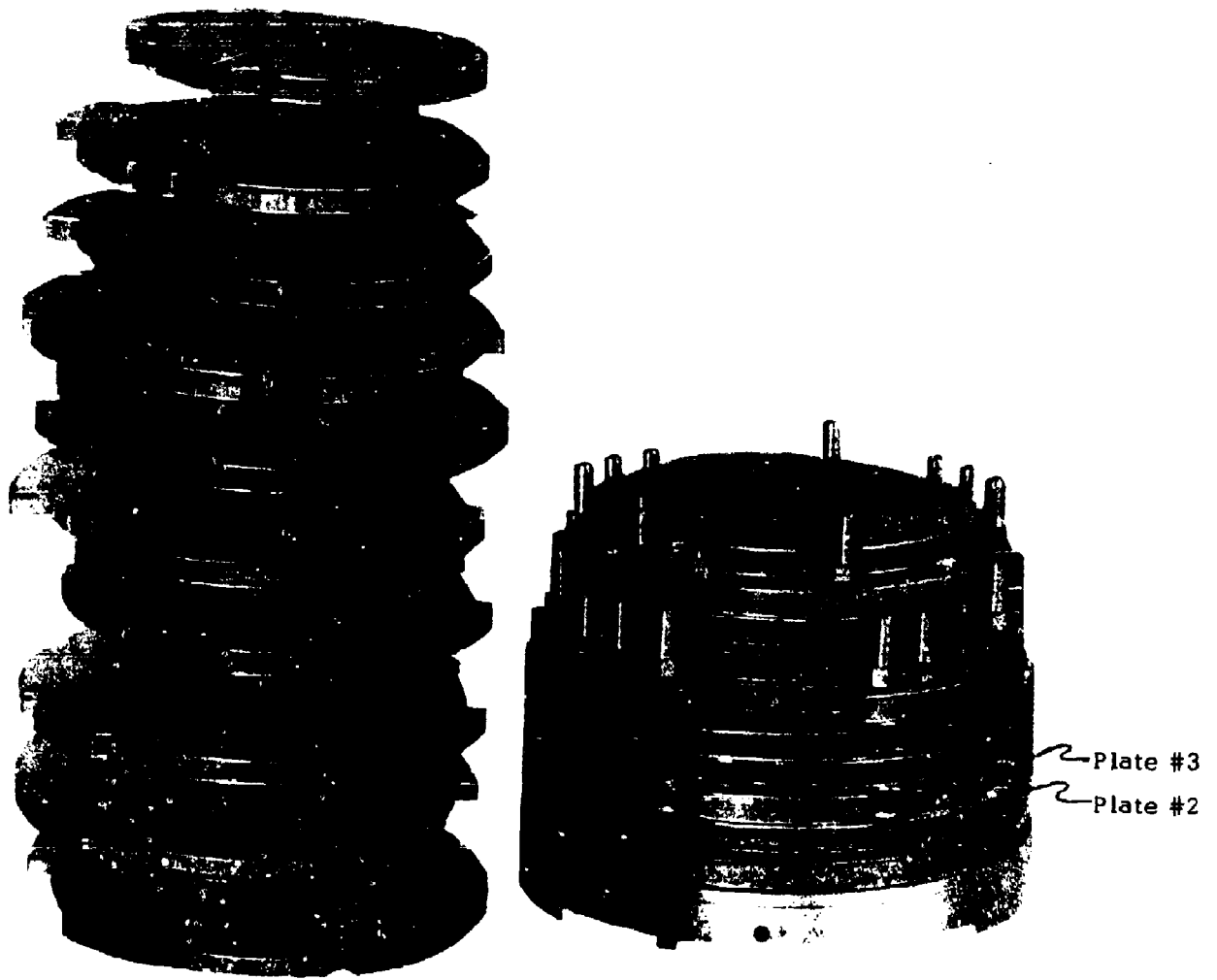Secondary Detection
Contamination Anomaly

168

Figure 89. B.E.C. Missile Control Fluidic Logic Package

were introduced; one, changes in supply pressure; two, inserting a small wire to simulate channel contamination; and three, blocking an unused output leg of a selected element.

a. Description of Circuit to be Tested

The B.E.C. Missile Control from which the selected circuit plates were chosen is shown in Figure 89. Both stacked and exploded views are shown, and the chosen circuit plates are marked as Plate #2 and Plate #3. The circuits built into these plates are shown in Figure 90. There are two identical, parallel circuits each of which accepts a more-or-less sinusoidal input signal. These inputs are amplified and shaped into pulses for use in other circuits in the control. Amplifying and pulse shaping is a common function in many digital systems, and was chosen as typical of digital circuitry because the characteristics required of it, such as high frequency response, positive switching, and acceptance of poor quality signals, are required throughout digital circuitry.

The circuit plates are round as befits a circuit for a round missile, and are mounted back-to-back. Transfer tubes provide interconnection between plates. Typical primary characteristics, shown as input and output waveforms, are shown in Figure 91. The input operates at a nominal frequency of 100 Hz.

b. Test Setup

The compactness of the missile control dictates the use of small detectors. Accordingly, piezoelectric bimorph crystals were chosen to detect the primary performance characteristics. They are small enough so that they were mounted without disturbing either the control stacking concept or the space requirements. Crystals were located as shown in Figure 90 to monitor both inputs and both outputs. A miniature pressure transducer was mounted near one of the crystals, monitoring one of the outputs, to serve as a check on the crystal performance. A B&K Model 4333 accelerometer was used to determine the secondary acoustic signature. As was done for the analog circuit module, preliminary testing was performed to determine the optimum location for the accelerometer. The accelerometer was mounted on Plate #3, as shown in Figure 90.

The output from the crystals and the pressure transducer were recorded using a light beam galvanometer type recorder. The acoustic signature was analyzed using a Panoramic recorder, and amplitude vs. frequency results recorded using an X-Y recorder.

c. Results of Varying Supply Pressure

The specified supply pressure to both circuit plates is 1.5 psig. Typical
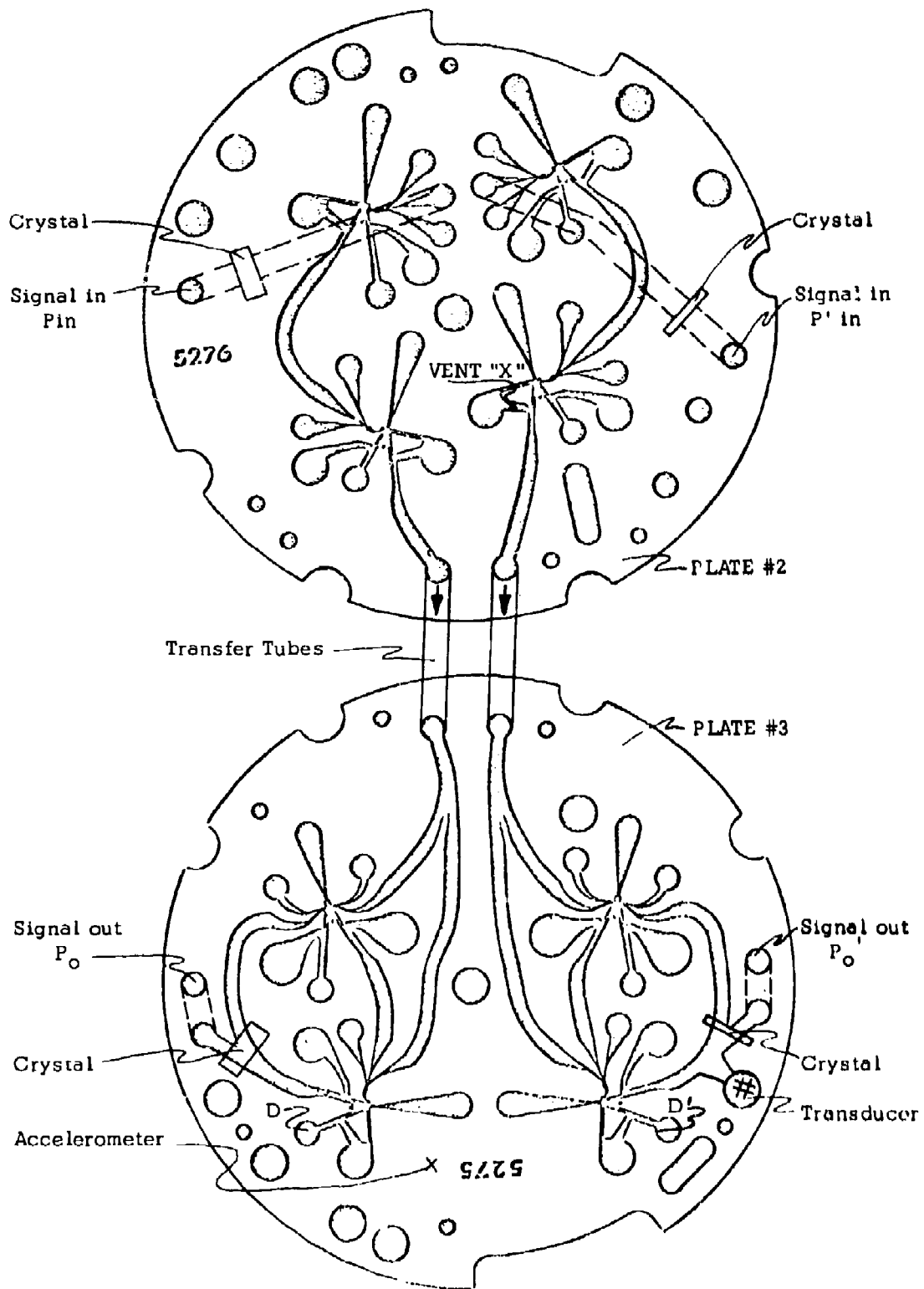
Figure 90. Amplifier (Plate #2) and Pulse Shaping (Plate #3) Circuits

171

Trace A-Output P'c - Transducer

Trace B-Output P'o - Crystal

Trace C-Input P'in - Crystal

Trace D-Output Po - Crystal

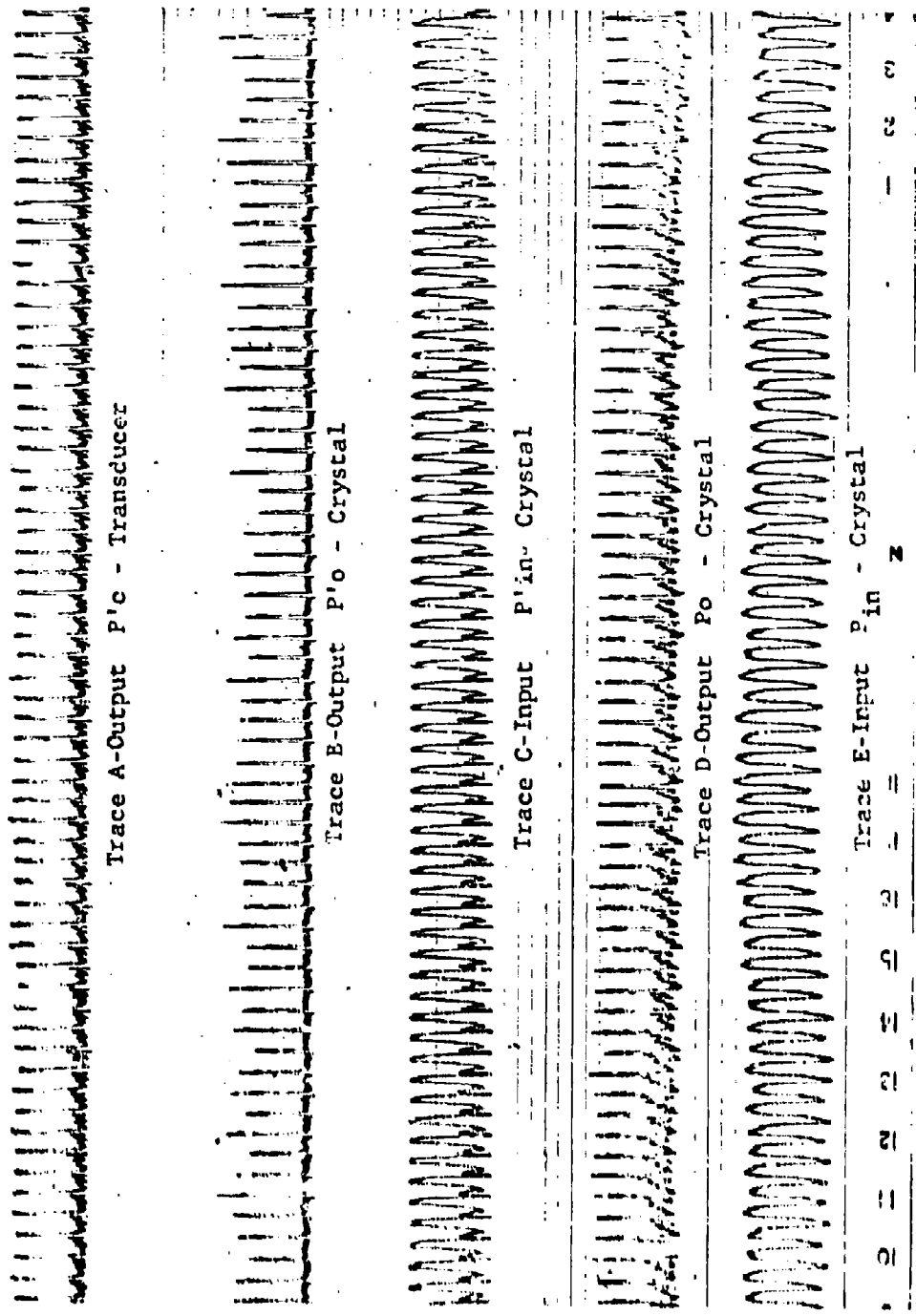Trace E-Input Pin - Crystal

Figure 61. Amplifier and Pulse Shaping Circuits
Primary Performance Monitoring
Satisfactory Performance

172

primary performance is shown in Figure 91. Degraded supply pressure is a typical system malfunction, so circuit performance at reduced pressure is of interest. The primary characteristics for three supply abnormalities are shown. The three abnormalities are supply for Plate #2 reduced to 1.0 and 0.5 psig, and supply for Plate #3 reduced to 1.0 psig. The operation is shown in Figures 92, 93, and 94, respectively.

The secondary acoustic signature as monitored by the accelerometer is shown in Figure 95, for various values of supply pressure to Plate #3. These curves are for normal supply to Plate #2, and for a steady-state (not sinusoidal) signal at the inputs. The changes in signature with supply pressure are clearly evident.

It was hoped that the accelerometer mounted on either plate could detect anomalies in either plate. However, the investigation to determine the optimum location for the accelerometer showed that the secondary acoustic signature from Plate #3 was strong enough to mask the signature from Plate #2, independent of location of the accelerometer. Thus, supply pressure causing anomalies in Plate #2 cannot be detected when Plate #3 is supplied with air.

Figure 96 shows the secondary acoustic signature for Plate #2 when Plate #3 is not supplied with air, and the input is steady-state, not sinusoidal. The change in signature with supply pressure (to Plate #2) is clearly evident.

Referring again to Figure 95, the (approximately) 8 KHz peak is seen to decline more rapidly than the (approximately) 12 KHz peak as the Plate #3 supply is decreased. Figure 96 shows the condition when the Plate #3 supply is reduced to zero. (The calibration of relative amplitude between Figure 95 and Figure 96 is different.)

The use of the secondary acoustic signature for circuit plates which are mechanically attached, as are these, is therefore somewhat limited. There are three routes the designer may choose.

1. Mechanically isolate the plates so that acoustic signals are not transmitted between plates, and use an accelerometer on each.

2. Provide a means for deactivating Plate #3 (shut off the supply).

3. Treat the pair of plates as the minimum replaceable sub-group; i.e., an entity, and determine the overall secondary acoustic signature degradation.

173

Trace A-Output P'o - Transducer

Unsatisfactory Performance

Trace B-Output P'o - Crystal

Trace C-Input P'in- Crystal.

Trace D-Output Po - Crystal

Trace E-Input P_{in} - Crystal

Figure 92. Amplifier and Pulse Shaping Circuit
Primary Performance Monitoring
Pressure Anomaly
$P_{s2} = 1.0$ psig

174

Trace A-Output P'o - Transducer

Trace B-Output P'o - Crystal

Trace C-Input P'in- Crystal

Trace D-Output Po - Crystal

Trace E-Input P_{in} - Crystal

4 5 6 7 8 9 10 11 12 13 14 15 16 17

Figure 93. Amplifier and Pulse Shaping Circuit
Primary Performance Monitoring
Pressure Anomaly
$P_{s2} = 0.5$ psig

Trace A-Output P'o – Transducer

Trace B-Output P'o – Crystal

Trace C-Input P'in – Crystal

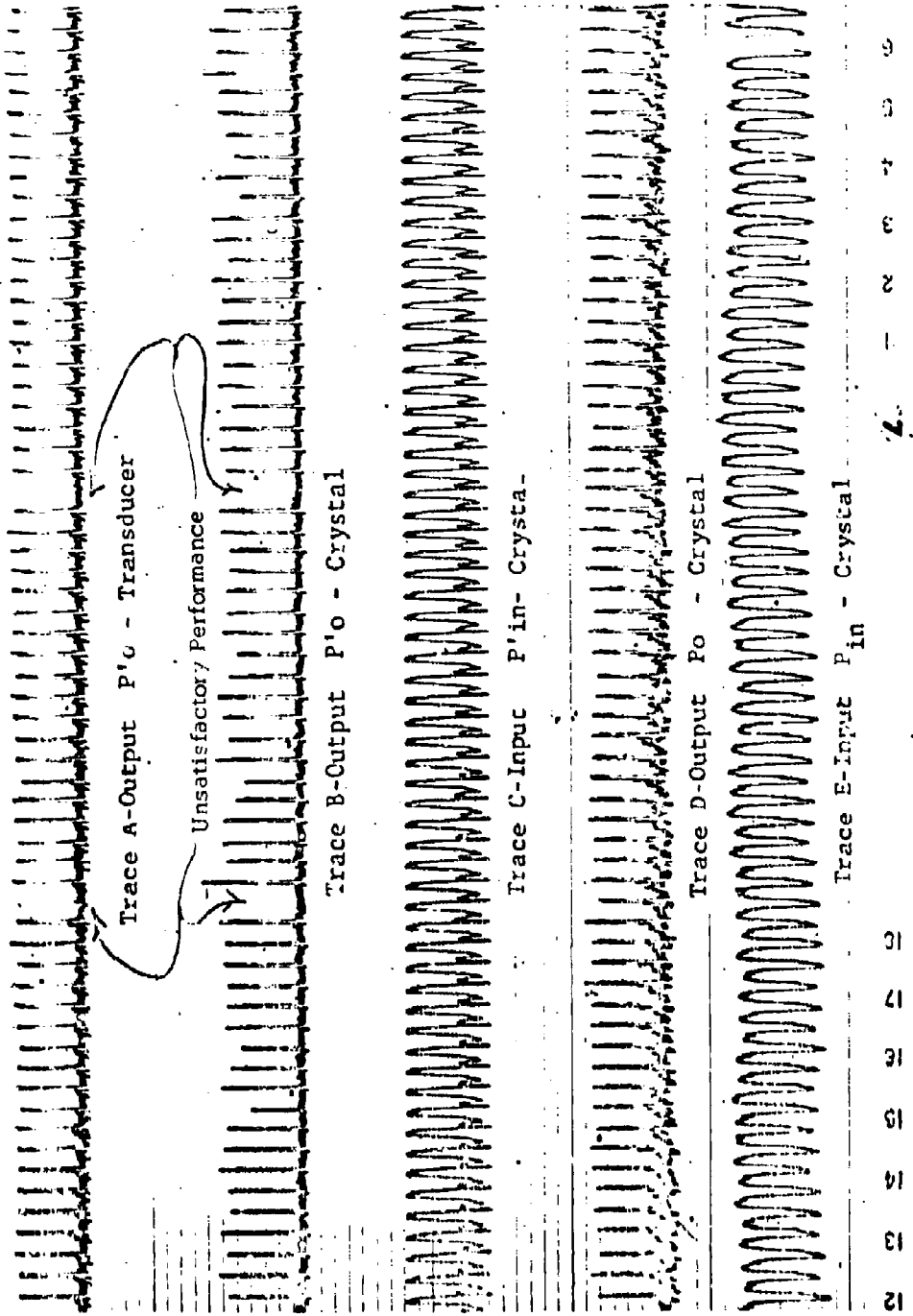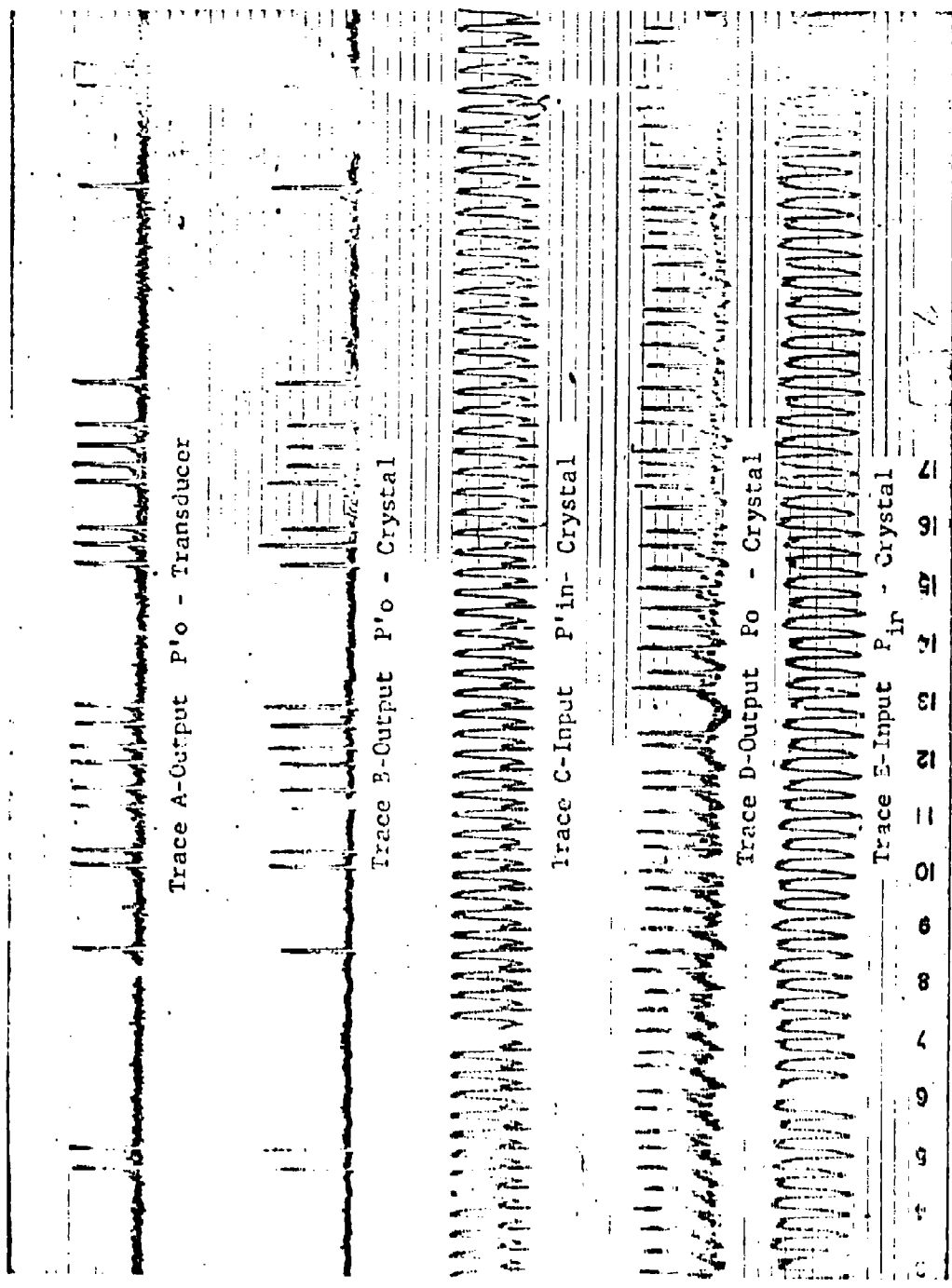Trace D-Output Po – Crystal

Trace E-Input P_in – Crystal
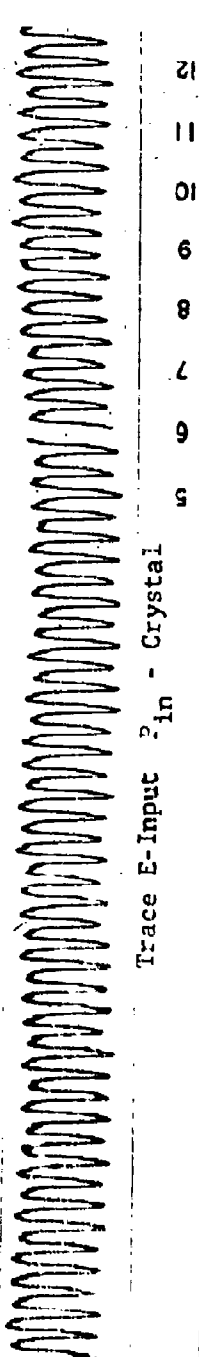
Figure 94. Amplifier and Pulse Shaping Circuits
Primary Performance Monitoring.
Pressure Anomalies
$P_{s3} = 1.0$ psig.

176

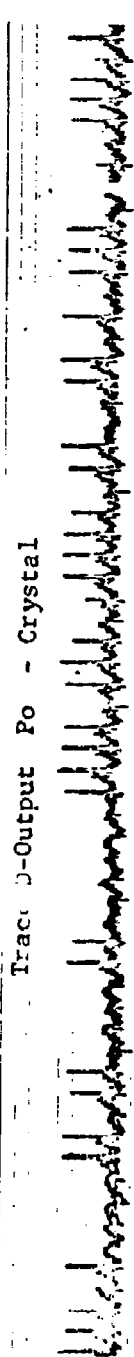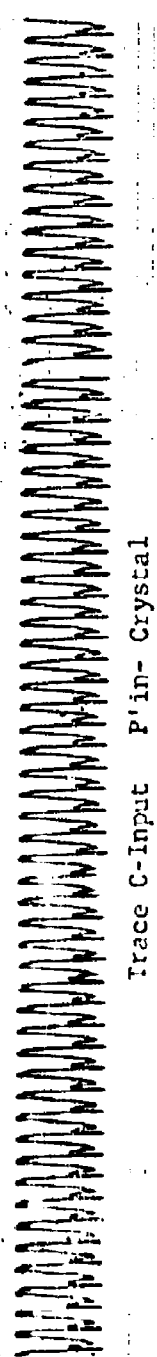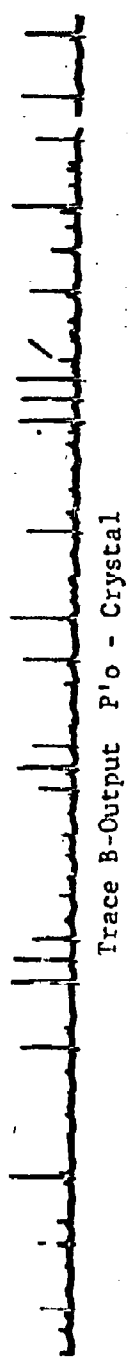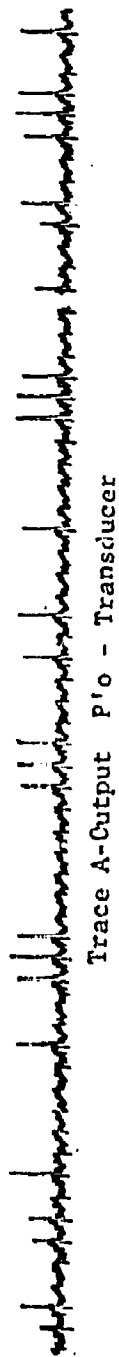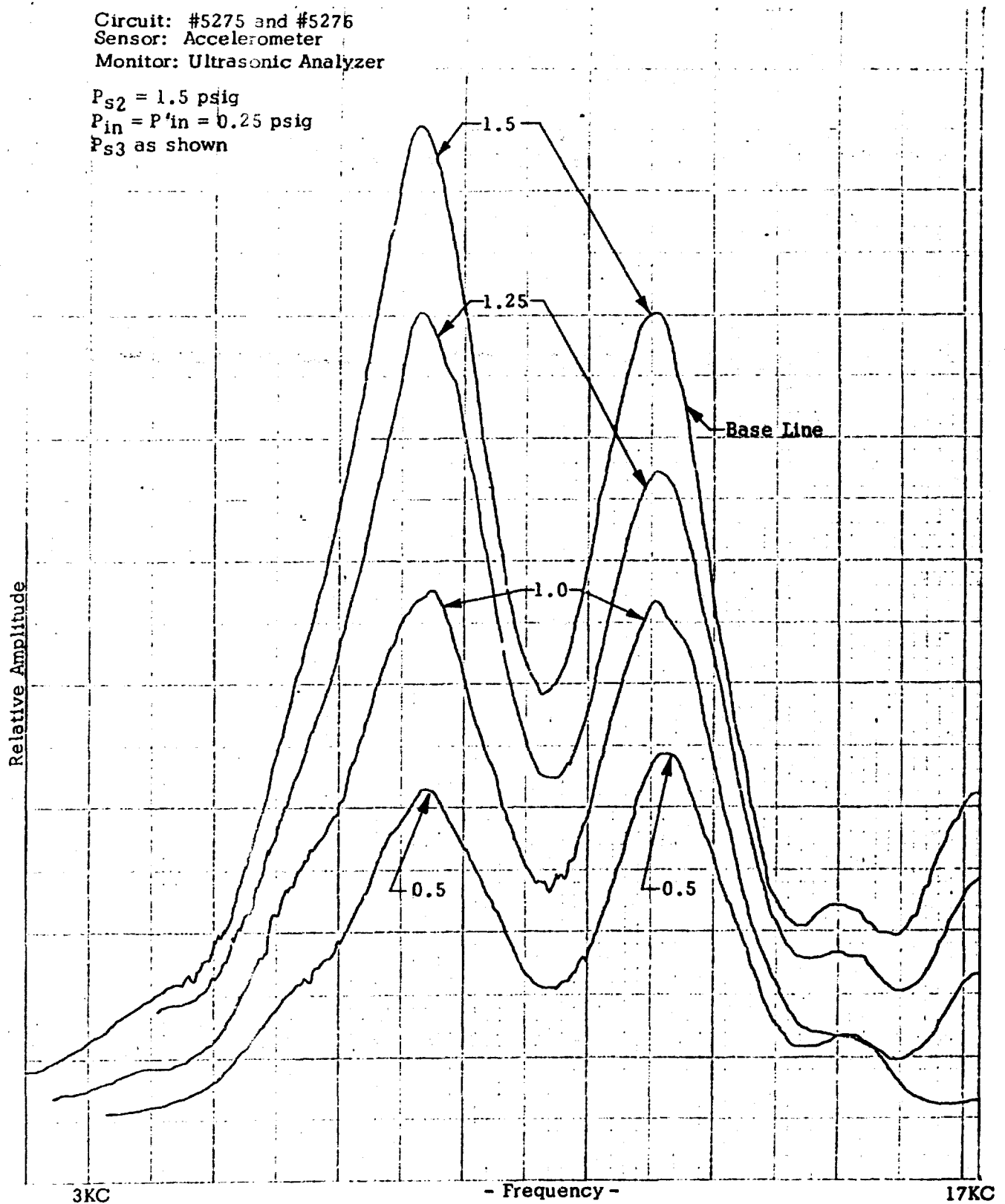Figure 95. Amplifier and Pulse Shaping Circuit Test
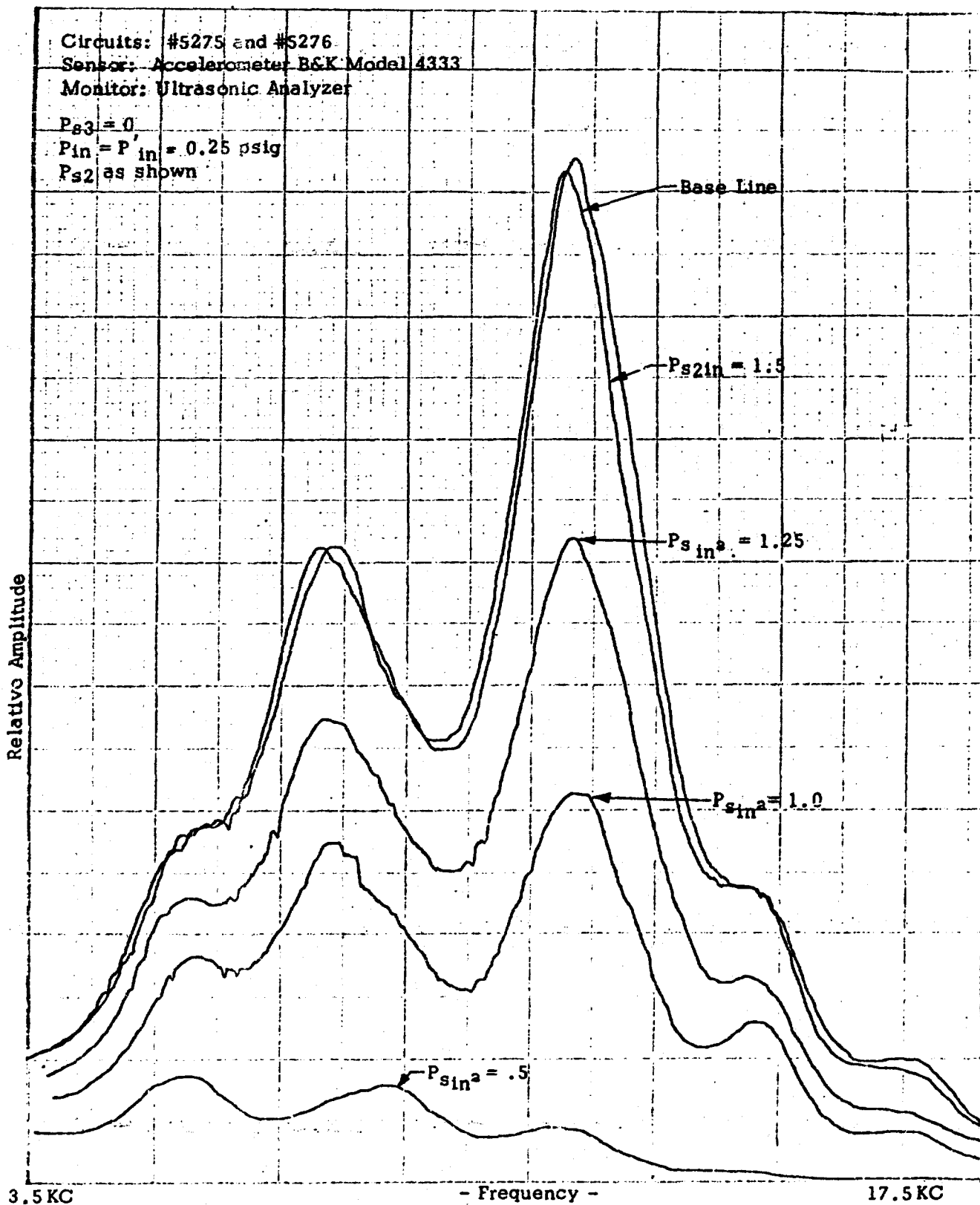Secondary Detection--P_{S3} Pressure Anomalies

Figure 96.　Amplifier and Pulse Shaping Circuit Test
Secondary Detection--P_{s2} Pressure Anomalies

178

d. Results from Simulated Contamination

Contamination, due to foreign particles, is a likely form of malfunction.
However, the inability to reproduce and quantify real contamination in
the circuit was discovered during the analog circuit investigations. Because
of those difficulties, it was decided to simulate the contamination by the
introduction of some physically real object. It was found that a small wire
introduced into an element vent produced a change in the secondary acoustic
signature without a concomitant change in the primary performance. The
location of the vent is shown as Vent X on Figure 90. The acoustic signatures
are shown on Figure 97. Again, this signature is obtained with a steady-state
input.

The change is appreciable, and indicates the possibility of detecting impending
failure since no change in functional performance with this level of anomaly
was observed.

e. Results from Blocked Vent

One of the anomalies which may occur in a Fluidic system is blockage of a
vent hole. Typical vents are shown in Figure 90 as D and D'. Blocking
these vents results in unsatisfactory primary performance, as shown in
Figure 98.

The secondary acoustic signature is markedly changed, as shown in Figure
99. The difference between D and D' is probably because the accelerometer
is not equidistant from the vents. This signature is obtained with a steady-
state signal.

3. HEALING OF MALFUNCTIONING CIRCUITRY

The primary investigations of this program have been directed toward detection
and location of Fluidic system malfunctions. Some of the malfunctions which
may occur are caused by an accumulation of contaminants within the channels
and passages. The combination of oil and carbon particles is known to degrade
performance if a sufficient quantity accumulates. It is thought that the oil
provides a wet surface on which the carbon particles accumulate, since neither
oil nor particles alone will accumulate.

It would be very desirable to have a technique for healing circuits in-place,
without having to remove or disturb the system. Since contamination due to
oil and particulate matter is a potential problem, some effort was directed
toward a healing technique.

179
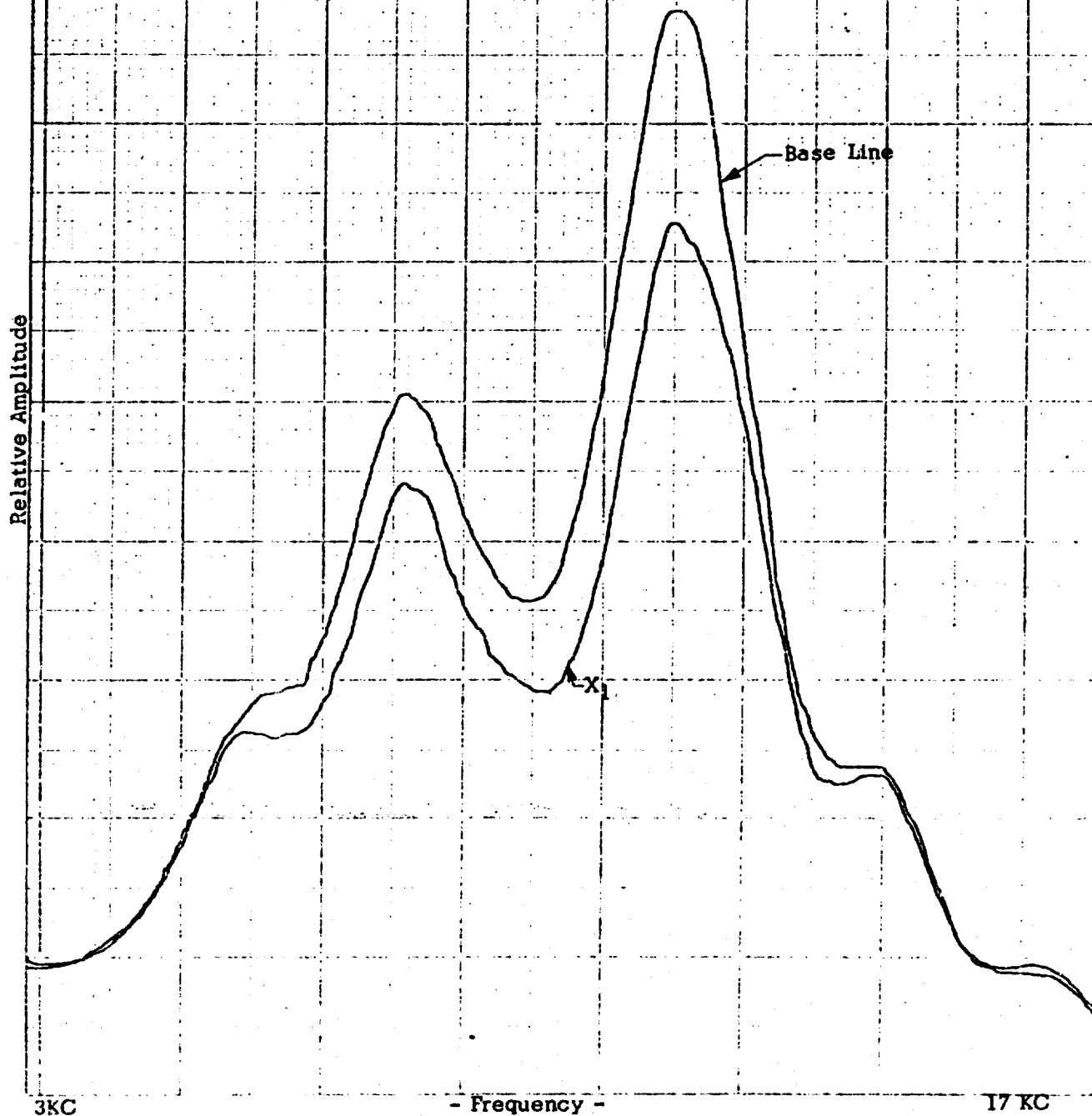
Figure 97. Amplifier and Pulse Shaping Circuit Test
Secondary Detection--Physical Anomalies

180

Trace A-Output P'o - Transducer

Unsatisfactory Performance

Trace B-Output P'o - Crystal

Trace C-Input P'in- Crystal

Trace D-Output Po - Crystal

Trace E-Input P_{in} - Crystal

Figure 98. Amplifier and Pulse Shaping Circuit
Primary Performance Monitoring
Physical Anomaly
D' output blocked off
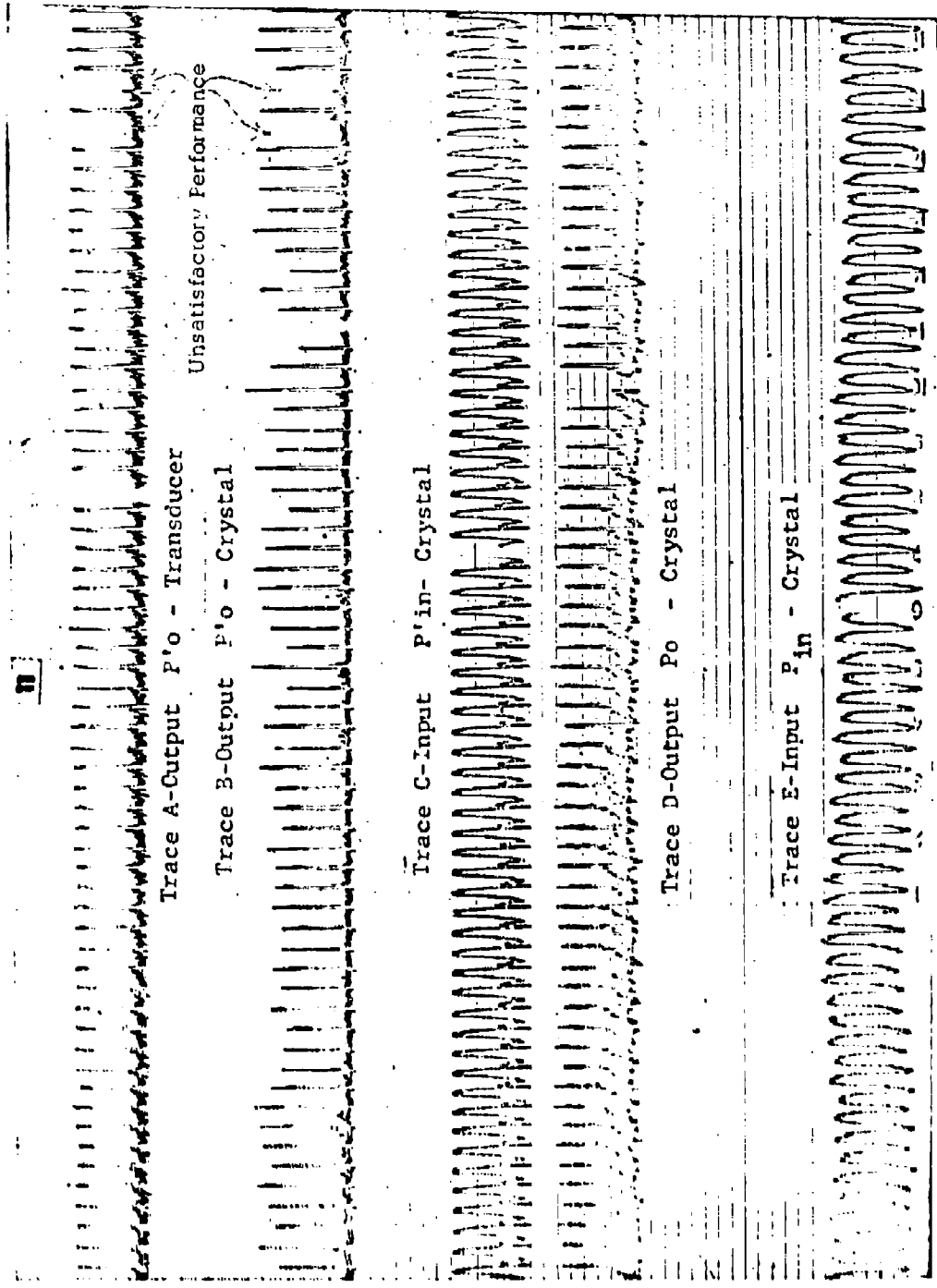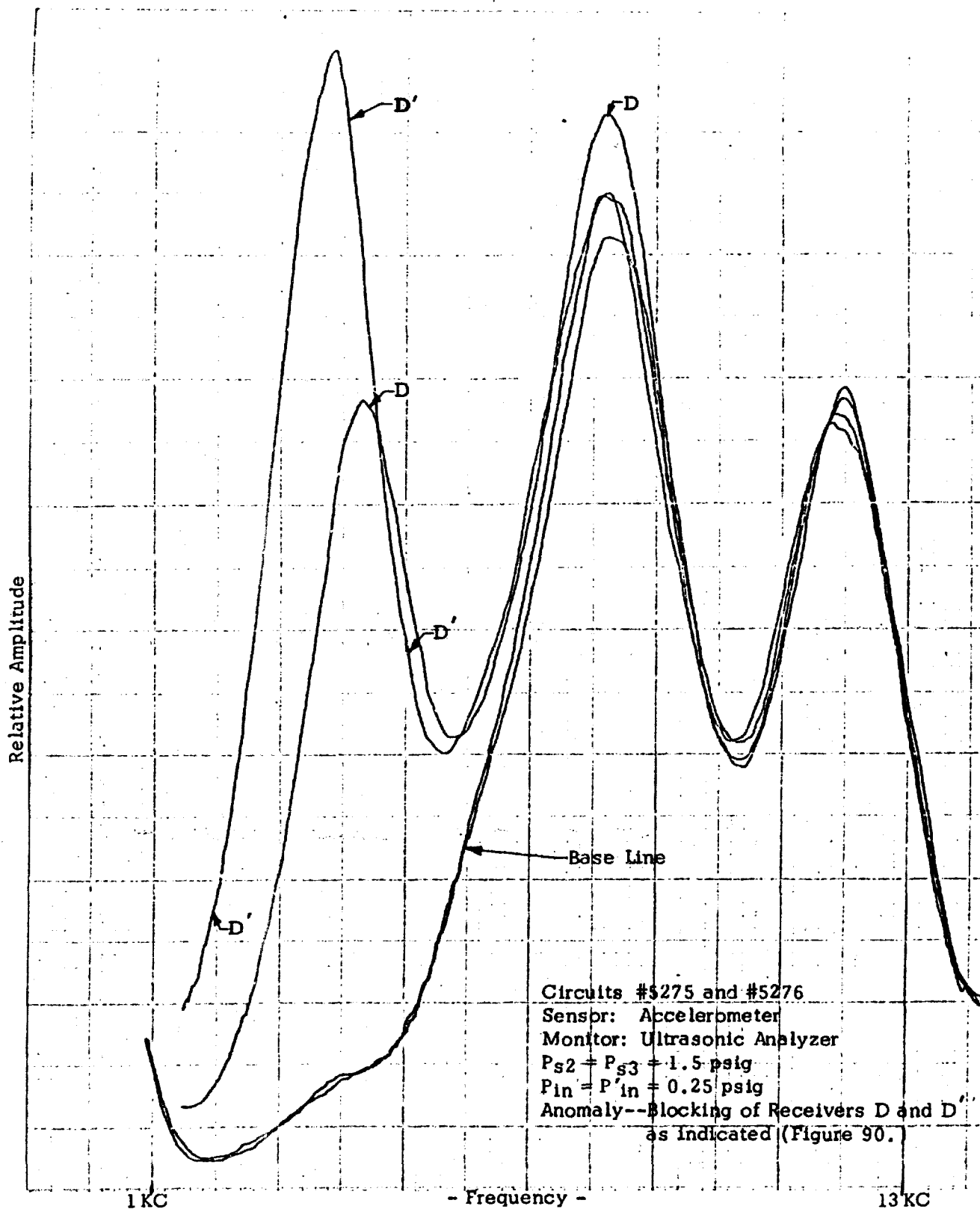
Figure 99. Amplifier and Pulse Shaping Circuit Test
Secondary Detection--Physical Anomalies

182

a. Introduction of Contamination

The introduction of contamination in meaningful, repeatable, quantitative amounts proved extremely difficult. This has been discussed in part 1. of Section VI. It was found that a drop of oil introduced into the supply port of an element or circuit, followed by dust particles added to the air stream, would produce degradation of primary performance. The oil used for this was commercially available ESSO Lube 20-20W motor oil. The dust consisted of particles that would pass through a 0.004" x 0.004" mesh. The change in primary characteristics of an analog circuit with three levels of contamination is shown in Figure 86 of part 2. of this section, and the change in the secondary acoustic signature is shown in Figure 87. Also, the change due to oil alone is shown in Figure 88.

b. Healing Procedure and Results

Freon TF DRL 714 is used as a degreasing agent in many industrial process. It is a liquid of ordinary temperature, is non-toxic, and nonflammable, and is known to not attack the materials used in both the Boiler control and the Missile control. Freon TF DRL 713, therefore, seemed a logical solvent to use to remove the contamination of oil and dirt.

Freon was flushed through the circuit, and the circuit allowed to "soak" for varying periods. It was found that after one hour, primary performance was returned to acceptable limits. Figure 100 shows the before and after primary performance for a single analog element. However, the secondary acoustic signature did not recover to its original character. A large amount of the contaminate was found to have built up in the porous plugs used in the vents of the amplifiers. These plugs have large open-area, and very low velocity so no significant degradation of primary characteristics results from contamination at these plugs. However, the particles did produce some change in acoustic properties, resulting in an inability to return the acoustic signature to its base line. In order to achieve the desired build up of contaminant in the receivers, an excessive and unrealistic amount of contaminant material was directed into the element, a large part of which deposited in the amplifier vent plugs. It is not highly probable that this level of vent contamination would occur under realistic conditions. It is expected that under realistic conditions, the signature should return to essentially the base line following solvent flushing.

c. Conclusions of Healing Study

The use of a solvent such as Freon TF DRL 714 has potential for removing certain kinds of contamination without disturbing or removing the system.
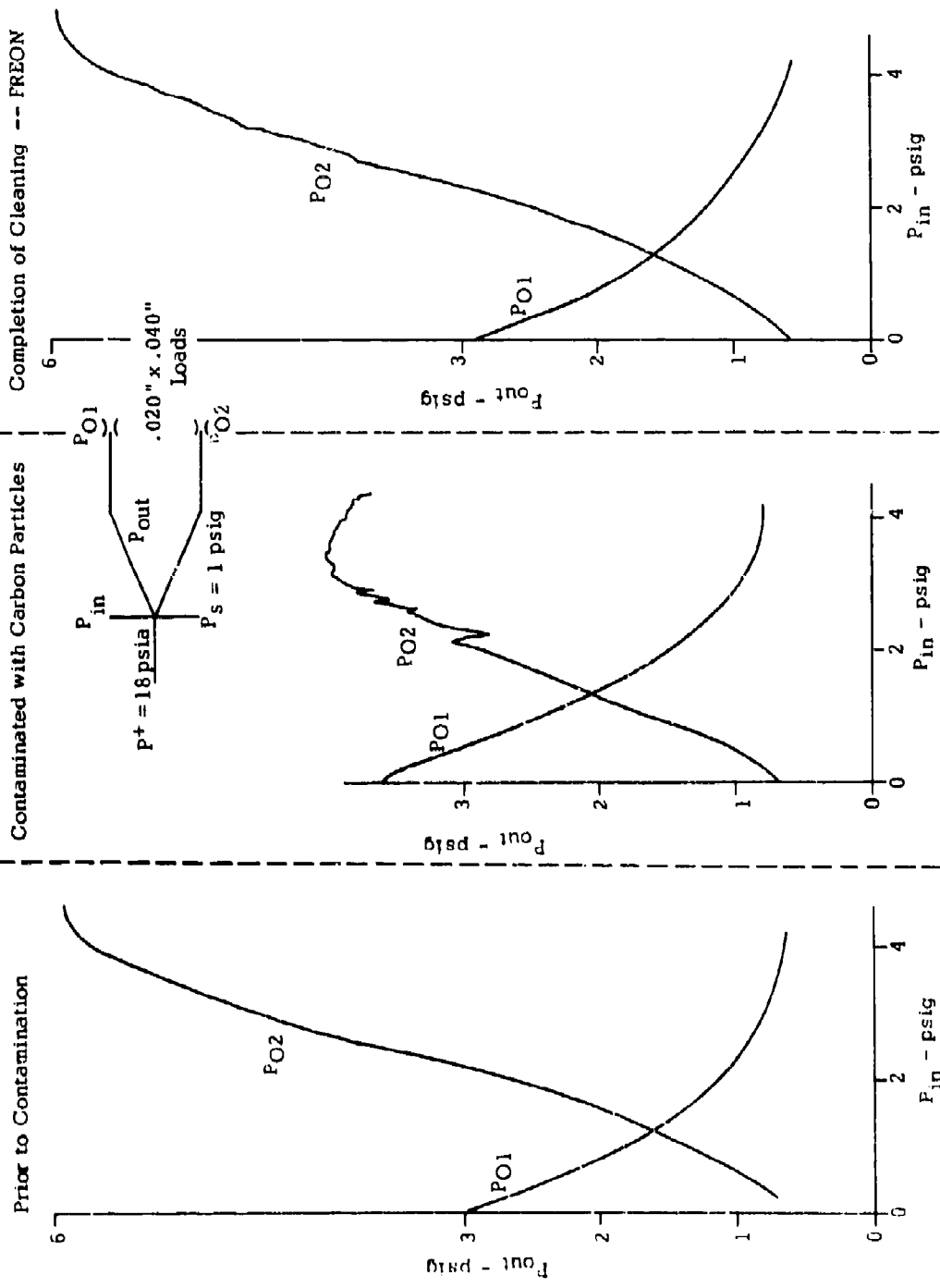
PRIMARY PERFORMANCE CHARACTERISTICS

Prior to Contamination

Contaminated with Carbon Particles

Completion of Cleaning -- FREON

Figure 100. Degradation and Healing Procedure -- Test

184

SECTION VII

DEMONSTRATION OF FEASIBILITY OF A CHECKOUT PROCEDURE FOR AN ANALOG CONTROL SYSTEM

This section describes the demonstration of a checkout procedure for an analog control system. The primary performance characteristics are used to determine whether the system is operating satisfactorily. Secondary acoustic signals are used to establish the anomaly causing primary performance malfunction. A description of the Fluidic circuitry and the instrumentation arrangement are included. The test procedure is enumerated, and the results from introducing various anomalies are shown in tabular form.

1. TEST CIRCUIT

The test circuit consists of the Fluidic Feedwater Controller which was developed by Bowles Engineering Corporation and successfully tested on a DLG-9 Boiler. This is the complete control system from which a portion was taken for the integrated circuit studies described in Section IV. The feedwater controller, shown diagrammatically in Figure 101 functions to automatically regulate the flow of feedwater into the boiler, acting to cause the water flow signal ($\dot{W}_W$) to follow the steam flow signal ($\dot{W}_S$), and to maintain boiler drum level (L) at the desired set point value (L_S). The output signal is water flow command ($\dot{W}_{WC}$) which operates a feedwater valve.

The Feedwater Controller is packaged in two modules, each of which contains one Fluidic circuit plate mounted on a manifold. These two modules, as they were set up for test, are shown in Figure 102, with the attenuator and logic module on the right and the reset module on the left. The Instrumentation Control Panel, monitoring their performance, is shown in Figure 103. The Fluidic circuits are shown in Figures 104 and 105.

2. INSTRUMENTATION ARRANGEMENT

The Feedwater Controller is basically a reset function, acting to control water flow as the time integral of the summation of the various signals. The most valid check of performance is to "close the loop" around the controller, apply known input signals, and examine the output response for operation within established limits. Two signals to close the loop must be generated, and two inputs must be set. The feedback signals required are $\dot{W}_W$ and L. $\dot{W}_W$ may be fed back directly from $\dot{W}_{WC}$ since these signals are of the same pressure range. In the boiler, L is related to water and steam flow approximately by the transfer function $L = \frac{k}{s}(\dot{W}_W - \dot{W}_S)$. This requires a time integral
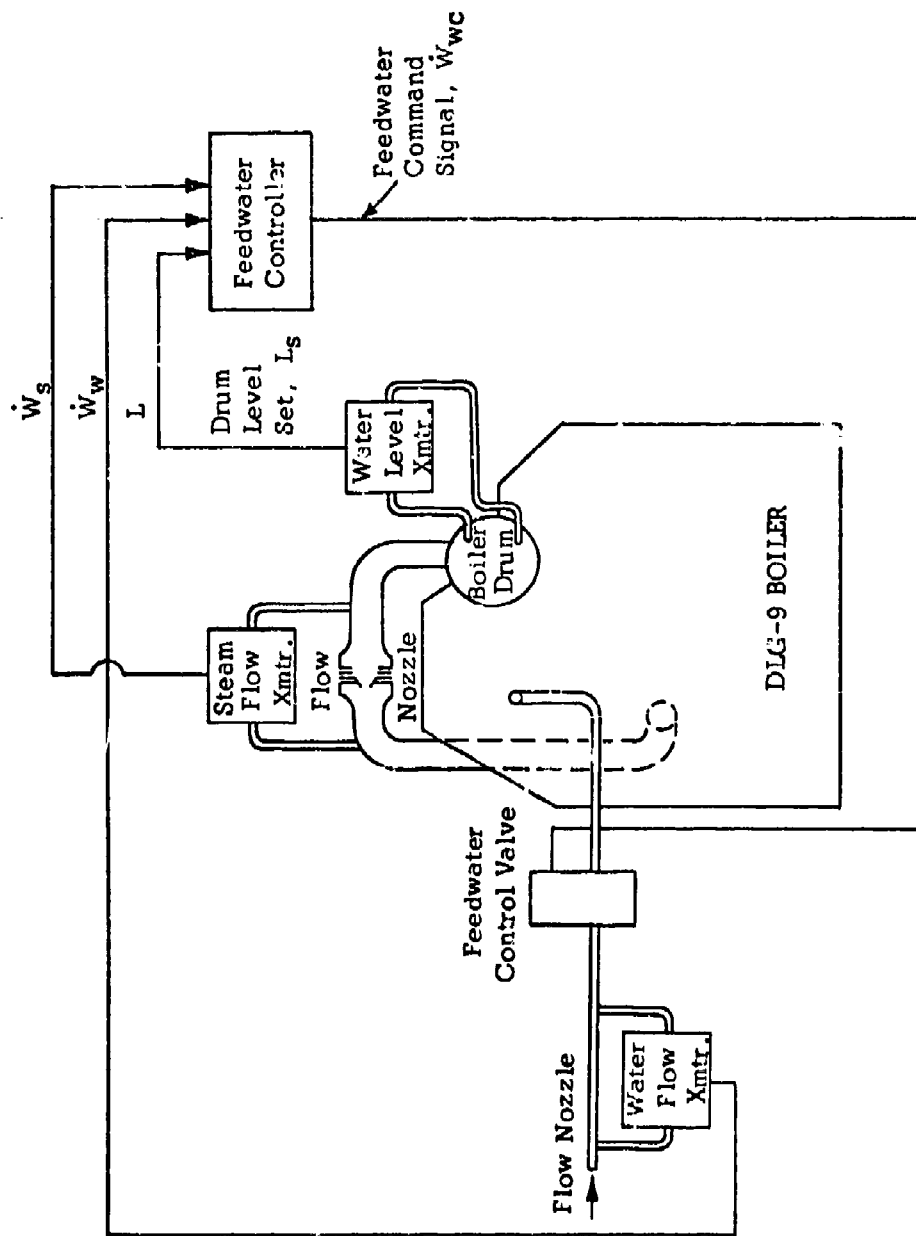
185

Figure 101. Diagrammatic Arrangement of DLG-9 Boiler Feedwater Control
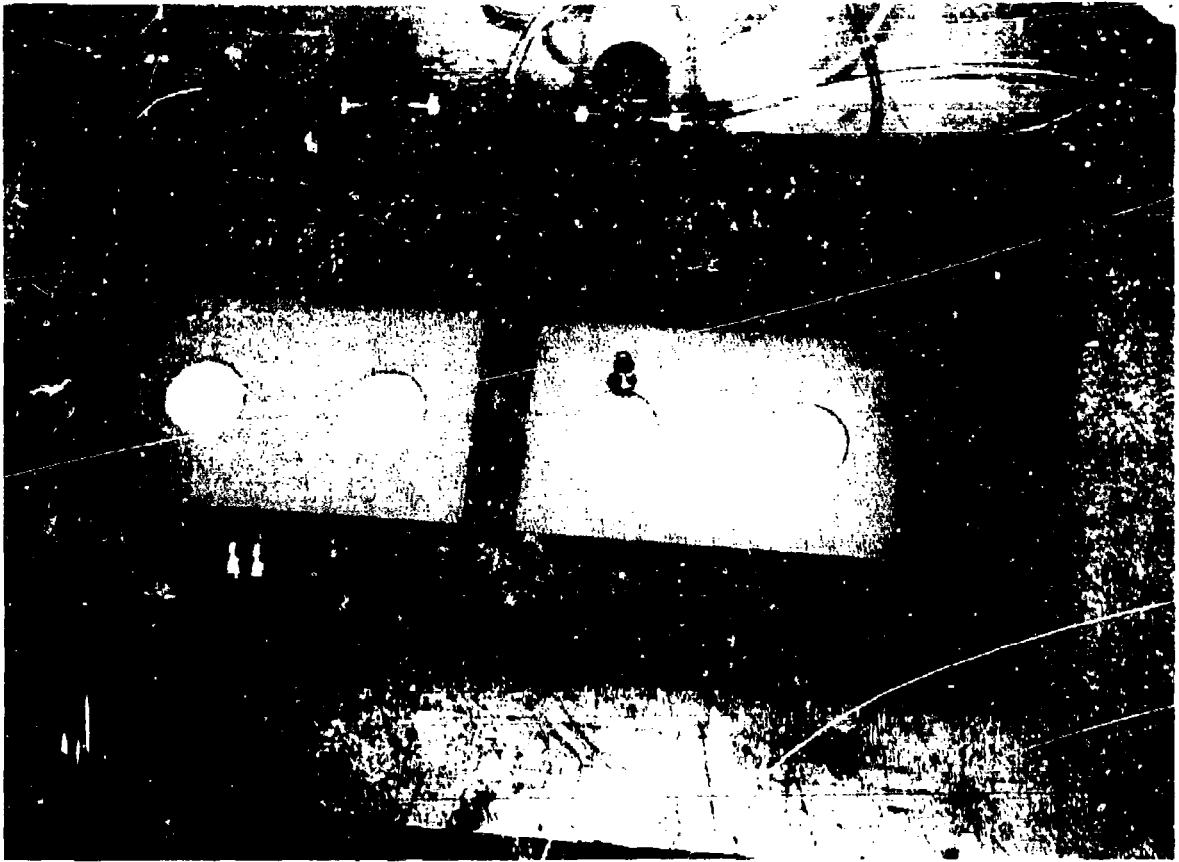
Figure 102. Feasibility Demonstration
Circuit Modules

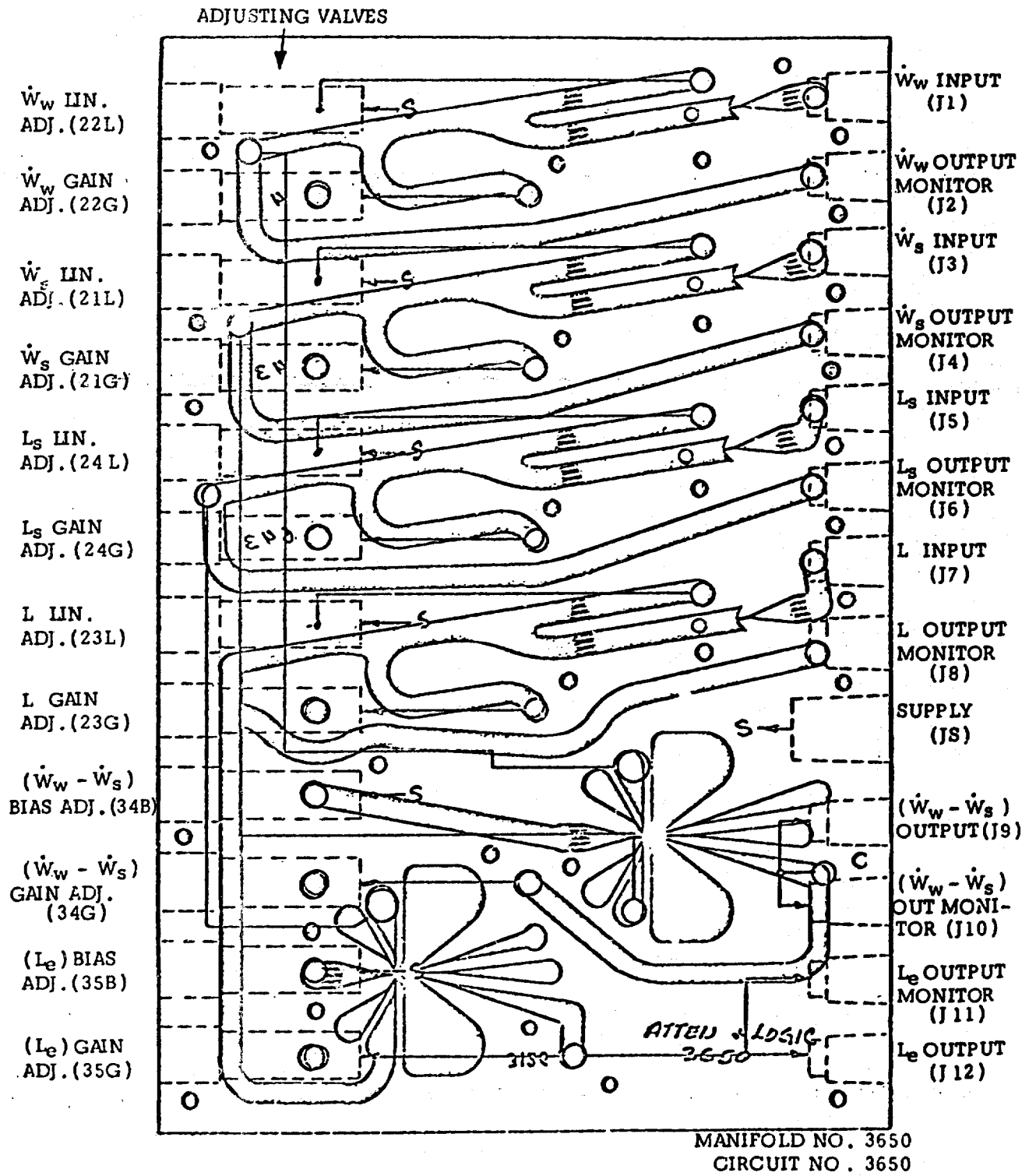187

Figure 103. Feasibility Demonstration
Test Setup

188

Figure 104. Feedwater Control Attenuators and Logic Module
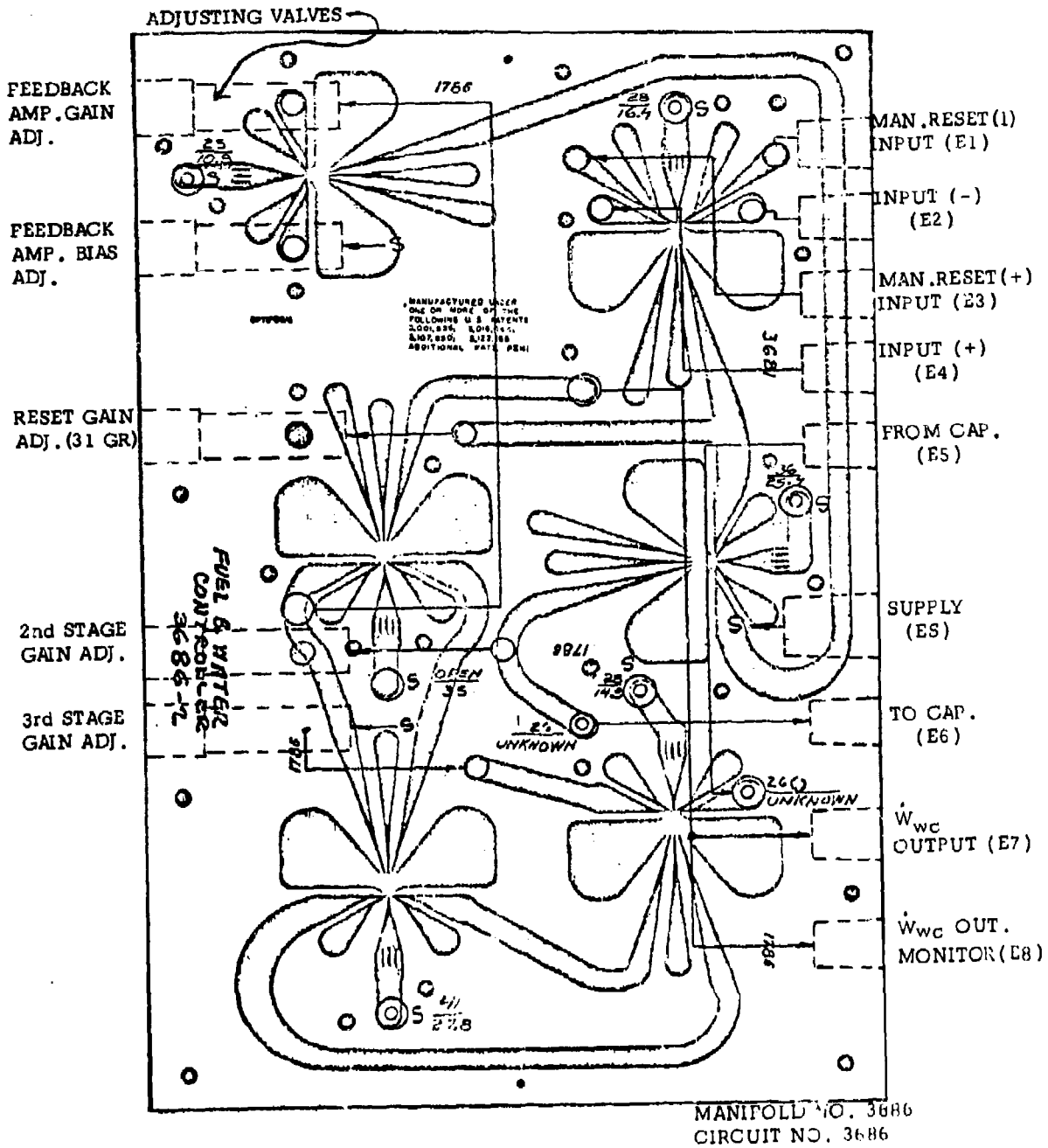
189

Figure 105. Water Flow Reset Controller Subcircuit Module

190

function which is achieved by converting $\dot{W}_W$ and $\dot{W}_S$ to electrical signals, electronically integrating, and converting back to pneumatics to generate L.

Flush mounted miniature pressure transducers of the type found suitable in Section V were used to convert $\dot{W}_W$, $\dot{W}_S$, and L to electrical signals. The signal $\dot{W}_W - \dot{W}_S$ was integrated using a Burr-Brown model 1507 operational amplifier, driving a model 1519 power booster. The power booster provided the electric signal to a Taylor, model 701T, electro-pneumatic converter.

Accelerometers of the type found suitable in Section V were mounted on the circuit plates. A separate accelerometer was mounted on each plate to detect the secondary acoustic signature of that circuit. Very little acoustic coupling exists between the circuits since they were interconnected with plastic tubing for these tests. The output of the accelerometers was analyzed by the Panoramic analyzer, and the output recorded on an X-Y recorder in the same manner as during previous tests.

A block diagram of the checkout setup is shown by Figure 106. The water flow control loop is shown closed by coupling the output of the reset module, $\dot{W}_{WC}$, to the water flow signal input, $\dot{W}_W$. Pressure transducers used to monitor the three active controller input signals are indicated. The means of generating the water level signal is shown, subtracting the output of the $\dot{W}_S$ transducer from the $\dot{W}_W$ transducer, integrating, and converting to a pneumatic water level signal, L, by use of an E/P converter. The L_S signal is a fixed set point value of 9 psig, hence need not be monitored by a pressure transducer during checkout.

The independent variable during checkout is the stream flow signal, $\dot{W}_S$. With the arrangement shown, the water flow and water level signals respond to changes in the steam flow signals in a manner similar to that occurring with the controller coupled to a boiler.

Figure 107 shows a schematic diagram of the electrical checkout circuitry used during the checkout demonstration. The pressure transducers monitoring $\dot{W}_W$, $\dot{W}_S$, and L, are each coupled through a bridge circuit to a Simpson Model 1327 wide view 3-1/2" 0-15 microammeter. Through the bias and gain adjustments provided, the ammeters are calibrated to read 4 to 14 microamps for a 4 to 14 psi pressure range applied to the pressure transducers. Power was supplied for the transducer circuitry by 4.5 volt batteries as shown, with switch S1 provided to switch on the power supplies during checkout.

The figure shows the electronic circuitry used to generate the water level signal. The water flow - steam flow differencing circuit includes a 25K and a 1K trimming potentiometer to equalize the gain of the two input signals, so that for $\dot{W}_W$ and $\dot{W}_S$ equal throughout the range, the differential signal

remains a constant. This constant is set to a value of zero volts by the shown biasing arrangement. The integration gain for the demonstration tests was setup for 50 sec^{-1}. The integrator output couples to the E/P converter. Switch S2 nulls the integrator when closed; it must be opened during checkout testing.

The two accelerometers, one for each of the circuit modules, are coupled to an ultrasonic analyzer through a selector switch, S4, as indicated, allowing for inputting from either one of the two accelerometers. The X axis of the Moseley X-Y recorder is coupled to the ultrasonic analyzer as shown, with the sweep generator of the recorder driving the frequency sweep of the analyzer. The recorder sweep generator was set for 0.5 in/sec, during the demonstration tests, driving the analyzer through a range of 10 KHz to 60 KHz. Switch S5b must be closed during checkout. The circuitry used to filter the analyzer output, and which coupled the analyzer output to the recorder Y axis, is defined by the figure. Switch S5 must be closed during checkout.

Switch S3 must be closed during checkout to couple the ±15 Volt power supply to the water level integrator circuit and to the op-amp of the ultrasonic analyzer driving circuit.

Figure 108 shows the arrangement selected for the demonstration to provide the required steady-state and dynamic steam flow input signals. A range of steady-state inputs are necessary for steady-state control accuracy testing. Checkout of dynamic response requires the inputting of a transient signal. The specification for the Feedwater Controller operating a boiler requires that the water level signal, L, may not vary from its set point by more than ±1.66 psi as the steam flow signal changes over 70% of full range in 45 seconds. The desired dynamic characteristics of the water flow controller which yield the above response when coupled to the boiler, may be transformed into an allowable closed loop response for the controller as coupled into the checkout arrangement. For a selected input ramp, an upper and lower limit to the change in L may be established.

The system of Figure 108 permits either manual setting of $\dot{W}_S$ at any value within the operating range, for steady-state tests, or provides a pre-set initial value of 5 psig for the ramp function, and the automatic generation of the ramp on command. Solenoid valves are used to implement the switching for convenience.

The pressure regulator is set for 35 psig during operation. The steam flow signal simulator is shown by the figure in the manual state. The manual/automatic solenoid is in the manual position, coupling the regulator to a valve which is used to manually regulate the pneumatic $\dot{W}_S$ signal inputted to the controller. The blocking solenoid valve is closed to prevent backflow

192

through the analog amplifier of the automatic ramp system.

The automatic generation of a ramp signal for dynamic testing is a two-step procedure. First, the selector solenoid valve and the blocking solenoid are actuated simultaneously, being coupled electrically. The "start ramp" solenoid remaining closed as shown. This provides a supply pressure and an input to the analog amplifier, with the orifice in the input line sized to cause a 5 psig output from the amplifier. This pre-set 5 psig signal provides a known steady-state input to the controller prior to the introduction of a transient.

The second step, following stabilizing of the system for the 5 psig input, is the opening of the "start ramp" solenoid valve, which automatically initiates a pre-established $\dot{W}_s$ ramp signal. This is accomplished by opening a second control input path to the amplifier which incorporates an RC lag. The orifices and capacitance tank were sized for the demonstration to generate a 7 psi ramp (5 to 12 psig) in 45 seconds.

Upon completion of dynamic testing, the steam flow simulator is reset to the manual mode by deenergizing all of the solenoid valves.

3.   DEFINITION OF A FEEDWATER CONTROLLER CHECKOUT PROCEDURE

The individual element and integrated circuit studies described in Sections V and VI have shown that satisfactory performance of an analog circuit must be established by use of primary performance characteristics. A method of determining these characteristics was determined, using flush-mounted miniature pressure transducers to measure pressures. Secondary acoustic signatures were shown to be valid for localizing the malfunction.

In order to implement these techniques in a useful manner, a step-by-step procedure must be established so that a minimum of system knowledge will be required of the using personnel. The test set-up for the Feedwater Controller has been described in the previous sub-section. The procedure has very few steps. A 35 psig supply is applied to the controller. First, steady-state performance is checked at three points. Second, the test ramp is introduced to determine dynamic performance. If these are all within limits, the system is serviceable. Should any step be outside limits, the secondary acoustic test is run to establish the cause of malfunction. A typical step-by-step chart is shown in Figure 109.

193

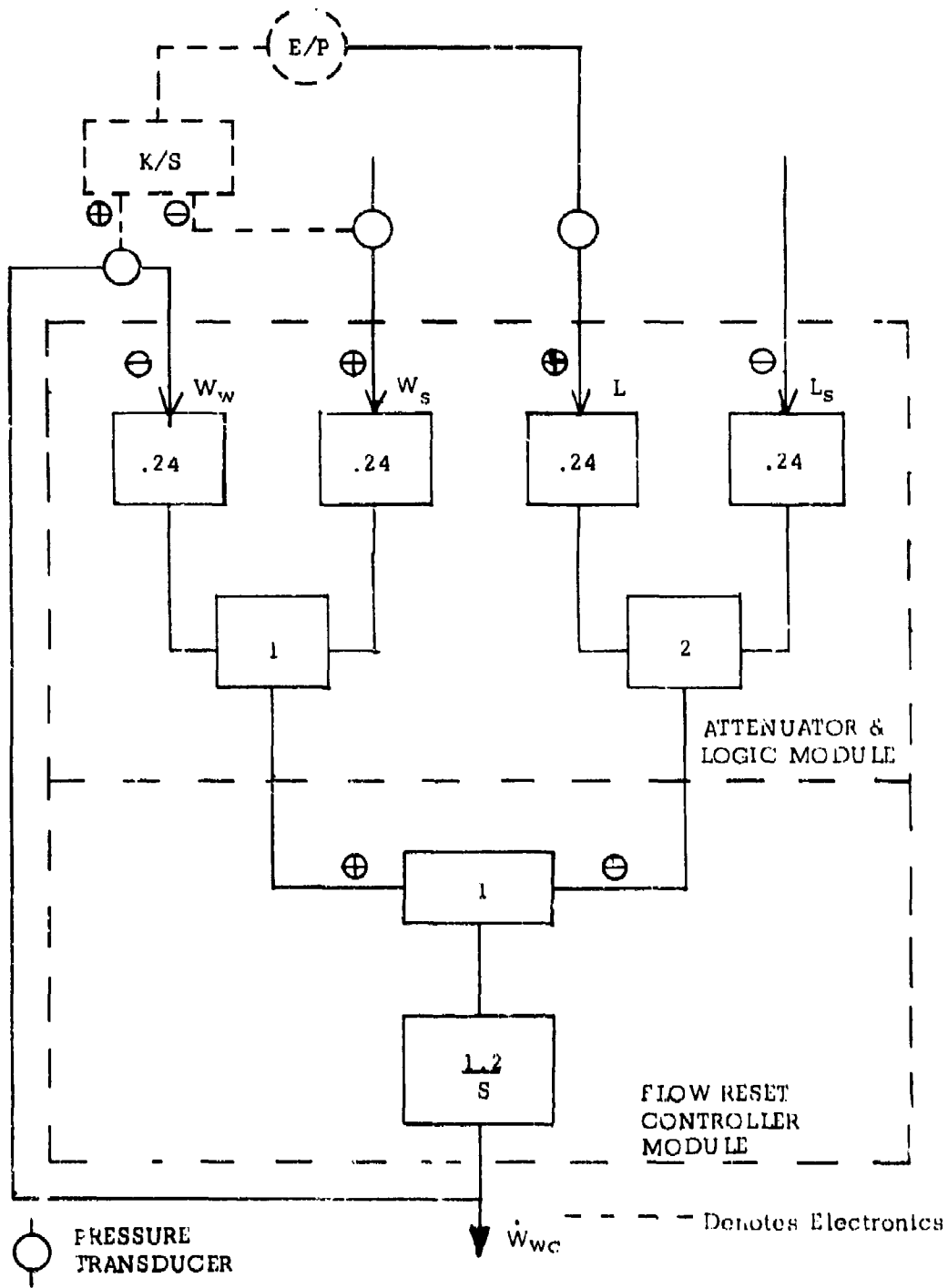Figure 106. Feedwater Controller Closed Loop
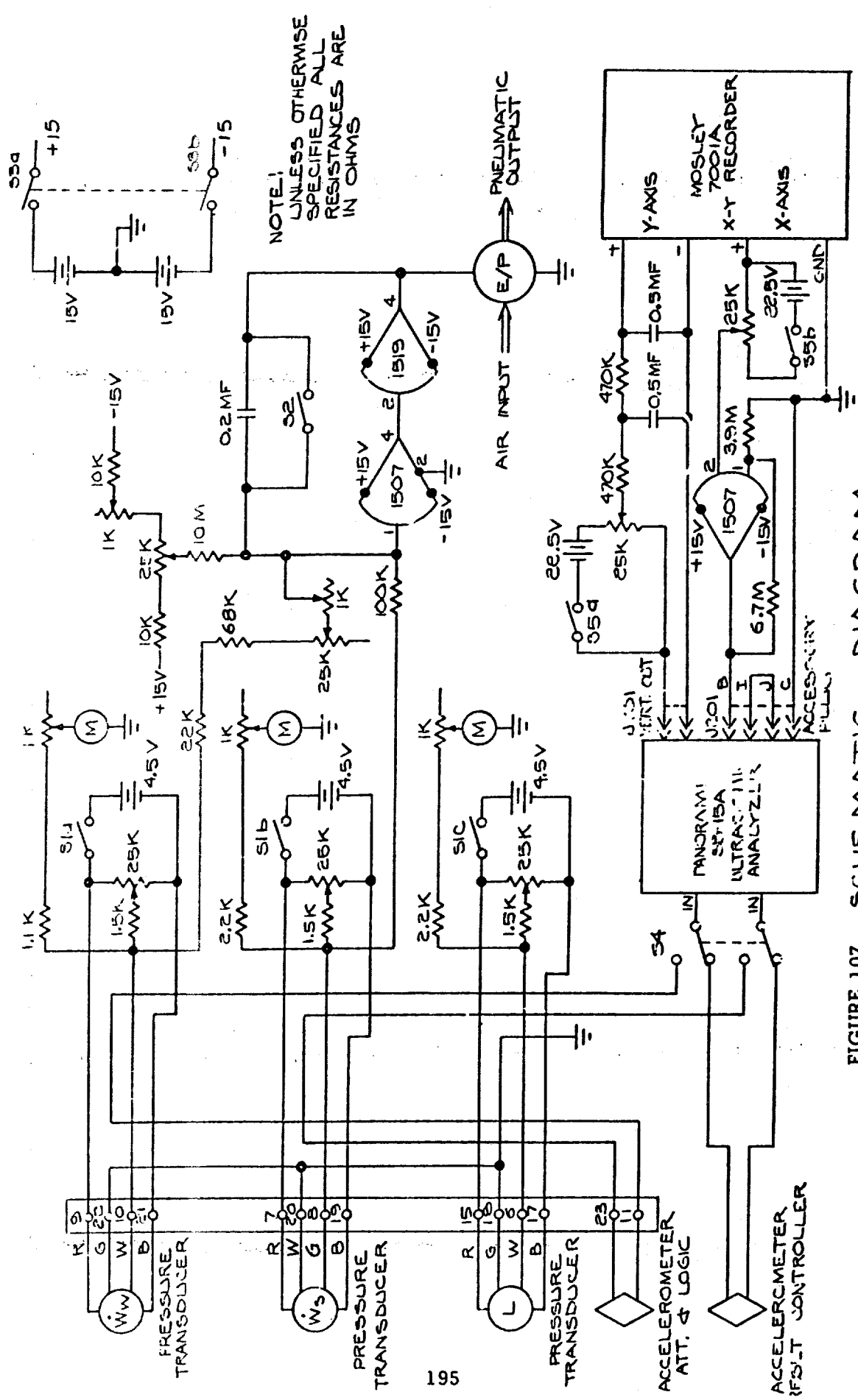Demonstration System

194

FIGURE 107. SCHEMATIC DIAGRAM
FEEDWATER CONTROLLER CHECKOUT CIRCUIT

NOTE!
UNLESS OTHERWISE
SPECIFIED ALL
RESISTANCES ARE
IN OHMS

195
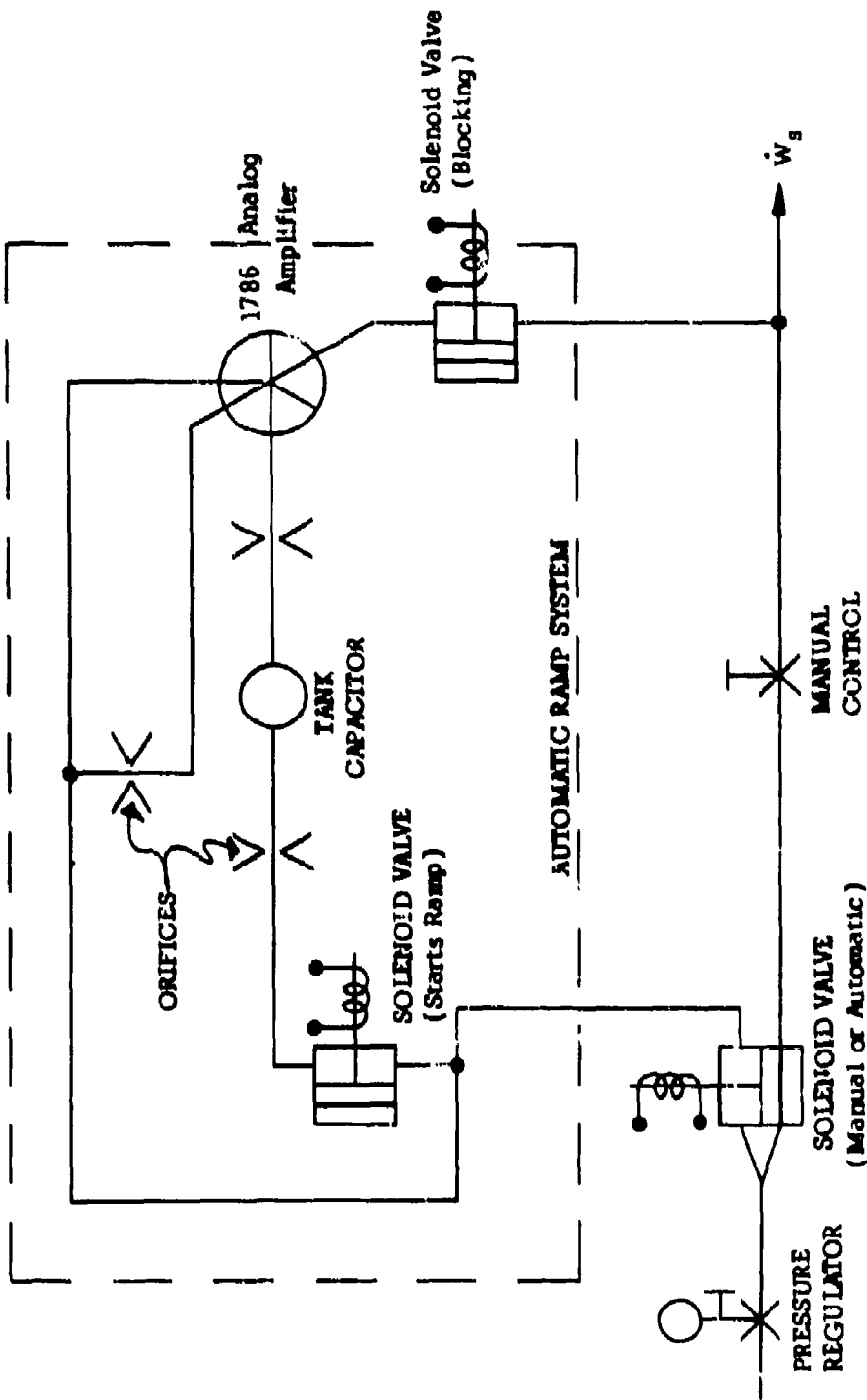
Figure 108. Steam Flow Signal Simulator

1. **Steady-State Performance**

    A.   Set $\dot{W}_S$ at   Measure $L_S - L$.

          4 psig   ____psig

          9 psig   ____psig

         14 psig   ____psig

    B.   Compare three values of $L_S - L$ from above. Maximum difference shall not exceed 0.42 psi between any two values. If maximum difference is within allowable limit, proceed to dynamic test.

    C.   If maximum difference exceeds allowable limit, perform acoustic signature test to isolate malfunction.

2. **Dynamic Performance**

    A.   Using dynamic test input, increase $\dot{W}_S$ 70% of range in 45 sec. Monitor $L_S - L$. $L_S - L$ shall fall within $L_S - 0.5$ psi as the upper limit and $L_S - 3$ psi as the lower limit.

    B.   If variation of $L_S - L$ is within allowable limits, system is operating as specified and is ready for service.

    C.   If variation is more than allowable limits, perform acoustic signature test to isolate malfunction.

3. **Acoustic Signature Test**

    A.   Set $\dot{W}_S$ at 9 psig.

    B.   Obtain acoustic signature using test set-up of Figure 107.

    C.   Compare acoustic signature with base line signature, and with reference signatures from known anomalies. Determine most likely cause of malfunction.

    D.   Perform adjustment, healing or removal procedure based on type of malfunction.

    E.   When malfunction corrected, repeat steady-state and dynamic tests to establish healing accomplished.

Figure 109. Checkout Procedure for Feedwater Controller

4. LABORATORY DEMONSTRATION OF CHECKOUT PROCEDURE FEASIBILITY

In order to verify that the primary performance characteristic testing and acoustic signature testing could provide a useful method of rapidly and accurately checking the operation of the Feedwater Controller, a laboratory demonstration was performed. Various anomalies were introduced, and both primary and secondary characteristics determined. Then, the anomalies were "healed" and return to base line conditions established.

As has been noted before in this report, introducing quantitative contamination proved impossible within the scope of this program. Also, removal of contamination proved difficult because large quantities were introduced rapidly, rather than wait for the slow build-up likely to occur in actual service. For this demonstration, then, contamination was simulated by the use of a small physical restriction in the receiver of one of the elements. This proved to be a reliable and repeatable means for inserting and removing contamination.

The anomalies introduced were as described below. The physical locations of these anomalies may be seen in Figures 104 and 105.

$P_{sL} = 30$ The supply pressure to logic module was set at 30 psig instead of the specified 35 psig.

$P_{sR} = 30$ The supply pressure to the reset (integrating) module was set at 30 psig instead of the specified 35 psig. Similarly, 33 and 25 psig were set.

$G_{2R} = 1/2$ turn   The second stage gain adjust valve in the reset module was advanced 1/2 turn.

Cap. Leak $= 0.017$ A leak equivalent to a 0.017" diameter hole was inserted in the line to the capacitor tank for the reset module.

198

W_S Leak = 0.017   A leak equivalent to a 0.017" diameter hole
                      was inserted at the $\dot{W}_S$ output monitor location
                      of Figure 104.

L_e Leak = 0.01   A leak equivalent to a 0.01" diameter hole was
                      inserted in the L_e signal line which interconnects
                      the logic and reset modules.

L_S = 8.0   The level set signal was set at a value of 8.0
                      psi instead of the nominal 9.0 psi.

Contamination In   The simulated contamination was inserted into
                      the output signal receiver of the ($\dot{W}_w - \dot{W}_S$)
                      relay amplifier.

The results of the introduction of these anomalies, one at a time, are shown
in Figure 110 (Chart). The magnitude of the anomaly was set in each case
to a value which caused primary performance to be at or near the limit of the
specification. Gross anomalies were not included, as their presence, and
location, is felt to be obvious. In each case, the secondary acoustic
signature exhibited readily observable changes, with the changes for each
different type of anomaly being distinguishingly different, thus defining the
anomaly.

5.   CONCLUSIONS

The testing of the Feedwater Controller has shown that a simple closed loop
test procedure can be used to determine whether primary performance
characteristics are within limits, and that such testing can be accurate
and quick. Also, it has been shown that the use of secondary acoustic
signatures can be used to determine type and location of malfunction,
provided base-line data have been established. Experience with systems
using this technique should quickly build up a store of signatures, making
its use evermore valuable.

Both techniques, primary characteristics and acoustic signature, require
the use of transducers mounted in the circuit at time of manufacture. Further
work must be done to reduce the space, weight, and economic penalty resulting
from the transducers, in view of the continuing effort to reduce the size and
cost of Fluidic control systems.

| Anomalies | Magnitude | Primary Performance | | Secondary Signature Changes | |
		S.S.	Dyn.	Logic Module	Int. Module
L_S	8.0 psig	Exc.	OK	(14 KC to 16 KC)↓(31 KC to 35 KC)↑	
L_e Leak	.01 Leak	Exc.	OK	(31 KC to 35 KC)↑	
Cap. Leak	.017 Leak	Exc.	Exc.		(10 KC to 60 KC except 41 KC)↓
$\dot{W}_S$ Leak	.017 Leak	Exc.	OK	(31 KC to 35 KC)↑(43 KC to 46 KC)↓	
Contam.	1/2	Exc.	OK	(31 KC to 35 KC)↓(41 KC to 50 KC)↓	
P_{SL}	30 psig	Limit	OK	(35 KC to 54 KC)↓	
P_{SR}	30 psig	Limit	OK		(10 KC to 60 KC)↓
	33 psig	OK	OK		(10 KC to 60 KC)↓
	25 psig	Exc.	OK		(10 KC to 60 KC)↓
G_{2R}	1/2 turn	Exc.	OK		(14 KC to 27 KC)↓(42 KC to 52 KC)↓

Legend---

Exc.	Exceeded performance specification
OK	Within specified limits
Limit	Border line case
↑	Increasing signature
↓	Decreasing signature
S.S.	Steady State
Dyn.	Dynamic

Figure 110. Feasibility Checkout Results (Performance Chart)

SECTION VIII

CONCLUSIONS AND RECOMMENDATIONS

The overall objectives of this circuit checkout have been met, and the feasibility of in-place checkout of Fluidic circuits and systems has been established. Some of the results were not foreseen at the outset, but no major obstacles were encountered. Much was learned, and much remains for further investigation before the techniques shown feasible during this study can become operational.

Because the work was divided into analog and digital circuits, and because the conclusions are somewhat different, analog and digital circuits are treated separately below. In real life, it is likely that Fluidic systems will consist of both analog and digital circuits.

It is necessary to point out that the conclusions drawn are based on the specific Fluidic elements, circuits, and systems examined during this program. The elements and circuits examined are thought to be typical of those which may be used in flight systems, so that generalization of the results is believed to be warranted. The detailed results will, of course, vary from element (type) to element, and from specific circuit to circuit.

1. ANALOG CIRCUIT CONCLUSIONS

The work of this program has shown that the secondary acoustic signature is a powerful tool for locating and characterizing analog system malfunctions, once the primary characteristics have shown the system to be malfunctioning. Primary performance characteristics are believed to be the only practical means of establishing that an analog circuit is operating within specified limits.

It was shown that the primary performance characteristics, i.e., output/input functions, may be easily determined, provided that this has been planned for from the beginning and proper sensors have been built into the circuit. It is expected that clever designs can minimize the number of primary variable sensors which must be built into the circuit or system. It is believed, also, that such sensors can be built into the circuits and systems without degrading reliability or performance, permitting checkout without disturbing the system in any way. This eliminates the problems of reconnection that sometimes occur when system elements are disconnected for checkout. Proper design of the primary sensor and its mounting can preclude system malfunction as a result of sensor failure.

The primary output/input characteristic can determine that the overall system is not operating correctly, and in some cases, can pin-point the cause. However, specific information as to the detailed location and type of malfunction can greatly reduce the time required for repair. For instance, knowledge that a low pressure is causing a malfunction suggested readjustment of the supply while knowledge that a channel has clogged suggests in-place cleaning with a solvent. Other indications can disclose which of several modules to replace. This type of information has been shown to be available in the secondary acoustic signature from analog circuits, if appropriate sensors are built into the circuitry. As in the case of primary sensors, proper selection of the secondary sensor and mounting precludes system malfunction as a result of sensor failure.

In summary, the use of built-in primary and secondary sensors has demonstrated the feasibility of an analog circuit checkout technique, which can determine that a system is functioning properly, and pin-point the malfunction if the system is out of limits.

2. DIGITAL CIRCUIT CONCLUSIONS

This program has shown the feasibility of using primary and secondary characteristics to determine whether a digital circuit is operating within limits, and if not can pin-point the cause of the malfunction. Because digital circuits transmit information using only two element states (i.e., 1 and 0), it was shown that less precise primary sensors are needed. In particular, the use of piezoelectric crystals could serve as primary sensors. These are easily mounted, quite inexpensive, and rugged enough for most applications.

Proper design of the sensors and mounting can preclude circuit malfunction in case of sensor failure, and checkout can be accomplished without disturbing the system in any way. Primary characteristics can determine that the circuit is operating within limits, and if it is not, the secondary acoustic signature can be used to determine the location and type of malfunction.

3. RECOMMENDATIONS

Many things remain to be done to move these techniques from feasibility to operability. Primary among these is the development of improved sensors. Both the primary and secondary sensors used in this program are costly. Development of sensors specifically for the task at hand seems likely to reduce the cost of the sensors. Circuit-sensor combinations may exist which will permit determination of both primary and secondary characteristics with the same sensor. This avenue of exploration should not be overlooked.

In digital circuits, the possibility of using only secondary acoustic signals deserves more attention. If it is shown that this can be done, simplification of sensors and associated instrumentation will result.

Little was done on this program with the problem of bringing out the electrical connections from the many sensors. Design studies in this area will eventually be needed, but perhaps deferred until the first application.

There exists the possibility of using Fluidic elements and techniques to bring both the signals to a more easily accessible point on the system. For instance, secondary acoustic signatures play a large role in pin-pointing the malfunction. It may be possible to provide acoustic transmission, much as used in commercial aircraft for movie sound, to bring the signals to a common location. If such is proven feasible, the secondary sensor would not need to be permanently mounted but could be "plugged in" where needed. Study should be directed to this area, and development undertaken if the study shows feasibility.

Another area that has not been touched on this program but which deserves study is the use of special input signals. It is possible that introduction of alternating signals, or pulse-type signals, can provide characteristic secondary signatures which can be interpreted to determine proper system operation. It may be feasible to introduce such signals without direct physical connection to the system, perhaps through the vents of selected elements. If this can be done, and if it can be combined with use of the acoustic signal transmission, no expensive built-in sensors would be required. Such a checkout technique would keep all the costly sensors and instruments "on the ground".

APPENDIX I

PRINCIPAL FLUIDIC DIGITAL ELEMENTS,
PERFORMANCE DEGRADATION
CAUSES AND SYMPTOMS
(TM-106)

TYPICAL ANALOG AMPLIFIER
PERFORMANCE CHARACTERISTICS
AND
ALLOWABLE PERFORMANCE DEVIATIONS
(TM-116)

Preceding Page Blank

PRINCIPAL FLUIDIC DIGITAL ELEMENTS,
PERFORMANCE DEGRADATION
CAUSES AND SYMPTOMS

AF33(615)-5296

by

P. Bauer

Bowles Engineering Corporation
9347 Fraser Street
Silver Spring, Maryland 20910

TABLE OF CONTENTS

Preceding Page Blank

PRINCIPAL FLUIDIC DIGITAL ELEMENTS,
PERFORMANCE DEGRADATION
CAUSES AND SYMPTOMS

AF33(615)-5296

1.0   INTRODUCTION

Fundamental element characteristics are discussed with respect to causes
and symptoms of performance degradation singly and in system circuits.
Reasons for failures (and their implications) are established to provide a
basis for detection and measurement of satisfactory or unsatisfactory
performance, anomalies, failures, and possible locations and causes of the se.

> NOTE: The basis for this discussion is given by the compatible
> family of digital logic circuit elements existing at BEC
> since 1964, represented by the following present
> elements: OR/NOR Gate (#4707), FLIP-FLOP (#4709),
> Passive AND Gates and several Binary Counter element
> types (such   circuit #4766). Furthermore, the great
> variety of system circuits manufactured (utilizing such
> elements) and tested in the past years provided the data
> for this discussion.
>
> It should be noted that the information given herein is
> based on BEC elements and circuits in common sizes
> (nozzles of 0.015 to 0.025 inches wide, element and
> channel depths of 0.04 inches), utilizing air around
> atmospheric conditions, and fabricated in Optiform,
> epoxy castings, and injection molded forms. However,
> it is most likely that such basic information is
> applicable to other Fluidic devices of a similar nature
> under similar circumstances and even under somewhat
> varied conditions, provided reasonable discretion is
> maintained in its interpretation.

2.0 PRIMARY CHARACTERISTICS

Quasi-Steady State Characteristics

As given by the enclosed three element catalog sheets, these characteristics
are presented as input (control) and output p/q relationships for a
constant supply pressure of 1 psig. Control pressures and flows, required
to switch an element into the alternate state and control pressures and flows
below which a monostable element returns to its stable state, are indicated
as regions or bands on the input p/q curves. These relationships are
plotted in one graph permitting the superposition of different element
characteristics for evaluation of compatibility in interconnections.

These characteristics are given in the form of wide regions or bands
encompassing hitherto tolerated (acceptable) performance deviations
under equal operating conditions, determined by large numbers of tested
elements (see Reference I). These measured regions also indicate that
(within these tolerances) fabrication rejects can be completely avoided; as
substantiated by the characteristics-originating measurements performed on
elements fabricated over a period of several months

The given characteristics apply to the element silhouettes, as identified by
their numbers, and also to their immediate successors, identified by the
following numbers:

	Original BEC No.	Latest BEC No.
OR/NOR	1715	4707
FLIP-FLOP	1425R	4709
Binary Counter	1391	4766

It should be noted that these tests are performed with regard to every
element's logic function, even though only as far as quasi-steady state
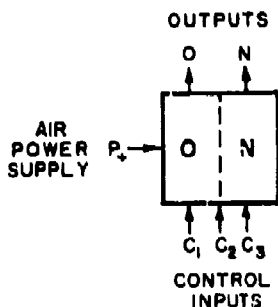is concerned.

3 INPUT OR/NOR No. 1715

This Pure Fluid Amplifier element supplies the OR and NOR logic functions for use in laboratory breadboards. In the absence of all control signals the NOR (N) leg provides an output. The OR (O) leg provides an output with either or all control signals present. An unused output or input should be vented to atmosphere.

This element used with others may be connected to demonstrate basic digital logic functions. However, if you contemplate circuit complexities of the order of a full adder or greater, you should contact the Bowles Engineering Corporation and we will consider the development of an integrated circuit of your required function. Thus, many problems arising in sychronous circuits, where timing and signal coincidence is important, may be eliminated.

This element is made of plastic and should not be heated above 150°F. The pressure fittings are barb type for 1/4 inch tubing.

LOGIC SYMBOL

OUTPUTS

O   N

AIR POWER SUPPLY P_+ → O | N

C_1 C_2 C_3

CONTROL INPUTS

SILHOUETTE
ACTUAL SIZE

O   N

C_3

C_2

C_1 — $\frac{.17}{.05}$ psig

P_+

P = 1.5 psig MAX.

STEADY STATE CHARACTERISTICS

INPUT

$P_+ = 1$ psig

OUTPUT

ON

OFF

SWITCHING AND RETURNING RANGE

PRESSURE, psig

VOL. FLOW (cu. in. / sec.)

* Price: $40.00 each
  Delivery: Within 30 days

Caution should be exercised to prevent dirt from entering the unit from the supply or input signal. Purge the supply line. This unit does not contain a filter. Do not overpressure.

* Price F.O.B. Silver Spring, Maryland. Subject to change without notice.   211

4 INPUT FLIP-FLOP No. 1425R

This Pure Fluid Amplifier element supplies the Flip-Flop logic function for use in laboratory breadboards. In the presence of a (C_0) control signal the O_0 leg provides an output. With a control signal at C_1 the O_1 leg provides an output. The signal remains present even after discontinuation of the input signal. The inputs on either side obey the "OR" function. An unused output or input should be vented to atmosphere.

This element used with others may be connected to demonstrate basic digital logic functions. However, if you contemplate circuit complexities of the order of a full adder or greater, you should contact the Bowles Engineering Corporation and we will consider the development of an integrated circuit of your required function. Thus, many problems arising in sychronous circuits, where timing and signal coincidence is important, may be eliminated.
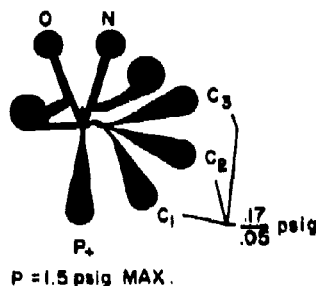
This element is made of plastic and should not be heated above 150°F. The pressure fittings are barb type for 1/4 inch tubing.
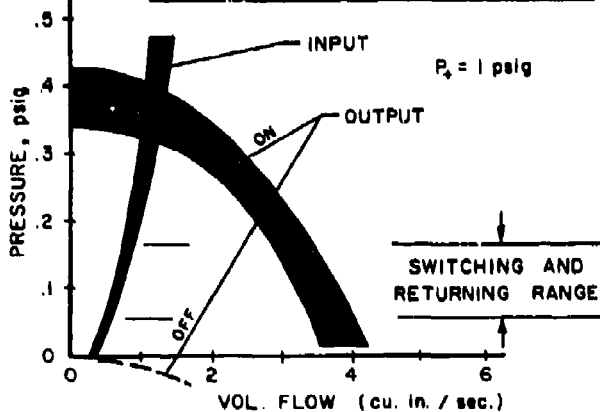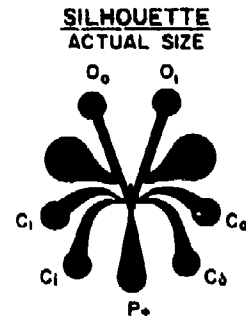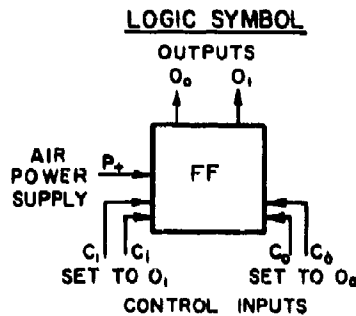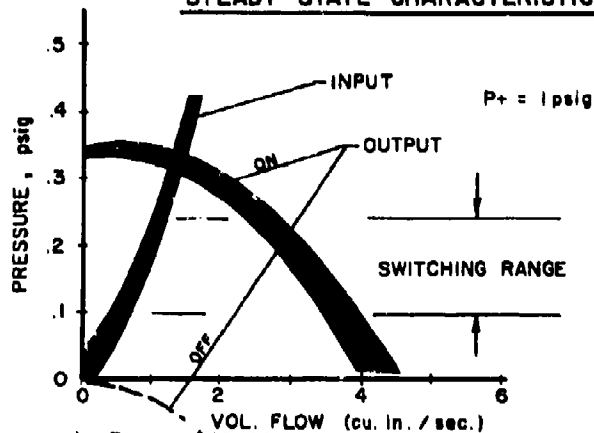
LOGIC SYMBOL

OUTPUTS

O_0 O_1

AIR POWER SUPPLY P_+ FF

C_1 C_1 C_0 C_0
SET TO O_1 SET TO O_0

CONTROL INPUTS

SILHOUETTE
ACTUAL SIZE

O_0 O_1

C_1 C_0

C_1 C_0

P_+

STEADY STATE CHARACTERISTICS

INPUT

OUTPUT

$P_+ = 1$ psig

ON

OFF

SWITCHING RANGE

VOL. FLOW (cu. In. / sec.)

PRESSURE, psig

* Price: $40.00 each

Delivery: Within 30 days

Caution should be exercised to prevent dirt from entering the unit from the supply or input signal. Purge the supply line. This unit does not contain a filter. Do not overpressure.

* Price F.O.B. Silver Spring, Maryland. Subject to change without notice.

212

BINARY COUNTER No. 1391

This Pure Fluid Amplifier element supplies the Binary Counter function for use in laboratory breadboards. This unit is a single input Flip-Flop and has a change of output for every complete input pulse. An unused output or input should be vented to atmosphere.

This element used with others may be connected to demonstrate basic digital logic functions. However, if you contemplate circuit complexities of the order of a full adder or greater, you should contact the Bowles Engineering Corporation and we will consider the development of an integrated circuit of your required function. Thus, many problems arising in synchronous circuits, where timing and signal coincidence is important, may be eliminated.

This element is made of plastic and should not be heated above 150°F. The pressure fittings are barb type for 1/4 inch tubing.

LOGIC SYMBOL

AIR POWER SUPPLY P_+ → | B.C. | O_0 O_1

SET TO O_1 CONTROL INPUT   SET TO O_0

SILHOUETTE
ACTUAL SIZE

O_0 O_1 ← P_+ S   R   C

STEADY STATE CHARACTERISTICS

P_+ = 1 psig

INPUT
OUTPUT
ON
OFF
SWITCHING RANGE

PRESSURE, psig

VOL. FLOW (cu. in./sec.)
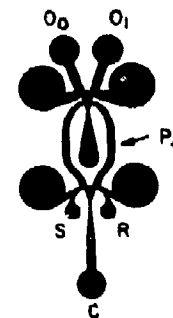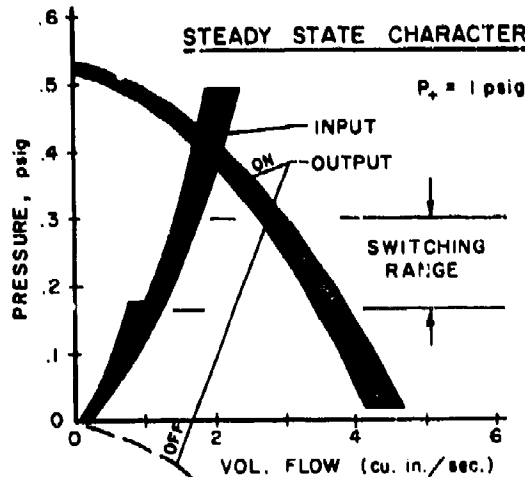
* Price: $40.00 each
Delivery: Within 30 days

Caution should be exercised to prevent dirt from entering the unit from the supply or input signal. Purge the supply line. This unit does not contain a filter. Do not overpressure.

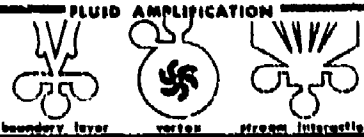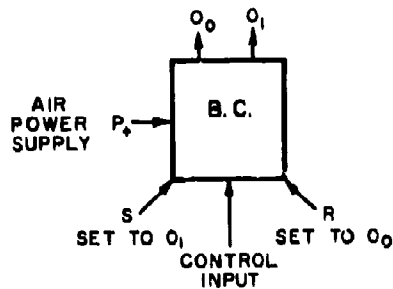* Price F.O.B. Silver Spring, Maryland. Subject to change without notice.

Dynamic/Transient Characteristics

Such characteristics are few and far between and their interpretation is rather questionable, mainly for two reasons:

1. All necessary operating conditions are not usually determinable; neither are all the conditions known under which characteristics were obtained. Transient characteristics are grossly affected by such "peripheral" conditions.

2. A large number of different and relatively complex measurements are needed to entirely specify a performance such that anomalies or deviations are definitely recognizable and interpretable.

However, some gross relationships can serve in a majority of cases for establishment of acceptable performance. Single elements and circuits in many instances lend themselves to a number of basic tests, as indicated in the following:

a. Waveform, pulse, and frequency response tests.

b. Switching/returning time or signal transition time tests.

c. Spurious noise tests.

d. Sound generation tests.

e. Transmission line tests.

f. Stability tests.

g. Feedback connection tests.

h. Jitter tests.

i. Cross-talk isolation tests.

Etc.

Characteristics as determined by the first three tests given above can be considered primary ones and are described below:

    a. Waveform, pulse, and frequency response.

        Any of the active elements (such as the OR/NOR, the FLIP-FLOP, and the Binary Counter) should accept single or repetitive waveforms, where each wave comprises only one monotonic rise and one fall, of various frequency contents, without excessive reflections and noise being generated at its input, which could in turn cause feedback sufficient to affect its own or other connected elements' correct operation. This applies over the frequency and amplitude range considered. Furthermore, such an element should respond such as to generate at its output a more or less square waveform of an also monotonical rise and fall character. This is relatively easy to detect by closely positioned input and output signal sensors when testing with a slow and clean rise and fall input signal; for example with rise and fall times of several tens of milliseconds or more.

Similarly, square waves (pulses) may be fed into an element of gradually increasing repetition rates or gradually decreasing widths, and sufficient amplitudes (see steady state characteristics). All elements should respond correctly and reliably, provided the input pulse width is more than 2.5 milliseconds (whether a pulse or an inversion of one is used), and the corresponding gaps before and after the pulse (or inversion) are at least 2.5 ms each.

Certain elements may respond to repetition rates higher than the implied maximum of 200 pps due to resonance effects. However, the criterion of a digital element's response is its performance with single pulses and pulse patterns, rather than with repetitive waveforms of oscillatory character. Therefore, repetitive waveform tests should be viewed with considerable care to avoid misleading interpretations. Such high frequency tests are of very little value, if any, for the determination of elements' digital speed capabilities, unless test conditions accurately reproduce all actual operating conditions and signals. Generally, the single short pulse test (as given above) of low duty cycle should be performed. A more valid test is one with such short pulse pairs and possibly triplets, but it requires special signal generating equipment.

The element response or speed (analogous to "analog element frequency response") is given in shortest accepted pulse width (or inversion). Its

215

actual frequency response may have to be considerably higher, but may be meaningless, as far as digital signal handling is concerned.

A further criterion has to be applied; a logic function has to be performed as a function of two or more input signals (with the exception of the inverter and the Binary Counter). As can well be visualized, two or more input signals arriving in time, such that coincidence or partial coincidence results, may logically be required to provide output signals as a function of the coincidence time. This time may well be shorter than the minimum accepted pulse width. Alternately, a time gap between two pulses arriving at different inputs may be shorter than the minimum accepted pulse width. In both cases elements will not respond correctly, in spite of input pulse widths larger than minimum accepted. Such fundamentals should be kept in mind. Other secondary effects, such as noise, jitter, interconnection line response, etc., generally degrade capabilities even further, as discussed in later sections.

b. Switching/returning time or signal transition time.

The relatively coarse determination of switching and returning delay (rise and fall or vice versa) and element signal transition delay establishes a primary element characteristic; i.e., whether or not an element is switching as required. Such tests can be performed simply by roughly measuring the time between an onset of an output change and the onset of the corresponding logically required input change. This corresponds to the signal transition delay when reasonably square waves are utilized at the input (i.e., waves, as generated by other correctly operating digital elements). Often it is sufficient for a coarse check to listen to an element output and input signal, although a rough-instrumented test will provide more reliable results. In the former case, correct function is assumed, when little or no delay (and noise) in the two signals can be audibly detected. In the latter case, measurements should indicate (across an element) signal transmission delays of less than a few milliseconds, with possibly detectable rise and fall times of less than 1-1/2 milliseconds.

c. Spurious noise.

Element (and circuit) inputs, outputs, and vents will immediately provide quality information, if checked with regard to noise level and kind in the various logic states. A coarse check can be made by the trained ear. However, a properly instrumented test will provide better results.

216

All elements should be quiet, except for a low amplitude audible hissing. No distinct tones should be detectable in any state. Instruments, such as the hot wire anemometer should indicate similarly a steady amplitude modulated with neither discernable discrete high or low frequency signals, and with a <u>minimum signal-to-noise ratio of 5:1</u> in any logical and steady state when correctly interconnected with a compatible element (does not apply to vents).

Interconnection Characteristics

Steady state interconnection characteristics are simply determinable. Pressure drop or resistance at utilized signal flows is the only characteristic needed to establish the steady-state interconnection quality. This pressure drop must never be higher than the available pressure margin between an element output signal channel and the interconnected next element (or elements, if fanned out) at signal flow levels. Under nominal operating conditions this amounts to no more than approximately 0.1 to 0.2 psid at approximately 2 cubic inches per second without fan-out in an interconnection, and correspondingly less if a fan-out exists or if higher signal flows are present due to several elements feeding one interconnection. Exact margins are determined from the particular element steady-state characteristics.

Transient and dynamic interconnection characteristics present special and complex problems and are separately classified as follows:

    a.   Frequency response of constant shape and size sections. Frequency response of other sections.

    b.   Transition sections.

    c.   Partial channel flow effects.

    d.   Effects of bends, corners, and edges.

    e.   Impedance match/mismatch and termination effects.

    f.   Fan-in/fan-out section effects.

    g.   Pure resistance effects.

    h.   Length effects (pure delay).

It is beyond the scope of this discussion to delve into closer details of the dynamic response of interconnections. However, several major effects, which are relatively easily measurable and which can provide valid data as to the performance, should be mentioned:

     Delay effects in an interconnection can be measured by conventional methods. It is possible to estimate whether or not an interconnecting line is suitable for the required task. If full channel flow is maintained and little waveform distortion occurs, signal propagation velocity should be close to the speed of sound over short low resistance channel lengths. Any longer delays measured are to be questioned. They may indicate separation of flow (signal) and can thus provide information on the state of the channel. For example, flow separation may occur due to dirt particles lodged in channel.

     Waveform degradation can similarly be measured between different locations. This can be caused for a variety of reasons: reflections, flow separation, obstructions of load nozzles, cross-sectional changes, sharp bends and edges, etc.

     Reflections can also be generally easily detected by tests with shortest pulses and measurement of the reflected pulse. Flow or pressure standing wave ratio can thus be established, which is directly a measure of the impedance mismatch. For example, one could determine the amplitudes of the incident and reflected waves at a suitable point along the line. Under the assumption that all signals (flow and pressure) in one direction are unidirectional, the flow or pressure standing wave ratio (FSWR or PSWR) equals to $\rho = \frac{p_{max}}{p_{min}} = \frac{q_{max}}{q_{min}}$, where p_{max} or q_{max} are maximum forward signal amplitudes, and p_{min} or q_{min} equal to these maximum amplitudes minus the respective reflected signal amplitudes. Thus, ρ can be determined, and with it the signal power effectively transmitted in the forward direction: i.e.

$$P_{transmitted} = P_{generated} \; \frac{1}{\rho}$$

3.0 SECONDARY CHARACTERISTICS

Secondary characteristics encompass effects of signal jitter, noise, oscillations (sound generation), cross-talk, back-pressure (load sensitivity, etc.

Signal jitter is one of the major sources of problems in circuitry. In general, it could be defined as the variation (in time) of an output signal with respect to a nominal reference time; usually the input signal. Two sources of jitter can be distinguished:

1.   Noise or unclear waveforms on input signal(s), power supply, vents, etc.

2.   Random or quasi-random fluid flow effects, such as turbulence, dirt particles, humidity changes, temperature changes, etc.

Jitter can mean fast changing variations or slow ones, such as possibly caused by power supply pressure or temperature variations.

Although, as it is generally known, noise does not propagate (and is not amplified) through digital elements, noise is transformed into jitter (in time) at each element. This is particularly true in Fluidic circuits where signal rise and fall times are generally of the order of magnitude of the shortest pulse widths utilized. Effectively, noise on an input signal or any of the other above mentioned sources affect the switching and returning points, such that these transitions occur at different times, for example with respect to the nominal input signal rise.

A reasonable guiding value for maximum permissible jitter per element due to all causes is extremely difficult to specify, due to its dependence on the signal-to-noise ratio. However, an element could be assumed to operate satisfactorily if it does not contribute more than 0.25 milliseconds of total jitter (under the assumption of a peak-to-peak signal-to-noise ratio of 5 or better).

Jitter values can be calculated from the following relationships:

$$N = \frac{S}{S/N}$$

$$\frac{t_j}{N} = \frac{t_{R,F}}{0.8S}$$

$$t_j = \frac{t_{R,F}}{0.8\ S/N}$$

N	=	Peak-to-peak noise amplitude
S	=	Peak-to-peak signal amplitude
S/N	=	Peak-to-peak signal-to-noise ratio
$t_{R,F}$	=	Signal rise or fall time respectively, as given between 10% and 90% of signal amplitudes
t_j	=	Jitter or total dispersion in time.

Jitter is additive through elements, such that each element contributes a certain amount of jitter t_j due to the signal-to-noise ratio at its input (and the other causes equivalent to noise components) to the input signal jitter. One might say that this is after all a statistical effect, which it is. The jitter dispersion probability distribution will crowd around median values, and probabilities will decrease with larger deviations. However, digital systems do not tolerate any misses or errors, and therefore total dispersion must be considered at all times. Similarly, peak-to-peak noise values must be used.

As already given in earlier sections, peak-to-peak signal-to-noise ratio of 5:1 or better must be maintained. Any elements generating oscillations (edgetones for example), particularly during switching or changes of state, must be evaluated with respect to such noise.

Cross-talk and back-pressure or load sensitivity are closely tied together. Input signals must not affect each other and output loading and output states must not affect input signal sources. Existing digital elements were designed to be thus unaffected and should perform in this way correctly. Furthermore, any load from zero to infinite resistance should be accepted without adverse effects.

4.0 ACCEPTABLE OPERATING CONDITIONS AND ALLOWABLE DEVIATIONS

Previously given characteristics and operating conditions represent nominal
situations. Acceptable deviations in conditions will cause acceptable
deviations in characteristics. Fundamentally, one has to differentiate
between deviations in operating condition- for one element or a part circuit
only (A) and those affecting the complete system equally and uniformly (B).
The following tabulations are thus differentiated and marked.

	(A)	(B)
Supply pressure (air):	1 psig, $\pm$ 25%	+200%, - 40%
Vent pressure (ambient):	14.7 psia, $\pm$ 1%	$\pm$ 30% (est.)
Output loads:	+0 to + ∞ resistance	
Temperature:	(see material specs.)	
Humidity:	Less than 100% relative	

5.0 SATISFACTORY PERFORMANCE AND ACCEPTABLE DEVIATIONS

These data are given in Sections 2 and 3 in this memorandum. Also see
Reference I.

6.0 ANOMALIES

Anomalies in power supply pressure distributi n can produce a variety of
results from excessive noise generation to complete failure. Two kinds of
such anomalies are considered common enough and, at the same time, not
always immediately apparent to warrant mention here: Power supply noise,
pulsing, and/or surges, resulting in noisy signals and thus excessive signal
jitter and even in extreme cases in spurious signals being generated in circuits,
can be troublesome, and it would be advantageous if pressure-to-noise ratio
could be kept above 10 (at nozzles). Uneven power supply distribution via
supply manifolds, due to high flow velocities in manifolds and feeder lines,
will cause failures of circuits if deviations exceed acceptable values given earlier.

Anomalies in venting in circuits will occur if vents are obstructed by packaging
and if common vent manifolds of insufficient volume are utilized. Results can
not be characterized due to the enormous variety possible.

Anomalies in physical configuration are similarly not characterizable
due to the great variety of effects possible, which can be caused by many
different deviations.

7.0 SPECIAL SYMPTOMS

Primary symptoms such as operational conditions or performance characteristics
and ones directly related to these are generally quite obvious (as given earlier)
and need not be mentioned here again.

Secondary symptoms may be useful to detect, particularly when integrated
circuits are involved.

Noise, tones, switching sounds, and state of element (sound intensity) can
be detected audibly and with microphones or anemometers suitably placed
near vents. Similarly, indirect performance sensing can be performed via
unused terminals of digital elements (inputs and outputs), which should
normally be vented.

Unconventional methods might include electrostatic sensing of states,
vibrational pick-ups, x-ray examination of construction (including moving
object for focusing), ultrasonic examination, infra-red examination, radio-
active tracer methods, etc.

Looking at a single digital element in an integrated circuit, where access
to input and output channels is not feasible, vents provide the only direct
means for sensing of element behavior. The following symptoms and probable
prime causes could be thus detected:

Symptoms	Prime Causes
Excessive noise in some or any state	Leaking, damage to shape, supply from elsewhere leaking or feeding in incorrectly - Potential Failure -
Extremely silent with no change on attempted switching	No supply and/or no control input
Whistle in any state	Probable edgetones, damage to power nozzle

222

Symptoms	Prime Causes
Whistle in some state	Too high supply pressure, damage to shape
Crackling in some or any state	S/N too low at input, leak, damage to shape, vent partially obscured. – Potential Failure –
No change of sound on attempted switching	Absence of input signals, asymmetry of shape, leak, obscured control nozzle, biased power nozzle.
Erratic switching on attempted regular repetitive excitation	Low frequency response, biased, leaking – Potential Failure –

There are a number of other symptoms, but very few uniquely distinguishable causes. Thus it may become impossible to tell anything beyond the probable location (which element) of a failure in a circuit.

8.0 REFERENCES

I.   BEC TM-73, "A Comprehensive Set of Compatible Digital Elements"

TYPICAL ANALOG AMPLIFIER
PERFORMANCE CHARACTERISTICS
AND
ALLOWABLE PERFORMANCE DEVIATIONS

AF 33(615)-5296

by

Edwin U. Sowers III

Bowles Engineering Corporation
9347 Fraser Street
Silver Spring, Maryland 20910

DATA ON
3126 ANALOG AMPLIFIER

1. OPERATING CONDITIONS

a.	P_S	3 to 35 psig
b.	Inputs (downstream)	5% to 25% P_S
c.	Load	Load area $\geq$ Control nozzle area

2. SATISFACTORY PERFORMANCE

The following data is based on a single side output (higher output leg), loaded with same area as that of amplifier control nozzles. Characteristics are different where load differs from above, as when bleeding from output to obtain a lower amplifier gain.

a.	Pressure Gain – at 22% of P_S output level, Bias = 10% P_S	2.3 to 2.5
b.	Max pressure recovery at saturation	37% to 40% P_S
c.	Operating Range – 3% linearity	10-13% P_S to 32-34% P_S
d.	Null Output – both inputs equal to 10% P_S	22% to 25% P_S
e.	Signal to Noise Ratio at frequency below 10 cps	≥ 100

3. ALLOWABLE DEGRADATION FROM ADJUSTED PERFORMANCE

The following data is based on requirements of the Boiler Controller, Combustion Control Logic, comprised of 3126 Amplifiers.

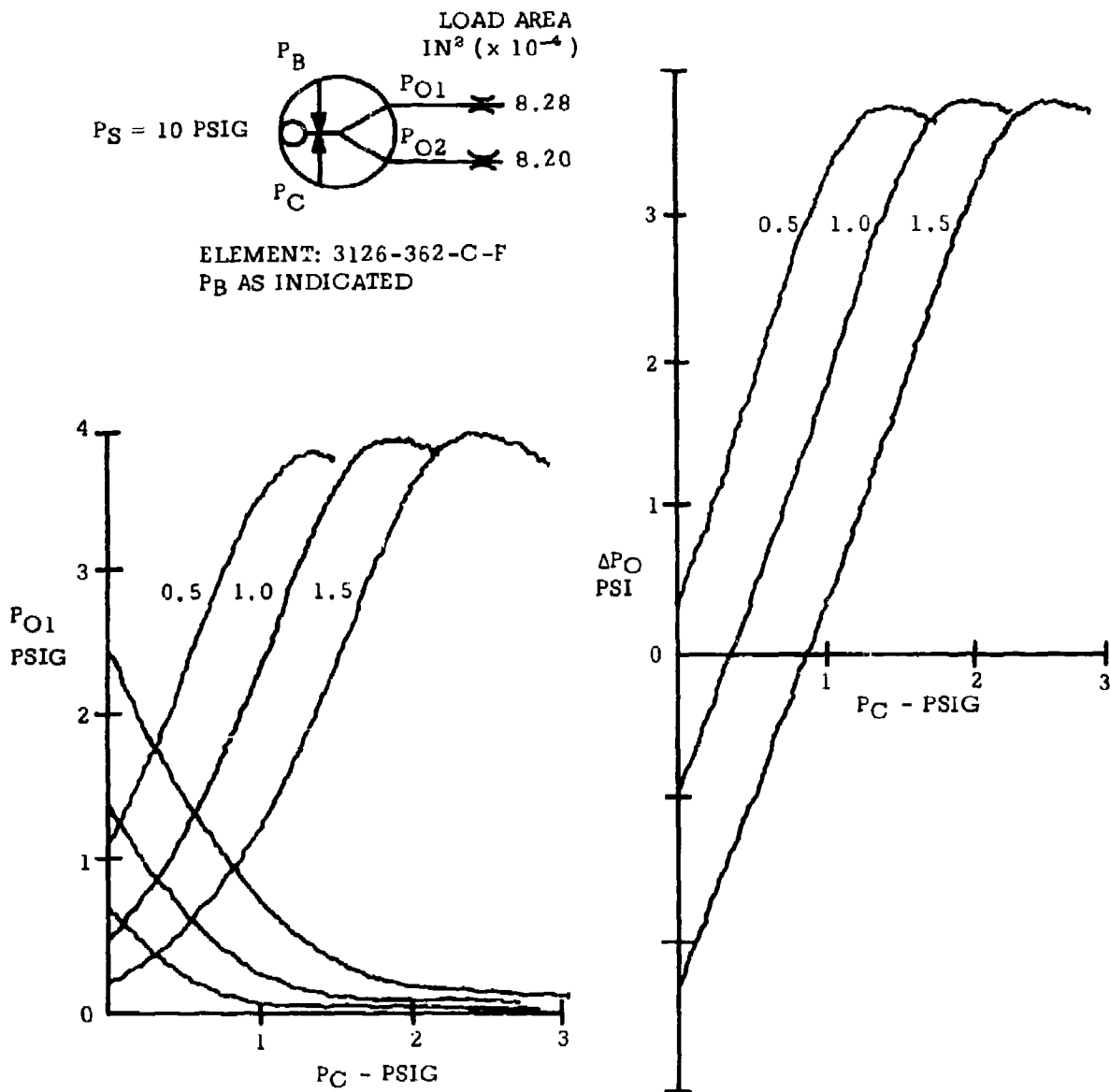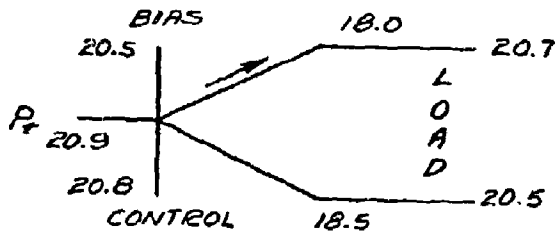|		
a.	Pressure Gain	$\pm$ 2% Gain change allowable
b.	Pressure Recovery	5% of maximum reduction allowable
c.	Operating Range	10% of range reduction allowable
d.	Output Null	$\pm$ 1% of operating range deviation
e.	Signal to Noise Ratio	No less than 100

227

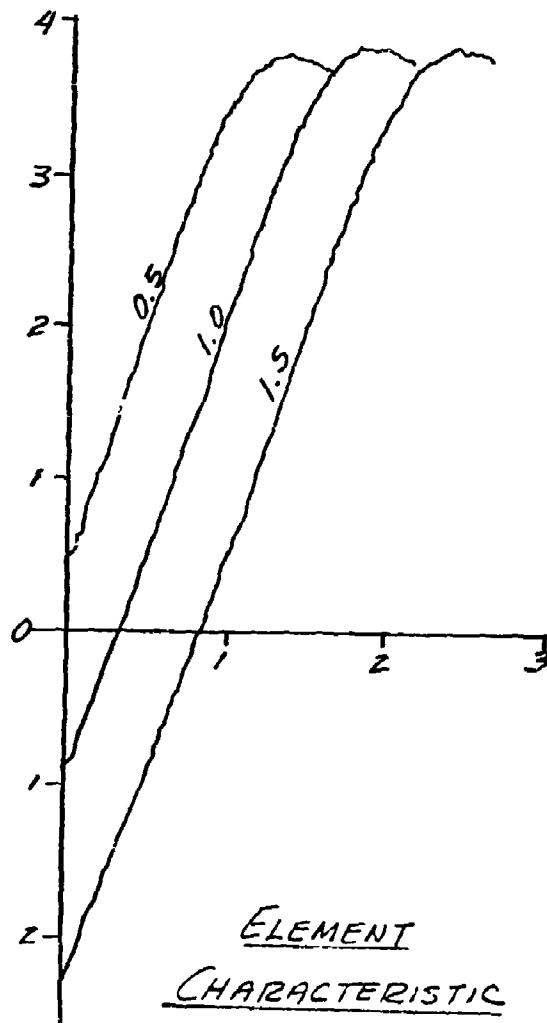Figure 1. Element Input/Output Pressure Characteristics
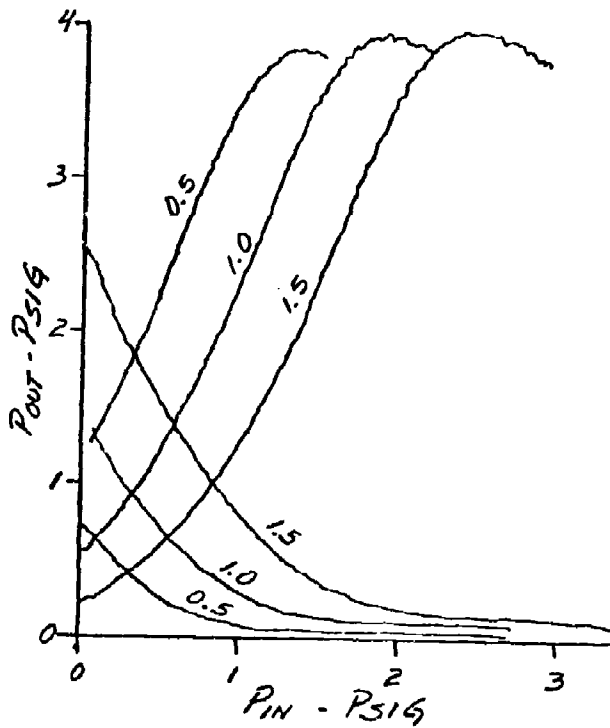
228

ELEMENT No. 3126-362-C-F

BIAS   18.0
20.5   20.7
                   L
Pᵣ   O
20.9   A
                   D
20.8   20.5
CONTROL   18.5

BIAS LEVELS INDICATED IN PSIG

ELEMENT

CHARACTERISTIC

229

3062Z

APPENDIX II

APPLICATION OF THERMISTORS
AS PERFORMANCE GAUGES
FOR FLUIDIC ELEMENTS
(TM-132)

APPLICATION OF THERMISTORS
AS PERFORMANCE GAUGES
FOR FLUIDIC ELEMENTS

AF 33(615)-5296

by

Dr. W. H. Walston, Jr.

Bowles Engineering Corporation
9347 Fraser Street
Silver Spring, Maryland 20910

Preceding Page Blank

TABLE OF CONTENTS

1.0 INTRODUCTION

An effective and inexpensive technique for determining the level of performance of Fluidic elements and circuits is desirable. In applications, such as boiler control systems, where units are operating continuously and break down is serious; a test which could indicate the impending failure of an element would be invaluable   In other applications, such as missile control systems, which are one-shot occurrences, the failure of one element often means failure of one phase of the mission or in some instances, of the entire mission. In such cases, it is mandatory to be able to quickly test the system operation just prior to launch. Such tests should indicate if any units are not performing properly and should detect the malfunctioning element so that it can be replaced as quickly as possible.

Since the performance of Fluidic elements is dependent upon pressure, any acceptable failure detection system must give an indication of the pressures at certain critical points. This can be accomplished either by measuring the pressure directly with pressure transducers or by measuring another variable such as temperature which can be related to pressure. In many cases, the first approach cannot be utilized due to space limitations. The expense of several permanently installed pressure transducers is also prohibitive in some instances. Thus it becomes necessary to accomplish pressure measurement by indirect means.

Thermistors offer much promise in this direction, but as will be seen in subsequent discussion, considerable analysis and development must be accomplished before a failure detection system based on temperature measurements alone becomes practical. Thermistors are inexpensive, space-saving, and relatively maintenance free. For these reasons they are ideal sensors for permanent installation in Fluidic circuits. They can

be installed and then used when necessary without elaborate preparation. Proper interpretation of the temperature readings indicates the pressure variation and thus the level at which the unit is performing. The degree of difficulty in properly interpreting the data increases as the number of variables such as stagnation temperature, ambient temperature, supply pressure, etc. increases. By consideration of the allowable variation in these variables, much useful information can be determined from the thermistor readouts.

Other than the difficulty associated with interpretation, the only other disadvantage of using thermistors is the time delay necessary to heat the thermal mass of the thermistor. This will be a problem only in dynamic applications where the change in pressure and/or temperature is rapid.

2.0 THEORY

Consider a converging nozzle fed by a constant area duct which is attached to a reservoir. Flow will be considered steady-state and one-dimensional. This appears schematically as:

Stagnation
Conditions

$V_o = 0$

T_o

p_o

ρ_o

V_1

T_1

A_1

V_2

T_2

A_2

Ambient conditions, T_a , ρ_a
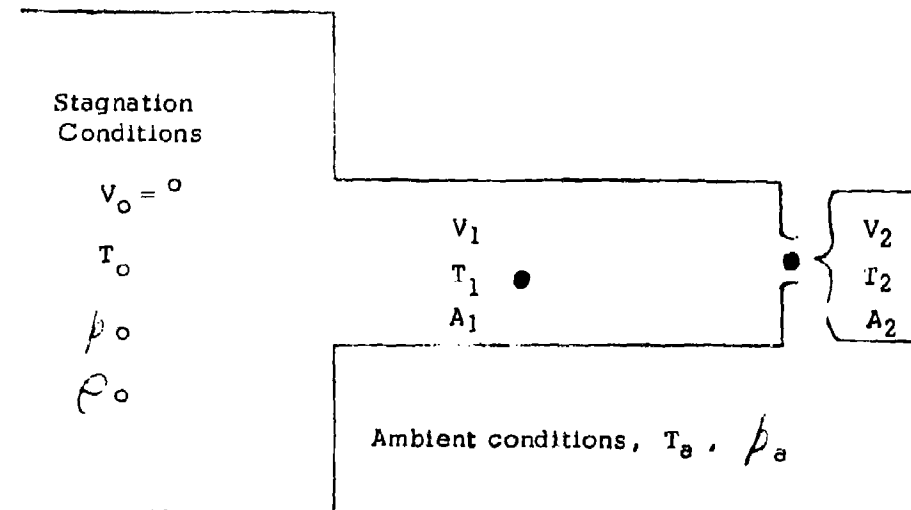
Thermistors may be located in the reservoir, in the line, at the nozzle exit, and in the ambient surroundings. Thermistors located in the reservoir and in the surroundings will give the temperatures directly. Those situated in the line and at the nozzle exit will not indicate T_1 and T_2 , but rather temperatures which are proportional to T_1 and T_2. This is due to the fact that the air is in motion at these locations. The actual indicated temperature will also be dependent upon the thermistor mounting. In many applications, the cross-sectional area of the line is so much larger than the nozzle throat area that the line conditions may be considered as stagnation conditions due to the low velocity.

237

Assume a perfect gas, air with $k = 1.4$.

$$p = \rho RT \qquad (1)$$

Assume isentropic flow.

$$\frac{T_1}{T_0} = \left(\frac{p_1}{p_0}\right)^{2/7} \qquad (2)$$

$$\frac{T_2}{T_0} = \left(\frac{p_2}{p_0}\right)^{2/7} \qquad (3)$$

$$\frac{T_2}{T_1} = \left(\frac{p_2}{p_1}\right)^{2/7} \qquad (4)$$

Events of interest are those which will result in a change in the various temperatures, in particular the temperature at the nozzle exit, T_2. Variations in T_2 will be picked up by the thermistor and, it is hoped, will give an indication of any impending malfunction or perhaps determine the cause of an existing malfunction.

The following events will result in a change in T_2:

      (1)   Change in T_0

      (2)   Change in p_0

      (3)   Change in A_2

      (4)   Change in T_a

Consider now each of these possibilities separately.

Case (1) T_0 change

$$T_2 = T_0 \left(\frac{p_2}{p_0} \right)^{2/7}$$

It is assumed here and in all subsequent calculations that the nozzle
flow is continuous and subsonic. This will result in the exit pressure
being equal to the ambient pressure for a nozzle exhausting into the
ambient surroundings. The variation of T_2 with changes in stagnation
temperature for various values of stagnation pressure is shown in Figure
1. It is assumed that the ambient pressure is 14.7 psia.

Case (2) p_0 change

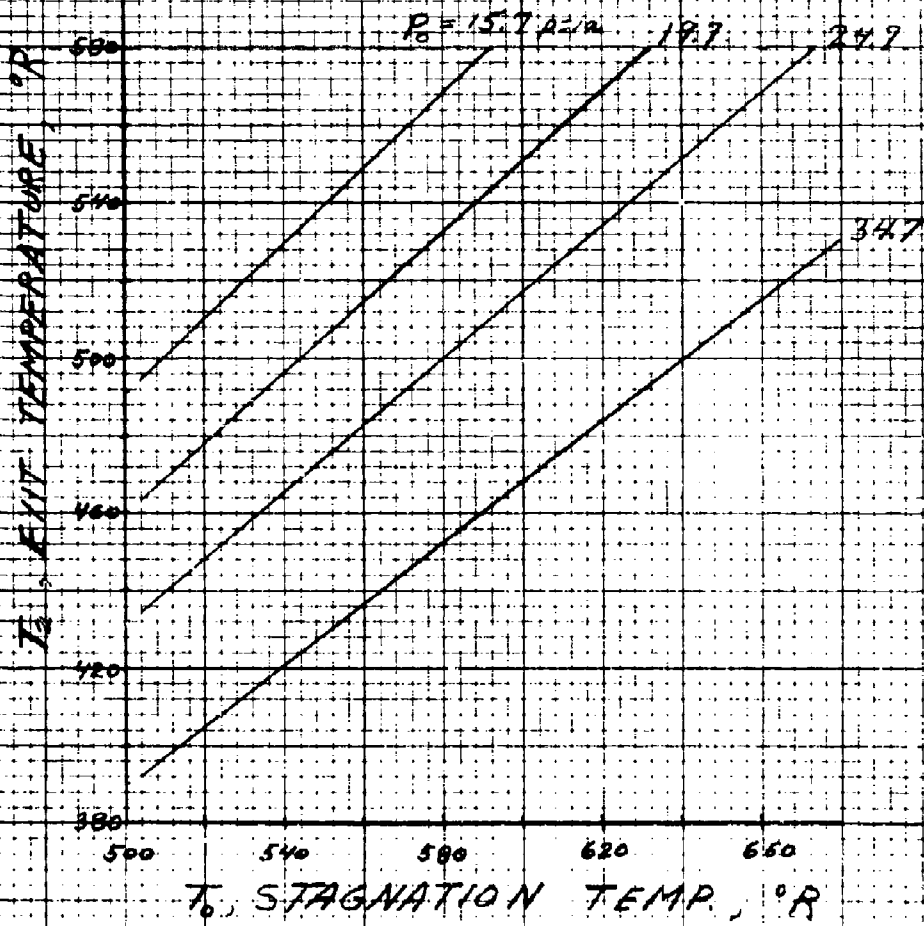$$T_2 = T_0 \left(\frac{p_2}{p_0} \right)^{2/7}$$

This variation is shown in Figure 2.

Case (3) A_2 change

This is of interest because nozzle contamination will result in a decrease
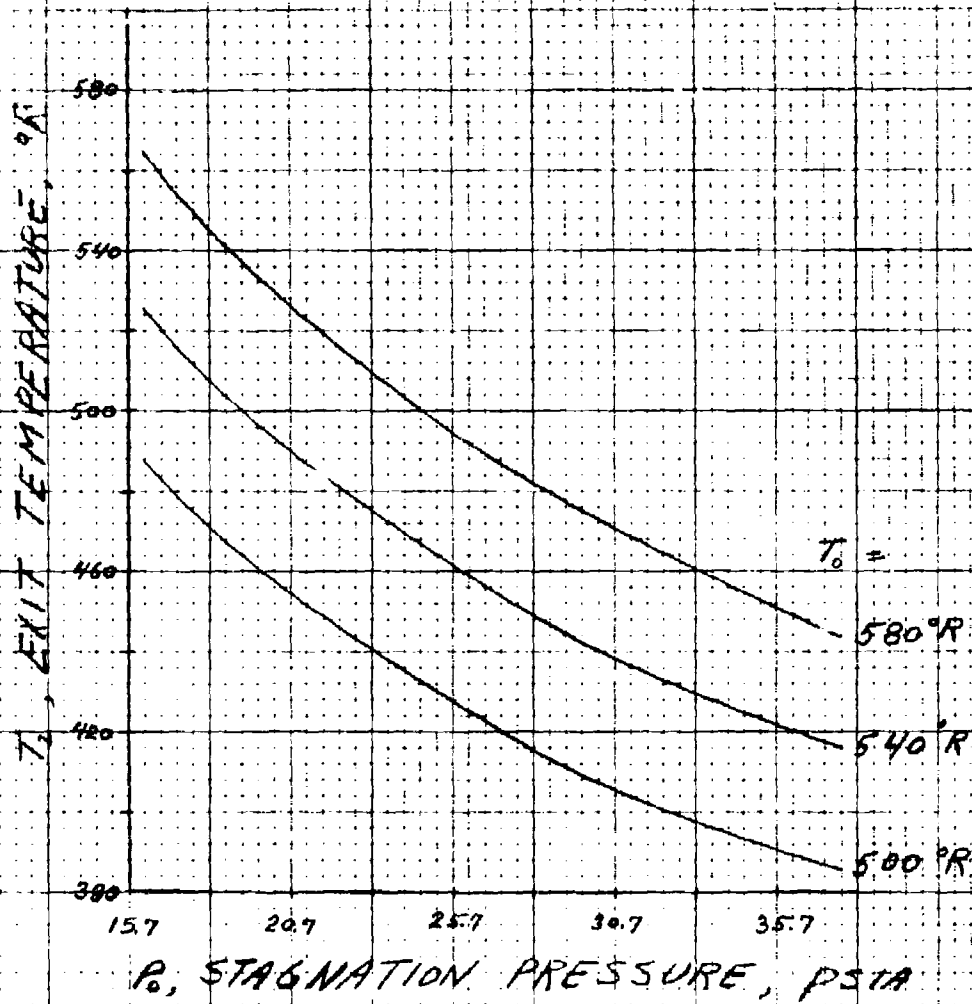in A_2. The relationship will be derived in terms of the pertinent variables.

Continuity equation:

$$\rho_1 V_1 A_1 = \rho_2 V_2 A_2 \tag{5}$$

239

TEMPERATURE VARIATION FOR
CHANGES IN T_0

FIGURE 1

240

TEMPERATURE VARIATION FOR
CHANGES IN P_0

FIGURE 2

Steady flow energy equations:

$$V_1^2 = 2 C_p (T_o - T_1) \tag{6}$$

$$V_2^2 = 2 C_p (T_o - T_2) \tag{7}$$

From continuity

$$V_1 = \left(\frac{\rho_2 \, A_2}{\rho_1 \, A_1} \right) V_2$$

Substituting into equation (6)

$$\left(\frac{\rho_2 \, A_2}{\rho_1 \, A_1} \right)^2 V_2^2 = 2 C_p (T_o - T_1)$$

or

$$V_2^2 = 2 C_p \left(\frac{\rho_1 \, A_1}{\rho_2 \, A_2} \right)^2 (T_o - T_1) \tag{8}$$

Equating the expressions for the exit velocity

$$(T_o - T_2) = \left(\frac{\rho_1 \, A_1}{\rho_2 \, A_2} \right)^2 (T_o - T_1)$$

which yields

$$\frac{T_o - T_2}{T_o - T_1} = \left(\frac{\rho_1 \, A_1}{\rho_2 \, A_2} \right)^2 \tag{9}$$

The density may be eliminated by use of the equation of state

$$\rho = \frac{p}{RT}$$

242

giving

$$\frac{T_o - T_2}{T_o - T_1} = (\frac{\rho_1 T_2}{\rho_2 T_1})^2 \; (\frac{A_1}{A_2})^2 \qquad (10)$$

The pressure may be eliminated by use of the isentropic flow assumption

$$\rho_1 = (\frac{T_1}{T_2})^{7/2} \rho_2 \qquad (11)$$

giving

$$\frac{T_o - T_2}{T_o - T_1} = (\frac{T_1}{T_2})^5 \; (\frac{A_1}{A_2})^2 \qquad (12)$$

which is the desired equation relating temperature changes to area changes. It is necessary to know the stagnation temperature in order to apply this equation. This can be determined by locating a thermistor in the reservoir. Some typical relationships are shown in Figures 3, 4, and 5.

Case (4) T_a change

The manner in which changes in the ambient temperature affects the thermistor readings (other than causing changes in stagnation temperature) will depend upon the type of mounting and on the material of which the circuit is fabricated. Consider that the thermistor is mounted in the channel wall and is flush with the surface.

243

$T_0 = 520\,°R$

$T_1 = 519\,°R$

$518\,°R$

$510\,°R$

$\dfrac{A_1}{A_2}$
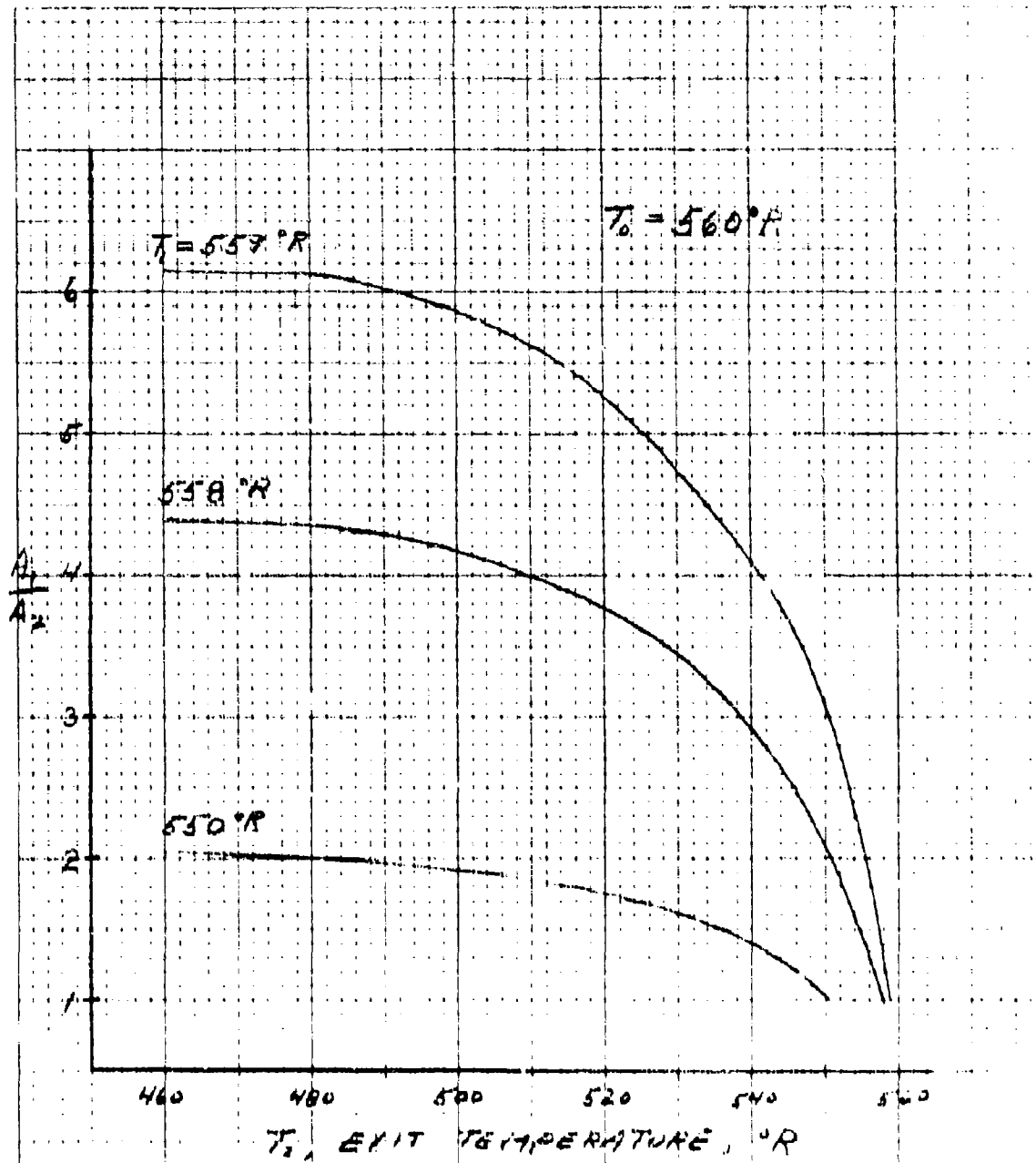
T_2, EXIT TEMPERATURE, °R
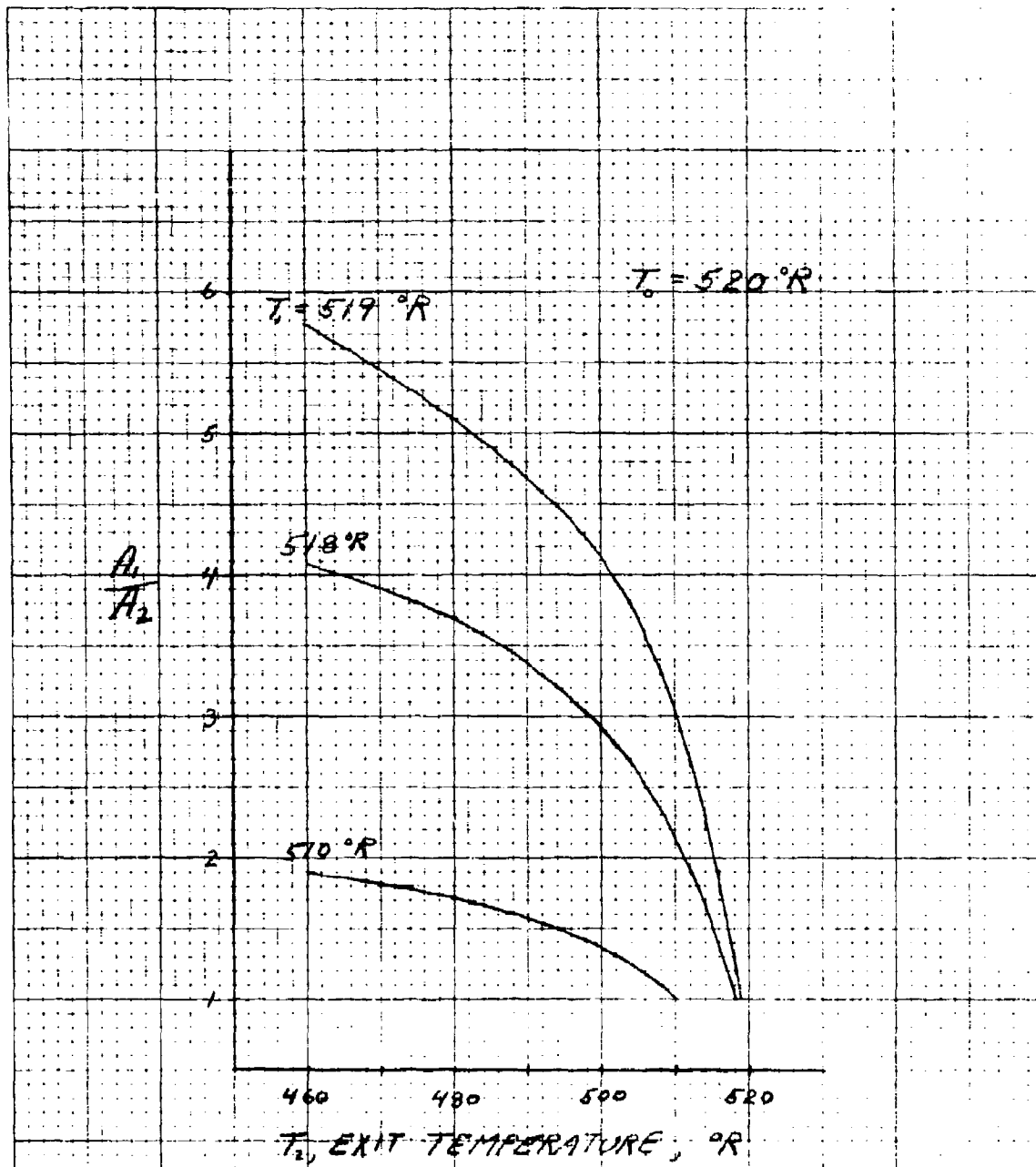
TEMPERATURE VARIATION FOR
AREA CHANGE
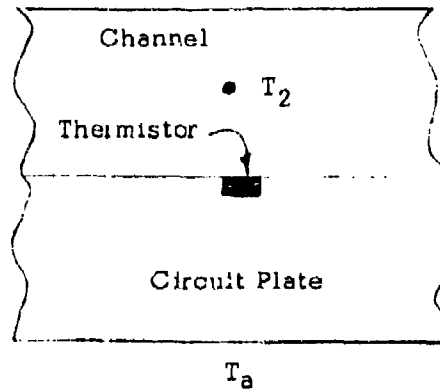FIGURE 3
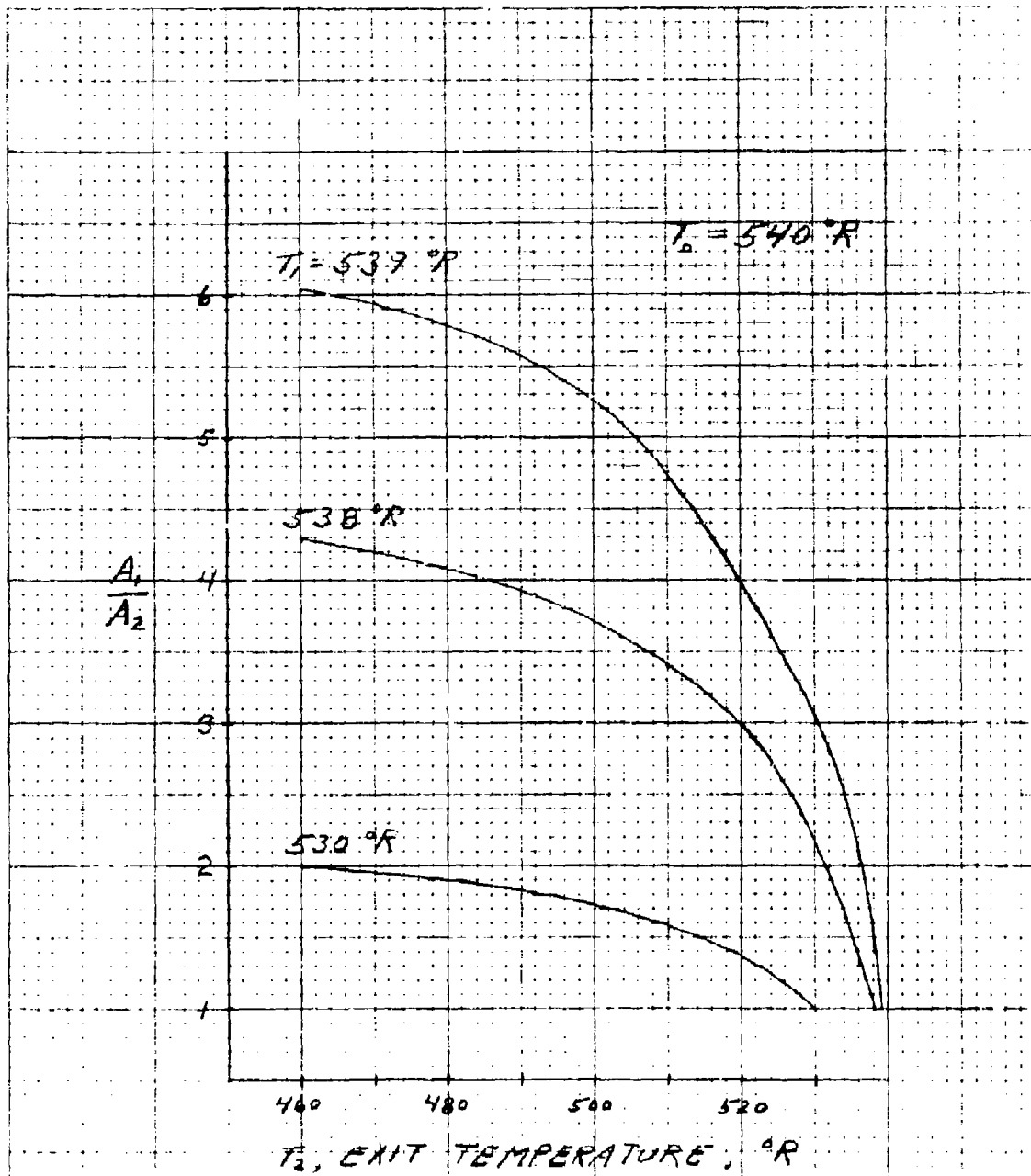
TEMPERATURE VARIATION FOR AREA CHANGE

FIGURE 4

245

TEMPERATURE VARIATION FOR
AREA CHANGE

FIGURE 5

Schematically, w have

T_2 is now the isentropic free-stream temperature. The thermistor does not measure this temperature but instead measures a temperature, T_3. T_3 is also not the stagnation temperature because it is not decelerated isentropically due to boundary layer effects and other irreversible effects. T_3 is also influenced by the ambient temperature T_a since the circuit plate material is a heat conductor. The accurate analytical determination of T_3 in terms of the other temperatures is a difficult task.

The problem would be simplified considerably if the wall were considered adiabatic, i.e., either an insulated wall or $T_a = T_3$. Then the temperature actually measured by the thermistor would be equal to the adiabatic wall temperature, T_{aw}.

$$T_3 = T_{aw}$$

This is a well-defined temperature and is expressed as

$$T_{aw} = T_2 + R_f (T_o - T_2) \tag{13}$$

where

$$R_f = \text{recovery factor}$$

This recovery factor has been determined experimentally for many cases and analytically for several specific conditions. This is discussed in some length in Heat Transfer by Giedt, p.199. Typical values are from 0.80 to 0.95. R_f may be expressed as

$$R_f = \frac{T_3 - T_2}{T_o - T_2} \tag{14}$$

In general, the circuit plate is not insulated and $T_a \neq T_3$. Therefore, the wall is not adiabatic and T_3 becomes a function of T_a as well.

$$T_3 = T_3 (T_o, T_2, T_a) \tag{15}$$

The recovery factor can be experimentally determined for non-adiabatic cases, but it too must then be considered a function of the ambient temperature. Unfortunately, an analytical expression for R_f is not available. Typical experimental data is given in Table 1, and compared to actual measurements in Figure 6. This is not intended to show a valid technique for determining R_f in general, but only that for given ambient conditions a constant value of R_f is valid over the range of temperature variations.

TABLE 1.

$$T_a = 74.3^\circ F \qquad T_o = 75^\circ F$$

$\frac{p}{p_o}$	T_1	T_3	T_2	(calculated theoretically for isentropic flow)
0 psig	74.3°F	75.0°F	--	
5	74.3	73.5	35°F	
10	74.3	71.5	4°	
15	74.3	70.5	-23°	
20	74.3	70.0	-42°	
25	74.3	69.0	-58°	
30	74.3	68.5	-72°	

Based on this data, a recovery factor of 0.95 to 0.96 is determined. Figure 6 shows these results.
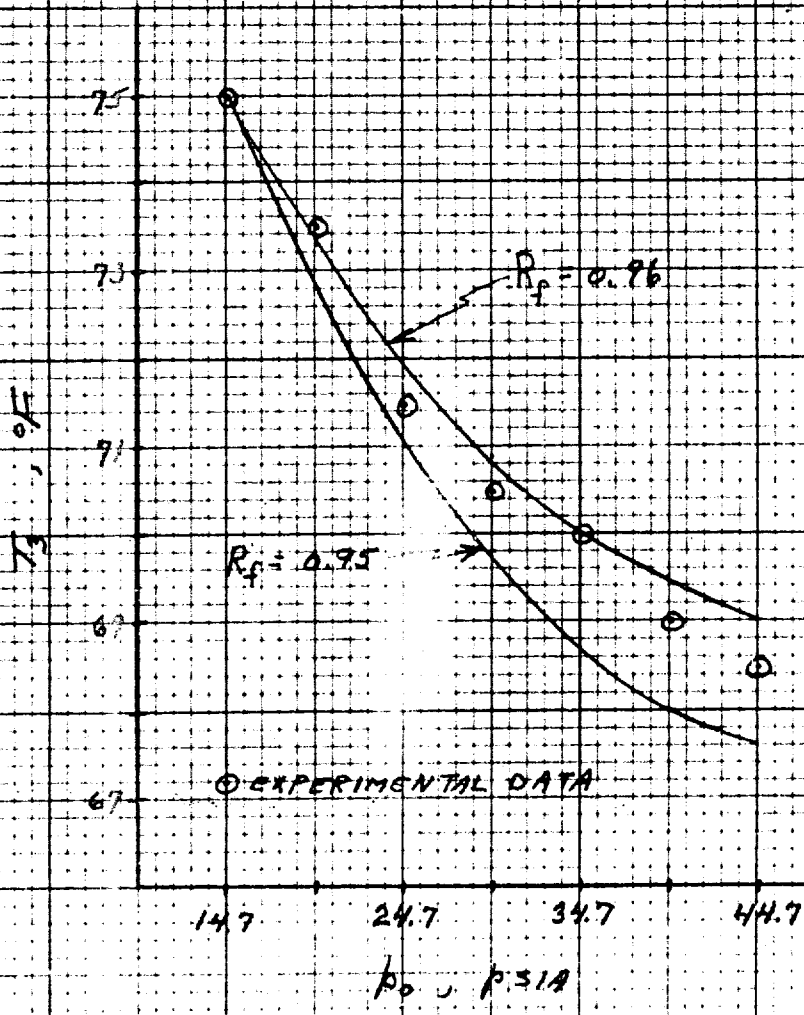
RECOVERY FACTOR

FIGURE 6

250

3.0 APPLICATIONS

Applications of the preceding theory to two specific problems is considered: (1) a boiler control system and (2) a missile control system. Typical values are chosen for the pressures and temperatures in order to obtain some indication of the order of magnitude of the changes which may be expected.

3.1 Boiler Control System

Both analog and digital elements are present in the boiler control system under consideration. Since the pressure required is significantly different for each, they will be discussed separately.

3.1.1 Analog Element

In the unit tested the nominal supply pressure is 10 psig. The element will function properly for variations of $\pm$ 3%, i.e., $\pm$ 0.3 psi. If the variation of supply pressure exceeds 3% the element malfunctions. We are interested then in determining variations in supply pressure of less than 3% which will give an indication of impending failure. The ambient temperature can possibly vary from $35^{\circ}F$ to $135^{\circ}F$ and the supply temperature should vary over approximately the same range.

The maximum acceptable variation in supply pressure gives a maximum variation of only $\pm$ $0.1^{\circ}F$ for the thermistor mounted in the wall of the nozzle (T_3). This is equivalent to a voltage output of $\pm$ 0.21 mv by the thermistor. The sensitivity of the thermistor offers no problem here, but the magnitude of the temperature change makes a proper interpretation of change

in supply pressure difficult if not impossible. The reason for this is the much larger variation in T_3 which is to be expected from changes in the ambient and supply temperatures. For example, a change of 10 degrees in the supply temperatures would cause a change of several degrees in T_3 (the actual change would depend on the pressure ratios). This change would overwhelm the small change due to supply pressure variation.

It thus appears at this time that this is not the optimum approach. Further investigation of the use of more than one thermistor in a bridge network offers the possibility of eliminating some of this difficulty. If other means of detecting P_o variations are too expensive or consume too much space, this approach may yet be fruitful. In other applications where the acceptable variation in supply is greater and/or the variation in ambient temperature is not so large, the above difficulties may be lessened considerably.

3.1.2 Digital Element

The nominal supply pressure is 1.0 psig with a minimum of 0.5 psig and a maximum of 1.25 psig. This is a rather large percentage variation, but a small variation in terms of psi.

Difficulties similar to those for the analog element are encountered. The variation in T_3 due to changes in supply pressure are much smaller than the variation which can be expected from ambient changes. The discussion for the analog element is thus also appropriate for the digital unit.

3.2   Missile Control System

The missile control system under consideration would operate from a supply manifold at 1.5 psig with a $\pm$ 5% variation. This would lead to small changes in T_3 similar to those discussed for the boiler control system. These changes would be undetectable when compared to temperature changes due to supply temperature variation.

4.0 CONCLUSIONS

Thermistors are proposed as a means for detecting the impending failure of a Fluidic element. In most cases, this failure is brought on by changes in certain pressures throughout the system. Thermistors measure temperatures which are functions of pressures, among other variables. If the temperature change due to pressure is comparable to or greater than the change due to variations in other parameters such as ambient temperature, then the thermistor is a useful detector. Unfortunately, for the cases considered in this report, namely, a boiler control system and a missile control system, this is not the case. Variations in temperature are due mainly to other temperature changes rather than supply pressure variations. The use of thermistors does not appear at this time to be a good method for determining the impending failure of these systems due to supply pressure changes.

It is believed, however, that further investigation of bridge networks utilizing thermistors can compensate for some of these difficulties. This investigation is recommended if other approaches prove to have their problems also.

In applications where the allowable variation in supply pressure is greater and for the variation in ambient temperature is less, thermistors should be considered as possible sensors for use in failure detection.

APPENDIX III

COMPATIBILITY OF SENSORS WITH
PACKAGING APPROACHES AND EFFECT
OF ENVIRONMENT ON SENSORS
(TM-147)

COMPATIBILITY OF SENSORS WITH
PACKAGING APPROACHES AND EFFECT
OF ENVIRONMENT ON SENSORS

AF 33(615)-5296

Dr. William H. Walston, Jr.
Edwin U. Sowers, III

TABLE OF CONTENTS

TABLE OF CONTENTS

1.0 INTRODUCTION

Bowles Engineering Corporation has engaged in a program to investigate sensors and instrumentation techniques which may be used to check out the state of performance of Fluidic Systems. The comparative evaluation of a group of candidate sensors includes consideration of the compatibility of the sensors with typical circuit packaging concepts, and consideration of the effects of environment on the sensors. The results of a study into these two areas of concern are summarized by this Technical Memorandum.

The candidate sensing techniques are as follows:

- o Microphone
- o Accelerometer
- o Anemometer
- o Miniaturized Pressure Transducers
- o Thermistors
- o Crystals
- o Infra Red Thermometer

The two types of packaging concepts considered for instrumentation will be described. Each sensor will be defined and the parameter sensed will be stated. Means of mounting each sensor to Fluidic circuitry will be presented. The compatibility of the candidate sensors with the two circuit packaging concepts will be discussed.

The sensitivity of each of the sensors to changes in the following ambient condition will be considered:

- o Temperature
- o Pressure
- o Humidity
- o Vibration
- o Acoustic Energy
- o Electromagnetic Energy

Preceding Page Blank

261

Conclusions will be presented as to the applicability of each of the sensors to instrumentation of integrated, packaged circuitry. Conclusions drawn from the study will be summarized.

2.0 PACKAGING CONCEPTS

The two most common concepts of packaging two-dimensional Fluidic circuitry are the modular concept and the stacked circuit concept. These two concepts are described in the following.

2.1 Modular Packaging Concept

The modular concept of packaging circuitry, with one or two circuit plates enclosed within a module, is highly desirable for a wide range of Fluidic control applications. Each module commonly houses one or more functional groupings of elements. The modules may be rack-mounted and appropriately interconnected. Adjustment and checking of each module may be accomplished independently, either prior to installation or when installed in a rack-mounted assembly. Individual faulty modules may be removed and repaired or replaced.

The module consists essentially of a circuit plate attached to one or both sides of a manifold, with the manifold supplying operating fluid to the circuit elements, providing element interconnection chanelling, and housing circuitry adjustment means. A protective cover is fitted over each of the circuit plates. Vented elements exhaust into the area between the circuit plate and the cover, through a porous filter in the cover to atmosphere. Figure 1 presents a simplified drawing of a typical circuit module.

There exists a significant space between the circuit plate and the cover. This space provides an ideal region for the location of sensors, particularly those sensors which offer the possibility of individually indicating the state of a functional grouping of elements.

2.2 Stacked Packaging Concept

An alternate approach to packaging is the stacking of multiple layers of two-dimensional circuitry, forming a more or less (monolithic) structure. The stringent dimensional and weight limitations of certain applications, as in a missile control system, require the high circuitry density afforded by this packaging approach.

Figure 2 shows a simplified sketch depicting the stacked packaging concept. Circuit plates, supply and vent plates, and channel interconnection plates are stacked in multiple layers with connections between plates made by means of internal transfer holes. A large number of functional circuit groupings are enclosed within the structure.

Porous Cover
Filter

Protective Cover

Circuit Plate

Circuit Sealing Plate

Supply, Input and
Output Connections

Circuit Plate

Element Vent

Level of Elements
and Interconnecting
Channels

Manifold

Interconnection
Manifold to
Circuit Plate

FIGURE 1. MODULAR CIRCUIT PACKAGE

Main Supply Passage

Elements and Interconnecting Channels

Transfer Hole, Manifold to Circuit Plate

Transfer Hole, Thru Manifold

Manifold Cover Plate

Vent

Vent Channel

Circuit Plate

Circuit Cover Plate

Manifold

Circuit Plate

Circuit Plate

Manifold
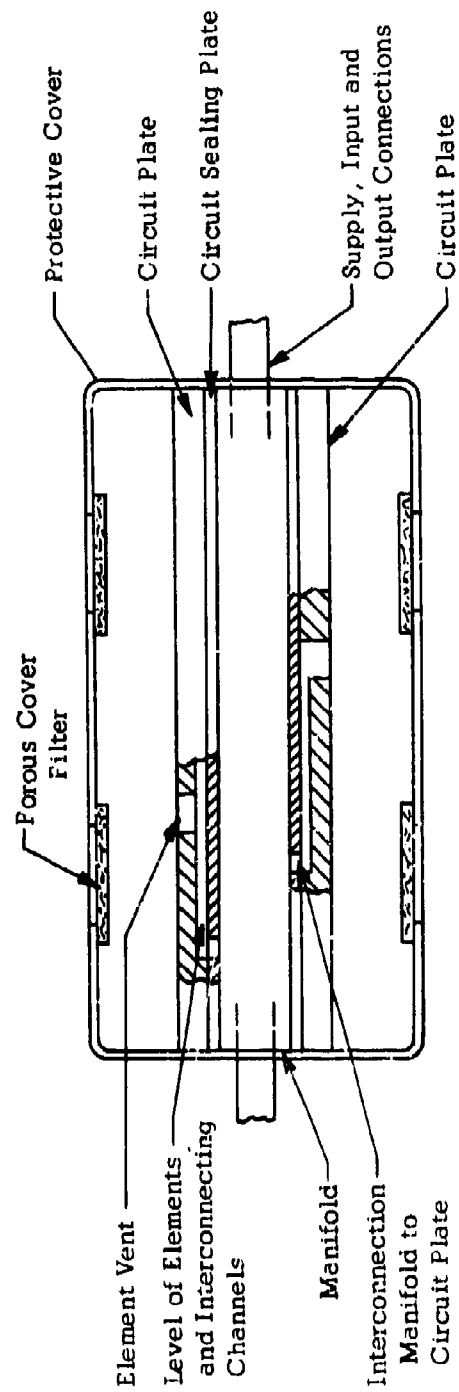
Circuit Plate
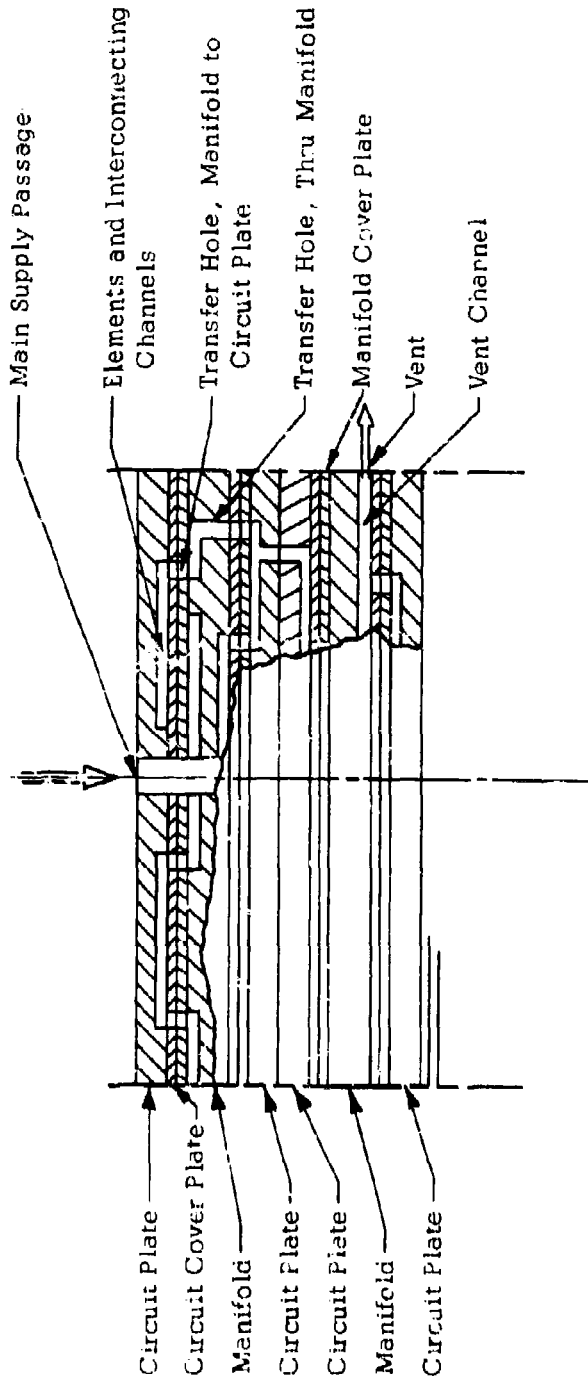
FIGURE 2. STACKED CIRCUIT PACKAGE

30374

Instrumentation of this type of a package is more difficult than in the case of a modularized approach. Available space for the mounting of instrumentation is limited. Vent areas are small. In most cases, the elements of a functional grouping, or subcircuit, do not vent into a common vent chamber.

It is expected that the mounting of sensors and the isolation and checkout of individual subcircuits will be more difficult in the case of stacked circuit packaging.

3.0   COMPATIBILITY OF SENSORS WITH CIRCUIT PACKAGE AND ENVIRONMENT

In the following, the compatibility of each of the considered sensors with
the two packaging concepts and with environmental conditions will be
individually investigated.

3.1   Microphone

The microphone under consideration is a Massa M-213 sound pressure
microphone, Massa Division Cohu Electronics, Inc., Hingham, Mass.
The size of this miniature piezoelectric type microphone is nominally
1/4" diameter x 5/8" length. It may be used in monitoring the acoustic
disturbances generated by a functioning flueric circuit.

3.1.1   Mounting Means and Package Compatibility

It is hoped that this sensor may be used to evaluate the operational
state of a grouping of Fluidic elements and consequently, may be
located at a position somewhat removed from the vented side of an
integrated circuit plate. When instrumenting a modularized circuitry
package, the microphone may be mounted to the module cover as
shown by Figure 3. The microphone, as shown, is bonded to a
mounting flange by means of a resilient potting material, such as
an RTV silicone rubber compound, to minimize transmission of high
frequency vibrations from the module cover to the microphone. This
mounting means allows for easy coupling and decoupling of the cable
assembly to the microphone external to the module cover. An
alternate attachment point of the microphone, using the same mounting
approach, is in the sides of the module cover. This would provide
improved accessibility of the coupling point where modules are
rack-mounted in close proximity.

The Massa microphone is not as well suited to a stacked circuit
arrangement as to the modularized package arrangement. The
considered objective of a microphone is to detect, by means of
acoustic disturbances, causes of malfunction within some group
of elements. It is considered that this can most satisfactorily be
accomplished where a group of elements vent into a common vent
region, with acoustic disturbances passing also through the vents
of each element into the vent region. By placing a microphone in
this region, as with the above described modular concept, the
single microphone may detect acoustic disturbances from each of a
group of elements. In the case of stacked circuitry, constrictions
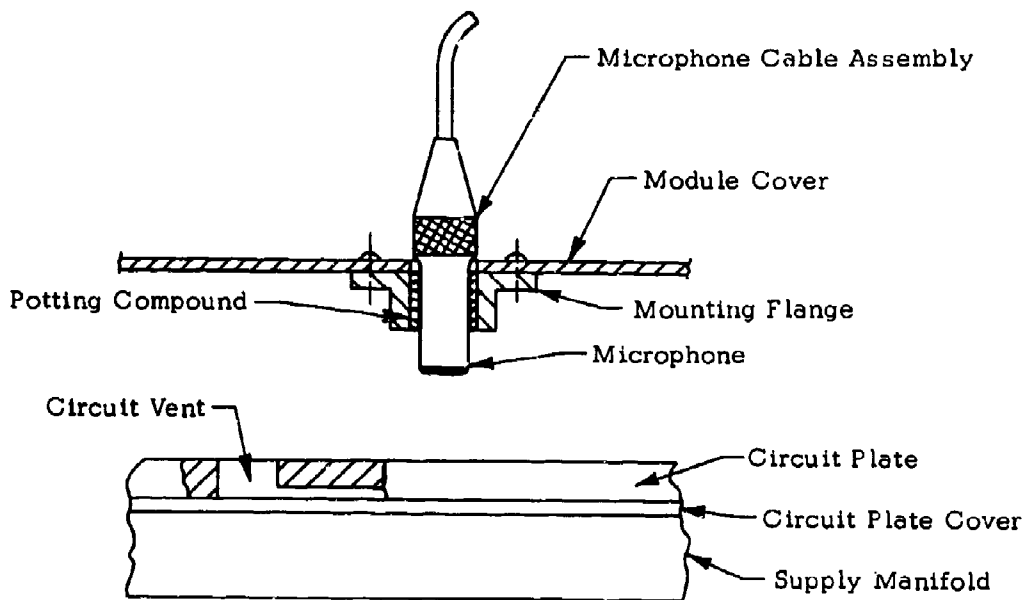impose! on element orientation and venting means by space

267

FIGURE 3.   MICROPHONE MOUNTING MEANS,
            MODULARIZED CIRCUIT PACKAGE

268

30375

limitations, frequently leads to an arrangement where groups of
elements do not vent into a common chamber into which a micro-
phone may be mounted. In such cases, the microphone does not
appear highly compatible with the stacked packaging concept.
Where space considerations do permit the inclusion of a common
and accessible vent region, it is probable that a suitable means
of incorporating the microphone may be established.

3.1.2   Environmental Effects

The permissible operating temperature range of the microphone is
-40° F to 160° F, the upper limit being set by the cements used
in the construction of the unit. However, high transient tempera-
tures of short duration will not damage the units. The active
element is ADP (ammonium dihydrogen phosphate), a piezo-
electric crystal. The upper limit of this crystal is approximately
200° F.

Temperature variation causes some changes in the piezoelectric
constants of the crystals as well as in the mounting adhesives.
If highly accurate measurements are required, a calibration curve
may possibly be needed for each microphone.

Environmental pressure changes have no effect on the operation of
the microphone.

The Massa microphone is sealed so that humidity is not a problem
in operation. The crystal itself has no lower humidity limit, but
it does pick up moisture from the ambient at humidities above 93
percent. This is, of course, prevented by the sealing of the
instrument.

Operation in the presence of a magnetic field does not affect the
performance of the microphone.

Vibration of the instrument may cause problems appearing as noise
in the output. The extent of the noise depends upon the amplitude
and frequency of the impressed vibration.

3.2   Accelerometer

The accelerometer under investigation is a B & K (Bruel and Kjaer)
Instruments, Inc., Model 4333. The nominal size of the piezo-electric
type accelerometer is 0.63 inches x 0.63 inches, and its nominal weight

is 12.7 grams. It has a frequency range of 2 to 14,000 KC (±1 d!)
and an acceleration range of 0.01 to 2,000 "g" with appropriate
instrumentation. This accelerometer may be used to determine the
vibrations of an operating Fluidic circuit. These vibrations may be
excited by acoustis signals.

3.2.1 Mounting Means and Package Compatibility

The accelerometer is mounted directly on the surface of the circuit
plate for the modular type of packaging. Mounting may be
accomplished by a threaded stud supplied by the manufacturer.
Correct measurement of high frequency vibrations is dependent
on the stiffness of the mounting. A typical arrangement is shown
in Figure 4, with the accelerometer located within the circuit cover.
In some cases, the clearance between the circuit plate and the
module cover may not be sufficient to accommodate the accelerometer.
In such instances, the accelerometer may extend through a clearance
hole in the cover plate. A flexible vibration-damping sealant should
then be used to seal the gap around the accelerometer, to prevent the
entrance of external contaminants into the element vent region under
the cover plate.

The accelerometer may be mounted in a similar manner to stacked
circuitry, as shown by Figure 5. To provide access to a circuit
plate within a stack, it may be necessary to allow the accelerometer
to extend through a number of adjacent circuit plates, orienting
circuitry in the adjacent plates to permit this. Smaller accelerometers
than the B & K unit are available, the size of which are much more
suitable to stacked circuitry than the B & K accelerometer. One
typical example is the Endevco Corporation Model 2222 microminiature
accelerometer. The size of this unit is 0.25" hex. x 0.20" thick. It
may be attached by means of an appropriate rigid adhesive. This
accelerometer, while it was not evaluated during the program, appears
to offer a good potential for use with compactly stacked circuitry.

3.2.2 Environmental Effects

The operating temperature range of the B & K accelerometer is
substantial, -320° F to 500° F, and is sufficient for any contemplated
applications. Slight sensitivity changes occur with temperature
variations and must be taken into account. Individual calibration
curves are supplied for each unit, enabling the correct sensitivity
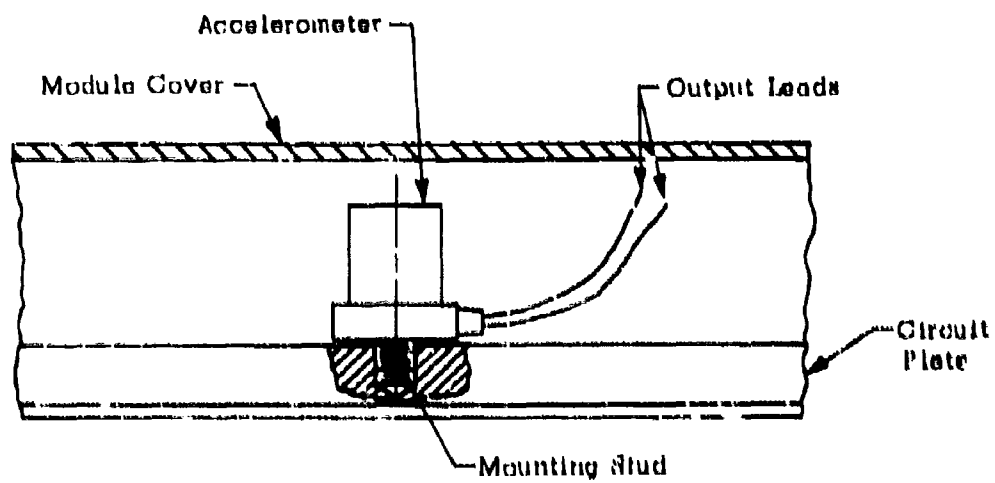to be found from these charts.

Accelerometer

Module Cover

Output Leads

Circuit Plate

Mounting Stud

FIGURE 4. ACCELEROMETER MOUNTED IN MODULAR CIRCUIT

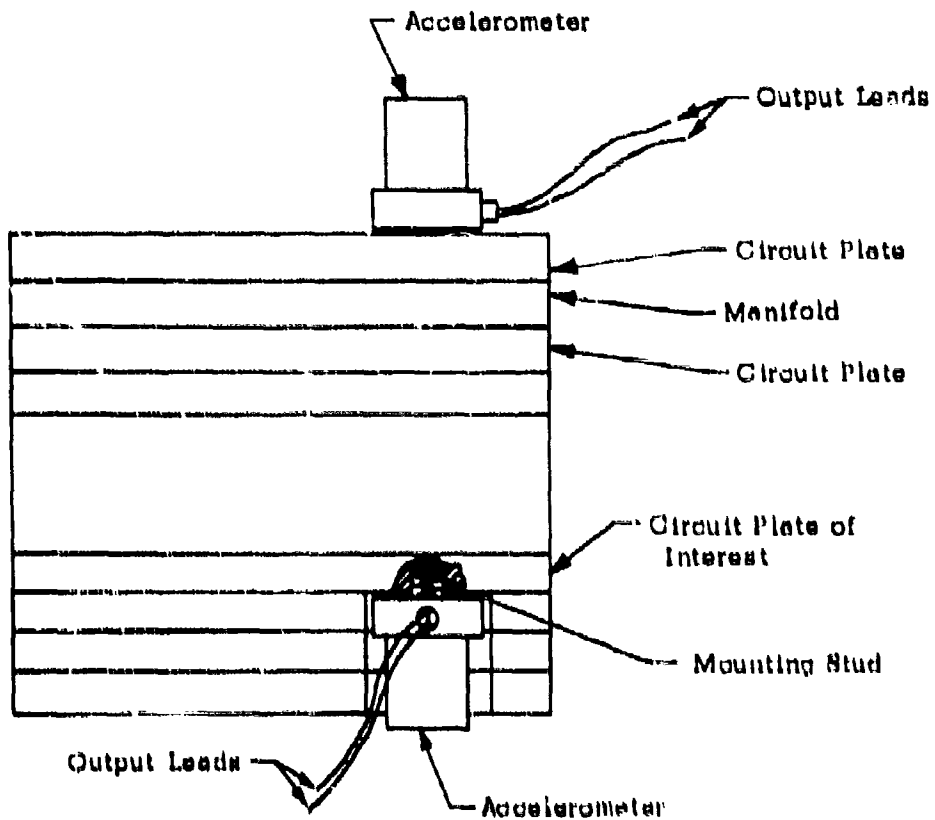FIGURE 5. POSSIBLE ACCELEROMETER MOUNTINGS FOR
STACKED CIRCUITS

272

The acoustic sensitivity of the element is 0.2 μV per μbar. This may be significant if the vibration being monitored is of small magnitude. The nominal voltage sensitivity including a calibrated connecting cable if 16 mV per "g". In some Fluidic application, it may be that the acoustic noise is significant when compared to the signal level. In such instances, some degree of acoustic isolation may be necessary.

Other possible areas of concern are electrostatic and magnetic fields. The magnetic sensitivity is 1 μV per gauss. In the applications under consideration, this is not expected to be a problem.

The unit is totally sealed so that humidity is of no concern. The ambient static pressure level has no effect, however, a varying pressure (such as a sound wave) could show up on the output as noise.

3.3 Constant Temperature Anemometer

The hot wire probe is a Disa miniature probe element 55A52. The wire material is platinum-plated tungsten approximately 0.45 mm. long and 0.005 mm. in diameter. The total length of the probe unit is 10.8 mm. and its overall diameter is 0.9 mm. Flow can be monitored in a selected region of a Fluidic element with a probe of this size.

3.3.1 Mounting Means and Package Compatibility

These miniature hot wire anemometer probes have the advantage of being smaller than most other sensors. This enables one to mount the element with less difficulty in the most suitable location. A major disadvantage of the probe is its fragility, thus requiring a mounting by which the probe can be easily replaced if damaged. An arrangement such as shown in Figure 6 offers this possibility. A suitable cement can be used for mounting the probe in the plug.

This type of mounting is especially suited for the modular package since the plug can be placed directly into the desired flow region. The leads may be taken out at any convenient location. Figure 7 depicts a typical arrangement.

The proper mounting of the probe in the stacked package is more difficult. The channel in which the measurements are needed must be accessible either directly or indirectly as shown in Figure 8, which depicts three possible mountings. In some cases, direct
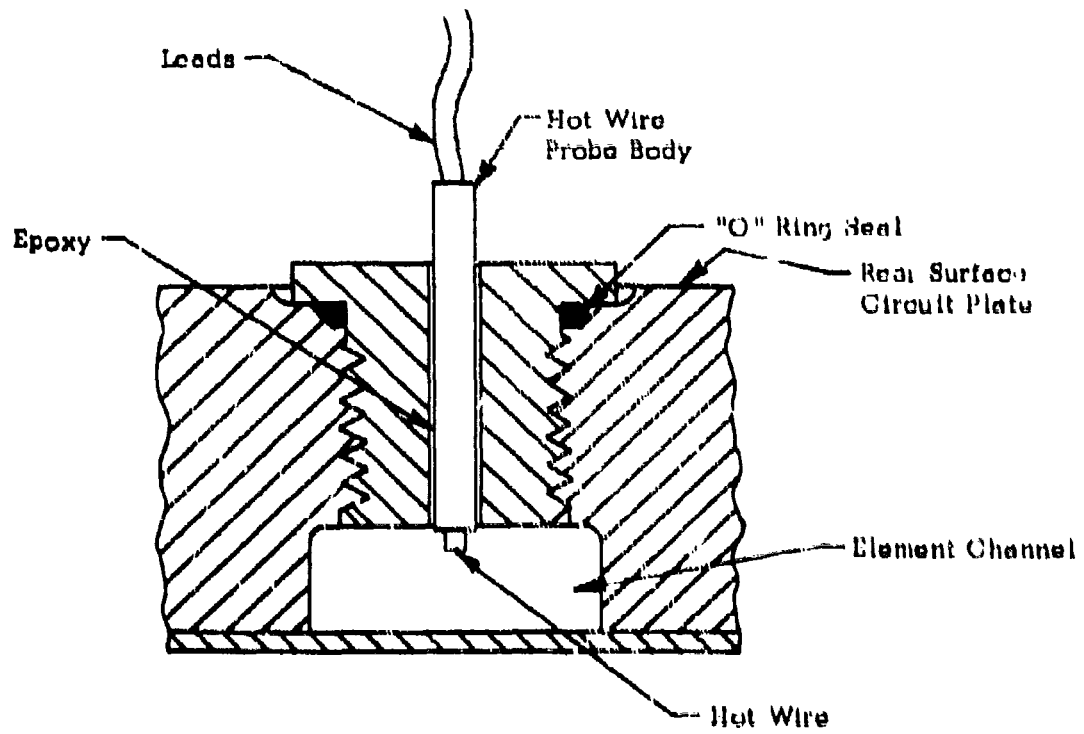
273

FIGURE 6. HOT WIRE PROBE MOUNTED IN PLUG ASSEMBLY

30378
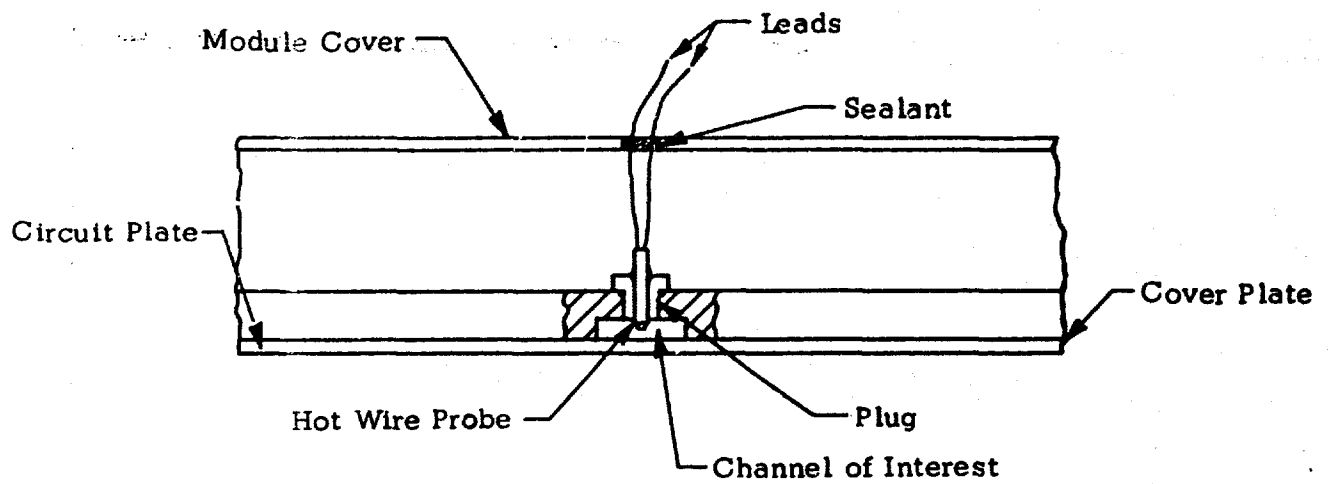
FIGURE 7.   HOT WIRE MOUNTING FOR MODULAR CIRCUIT

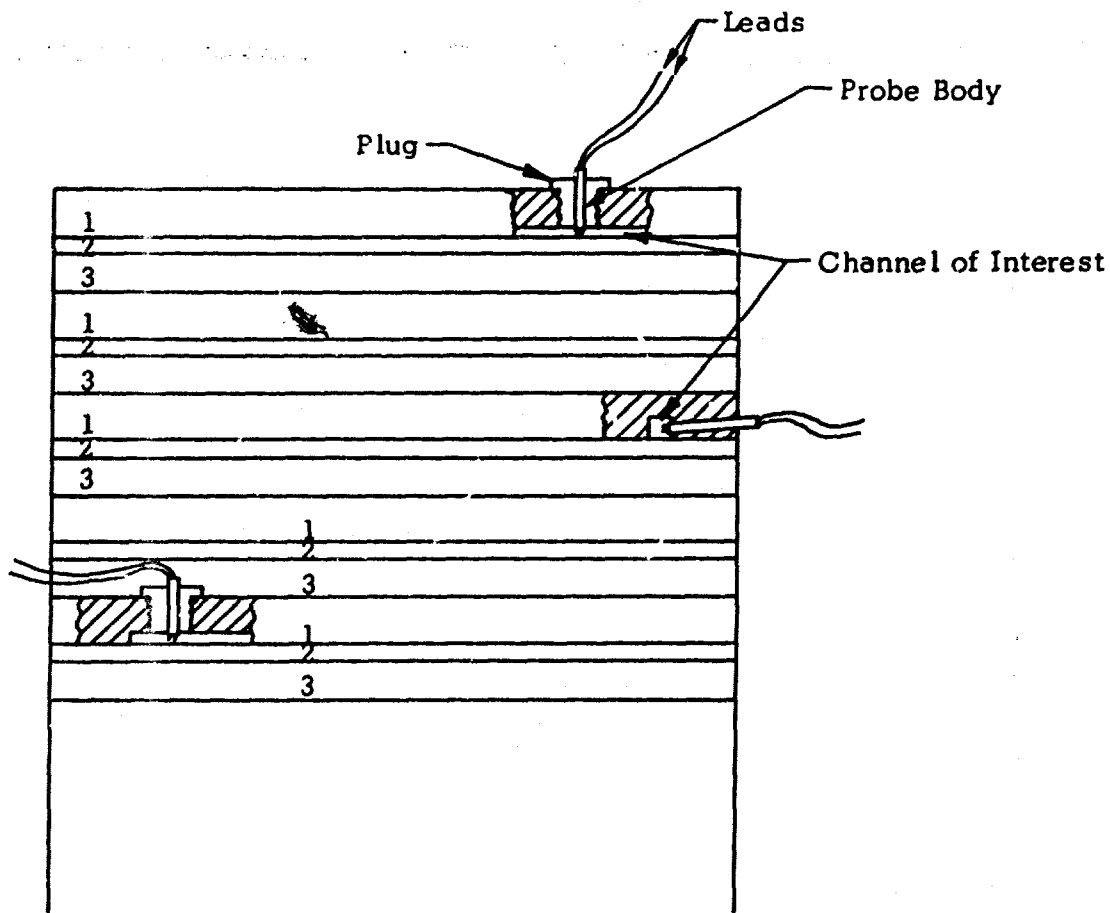1 - Circuit Plate

2 - Cover Plate

3 - Manifold

FIGURE 8. HOT WIRE MOUNTING FOR STACKED CIRCUIT

276

bonding of the probe into a hole in a circuit plate may be necessary as where mounting the probe nominally parallel to the circuit plate. If circuits are designed with the incorporation of probes in mind, it should be possible to place the channels in such a way so as to be accessible.

3.3.2 Environmental Effects

A constant temperature anemometer system maintains the resistance of the hot wire at a constant value by holding the wire temperature at a constant level. Thus, environmental temperature changes could cause changes in the wire temperature and consequently changes in the anemometer output signal.

Ambient temperature changes do not in general affect calibration of the anemometer unless the temperature differential is sufficient for heat to be conducted through the probe element to the wire itself. Changes in the stream temperature exert considerable effect on the hot wire output; less current is required to maintain the wire at a constant temperature for a given stream velocity as the stream temperature increases.

Ambient pressure changes do not influence the system. However, variations in the stream pressure do effect the anemometer output signal. For example, an increase in the static pressure of the stream increases the cooling capacity of the fluid. Therefore, for a given stream velocity the fluid exerts a larger cooling effect on the hot wire, requiring a larger current to maintain constant wire temperature.

Changes in the ambient humidity have no effect on the calibration. Increases in the humidity of the stream gas result in an increased cooling effect. The result is then similar to the pressure increase described above, i.e., an increase in current.

If the effects of temperature, pressure, and humidity changes an anemometer calibration are greater than allowable, it is expected that these effects can be minimized through use of multiple anemometers and appropriate nulling electronic circuitry. Calibration shifts are of concern in the case of analog circuitry, where the accurate detection of signal levels is necessary. In the case of digital circuitry, however, calibration shifts are not so critical. In this instance, the detection of digital changes in flow and time relationships between flow pulses are of more concern than accurate representation of flow levels.

277

The hot wire is a very sensitive element and consequently any
vibrational disturbances with sufficient amplitude to give the wire
an additional imposed velocity relative to the stream are picked up
and read out as though these are fluctuations in the stream velocity.
It is anticipated, however, that if this should be encourntered, the
fluctuation amplitudes would be small compared to the signal changes
of interest.

Acoustic noises and magnetic disturbances should not be a problem
with the anemometer.

As with any hot wire, contamination or build-up of foreign material
on the wire will, in time, change the calibration with the probe
incorporated into a plug, as per Figure 6, removal for cleaning is
facilitated.

3.4   Miniaturized Pressure Transducer

The transducer under consideration is a Scientific Advances, Inc., Model
SA-SD M-6H. It is a bi-directional differential pressure transducer which
uses a movable diaphragm and a strain gauge bridge as the active elements.
The size of the sensor is 0.25 inches diameter and 0.25 inches thick. The
sensor is well suited to flush-mounting into element channels for use in
monitoring operating pressure signals.

3.4.1   Mounting Means and Package Compatibility

The pressure transducer may be readily flush-mounted into circuit
channels as shown by Figure 9. A 1/2 inch diameter hole is bored
from the rear of the circuit plate with a flat-bottomed end mill, to a
depth where it just breaks through the bottom of the channel. The
pressure transducer is inserted into the hole until it bottoms. A
fillet of bonding material is then placed around the transducer at
the rear surface of the circuit plate. This fixes the transducer in
place and provides the required seal. A bonding material which may
be dissolved by a solvent, as may Duco cement, permits the transducer
to be removed if necessary.

The size of the sensor and the means of installation are compatible with
both the modular and the stacked circuit packaging concepts. In the
latter case, it may be necessary to arrange the circuitry in a plate
adjacent to the plate being instrumented so that the rear of the transducer
may be extended into the adjacent plate. Where using atmospheric
pressure as a reference (measuring signals in psig), the rear of the trans-
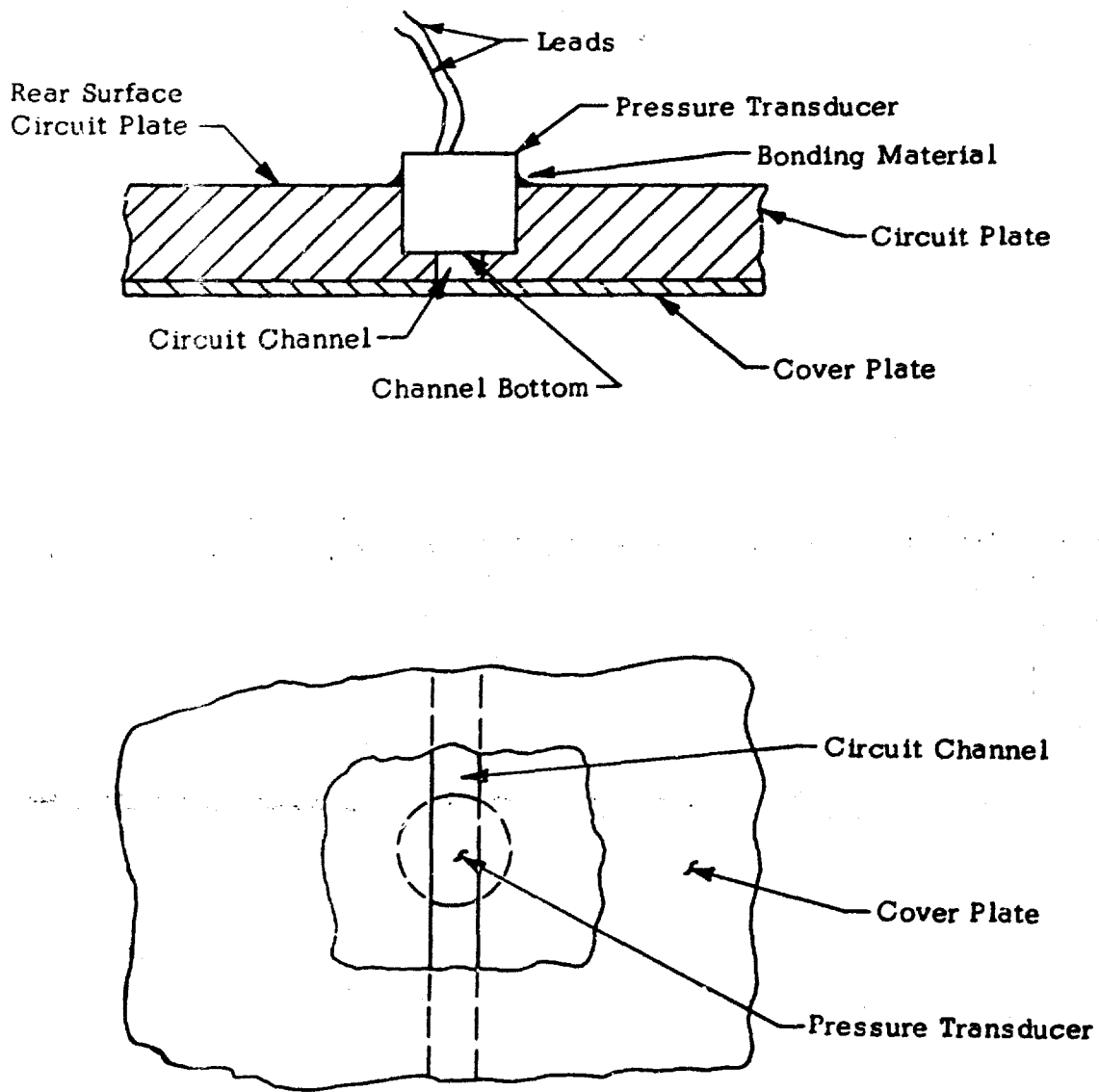ducer must be exposed to atmospheric pressure.

278

FIGURE 9. MINIATURIZED PRESSURE TRANSDUCER INSTALLATION

3.4.2 Environmental Effects

Temperature variations affect the sensitivity and zero point of the transducer. Precise information regarding each individual element is supplied with the transducers by the manufacturer. Models are available with and without temperature compensation. Typical effects for the uncompensated model are a zero shift of 0.2 per cent of full scale per °F and a sensitivity variation of 0.2 per cent of full scale per °F. The compensated model is significantly better with variations of 0.05 to 0.01 per cent of full scale per °F. Operating temperature ranges vary depending upon the specified requirements. Typical ranges are from -40°F to 150°F and from -100°F to 300°F. The model selected will depend upon the pressure level changes of interest and the environmental temperature changes encountered in specific applications.

Ambient pressure variations will not influence the reading unless of course ambient is being used as the reference pressure. Operating pressure ranges vary with requirements. Elements tested had ranges of ±2 psi and ±15 psi.

Humidity is not a problem for most applications, although the performance may be somewhat impaired if operated in a high humidity for an extended period of time.

Vibrations, acoustic disturbances, and magnetic fields have little or no effect on the performance of this sensor.

3.5 Thermistors

A variety of bead-type thermistor probes from Fenwal Electronics are considered. These beads are small in size being typically 0.04 inches in diameter with smaller or larger sizes readily available. These thermistors may be used to monitor either the stream temperature or the resulting temperature of the circuit plate. This temperature gives an indication of the state in which the Fluidic circuit is operating. The mass of the thermistor must be heated up to this temperature to give a proper reading which necessarily requires a certain amount of time. This time delay presents a disadvantage for dynamic analysis of Fluidic circuits.

3.5.1 Mounting Means and Package Compatibility

The small overall size of the thermistor enables it to be more easily mounted than some of the other sensors. It may be cemented on the inside or outside of the circuit plate, or if size permits, in the stream itself. When located in the stream itself, however, the size of the thermistor bead may be significant in comparision to the cross-sectional area of the channel. Thus, the bead may change the operating characteristics of the Fluidic element.

Bead thermistors are easily mounted in the modular package. Figure 10 shows typical thermistor mountings for the modular concept. Where mounted within the circuit plate, a hole slightly larger than the thermistor is drilled from the rear of the circuit plate to a depth where it nearly breaks through into the channel. Then the thermistor is potted within the hole, locating it against the bottom of the hole. It is important that the potting around the thermistor be continuous (no air bubbles) to prevent any thermal isolation from the channel bottom.

3.5.2 Environmental Effects

The thermistor output depends on the resistance of the element. This resistance is solely a function of the temperature of the thermistor. Therefore, pressure, humidity, vibrations, acoustic disturbances, and magnetic fields will have no effect on the calibration or performance of the thermistor. Of course, it will pick up any environmental temperature changes which may be transmitted to the bead itself.

3.6 Piezoelectric Crystals

The piezoelectric crystals are PZT Bimorph ceramic material manufactured by the Piezoelectric Division of Clevite Corporation. These elements consist of two layers of piezoelectric material with a layer of metal sandwiched between them. This construction allows smaller forces to be adequately handled. They are used in Fluidic circuits as pressure transducers. The main advantage of these crystals is their extremely low cost compared to commercial pressure transducers. The thickness of the plate is 0.024 inches with the shape variable according to the application.

3.6.1 Mounting Means and Package Compatibility

A technique for flush-mounting the crystal to the bottom of a circuit channel is shown by Figure 11. An elongated slot, the width being that of the crystal is milled into the circuit plate from the rear surface.
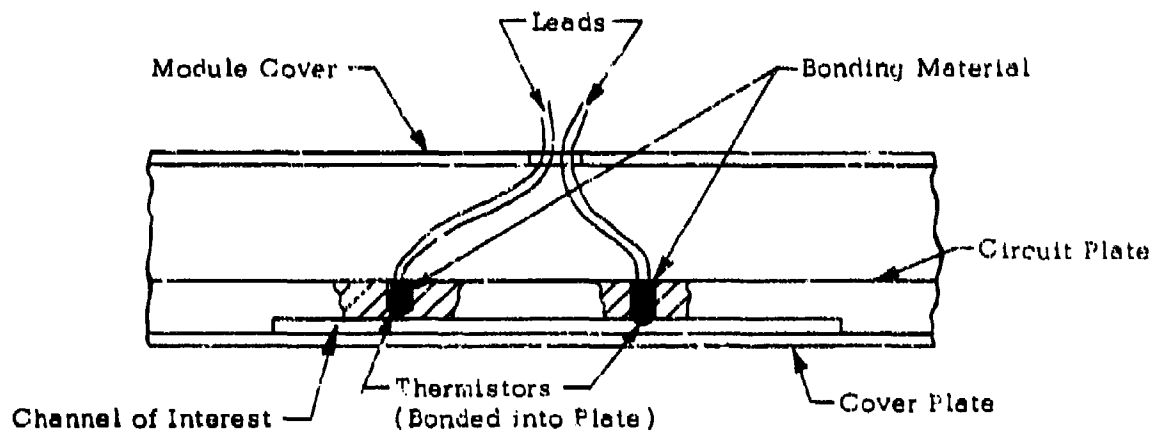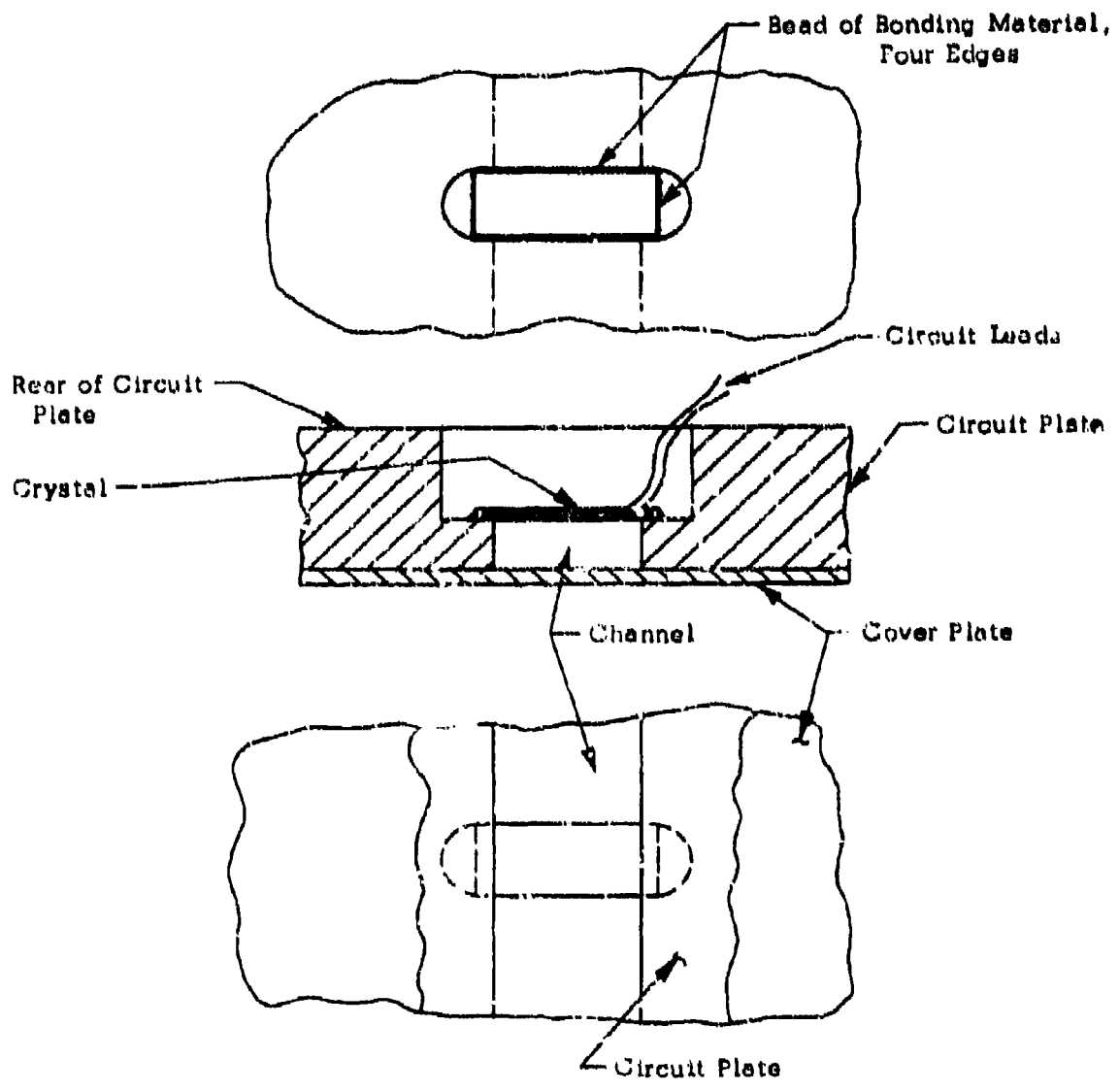
FIGURE 10. THERMISTOR MOUNTING FOR MODULAR CIRCUIT

FIGURE 11. MOUNTING OF FLAT PIEZOELECTRIC CRYSTAL
IN CIRCUIT PLATE

283

The depth of this flat-bottomed milled slot is such as to just break through the channel bottom. The crystal, with leads attached, is placed on the bottom of this channel and bonded into place with a bead of cement, such as Duco, around the four outer edges of the crystal.

The means of installing the crystal is applicable to both the modular and stacked circuit packaging concepts. In the latter case, it may be necessary to design into the stacked structure means to couple the space behind the crystal to ambient pressure.

3.6.2   Environmental Effects

The ceramic material of the Bimorph crystal has a high Curie point, well above 500°F, so the operating range is more than sufficient for the contemplated applications. The characteristics of the piezo-electric crystals are temperature dependent, however. Precise calibration curves are not available for the Bimorph-type of construction since the variation in properties due to temperature changes depends extensively on the shape of the element and its mounting characteristics. Given a specific size, shape, and type of mounting for a particular crystal; calibration curves can be determined. This calibration may vary somewhat from element to element due to variations in the mounting.

Pressure variation have no effect on the properties of the crystal itself. In most Fluidic applications, it is expected that the crystal will be used to indicate gauge pressures, in which case, ambient fluctuations will not affect the calibration. For determination of absolute pressures, a change in ambient pressure causes a shift of the zero point.

A humidity level of 90 to 95 percent does not harm the unprotected crystals. If extended service is expected at a higher humidity, then the crystals should be sealed. This does not affect their utility but does add to their cost.

3.7   Infrared Thermometer

A Barnes Engineering Company portable infrared thermometer, Model PRT-4, was investigated as a means of evaluating the applicability of I.R. sensing techniques to Fluidic system checkout. The potential afforded by I.R. techniques is in the determination of the thermal map of a functioning circuit, with deviations from the reference map indicating

284

the presence of an anomalous condition. While the I.R. thermometer model used during the program provided an approach to investigating the technique, it is not itself considered applicable to in-place flight line checkout procedures which are under consideration in the present program, due to its size and the need to scan to obtain a thermal map. It was considered that if highly satisfactory results were realized from the evaluation of I.R. techniques, more applicable I.R. sensing means could be found or perhaps developed.

3.7.1 Mounting Means and Package Compatibility

The size of the I.R. thermometer head is 5-1/2 inches diameter x 5 inches long. The target distance is one (1) foot to infinity. These characteristics are considered to prohibit suitable mounting to Fluidic circuitry and are not compatible with either the module or stacked circuit packaging concepts.

3.7.2 Environmental Effects

Variations in ambient temperature which effect changes in temperature of the surface of a Fluidic circuit plate being monitored are detected by the I.R. thermometer. The significance of this is appreciably minimized where concerned primarily with temperature profiles, as with a thermal map, rather than absolute temperatures values. Greatest accuracy in the use of I.R. mapping techniques may, of course, be realized where reference maps are made for the actual ambient temperature condition.

Other changes in environment, such as pressure, humidity, vibrations, acoustic disturbances and magnetic field have no effect on the operation of the thermometer.

4.0 CONCLUSIONS

The mounting of sensors (excluding the I.R. thermometer) on most modular packages offers no difficulty since space is generally available. It is more difficult to properly mount sensors in or on stacked or laminated circuits due to the density of the elements and the lack of available space. For these applications, it will be necessary in most cases to design the circuit with the sensing requirements in mind.

In most cases, the performance of a sensor is influenced to some degree by the environment to which it is subjected. It is necessary to carefully examine the effects of environmental conditions before selecting a particular sensor for use in a Fluidic system checkout application.

The microphone under consideration is compatible with the modular package, but it appears to be unsuitable for the stacked circuits. Environmental effects can be satisfactorily accounted for in the contemplated applications, with particular consideration directed to environmental acoustic noise.

The piezoelectric accelerometer is easily mounted on the modular package. Its use with a stacked circuit is dependent on the accessibility of the desired mounting location. It is considered that adequate corrections can be made for environmental effects with particular attention directed to environmental acoustic noise and high frequency vibration of the Fluidic circuit structure.

Miniature constant temperature anemometers are readily mounted on modular circuits, and in many cases, can be placed in stacked circuits, although more difficulty is expected. In either case, the mounting must be suitable for easy replacement of the probe element. Variation in stream conditions such as temperature, pressure, and humidity, where sufficient to be significant, may require the use of calibration curves or multiple anemometer installations and appropriate electronic circuitry to null out those effects.

The pressure transducer under consideration can be suitably mounted on either the modular or the stacked package. Temperature variation is the only environmental effect which is troublesome, and this can be largely overcome by the use of a temperature compensated transducer which is available.

Thermistors can be mounted on either type of package with less difficulty than most sensors due to their small overall size. Temperature change is the only environmental change which is of concern in the use of those elements, and may require the use of multiple thermistor installation and nulling electronic circuitry.

Piezoelectric crystals are satisfactory for use either with modular or with stacked packages. Environmental effects can be adequately accounted for in most instances. It is considered probable that for digital circuitry, to which the crystal is best suited, any calibration changes caused by environmental variations will be acceptable.

The infrared thermometer offers no mounting problems since it senses from a distance. With the exception of its somewhat limited temperature range, environmental changes are of no consequence. Preliminary tests indicate that this device is not suitable for the contemplated applications due to its size and insensitivity.

The infrared thermometer investigated during this program is not compatible with either packaging concept. It was selected as a practical means of evaluating the I.R. sensing concept, appreciating the need to find or develop a more suitable I.R. sensor if the technique proved highly satisfactory. Environmental temperature change is the only environmental condition of concern, this effect being minimized by the fact that temperature profiles rather than absolute temperatures are of most concern.

DOCUMENT CONTROL DATA - R & D

(Security classification of title, body of abstract and indexing annotation must be entered when the overall report is classified)

1. ORIGINATING ACTIVITY (Corporate author)	2a. REPORT SECURITY CLASSIFICATION
BOWLES ENGINEERING CORPORATION 9347 Fraser Street Silver Spring, Maryland 20910	UNCLASSIFIED
	2b. GROUP N/A

3. REPORT TITLE

Checkout Techniques for Fluidic Systems

4. DESCRIPTIVE NOTES *(Type of report and inclusive dates)*

Final Report

5. AUTHOR(S) *(First name, middle initial, last name)*

Sowers, Edwin U., III
Sekowski, F. Ray

6. REPORT DATE	7a. TOTAL NO. OF PAGES	7b. NO. OF REFS
November 1968	287	
8a. CONTRACT OR GRANT NO. AF 33(615)-5296	9a. ORIGINATOR'S REPORT NUMBER(S)
b. PROJECT NO. 8174	R-9-10-68
c. Task 817412	9b. OTHER REPORT NO(S) (Any other numbers that may be assigned this report) AFAPL-TR-68-68

10. DISTRIBUTION STATEMENT This document is subject to special export controls and each transmittal to foreign governments or foreign nationals may be made only with prior approval of Support Technology Division (APF), Air Force Aero Propulsion Laboratory, Wright-Patterson Air Force Base, Ohio 45433.

11. SUPPLEMENTARY NOTES	12. SPONSORING MILITARY ACTIVITY
N/A	Air Force Aero Propulsion Laboratory Wright-Patterson Air Force Base, Ohio

13. ABSTRACT

(SEE ATTACHED SHEET)

DD FORM 1473 (1 NOV 65)

Supplement to DD Form 1473

13. Abstract

Bowles Engineering Corporation has demonstrated the feasibility of checkout techniques for Fluidic circuitry. Sensors, instrumentation techniques, and checkout procedures have been defined which has been shown, by laboratory tests, to be successful in establishing levels of functional performance, and in isolating causes of circuitry malfunctions. The program was sponsored by the Air Force Aero Propulsion Laboratory.

It has been established that the most accurate means of establishing level of functional performance, to determine if the performance of a system is satisfactory or is outside of allowable limits, is through the use of primary sensors, such as certain pressure transducers and piezoelectric crystals. Primary sensors detect functional signals directly.

Acoustic sensing techniques, a secondary sensing procedure, has been applied, with a high level of success, to the isolation of anomalies causing malfunction. An accelerometer has been mounted to a circuit plate to sense the secondary acoustic energy generated by a group of operating elements on the circuit plate. This sensed acoustic signal has been converted into an amplitude vs. frequency acoustic signature, through the use of sonic and ultrasonic spectrum analyzers. It has been demonstrated that different anomalies cause distinguishingly different changes in the acoustic signature, thus permitting detection and definition of the anomalies causing malfunctions. The results realized in the isolating of malfunction causes through the use of secondary acoustic techniques is considered to be highly significant.

The present report presents the results of the checkout techniques program, during which the applicability of a group of candidate sensors were evaluated for use in the checkout of both analog and digital circuitry.

14. KEY WORDS	LINK A		LINK B		LINK C	
	ROLE	WT	ROLE	WT	ROLE	WT
Fluidic Control Systems						
Checkout Techniques						
Acoustic Sensing						
Non-Destructive Testing						
Secondary Effect Sensing						